Antigen presentation and T cell regulation by intestinal epithelial cells



Cornelia Heuberger

Lincoln College

University of Oxford

A thesis submitted for the degree of

Doctor of Philosophy

Michaelmas 2021

For Susanne

Acknowledgements

First of all, I would like to thank my supervisors Prof Kevin Maloy and Prof Fiona Powrie for their great supervision and guidance throughout my DPhil. They continuously challenged me to see the broader context of my work and allowed me to develop my independence in scientific thinking and experimental planning. I especially value their passion for science and would like to thank them for their encouragements and support throughout my DPhil studies.

This thesis would not have been possible without the continuous support and guidance by my Post-Doc supervisors Dr Johanna Pott and Dr Emily Thornton. I would like to thank both for their day-to-day help in the lab, for always being available to discuss new results, their unlimited support during any challenge I faced, their enthusiasm for science, and all the laughter and tears they shared along the way. I am so grateful to both of you for making my DPhil studies in Oxford the fantastic experience it was.

I had the fantastic opportunity to be part of both Kevin's and Fiona's lab and met so many wonderful people throughout the years. I would like to thank everyone for their helpful discussions and feedback, their support with experimental work, their emotional companionship and for the great environment they created in both labs. Firstly, the Maloy lab. I would like to thank Alison, Andrea, Belen, Cristina, Kelsey and Theo for making the lab a fun place to work at and for becoming great friends. The large group of Powrie's, where I would like to especially thank Alice, Alina, Claire, Elizabeth, Samuel, Matthias, Mathilde, Natasha, Raphael and Yisu.

To Prof Michael Dustin and Prof Gad Frankel for examining this thesis.

To the Medical Research Council for their generous DPhil funding awarded to me through the MRC Industrial Strategy Studentship.

To all the PSB and BSU staff for their support with animal husbandry. To the facility teams and people working in administration. To all the people working at the Sir William Dunn School of Pathology and Kennedy Institute of Rheumatology

for their collaborative spirit.

To Lincoln College Boat Club, which was a great component of my live in Oxford. So many wonderful people were part of the rowing team and I am thankful for the memories we created together. Thank you for providing me with the balance to a busy day in the lab, for the endless hours shared on the erg and the wonderful times we had out on the water.

To Barbara, Kaspar and Thomas for being the best flat mates I could have asked for, but more importantly, for being great friends in Oxford and beyond. Thank you for being my Oxford surrogate family. To my house mates Jacqueline, Isabel and Pete for sharing delicious meals and late-night teas together throughout my final DPhil year.

To my friends Athena, Daniel, Eirian, Emma, Gareth, Johannes, Josephine, Kasia and Sofie for all their support throughout this journey and for making this Oxford experience so special and memorable.

To my family and my partner Wolfgang for their unconditional support. This thesis would not have been possible without them and I am immensely grateful for them.

Abstract

Major histocompatibility complex (MHC) class II expression by intestinal epithelial cells (IECs) has been described in inflammatory bowel disease patients. However, the role of epithelial antigen presentation in the maintenance of immune homeostasis remains unclear. We determined that colonic IECs possess important features of antigen presenting cells, as they express MHC class II in response to IFNγ signalling, are able to take up and to process antigen and express the co-inhibitory molecule programmed death-ligand 1. Using targeted deletion of MHC class II expression in IECs, we demonstrated that colonic IEC antigen presentation plays a minor role in controlling colonic inflammation but might be important in facilitating the resolution of chronic inflammation. Small intestinal IECs express MHC class II at steady state and loss of epithelial antigen presentation at this tissue site resulted in the near loss of CD8$\alpha\alpha^+$ CD4$^+$ IELs. However, the functional consequences of this loss remain to be determined. In addition, we investigated the role of epithelial antigen presentation in modulating regulatory T cell responses and demonstrated that loss of caecal IEC MHC class II expression resulted in increased FoxP3 expression and IL-10 production by *H. hepaticus*-specific CD4 T cells in *H. hepaticus* colonised mice during intestinal inflammation. An experimental repeat, characterised by lower caecal IEC MHC class II expression, did not show these CD4 T cell changes, highlighting the importance of the tissue microenvironment in supporting antigen-specific CD4 T cell responses by IECs. To further dissect the importance of epithelial antigen presentation, *in vitro* colonic organoid and *H. hepaticus*-specific CD4 T cell co-cultures were established. This co-culture system revealed that IECs activate microbe-specific CD4 T cells in an antigen specific manner and modulate their effector phenotypes and functions. These results show, that IECs can function as non-conventional antigen presenting cells but the functional consequences of epithelial antigen presentation *in vivo* require further investigations.

Declaration of authorship

Data presented in this thesis are all from the authors' own experiments, other than the colonic organoid stimulations presented in Figure 3.4 G, which were performed by Dr. Elizabeth Mann, Kennedy Institute of Rheumatology, University of Oxford. As well as the chronic DSS histology assessment in Figure 5.25, which was performed by Dr. Mathilde Pohin, Kennedy Institute of Rheumatology, University of Oxford.

Parts of the introduction of this thesis were submitted for authors' own publication and remain largely unaltered from the published material [1]. Published contents are clearly highlighted in the relevant sections. Co-authors (Prof. Kevin Maloy and Dr. Johanna Pott) were notified and agreed with the reproduction of the mentioned published material in this thesis.

Contents

List of Figures **xi**

List of Tables **xv**

List of Abbreviations **xvi**

1 General Introduction **1**
- 1.1 The mucosal immune system . . . 1
- 1.2 Inflammatory Bowel Disease . . . 3
- 1.3 Experimental murine models of intestinal inflammation . . . 6
  - 1.3.1 *Citrobacter rodentium* infection . . . 7
  - 1.3.2 *Helicobacter hepaticus*+ anti-IL-10R-driven model of colitis . . . 9
  - 1.3.3 Dextran sodium sulphate-induced colitis . . . 10
- 1.4 Intestinal epithelial cells . . . 11
- 1.5 *Ex vivo* analysis of IEC functions: organoids . . . 15
- 1.6 MHC class II expression and localization in IECs . . . 17
- 1.7 The MHC class II processing and presentation pathway . . . 20
- 1.8 IECs show limited expression of co-stimulatory molecules . . . 23
- 1.9 Mucosal T cells . . . 24
  - 1.9.1 Th1 cells . . . 26
  - 1.9.2 Th2 cells . . . 27
  - 1.9.3 Th17 cells . . . 28
  - 1.9.4 Treg cells . . . 29
  - 1.9.5 Intestinal epithelial lymphocytes . . . 34
- 1.10 Host T cell-microbial cross talk . . . 37
- 1.11 Aims of the thesis . . . 40

2 Materials and Methods **42**
- 2.1 Mice . . . 42
- 2.2 Genotyping . . . 43
- 2.3 Bacterial culture . . . 44
  - 2.3.1 *Citrobacter rodentium* . . . 44
  - 2.3.2 *Helicobacter hepaticus* . . . 44

2.4 *In vivo* models . . . 44
2.4.1 *H. hepaticus* models . . . 44
2.4.2 *C. rodentium* model . . . 45
2.4.3 Chronic DSS model . . . 45
2.5 Assessment of intestinal and systemic inflammation . . . 46
2.5.1 Quantification of *C. rodentium* colonization . . . 46
2.5.2 Histological assessment . . . 46
2.6 Cell isolation, enrichment and sorting . . . 51
2.6.1 Isolation of spleen and lymph node cells . . . 51
2.6.2 Isolation of colonic lamina propria lymphocytes . . . 51
2.6.3 Isolation of colonic intestinal epithelial lymphocytes . . . 52
2.6.4 Isolation of colonic intestinal epithelial cells . . . 52
2.6.5 Isolation of small intestinal lamina propria lymphocytes . . . 52
2.6.6 Isolation of small intestinal intestinal epithelial cells and intestinal epithelial lymphocytes . . . 53
2.7 Flow cytometry . . . 54
2.7.1 Surface staining . . . 54
2.7.2 Restimulation for cytokine production . . . 55
2.7.3 Intracellular cytokine staining . . . 55
2.7.4 Intracellular transcription factor staining . . . 55
2.7.5 Fluorescence activated cell sorting and adoptive transfer of HH7-2tg CD4 T cells . . . 56
2.8 Quantification of cytokine levels . . . 56
2.9 Gene expression analysis . . . 58
2.9.1 Tissue processing for RNA isolation . . . 58
2.9.2 Organoid processing for RNA isolation . . . 58
2.9.3 RNA isolation and quantitative PCR (qPCR) . . . 58
2.10 Intestinal 3D organoid culture . . . 59
2.10.1 Isolation of primary intestinal epithelial cells and culturing of intestinal epithelial 3D organoids . . . 59
2.10.2 Cytokine stimulation of intestinal 3D organoids . . . 60
2.10.3 Organoid co-culture with HH7-2tg CD4 T cells . . . 61
2.11 Fluorescence microscopy . . . 62
2.11.1 Fluorescence microscopy of paraffin embedded tissue . . . 62
2.11.2 Fluorescence microscopy of OCT embedded tissue . . . 63
2.11.3 Fluorescence microscopy of organoids . . . 63
2.12 Statistics . . . 64

3 Colonic IECs have the machinery to function as non-conventional antigen presenting cells 65
3.1 Introduction . . . 65
3.2 Results . . . 70
3.2.1 MHC class II deficiency of IECs in H2-Ab1^{VC} mice . . . 70
3.2.2 MHC class II mRNA is expressed by cIECs . . . 72
3.2.3 MHC class II protein is expressed by cIECs . . . 77
3.2.4 IECs can take up and process antigen . . . 80
3.2.5 MHC class II deletion in IECs of H2-Ab1^{VC} mice is not totally efficient . . . 83
3.2.6 Lack of MHC class II expression by cIECs does not result in intestinal pathology at steady state . . . 85
3.3 Discussion . . . 92

4 Role of MHC class II expression by small intestinal IECs 103
4.1 Introduction . . . 103
4.2 Results . . . 105
4.2.1 MHC class II is increasingly expressed by IECs along the small intestinal tract . . . 105
4.2.2 MHC class II expression by siIECs is important for CD8$\alpha\alpha^+$ CD4$^+$ IEL homeostasis . . . 108
4.3 Discussion . . . 114

5 Role of MHC class II expression by colonic IECs during intestinal inflammation 118
5.1 Introduction . . . 118
5.2 Results . . . 123
5.2.1 MHC class II expression on cIECs does not impact acute intestinal inflammation triggered by *Citrobacter rodentium* infection . . . 123
5.2.2 MHC class II deficiency by cIECs does not influence chronic intestinal inflammation . . . 129
5.2.3 MHC class II expression by cIECs is potentially important during the resolution of chronic intestinal inflammation . . . 138
5.2.4 MHC class II expression by cIECs does not influence intestinal inflammation induced by chronic DSS treatment . . . 156
5.3 Discussion . . . 166

6 The role of MHC class II expression by colonic and caecal IECs in modulating CD4 T cell responses to *H. hepaticus* 175
6.1 Introduction 175
6.2 Results 179
6.2.1 *H. hepaticus* specific CD4 T cell modulation by MHC class II expression by IECs *in vivo* 179
6.2.2 HH7-2tg CD4 T cells are activated and their effector functions modulated by colonic organoid MHC class II expression . . . 192
6.3 Discussion 208

7 General discussion 218

References 223

List of Figures

1.1 Structural organisation of the intestinal epithelium. 14
1.2 Schematic overview of intestinal organoid culture. 17
1.3 The MHC class II processing and presentation pathway. 22

3.1 Successful deletion of MHC class II expression by IECs in H2-Ab1^{VC} mice. 71
3.2 IFNγ is a potent inducer of MHC class II and CIITA mRNA expression in cIEC organoids. 74
3.3 MHC class II mRNA expression levels by cIECs can be robustly detected after 6 h of IFNγ. 75
3.4 Selected TLR and NOD2 ligands do not induce MHC class II mRNA expression in H2-Ab1^{VC} and H2-Ab1$^{fl/fl}$ colonic organoids. 76
3.5 MHC class II protein expression can be robustly detected after 16 h of IFNγ treatment. 78
3.6 MHC class II protein is located at the cell surface and intracellular in H2-Ab1$^{fl/fl}$ cIECs after IFNγ treatment. 79
3.7 CIECs can take up and process protein. 82
3.8 MHC class II^{+} intestinal crypts are present on rare occassions in H2-Ab1$^{fl/fl}$ cIECs. 84
3.9 H2-Ab1^{VC} mice show low but significantly increased histopathology scores in the caecum. 87
3.10 Increased Th cell frequencies and numbers in the colonic lamina propria of aged H2-Ab1^{VC} mice. 88
3.11 Comparable effector cytokine expression by colonic lamina propria CD4^{+} T cells in aged H2-Ab1^{VC} and H2-Ab1$^{fl/fl}$ littermates. 89
3.12 Lack of MHC class II expression by cIECs does not impact MHC class I and II expression by B220^{+} cells in MLNs. 90
3.13 Reduced MHCII^{+} CD11c^{+} frequencies in the MLNs of aged H2-Ab1^{VC} mice. 91

4.1 Schematic of small intestinal sections. 106
4.2 SiIECs show increased MHC class II expression in the distal area of the SI. 107

4.3 Significantly reduced CD8$\alpha\alpha^+$ CD4$^+$ IEL frequencies and increased conventional CD4$^+$ IEL frequencies in the ileum of H2-Ab1^{VC} mice. 111
4.4 Increased FoxP3 and RoRγt expression by conventional CD4$^+$ IELs in the ileum of H2-Ab1^{VC} mice. 112
4.5 Effector function analysis of CD8$\alpha\alpha^+$ and conventional CD4$^+$ IELs in the ileum. 113

5.1 *C. rodentium* infected H2-Ab1^{VC} and H2-Ab1$^{fl/fl}$ mice show comparable body weight loss and similar spleen weight. 125
5.2 *C. rodentium* infection induces IEC MHC class II expression in H2-Ab1$^{fl/fl}$ mice. 126
5.3 *C. rodentium* infected H2-Ab1^{VC} and H2-Ab1$^{fl/fl}$ mice show similar tissue adherent and planktonic bacteria in intestinal tissues and caecal content. 127
5.4 *C. rodentium* infected H2-Ab1^{VC} and H2-Ab1$^{fl/fl}$ mice exhibit comparable pathology. 128
5.5 *H. hepaticus* + anti-IL-10R treated H2-Ab1^{VC} and H2-Ab1$^{fl/fl}$ mice show comparable body weight loss and similar spleen weight. 132
5.6 *H. hepaticus* + anti-IL-10R treated H2-Ab1^{VC} and H2-Ab1$^{fl/fl}$ mice show comparable histopathology scores. 133
5.7 *H. hepaticus* + anti-IL-10R treatment induces MHC class II expression by cIECs in H2-Ab1$^{fl/fl}$ mice. 134
5.8 Colonic CD4$^+$ IEL frequencies of *H. hepaticus* + anti-IL-10R treated H2-Ab1^{VC} and H2-Ab1$^{fl/fl}$ mice are comparable. 135
5.9 Lamina propria CD4$^+$ T cell frequencies of *H. hepaticus* + anti-IL-10R treated H2-Ab1^{VC} and H2-Ab1$^{fl/fl}$ mice are comparable. 136
5.10 SHelAg treatment induced cytokine production by LPLs of *H. hepaticus* + anti-IL-10R treated H2-Ab1^{VC} and H2-Ab1$^{fl/fl}$ mice. 137
5.11 Reduced spleen weight but comparable body weight of H2-Ab1^{VC} mice during the resolution phase of *H. hepaticus* + anti-IL-10R treatment. 144
5.12 Delayed resolution of inflammation of *H. hepaticus* + anti-IL-10R treated H2-Ab1^{VC} mice. 145
5.13 Comparable colonic CD4$^+$ IEL frequencies during the resolution of chronic inflammation. 146
5.14 Comparable Treg and Th17 frequencies during the resolution of chronic inflammation between H2-Ab1^{VC} and H2-Ab1$^{fl/fl}$ littermates. 147
5.15 Comparable cytokine and AMP expression, as well as proliferation and stemness status in colonic tissue of H2-Ab1$^{fl/fl}$ and H2-Ab1^{VC} mice during resolution of chronic inflammation. 148

5.16 Increased TNFα and IFNγ production by MLN Th cells of H2-Ab1^{VC} mice during the resolution phase of *H. hepaticus* + anti-IL-10R treatment. 149
5.17 Comparable spleen weight during the resolution phase of *H. hepaticus* + anti-IL-10R treatment at the new SPF-B animal facility. 150
5.18 Comparable resolution of inflammation of *H. hepaticus* + anti-IL-10R treated H2-Ab1^{VC} mice in new SPF-B animal facility. 151
5.19 Upregulated MHC class II expression by cIECs during the resolution of inflammation of *H. hepaticus* + anti-IL-10R treated H2-Ab1$^{fl/fl}$ mice. 152
5.20 Reduced colonic CD4^{+} IEL frequencies in H2-Ab1^{VC} mice during the resolution of chronic inflammation in the new SPF-B animal facility. 153
5.21 Comparable Treg and Th17 frequencies during the resolution of chronic inflammation between H2-Ab1^{VC} and H2-Ab1$^{fl/fl}$ littermates in the new SPF-B animal facility. 154
5.22 Comparable TNFα and IFNγ production by MLN Th cells of H2-Ab1^{VC} mice during the resolution phase of *H. hepaticus* + anti-IL-10R treatment in the new SPF-B animal facility. 155
5.23 MHC II expression on IECs does not affect recovery from chronic DSS colitis. 159
5.24 IECs express MHC class II during chronic DSS treatment in H2-Ab1$^{fl/fl}$ mice. 160
5.25 Histopathology scores of colonic sections of chronic DSS treated H2-Ab1$^{fl/fl}$ and Ab1^{VC} mice. 161
5.26 Myeloid gating strategy for chronic DSS. 162
5.27 Comparable myeloid cell populations during chronic DSS treatment in H2-Ab1^{VC} and H2-Ab1$^{fl/fl}$ mice. 163
5.28 Reduced cell numbers in distinct myeloid populations in H2-Ab1^{VC} mice detected in the first chronic DSS experiment. 164
5.29 Comparable Treg and Th17 frequencies during chronic DSS treatment of H2-Ab1^{VC} and H2-Ab1$^{fl/fl}$ littermates. 165

6.1 Experimental design of adoptive HH7-2tgIL10GFP CD4 T cell transfer. 181
6.2 *H. hepaticus* colonisation induces MHC class II expression by IECs in the caecum and colon of H2-Ab1$^{fl/fl}$ mice. 182
6.3 Increased IL-10 and FoxP3 expression by HH7-2tgIL10GFP CD4 T cells in the caecal lamina propria of H2-Ab1^{VC} mice. 183
6.4 Comparable IL-10 and FoxP3 expression by HH7-2tgIL10GFP CD4 T cells in the colonic lamina propria of H2-Ab1^{VC} mice and H2-Ab1$^{fl/fl}$ littermates. 184

6.5 Comparable IL-10 and FoxP3 expression by HH7-2tgIL10GFP CD4 T cells in context of lower MHC class II expression by caecal IECs. 188
6.6 *H. hepaticus* colonisation induces MHC class II and PD-L1 expression by IECs in the caecum and colon of H2-Ab1$^{fl/fl}$ mice. 189
6.7 MHC class II and PD-L1 expression by caecal and colonic IECs show very strong positive correlation. 190
6.8 Experimental setup of colonic organoid and CD4 T cell co-culture and culture conditions. 197
6.9 Three day co-culture of HH7-2tg CD4 T cells with colonic H2-Ab1$^{fl/fl}$ organoids. 198
6.10 Upregulation of PD-1 and CD44 expression by HH7-2tg CD4 T cells upon antigen specific activation by cIECs. 199
6.11 Flow cytometric analysis of PD-1 and CD44 expression by HH7-2tg CD4 T cells upon antigen specific activation by cIECs. 200
6.12 Co-culture supports central memory T cell differentiation. 201
6.13 Upregulation of RoRγt and T-bet but not FoxP3 expression by HH7-2tg CD4 T cells upon antigen specific activation. 202
6.14 Upregulation of RoRγt and T-bet but not FoxP3 expression by HH7-2tg CD4 T cells upon antigen specific activation. 203
6.15 Antigen specific activation of HH7-2tg CD4 T cells by MHC class II expressing cIECs supports RoRγt and T-bet expression. 204
6.16 Upregulation of IFNγ, IL-17A and TNFα cytokine production upon antigen specific activation of HH7-2tg CD4 T cells. 205
6.17 Upregulation of IFNγ, IL-17A and TNFα cytokine production upon antigen specific activation of HH7-2tg CD4 T cells. 206
6.18 Antigen specific stimulation of HH7-2tg CD4 T cells leads to IFNγ release. 207
6.19 Schematic overview of antigen-specific interaction of HH7-2tg CD4 T cell with colonic organoids. 213

List of Tables

1.1 MHC class II expression by intestinal epithelial cells 19

2.1 Histological scoring of *C. rodentium* induced colitis 48
2.2 Histological scoring of *H. hepaticus* + anti-IL-10R induced colitis . 49
2.3 Histological scoring of chronic DSS induced colitis 50
2.4 List of antibodies used in this study 57
2.5 HH7-2tg CD4 T cell FACS panel 58
2.6 Media supplements to support colonic organoid growth *ex vivo*. . . 60

List of Abbreviations

A/E . . . . . attaching and effacing.

AMP . . . . . antimicrobial peptide.

APC . . . . . antigen presenting cell.

βMe . . . . . beta mercaptoethanol.

C. rodentium Citrobacter rodentium.

CDC42 . . . . cell division control protein 42 homolog.

CD . . . . . Crohn's disease.

CFU . . . . . Colony forming units.

cIEC . . . . . colonic intestinal epithelial cell.

cIEL . . . . . colonic intestinal epithelial lymphocyte.

CIITA . . . . . class II major histocompatibility complex transactivator.

CLIP . . . . . class II-associated invariant-chain peptide.

cmIEC . . . . caecal intestinal epithelial cell.

CpG . . . . . cytosine-phosphate-guanine.

DAMP . . . . damage-associated molecular pattern.

DAPI . . . . . 4',6-diamidino-2-phenylindole.

DSS . . . . . dextran sulfate sodium.

EDTA . . . . . ethylenediaminetetraacetic acid.

EGF . . . . . epidermal growth factor.

ELISA . . . . . enzyme-linked immunosorbent assay.

ER . . . . . endoplasmic reticulum.

FoxP3 . . . . . forkhead box P3.

GvHD . . . . . graft-vs-host disease.

GWAS . . . . . Genome-wide association studies.

H. hepaticus . Helicobacter hepaticus.

HFD . . . . . high fat diet.

Hprt . . . . . hypoxanthine phosphoribosyl transferase.

H& E . . . . . haematoxylin and eosin.

i.g. . . . . . intragastrically.

i.p. . . . . . intraperitoneally.

i.v. . . . . . intravenously.

IBD . . . . . inflammatory bowel disease.

ICAM-1 . . . . intercellular adhesion molecule-1.

ICOS-L . . . . inducible co-stimulatory ligand.

IDO . . . . . indoleamine 2,3-dioxygenase.

IEC . . . . . intestinal epithelial cell.

IEL . . . . . intestinal epithelial lymphocyte.

IFN . . . . . interferon.

Ig . . . . . immunoglobulin.

Ii . . . . . MHC class II invariant chain.

ISC . . . . . intestinal stem cell.

iTreg . . . . . induced Treg.

LEE . . . . . locus of enterocyte effacement.

LFA-1 . . . . . lymphocyte function-associated antigen-1.

LPS . . . . . lipopolysaccharide.

LP . . . . . lamina propria.

MAMP . . . . microbial-associated molecular pattern.

MFI . . . . . median fluorescent intensity.

MHC . . . . . major histocompatibility complex.

MIIC . . . . . MHC class II compartment.

MLN . . . . . mesenteric lymph node.

MNP . . . . . mononuclear phagocytes.

mRNA . . . . messenger RNA.

MVB . . . . . multi-vesicular bodies.

NGS . . . . . normal goat serum.

NOD2 . . . . . nucleotide-binding oligomerization domain 2.

NOS2 . . . . . nitric oxide synthase 2.

NO . . . . . nitric oxide.

OD . . . . . optical density.

ON . . . . . overnight.

P/S . . . . . Penicillin/Streptomycin.

PBS . . . . . Phosphate buffered saline.

PCR . . . . . polymerase chain reaction

PD-1 . . . . . programmed death 1.

PD-L1 . . . . . programmed death ligand 1

pi . . . . . post infection.

PMA . . . . . Phorbol 12-myristate 13-acetate.

PPL . . . . . Project License.

PRR . . . . . pattern recognition receptor.

ROR . . . . . retinoic acid receptor-related orphan nuclear receptor.

RTqPCR . . . real time quantitative polymerase chain reaction.

RT . . . . . room temperature.

Runx3 . . . . . runt-related transcription factor 3.

SFB . . . . . segmented filamentous bacteria.

siIEC . . . . . small intestinal epithelial cell.

SI . . . . . small intestine.

SPF . . . . . specific pathogen-free.

STAT . . . . . signal-transducing activators of transcription.

T3SS . . . . . type 3 secretion system.

TA . . . . . transient-amplifying cell.

TF . . . . . transcription factor.

TGF . . . . . transforming growth factor.

TGF . . . . . transforming growth factor.

tg . . . . . transgenic.

ThPOK . . . . T helper–inducing POZ/Krüppel-like factor.

Th . . . . . T helper.

TLA . . . . . thymus leukaemia antigen.

TLR . . . . . Toll-like receptor.

TMB . . . . . 3,3',5,5'-Tetramethylbenzidine.

TNF . . . . . tumor necrosis factor.

Treg . . . . . regulatory T.

UC . . . . . ulcerative colitis.

1 General Introduction

Contents

1.1 The mucosal immune system 1
1.2 Inflammatory Bowel Disease 3
1.3 Experimental murine models of intestinal inflammation 6
1.3.1 *Citrobacter rodentium* infection 7
1.3.2 *Helicobacter hepaticus*+ anti-IL-10R-driven model of colitis 9
1.3.3 Dextran sodium sulphate-induced colitis 10
1.4 Intestinal epithelial cells 11
1.5 *Ex vivo* analysis of IEC functions: organoids 15
1.6 MHC class II expression and localization in IECs . . . 17
1.7 The MHC class II processing and presentation pathway 20
1.8 IECs show limited expression of co-stimulatory molecules 23
1.9 Mucosal T cells 24
1.9.1 Th1 cells 26
1.9.2 Th2 cells 27
1.9.3 Th17 cells 28
1.9.4 Treg cells 29
1.9.5 Intestinal epithelial lymphocytes 34
1.10 Host T cell-microbial cross talk 37
1.11 Aims of the thesis 40

1.1 The mucosal immune system

The mucosal immune system comprises the gastrointestinal, respiratory and urogenital tract. These tissue sites are in constant interaction between microbes, resident

tissue cells and the immune system and are the major interface between the host and the external environment. The mucosal surface of the gastrointestinal tract provides a barrier against chemical, physical, and microbial insults while maintaining the absorption of nutrients and water. The mucosal immune system consists of a diverse community of innate and adaptive immune cells and has the unique challenge to distinguish harmless antigens derived from food and microbiota from harmful pathogens.

The gastrointestinal tract forms a continuous tube, consisting of different segments, which have a similar architecture. The common architecture can be divided into four layers: the mucosa, the submucosa, the muscularis propria and the serosa. The mucosa surrounds the gastrointestinal lumen and itself consists of three layers. The innermost layer, the intestinal epithelium, is formed by intestinal epithelial cells (IECs) and faces the intestinal lumen. The epithelium is supported by the lamina propria, a layer of connective tissue. Both epithelium and lamina propria are key immunological effector sites, hosting the majority of the intestinal immune cells. Underneath these two layers lies the muscularis mucosae, a thin muscle layer [2].

The small intestine can be divided into three segments, the duodenum begins after the pylorus of the stomach, followed by the jejunum and finally the ileum. The small intestine is followed by the large intestine. The caecum has a sac-like structure and leads into the proximal, mid and distal colon and the rectum. The gastrointestinal tract exhibits functional differences along its length, with the small intestine being important for the digestion of food and absorption of nutrients, while the large intestine mainly re-absorbs water and forms a large reservoir for the gut microbiota. [3]

The microbiota is a complex community of micro-organisms, consisting of predominantly bacteria, viruses, fungi, protozoa and archaea. The concentration

of bacteria increases from the small intestine towards the large intestine and is estimated in the order of 100 trillion (10^{14}) microbes [4] [5]. The microbiota plays an important role in the education of the intestinal immune system. In germ free mice, which are devoid of microbiota, the immune system has not been shaped by microbial interactions and is impaired in its development, showing defects in the development of mature lymphoid tissues, antibody production and T cell development and functions (reviewed in [6]). The microbiota and the immune system maintain a symbiotic relationship. Distinct symbiotic bacteria provide benefits to the host: they break down complex food components, providing essential nutrients to the host and they prevent the colonisation of potential pathogens through niche competition.

The intestinal immune system strives to maintain a homeostatic relationship with the microbiota by balancing pro-inflammatory immune responses towards pathogens with anti-inflammatory pathways involved in the maintenance of tolerance to harmless antigens. However, the disruption of the microbiota, through administration of antibiotics or changes in diet, can result in a misdirected immune response against self, microbiota-derived, or environmental antigens [7] and has been associated with systemic autoimmune and inflammatory diseases, such as inflammatory bowel disease (IBD), cancer and obesity [8–10]. These changes in the taxonomic composition of the microbiota, especially the loss of commensal bacteria diversity, relative to healthy controls is referred to as 'dysbiosis'. Whether dysbiosis is the cause or a consequence of these pathologies is currently not understood.

1.2 Inflammatory Bowel Disease

Inflammatory bowel disease (IBD) is a chronic, relapsing inflammatory disease of the gastrointestinal tract, which includes Crohn's disease (CD) and ulcerative colitis (UC). CD can affect any part of the gastrointestinal tract, whereas UC is restricted to the colon [11]. In addition, the inflammation in CD can be transmural, affecting all layers of the bowel from the mucosa to the serosa, whereas the inflammation in UC is mostly confined to the colonic mucosa [12]. The characteristic histological

findings of the disease include crypt abscesses, goblet cell depletion and immune cell infiltration [13]. Inflammation of the gastrointestinal tract results in abdominal pain, weight loss and diarrhoea [13]. IBD is mainly diagnosed in adolescence or early adulthood, with a UK incidence rate of 23 per 100000 person-years for UC and 14.3 per 100000 person-years for CD between 2000 and 2018 [14].

The precise aetiology of IBD is not fully understood and multiple factors are thought to contribute to the immunopathogenesis, including genetic, microbial, environmental and host immune factors [15]. The dysregulated immune response is thought to be partly directed towards the microbiota and studies were initially focused on adaptive immunity, but have expanded in recent times to include tissue cells, which display immunoregulatory functions [15].

$CD4^+$ T cells play an important part in driving the pathogenesis in human IBD. Since the late 1980s, T helper (Th) cells have been grouped into distinct subsets, according to their cytokine production and associated functions, with Th1 and Th2 cell representing the original subsets [16]. CD was originally described to be a Th1 cell mediated disease, with high levels of IFNγ [17, 18], whereas UC was associated with an expanded Th2 response, driven by IL-4 and IL-13 [19, 20]. However, more recent studies have demonstrated that both CD and UC patients have elevated IL-17 and IL-22 levels in the gut mucosa, cytokines associated with a Th17 response [21–24]. Therefore, the classical Th1/Th2 paradigm has been revised. The cytokine IL-23, primarily produced by activated macrophages and dendritic cells, stabilises the Th17 lineage and lack of IL-23 was accompanied by reduced expression of TNFα, IFNγ and IL-6, as well as reduced intestinal inflammation, in experimental T-cell mediated mouse models [25–27]. In addition, regulatory T (Treg) cells suppress pro-inflammatory immune responses against microbial and food antigens, and thereby maintain intestinal homeostasis. T cell transfer models have shown that Treg cells protect from intestinal inflammation [28–30] and Treg

cell transfer after disease induction cures established intestinal inflammation [31].

The role of the microbiota in triggering IBD has been extensively studied. Analysis of patient stool and mucosal samples revealed alteration in the intestinal microbiota, or dysbiosis, characterised by decreased commensal bacteria diversity and a shift in bacterial composition (reviewed in [8]). Reduced diversity in the phyla Firmicutes and Bacteroides have been described [32–34]. Murine models of colitis support the role of the microbiota in contributing to the pathogenesis, as mice treated with antibiotics, or housed in a germ free environment, show ameliorated disease (reviewed in [35]). In addition, the oral transfer of colitogenic fecal microbiota into healthy mice was shown to enhance disease susceptibility [36–38]. Although these fecal transfer experiments suggest a crucial role for the microbiota in driving the pathogenesis of IBD, it is not clear whether dysbiosis is a cause or consequence of intestinal inflammation.

In addition, the genetic make-up of the individual plays an important role in the development of IBD. Epidemiological studies suggest a strong genetic contribution to IBD susceptibility, with a high risk of IBD development of first-degree relatives of IBD patients [39]. Genome-wide association studies (GWAS) have provided further insights into genetic definitions of host susceptibility, identifying both innate (NOD2, CARD9) and adaptive (TNFSF15, PTPN2, IL12B) immune pathways in IBD (reviewed in [40, 41]). These findings opened up the idea that innate immune sensing might play an important role in the development of IBD. In addition, GWAS identified a protective variant in *IL23R*, the gene encoding a subunit of the receptor for the pro-inflammatory cytokine IL-23 [42]. Genetic variants of monogenic traits can lead to early-onset IBD, with the mutations in the IL-10 receptor genes *IL10RA* and *IL10RB* being one of the first hypomorphic alleles described to reduce IL-10 signalling and causing severe intestinal inflammation [43]. These genetic studies highlight that a single genetic defect in regulatory pathways can results in impaired tolerance, which results in intestinal inflammation. They

played an important role in identifying pathways associated with disease pathology. However, the heterogeneous immunopathology of IBD and low disease penetrance in individuals carrying disease-susceptibility alleles suggest that complex interactions between multiple host and environmental factors cause IBD.

The major goal of IBD treatment is the reduction of intestinal inflammation, which relieves disease symptoms and ideally result in long-term disease remission. Although much progress has been made in understanding the multiple genetic and environmental factors contributing to disease pathology, no cure exists. Classic immunosuppressive drugs include azathioprine or methotrexate, which are used for the induction and maintenance of disease remission [44, 45]. Several new drugs have been used in IBD therapy, including anti-TNF agents, which decrease the disease severity of many patients [45, 46]. However, not all patients respond to anti-TNF therapy. There is still a large unmet need for new therapeutic agents, with many of the novel therapeutic approaches accepting the challenge to tailor therapies to individual patient's disease pathology.

1.3 Experimental murine models of intestinal inflammation

Experimental murine models of IBD have substantially improved our understanding of intestinal homeostasis and how a breakdown of intestinal homeostasis can lead to intestinal inflammation, building the foundation for the development of new therapeutic strategies. A number of murine models of colitis have been described, although not a single model recapitulates the complexity of the immunopathology. Each model recapitulates different aspects of the disease and mouse models can be divided into either chronic or acute models, and those that are driven either by innate and/or adaptive immune responses. The experimental mouse models can broadly be divided into four groups: (1) genetically modified animals exhibiting pathology; (2) chemical disruption of the intestinal epithelium; (3) adoptive transfer

models of colitis and (4) administration of infectious agents.

1.3.1 *Citrobacter rodentium* infection

Citrobacter rodentium (*C. rodentium*) is a gram-negative, non-invasive, enteric murine attaching and effacing (A/E) pathogen. It is transmitted via the fecal-oral route and causes a transient colitis [47]. Initially, *C. rodentium* colonises the caecum, specifically the caecal lymphoid patch, and later the colon and caecum [48] Depending on the mouse strain, *C. rodentium* levels peak between day 4-12 post infection (pi) and is cleared from the colon by day 21-28 pi [49, 50]. Colonisation by *C. rodentium* is mediated via intimate adherence to IECs and the formation of attaching and effacing lesions, which are characterized by effacement of the brush border microvilli and localised reorganisation of the host actin cytoskeleton to form pedestal-like structures at the attachment site [47, 51].

The pathogenicity island called locus of enterocyte effacement (LEE) mediates the formation of A/E lesions and encodes multiple virulence factors, including components of the type 3 secretion system (T3SS) [52]. *C. rodentium* shares its virulence genes and infection strategy with the human enteropathogenic and enterohaemorrhagic *Escherichia coli* (EPEC and EHEC) and is therefore widely used to study host-pathogen interactions in immunocompetent mice [53].

In addition, *C. rodentium* infection is used to study intestinal inflammation disorders, such as UC and CD [54]. The colonic pathology of *C. rodentium* infection has common features with other mouse models of colitis. During the establishment phase of *C. rodentium* infection (1-3 d pi) dendritic cells secrete IL-23, which induces the production of IL-22 and IL-17 by type3 innate lymphoid cells. IL-22 in turn acts on IECs to induce the secretion of antimicrobial peptides (AMPs) [50]. After one week of *C. rodentium* colonisation, the formation of A/E lesions caused excessive epithelial regeneration, which leads to thickening of the colonic mucosa and epithelial

cell hyperplasia, including crypt elongation and goblet cell loss [55, 56]. Neutrophils get recruited into the tissue and participate in the IL-22 secretion [50]. Th1 and Th17 cells infiltrate the inflamed mucosa, secreting IL-17A, IFNγ and TNFα [50, 54]. The pathology is partly driven by T and B cells, as mice deficient in these cell populations develop less severe disease [57]. Clearance of *C. rodentium* is mediated by both innate and adaptive immune responses and is thought to occur in multiple stages. First, epithelial repair re-establishes the epithelial barrier, limiting the translocation of luminal antigen into the mucosa. Then the adaptive immune response mediates the later stages of the clearance of the infection, through $CD4^+$ T cell dependent IgG responses [57–59]. Finally, neutrophils mediate the killing of bacteria through phagocytosis, formation of neutrophil extracellular traps and release of toxic granule content [50, 60]. The adaptive immune responses are orchestrated by IL-23 secretion from innate immune cells. IL-23 and transforming growth factor (TGF) β induce a potent Th17 response, which is characterised by IL-17 expression, which is more pronounced than the Th1 response, producing IFNγ [61]. Mice lacking IL-23 fail to clear *C. rodentium* infection and show higher mortality rates than wild type mice [61]. In addition, IL-22 is produced in the inflamed intestine and provides protection against *C. rodentium* infection by promoting epithelial repair and antimicrobial peptide production [62].

C. rodentium infection modulates the gut microbiota. During *C. rodentium* outgrowth, the total numbers of colonic host bacteria decrease and the bacterial composition is altered [63, 64], which may affect pathogenesis and bacterial clearance. Indeed, the commensal *Segmented filamentous bacteria* (SFB) can induce IL-22 and IL-17 production by Th17 cells, which resulted in increase resistance towards *C. rodentium* infection [65]. *C. rodentium* infection initiates a variety of innate and adaptive immune responses, which makes it an useful model to investigate both protective immunity as well as inflammatory responses in the intestine.

1.3.2 *Helicobacter hepaticus*+ anti-IL-10R-driven model of colitis

Helicobacter hepaticus is a gram-negative Proteobacteria, which grows in microaerophilic conditions. It was initially isolated from the livers of immunocompetent A/JCr mice and implicated in the development of chronic hepatitis and liver cancer but was also shown to colonise the murine large intestine [66, 67]. While *H. hepaticus* can chronically colonise immunocompetent mice without causing overt disease, it has been associated with the induction of colitis in immunodeficient mouse strains [68, 69]. It has been established that *H. hepaticus* leads to the development of chronic inflammation of the caecum and colon (typhlocolitis) in IL-10 deficient mice [70, 71], which can be reproduced by blocking IL-10R signalling using an antibody targeting the IL-10R (anti-IL-10R) in wild-type C57BL mice [25].

The inflammatory response of IL-10 deficient mice against *H. hepaticus* is driven by a type 1 cytokine response, characterised by IL-12, tumor necrosis factor (TNF) α and Interferon (IFN) γ secretion [70, 72]. Furthermore, mice treated with anti-IL-10R develop colitis, driven by increased expression of INFγ and IL-17 in the colon and mesenteric lymph nodes (MLN). Additional studies have established IL-23 as a driver of intestinal inflammation. Mice deficient in IL-12p40 (a common subunit of IL-12 and IL-23) but not IL-12p35 (a subunit of IL-12, but not IL-23) were resistant to the development of intestinal inflammation by *H. hepaticus* infection and anti-IL-10R treatment [25] or did not develop spontaneous colitis in IL-10 deficient mice [73]. These studies show that IL-23 is driving the pathogenic Th1 and Th17 responses during intestinal inflammation. IL-23 is produced by activated $CD11c^+$ mononuclear phagocytes [74] in response to microbial stimulation (reviewed in [75]). However, *H. hepaticus* infection alone of wild type mice induces Treg cell responses, which inhibits the development of intestinal inflammation [76].

Chronic intestinal inflammation is most pronounced in the caecum and proximal colon, the primary sites of *H. hepaticus* colonisation, but affects the entire large

intestine. Pathology is characterised by epithelial hyperplasia, goblet cell depletion and infiltration of mononuclear leukocytes into the lamina propria [25]. In severe cases, the development of crypt abscesses, ulceration and tissue oedema can be observed [25].

The *H. hepaticus* and anti-IL-10R chronic colitis model highlights the interplay of microbial and host factors in immunopathology and serves as a unique experimental model of host-microbe maladaptation. It illustrates that certain members of the intestinal microbiota have the potential to cause disease if intestinal homeostasis is disturbed and organisms with such abilities have been classified as pathobionts. Thus, *H. hepaticus* infection can be used to study immunological processes driving IBD pathogenesis.

1.3.3 Dextran sodium sulphate-induced colitis

Dextran sulfate sodium (DSS), a water-soluble sulphated polysaccharide, can be administered to mice in the drinking water. Due to its toxicity to colonic epithelial cells [77], it causes disruption of the epithelial layer, allowing the entry of luminal contents and antigens into the mucosa, resulting in rapid intestinal inflammation [78, 79]. If administered for a short period, DSS treatment leads to acute colitis, which is characterised by weight loss, bloody diarrhoea, ulcer formation and neutrophil infiltration into the mucosa and submucosa of the colon [78, 80] and thereby resembles many human UC-like pathologies. Importantly, acute DSS can be induced without the help of adaptive immune cells, as intestinal inflammation develops in severe combined immunodeficient (SCID) [81] and Rag2-/- [82] mice (both lacking mature B- and T- cells), suggesting that the innate immune responses are sufficient to drive intestinal inflammation.

The acute DSS model is widely used due to it simplicity, rapidity and reproducibility. However, the treatment regime can easily be adapted and multiple treatment cycles allow the modeling of relapsing and chronic forms of intestinal inflammation.

Between DSS treatment cycles, mice are administered normal drinking water, which allows for the recovery from intestinal inflammation. The chronic colitis model can therefore be used for the investigation of tissue regeneration and chronic wound healing [79]. In chronic DSS colitis, T cells accumulate in the inflamed mucosa, showing changes in Th1/Th2 cytokine expression [83].

The alterations of the intestinal epithelium caused by DSS treatment result in abnormal interactions of the host with luminal antigens, which contribute to disease. Within three days, DSS induced colitis leads to changes in the composition of the gut microbiota, with reduced microbial diversity [84]. DSS treatment led to a decrease in members of the phyla Bacteriodetes, Tenericute and Lactobacillus [84, 85], with an increase in *Enterobacteriaceae*, *Akkermansia* and *Desulfovibrio* [84, 85].

1.4 Intestinal epithelial cells

The following section is my own work and has been published [1].

The intestinal epithelium is composed of a single layer of columnar IECs. It facilitates the absorption of metabolites and water while compartmentalizing the immune cells residing in the lamina propria from the microbiota in the lumen. Its large surface is formed by millions of crypt–villus units [86]. Each villus, a finger-like structure extending into the lumen, is surrounded by multiple crypts. In the small intestine, the villi are composed of post-mitotic IECs and their length decreases along the gastrointestinal tract. In the colon, villi are lacking and the crypts open into a flat epithelium.

To maintain the epithelial barrier in the face of constitutive exposure to a vast microbiota and mechanical stress caused by peristaltic movement, it is constantly replenished by ISCs. ISCs reside at the bottom of the crypt and give rise to progenitor cells, called transient-amplifying cells (TAs) that proliferate and

differentiate into mature IECs. The epithelium consists of at least six different mature cell types, which can be separated into absorptive (enterocytes and M cells) and secretory (Paneth, goblet, enteroendocrine and tuft cells) cells [87, 88]. The structural organisation of the intestinal epithelium is shown in Figure 1.1.

Enterocytes make up around 80 % of mature IECs that line the epithelium [89]. Their main function is to take up nutrients and transport them across the epithelium. Microfold cells (M cells) are located above gut-associated lymphoid tissue (GALT) [90]. M cells are absorptive cells specialised in the phagocytosis and transcytosis of luminal antigen and their release into the underlying immune cell containing tissue [91]. Paneth cells reside at the bottom of the small intestinal crypt [92]. They are known to both support the ISCs by producing growth factors and to protect the ISCs by secreting microbicidal proteins and peptides. Goblet cells secrete mucins, which form a protective layer on the intestinal epithelium [93, 94]. In addition they were shown to support mucus barrier integrity by secreting factors such as the mucin crosslinking agent trefoil factor 3 [95]. Enteroendocrine cells specialise in the production of hormones that regulate the digestive functions. They represent approximately 1 % of the IEC population and individual subtypes are determined by the specific hormones they release [96]. The rarest IEC population comprises tuft cells, which express chemosensory receptors. Their precise function however remains poorly understood. Recently, they were shown to be important in the defence of helminth infection and their cell numbers were regulated by type 2 cytokines [97, 98]. With the exception of Paneth cells, all cell types described above can be found in both the small intestine and the colon. Paneth cells however are unique to the small intestinal stem cell niche. The colonic intestinal stem cell niche is supported by the subepithelial mesenchymal cells [99, 100], as well as Reg4+ deep crypt secretory cells [101–103].

The intestinal epithelium plays a vital part in maintaining immune homeostasis with the commensal microbiota, partly because it limits the physical interaction of

the microbiota with the immune cells residing in the lamina propria. This physical barrier is enforced by inducible defence mechanisms; recognition of the microbiota by IECs can trigger their activation and expression of mediators, such as chemokines or cytokines, which subsequently can activate local immune cells [104, 105]. These defences are activated by pattern recognition receptors (PRRs), which recognize microbial-associated molecular patterns (MAMPs) or damage-associated molecular patterns (DAMPs) released from the host cells. IECs express a variety of different PRRs, and signalling through Toll-like receptors (TLRs) was shown to maintain barrier function [104, 105]. IECs are structurally polarized – their apical surface faces the intestinal lumen, whereas their basolateral membrane is in contact with the lamina propria – and TLR activation can lead to different cellular responses depending on the localization at either the apical or basolateral membrane [106–108]. Additionally, TLR expression levels by IECs change along the intestine with small intestinal IECs (siIECs) generally expressing lower levels than colonic IECs (cIECs) [107], which corresponds to the much lower levels of microbiota found in the small intestine. Specialized IEC populations may also detect and directly respond to distinct pathogens; for example, tuft cells have recently been demonstrated to participate in immunity against some parasitic worms through release of IL-25 that promotes type II responses [87, 97, 98, 109].

Although it is clear that IECs make crucial contributions to barrier integrity and innate immune pathways, evidence of their participation in antigen-specific immune reactions is more equivocal. Nevertheless, their ability to express major histocompatibility complex (MHC) class II proteins, as well as associated processing molecules, suggests that IECs may function as non-conventional antigen-presenting cells (APCs).

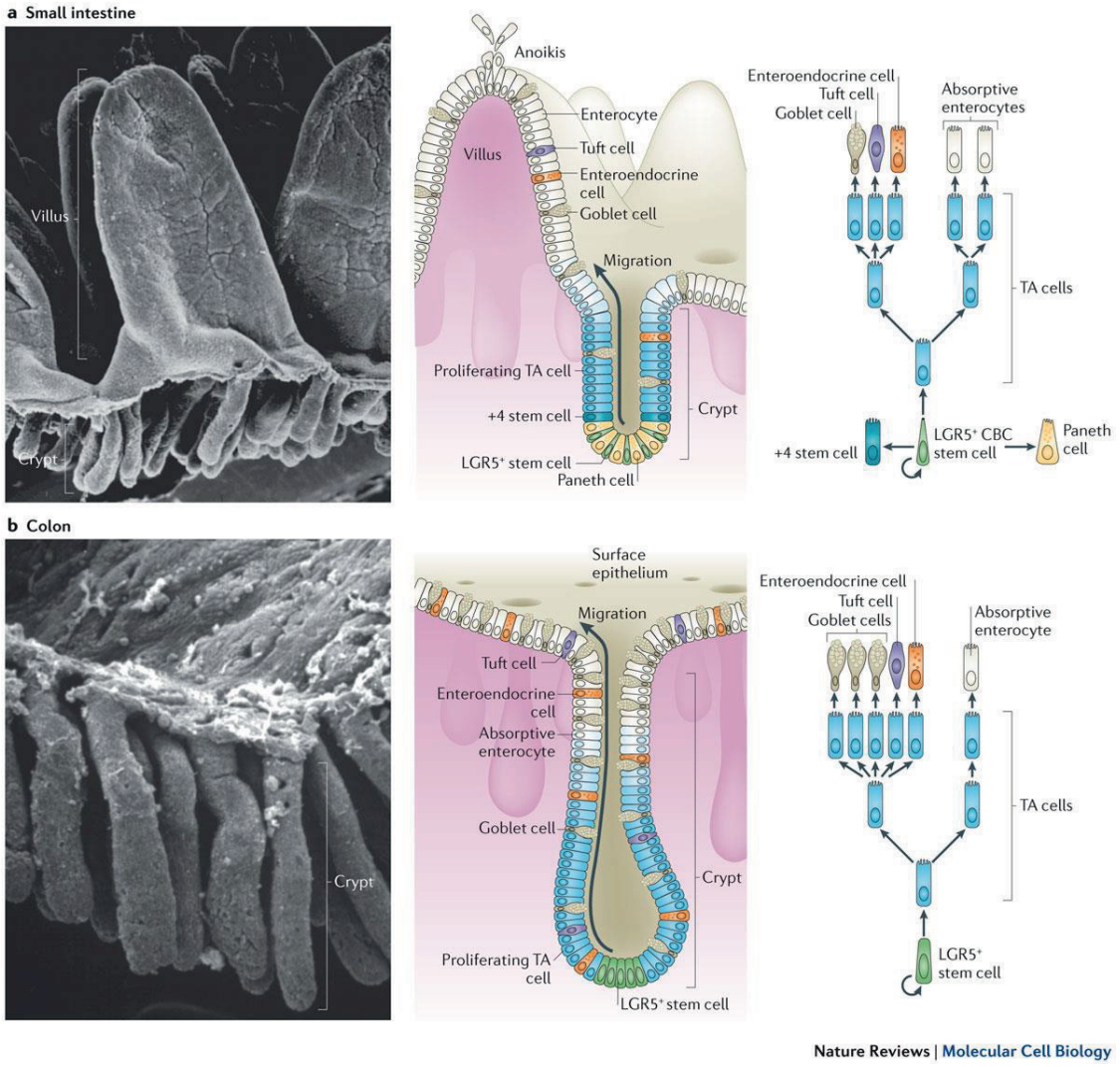


Figure 1.1: Structural organisation of the intestinal epithelium. (A) In the small intestine (scanning electron micrograph shown in the left panel), Lgr5$^+$ stem cells are intercalated with Paneth cells at the bottom of the intestinal crypt and can be restored by +4 stem cells in case of necessity (middle panel). Lgr5$^+$ cells generate transit-amplifying (TA) cells, that rapidly proliferate and differentiate into various kinds of mature cells (enterocytes, tuft cells, goblet cells and enteroendocrine cells) along the villi. They thereby constantly replace epithelial cells, which reached the tip of the villi and died by anoikis. The epithelial turnover occurs every 3-5 days. The differentiation hierarchy of stem cells and differentiated IECs is shown in the right panel. (B) In the colon (scanning electron micrograph shown in the left panel), Lgr5$^+$ stem cells are located at the base of the crypt and generate TA cells that rapidly proliferate (middle panel). TA cells differentiate into different mature IEC subsets (goblet cells, enterocytes, enteroendocrine cells and tuft cells), as shown in the differentiation hierarchy tree on the right panel. Epithelial turnover happens every 5–7 days. Figure taken from [110]. Reprinted by permission from Copyright Clearance Center: Springer Nature; Nature Reviews Molecular Cell Biology; Adult intestinal stem cells: critical drivers of epithelial homeostasis and regeneration; Barker, Nick (2013).

1.5 *Ex vivo* analysis of IEC functions: organoids

The experimental mouse models of colitis discussed in section 1.3 recapitulate multiple features of the complex immunopathologies of IBD. However, they lack the convenience of targeted and precise manipulation of cell line work. Cell lines on the other hand often originate from carcinoma cells and its therefore unlikely that their behaviour reflects that of healthy cells. IECs have a rapid turnover rate. Within 3-5 days, they differentiate from ISC to mature IECs, which undergo cell death through anoikis once they reach the villus tip and lose cell-cell contact [110]. Uncontrolled loss of cell-cell contact of IECs has detrimental effects to intestinal homeostasis, allowing translocation of luminal antigen into the mucosa. Therefore, IECs losing cell-cell contact die and are pushed out of the epithelium to maintain an intact epithelial barrier. This key feature of IEC biology has hindered the *ex vivo* study of isolated, primary, single IECs as they can not be kept in long-term cell cultures.

In 2009, Sato et al. [111] developed a 3D culture system, which allowed the long term propagation and differentiation of $Lgr5^+$ ISC *ex vivo*. The minimal intestinal stem cell niche environment is replicated through the supplementation of the culture media with key ISC supporting factors and the provision of a 3D matrix. The stem cell niche is supported by the following essential factors: epidermal growth factor (EGF), R-spondin, the bone morphogenetic protein (BMP) signalling inhibitor Noggin and Wnt3A (see table 2.6 [92, 111]). Small intestinal organoid cultures do not need Wnt3A supplementation, as Paneth cells are part of the small intestinal crypt base and provide this signal to neighbouring ISCs. In contrast, colonic organoid cultures are devoid of Paneth cells. Mesenchymal cells produce Wnt pathway component *in vivo* and colonic organoid cultures therefore rely on Wnt3A supplementation for their self-renewal [92, 112]. The intestinal epithelial growth is supported by a growth matrix (laminin-rich matrigel).

Once embedded in the growth matrix, isolated intestinal crypts rapidly seal off their upper opening, forming symmetric spheres, called organoids. As the organoids grow, they rebuild the crypt-villus structure, containing ISC at the crypt base, which are flanked by their differentiated progeny [111]. These crypt-like structures protrude into the luminal cavity, which is successively filled with apoptotic cells as the organoids grows, resembling the *in vivo* intestinal epithelium [111]. As the organoid lumen fills with dead cells over time, organoids have to be regularly passaged to avoid bursting. They can be propagated for extended periods [92, 111, 113]. A schematic overview of an intestinal organoid culture is shown in Figure 1.2.

As organoids are 3D structures, the apical membrane of IECs faces the organoid lumen and is not accessible for stimulations. In contrast, the basolateral membrane faces outwards and can be exposed to a variety of stimuli. 3D organoids are therefore suitable for the investigation of interactions between IECs and other cell types. Recently, co-cultures have been successfully established with intraepithelial lymphocytes [114, 115], fibroblasts and enteric nerves [116]. In addition, polarised, collagen supported 2D IEC monolayers can be established, with the apical membrane exposed upwards. This allows the administration of pathogens or substances from the apical side [117].

Organoids can be grown from multiple adult human and mouse tissues [92, 111, 118], including small intestine [111], colon [92], stomach [119], pancreas [120] and liver [121, 122]. The establishment of large patient-derived organoid biobanks can support drug discovery and test the efficacy of specific drugs for individual patients [123–125].

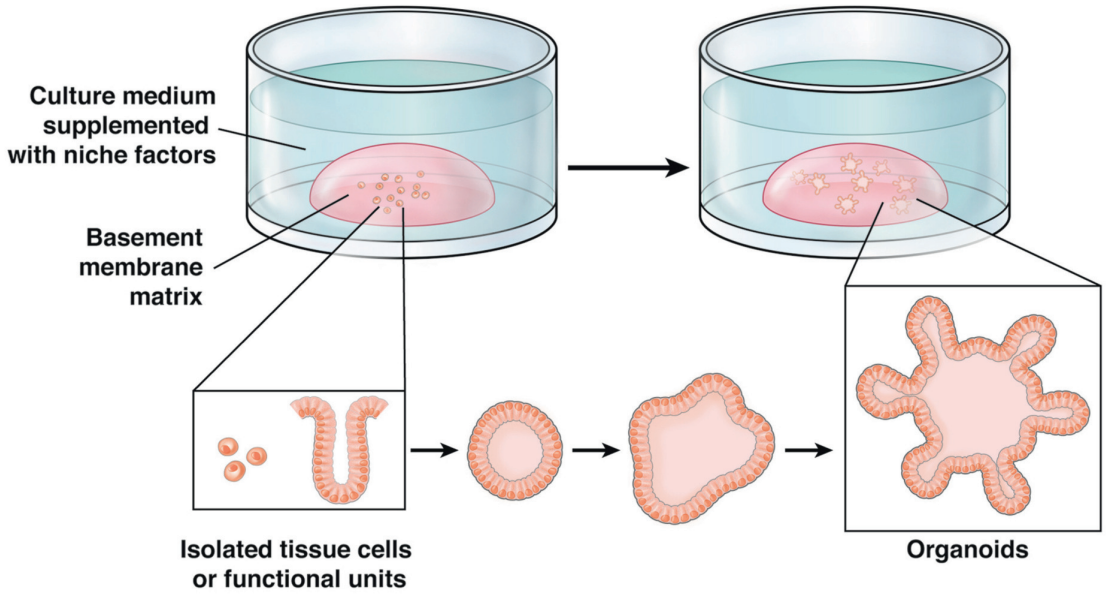


Figure 1.2: Schematic overview of intestinal organoid culture. A schematic summarising the establishment of an intestinal organoid culture. At the start, isolated intestinal stem cells or functional crypt units are embedded in extracellular matrix domes. The crypt units seal themselves off and the stem cell renewal is supported by media, supplemented with essential intestinal stem cell niche growth factors. Under this condition, they build 3-D structures. Small intestinal organoids build distinct crypt-villus domains, which are arranged around a central luminal cavity. The apical side of the intestinal epithelial cells faces towards the lumen, while the basolateral membrane is in contact with the extracellular matrix. Intestinal organoids build 3-D structures within one week before they have to be dissociated and re-seeded. Figure taken from [126]. Reprinted by permission from Copyright Clearance Center: Gastroenterology; Reviews in Basic and Clinical Gastroenterology and Hepatology; Modeling Human Digestive Diseases With CRISPR-Cas9–Modified Organoids; Fujii, Masayuki (2019).

1.6 MHC class II expression and localization in IECs

The following section is my own work and has been published [1].

Several decades ago, it was shown that IECs were able to express MHC class II molecules, thereby possessing an important prerequisite to function as non-conventional APCs [127–130]. Human siIECs constitutively express MHC class II molecules [128, 130–133], and it was noted that this was most evident at the tip of the villus. However, it was recently reported that murine ISC subsets at the base of the small intestinal crypts also express MHC class II under homeostatic

conditions [134]. In contrast, cIECs do not express MHC class II molecules under healthy, steady-state conditions. However, MHC class II is upregulated both in human and in murine small intestinal and colonic IECs under inflammatory conditions, including the immune-mediated disorders IBD, coeliac disease and graft-vs-host disease (GvHD), as well as during infections with *Salmonella enterica* or *Heligmosomoides polygyrus* [131, 134–138] (Table 1.1). Hershberg et al [139] demonstrated that in the presence of the pro-inflammatory cytokine IFNγ, human colonic IEC-like cell lines express MHC class II on their cell surface as well as Ii and HLA-DM. They also showed that, without additional activation, these human colonic IEC-like cell lines were able to process and present antigen from the apical surface of cIECs, but only when high concentrations of antigen were present [139]. Moreover, when the human colonic IEC-like cell line was transfected with class II transactivator (CIITA), mimicking pro-inflammatory conditions, the IECs were able to take up and process antigen from both the basolateral and apical membrane [140].

In terms of localization of MHC class II molecules in IECs, using a human colonic cell line transfected with a MHC class II construct, MHC class II was shown to be predominantly located at the basolateral membrane [140]. However, analyses of human and rat siIECs showed MHC class II molecules located at basolateral, lateral and apical membranes as well as in intracellular vesicular structures [133, 135, 145]. The uptake of antigen is mainly mediated by the endosomal pathway, where early endosomes progressively develop into the late endosomal structure MIIC. The latter can be divided into distinct compartments according to ultrastructural morphology, which includes multi-vesicular bodies (MVB) [146]. Several studies characterized the localization of MHC class II molecules within IECs in endoscopic biopsies of healthy controls and IBD patients [133, 147] as well as human small intestinal organoids [148]. In the healthy human gut, the late endosomal structure MVB harboured the majority of MHC class II molecules, but they were also observed at the basolateral cell membrane with faint expression at the apical membrane [133, 147]. The localization of MHC class II in late endosomal structures

	Small Intestine	Colon	Species
Homeostasis			
Steady state [128, 130–133, 137]	+	-	Human, Mouse
Germ free [137, 141]	-	N.d.	Human
MyD88-/- Trif-/- [137]	-	-	Human
Rag-/- IL-2rg-/- [137]	-	N.d.	Human
Inflammation/Infection			
Coeliac disease [131, 142–144]	++	N.d.	Human
Inflammatory bowel disease [135, 136, 138]	++	++	Human
Graft-versus-host disease [137]	++	N.d.	Mouse
Salmonella enterica [134]	++ (siISC)	N.d.	Mouse
Heligmosomoides polygyrus [134]	++ (siISC)	N.d.	Mouse

Table 1.1: MHC class II expression by intestinal epithelial cells: Various factors contribute to the expression of MHC II molecules by IECs under different conditions. During homeostasis, small intestinal IECs (siIECs) express MHC class II, whereas colonic IECs (cIECs) do not. Homeostatic MHC class II expression by siIECs was described to be dependent on the microbiota as well as Toll-like-receptor signalling via MyD88/TRIF and the presence of innate and adaptive lymphocytes. During inflammatory conditions, MHC class II expression was upregulated in IECs and intestinal infections led to an increase in MHC class II expression in small intestinal stem cells (siISCs).
+: MHC class II is expressed.
-: MHC class II is not expressed.
++: MHC class II expression is upregulated.
N.d.: not determined.

was also detected in human siIEC organoids [148]. Bär et al showed that in inflamed samples from Crohn's disease (CD) and ulcerative colitis (UC) patients, the expression of MHC class II molecules increased at the basolateral membrane, which was accompanied with a decrease of MHC class II molecules located in MVB [147]. These observations support the hypothesis that MHC class II molecules get transported from MVB to the basolateral membrane during inflammation and that this redistribution potentially allows IEC to present antigen to $CD4^+$ T cells in the lamina propria during such conditions.

1.7 The MHC class II processing and presentation pathway

The following paragraph is my own work and has been published [1].

The MHC class II antigen processing and presentation pathway is a highly regulated process which involves many accessory proteins. As the newly synthesized MHC class II molecules are located in the endoplasmic reticulum (ER), the premature binding of peptides in the ER needs to be prevented. Therefore, the MHC class II molecules assemble with the MHC class II invariant chain (Ii or CD74), part of which occupies the peptide-binding groove of the MHC class II molecule, thus preventing the binding of other peptides [149, 150]. The complex travels through the endosomal pathway where Ii gets progressively trimmed until MHC class II only contains the short class II-associated invariant-chain peptide (CLIP) [149, 151]. The cleavage of Ii to CLIP is thought to occur in the acidic MHC class II compartment (MIIC) late in the endosomal pathway. Within MIIC, binding of the MHC class II-like molecule HLA-DM to the MHC class II molecule: CLIP complex catalyses the release of CLIP from the peptide-binding groove and stabilizes the empty MHC class II molecule to allow the binding of antigenic peptides [152–154]. Endocytosed proteins from extracellular origin as well as self-proteins are initially proteolysed in endosomal and lysosomal antigen processing compartments, which generates peptide fragments. In addition to antigenic peptides from extracellular origin, MHC class II molecules can also cross-present cytosolic self-antigen and foreign antigen processed by autophagy. This naturally occurring process directs damaged organelles and cytosolic proteins into autophagosomes during stress or starvation. The cargo is subsequently transported via the endosomal pathway into lysosomes where they are degraded and the resultant peptides may encounter MHC class II molecules embedded in the membrane [155–157]. Thus, MHC class II molecules can present a highly diverse repertoire of peptides which originate from a range of cellular compartments of APCs [155, 158, 159]. After the MHC class II containing vesicle fuses with the antigenic peptide containing compartment,

the peptides can bind to MHC class II molecules on their way to the cell surface. The stable MHC class II:peptide surface complexes can be recognized by cognate antigen-specific $CD4^+$ T cells. A schematic overview of the MHC class II processing and presentation pathway is shown in Figure 1.3.

Phagocytosis or receptor-mediated endocytosis mediate the uptake of pathogens into the endocytic pathway. Their proteins are degraded into antigenic peptides and presented by MHC class II molecules to $CD4^+$ T cells (reviewed in [161]). Many pathogens developed strategies to circumvent immune recognition by producing proteins called immunoevasins. Some immunoevasins inhibit the surface expression of MHC class II molecules. The US2 protein by *Human cytomegalovirus* targets HLA-DR and HLA-DM molecules for degradation by proteasomes (reviewed in [161]). The BZLF2 protein by *Epstein-Barr virus* interacts with cell surface and intracellular MHC class II, thereby interfering with CD4 Tcell activation and possibly the presentation of antigenic peptides (reviewed in [161]). In addition, pathogens have been described to interfere with the endocytic pathway. For example, *Herpes simplex virus 1* glycoprotein B redirects MHC class II molecules to MVBs, thereby increasing the secretion of MHC class II molecules via exosomes and reducing cell surface expression (reviewed in [160]).

Defects in the expression of MHC class II molecules by the host can lead to severe immunodeficiency. As the thymus lacks MHC class II molecules, CD4 T cells can not be positively selected and only few develop. In addition, APCs lack MHC class II expression and can not activated the remaining few CD4 T cells in an antigen specific manner. However, MHC class I expression is normal and CD8 T cells develop normally [162]. This disease is known as bare lymphocyte syndrome, or MHC class II deficiency. It is caused by mutations in one of several genes encoding gene-regulatory proteins required for transcriptional activation of MHC class II promoters. These genes include *CIITA*, *RFXANK*, *RFX5* and *RFAP*

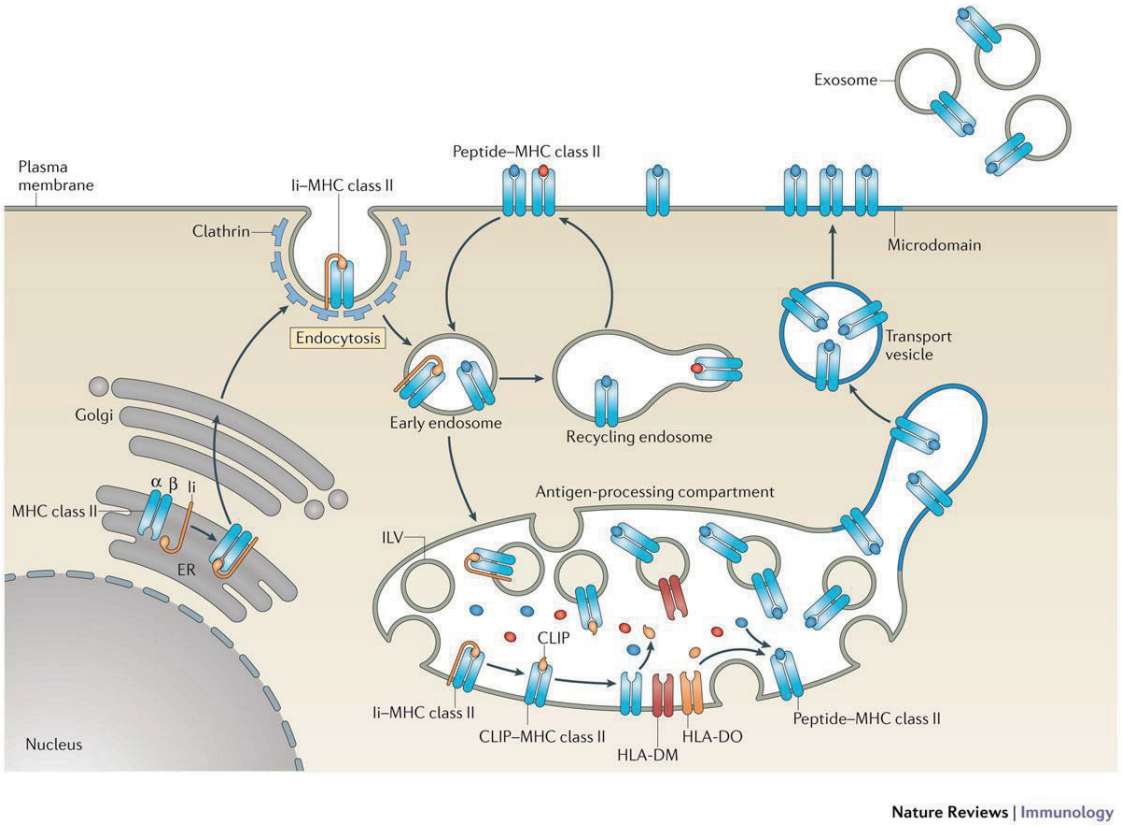


Figure 1.3: The MHC class II processing and presentation pathway. The newly synthesised MHC class II molecule associates with the invariant chain (Ii) in the endoplasmic reticulum (ER), to prevent binding of peptides located in the ER. The Ii-MHC class II complexes traffics through the Golgi apparatus, are delivered to the cell surface and internalised by clathrin-mediated endocytosis. The Ii-MHC class II complexes then traffic to multivesicular antigen-processing compartments, where some are located in intraluminal vesicles (ILVs) of multivesicular bodies (MVBs). The Ii molecules is cleaved by acid proteases until only a short peptide is still bound to the MHC class II molecule, termed class II-associated invariant chain peptide (CLIP). CLIP remains in the peptide-binding groove until it is removed by the enzyme HLA-DM, thereby allowing the binding of antigenic peptide. The activity of HLA-DM is regulated by HLA-DO. Peptide:MHC class II complexes located in ILVs fuse with the MVB membrane and are trafficked to the plasma membrane. If an entire MVB fuses with the plasma membrane, its ILVs are released in the form of exosomes. Peptide:MHC class II complexes located at the cell surface can be internalised and recycled. Figure taken from [160]. Reprinted by permission from Copyright Clearance Center: Springer Nature; Nature Reviews Immunology; The ins and outs of MHC class II-mediated antigen processing and presentation; Roche, Paul (2015).

(reviewed in [162, 163]). MHC class II deficiency illustrates the importance of CD4 T cells in adaptive immunity to most pathogens.

1.8 IECs show limited expression of co-stimulatory molecules

This following section is my own work and has been published [1].

After the binding of the TCR to the MHC class II:peptide complex, co-stimulatory molecules co-localize to the complex. Co-stimulatory signal transduction shapes the flavour of the T cell response. Depending on the ligand, it can either promote or inhibit T cell activation, differentiation and function. Co-stimulatory molecules include CD80, CD86, CD40 and inducible co-stimulatory ligand (ICOS-L). Conversely, programmed death ligand 1 (PD-L1) is a co-inhibitory molecule that transduces an inhibitory signal into T cells [164].

Conflicting results have been generated whether IECs are capable of delivering co-stimulatory or co-inhibitory signals. The co-stimulatory molecules CD80, CD86 and CD40 were reported to be expressed at the mRNA level in healthy human IECs [132, 165]. In contrast, another study reported a lack of CD80/CD86 mRNA expression in murine siIECs, even after IFNγ treatment [166]. Moreover, the detection of these molecules at the protein level appears to be driven by inflammation in the tissue. Similarly, while some studies reported an absence of CD80, CD86 and CD40 protein expression in healthy human IECs [132, 167] and CD80/CD86 protein expression in cIECs in UC patients [168], others reported CD86 protein expression by cIECs in UC patients [165] and CD40 protein expression was detected in inflamed colonic and ileal IECs of CD and UC patients, as well as in IEC-like cell lines after IFNγ stimulation [167]. In addition, CD80 protein levels were upregulated on siIECs during GvHD [137].

Although mRNA for both the co-stimulatory molecule ICOS-L and the co-inhibitory molecule PD-L1 were detected in healthy and inflamed cIECs of IBD patients, only low surface expression of ICOS-L and PD-L1 was detected in patient cIECs, with PD-L1 being more highly expressed by cIECs in CD than in UC patients [169].

Taken together, mRNA for different co-stimulatory and co-inhibitory molecules appears to be expressed by IECs both at steady-state and under inflammatory conditions. Although the detection of surface expression of co-stimulatory and co-inhibitory molecules was not consistent across the different studies, when detected these molecules were expressed at low levels and were mainly present in inflamed tissue. Therefore, there is no clear evidence that IECs can provide sufficient co-stimulatory signals to activate naïve $CD4^+$ T cells. However, as noted below, intestinal T cell populations mainly comprise activated effector and regulatory T cells that are less dependent on co-stimulatory signals for triggering of their effector functions [170]. Thus, it seems likely that IECs modulate Teff and Treg cell responses to maintain intestinal homeostasis.

1.9 Mucosal T cells

The gastrointestinal tract harbours the largest fraction of lymphoid cells in the human body. These cells are located in several compartments, including the gut-associated lymphoid tissue (GALT), intestinal lamina propria and epithelium. The lymphoid cells differ in their cell phenotype and function depending on the tissue sites and comprise unconventional and classical T cell subsets. In healthy individuals, T cells are a natural component of the cell types present at mucosal surfaces. The small intestine harbours the largest T cell numbers and they are located in the epithelium, lamina propria, Peyer's patches (PP) and isolated lymphoid follicles [171]. The large intestine accommodates slightly fewer T cells, residing in the

epithelium, lamina propria and isolated lymphoid follicles.

CD4 T cells predominate in the lamina propria and CD8 T cells in the gut epithelium. T cells residing in the epithelial layer are termed intraepithelial lymphocytes (IELs) and are distinct from lamina propria lymphocytes. Both small intestinal and colonic IELs are predominantly $CD3^+$ [172]. The small intestinal IELs mainly express CD8 and comprise equal TCR$\alpha\beta$ and TCR$\gamma\delta$ subsets [172]. In contrast, in the large intestine the majority of IELs were $CD4^-$ TCR$\alpha\beta^+$ [172]. In the small intestinal epithelium one IEL per 10 IECs can be found. In the large intestine this frequency is reduced to one IEL per 40 IECs [172]. The unique location of IELs allows them to recognise and eliminate infected IECs and support the repair of the epithelium after tissue damage.

Intestinal $CD4^+$ T cells plays an important role in orchestrating the adaptive immune response in the gastrointestinal tract. $CD4^+$ T cells comprise a diverse range of cell subsets, with unique phenotypes and functions. As the $CD4^+$ T cells reside in the mucosa of the intestine, they are continuously exposed to environmental and microbial factors and have the unique challenge to quickly adapt their immune responses to the diverse challenges encountered, protecting the host from foreign antigens while remaining tolerant to commensal- and food-antigens. For a fast and effective response, $CD4^+$ T cells rely on the continuous communication with antigen-presenting dendritic cells, often helped by IECs. For an effective division of labour, $CD4^+$ T cells differentiate into different effector and regulatory subsets, which can exert pro-inflammatory and regulatory functions. It is of crucial importance that the balance of pro- and anti-inflammatory CD4 T cell responses is maintained, as the impairment of either inflammatory or regulatory pathways can result in the development of inflammatory disorders, such as IBD. Patients suffering from IBD experience a heavy infiltration of $CD4^+$ T cells into the gut mucosa (reviewed in [173]).

1.9.1 Th1 cells

$CD4^+$ T cells differentiate into Th1 cells in response to intracellular pathogens (including parasites, viruses, and intracellular bacteria). The Th1 differentiation is initiated by dedritic cells and macrophages releasing type I interferons (IFNα and IFNβ) and IL-12. The latter activates the production of IFNγ, which acts in an autocrine manner, generating a positive feedback loop to facilitate more IL-12 production. Both IFNγ and IL-12 are needed to induce Th1 differentiation [174]. IFNγ signalling to naïve $CD4^+$ T cells stimulates the JAK1/2-STAT1 signalling pathway, which activates the transcription factor (TF) signal-transducing activators of transcription (STAT) 1, which induces the expression of the TF T-bet. T-bet itself induces the expression of IFNγ and IL-12R. IL-12 can now bind to IL-12R on the cell surface of Th1 cells and promotes the production of effector cytokines [174–176]. Differentiating Th1 cells secrete IFNγ, which act on surrounding naïve $CD4^+$ T cells and thereby supporting the differentiation of more Th1 cells. IL-27, a member of the IL-12 cytokine family, can also induce T-bet expression, mediated through JAK1/2-STAT1 signalling [177, 178].

Th1 cells have been implicated in intestinal inflammation. The majority of $CD4^+$ T cell clones located in the colonic mucosa of CD patients produce high levels of IFNγ, but not IL-4, when compared to patients with non-inflammatory gut disorders [17]. These findings are supported by data generated with experimental mouse models. The adoptive transfer of naïve $CD4^+$ $CD45RB^{hi}$ T cells into SCID hosts resulted in a strong Th1 polarised cytokine response and the treatment with anti-IFNγ antibodies successfully prevented the development of intestinal inflammation [179]. In addition, the TF T-bet was described to be essential and sufficient to drive Th1 mediated colitis [180]. These findings stand in contrast to a study by Krausgruber et al [181]. They showed that T-bet expression by CD4 T cells was dispensable for their pathogenicity in a adoptive T cell transfer model. Instead, T-bet was critical in mediating IL-23-driven colitogenic $CD4^+$ T cell responses [181].

1.9.2 Th2 cells

$CD4^+$ T cells differentiate into Th2 cells in response to extracellular parasites or allergens, which promote the production of IL-4 from innate immune cells, such as basophils or mast cells [182, 183]. IL-4 activates STAT6 signalling [184–187], which in turn induces the lineage specific TF GATA3 [188, 189]. GATA3 activates the expression of multiple effector cytokines, associated with a Th2 response, including IL-4, IL-5, and IL-13 [190]. In addition, it can positively regulate its own expression by binding to its regulatory elements. GATA3 is essential for Th2 differentiation [191] and was described to downregulate STAT4, thereby suppressing Th1 differentiation [192]. Th2 cells also produce IL-25, which, together with IL-4, supports B cell class switching to produce immunoglobulin (Ig) E antibodies, to fight parasitic infection, and promote the recruitment of basophils, eosinophils and mast cells [193]. Basophils and eosinophils haven been reported to respond the chitin, a fungal and helminth parasite polysaccharide. Chitin challenge of mice lead to the recruitment of basophils and eosinophils into the tissue [194]. Helminth expulsion is mediated through increased Th2 IL-4 and IL-13 production [195]. In addition, Th2 cytokines can promote allergic responses, by promoting the secretion of IgE. IgE complexes binds to the high affinity IgE receptors expressed by basophils and mast cells, initiating the secretion of cytokines and inflammatory mediators, such as histamine, heparin and serotonin (reviewed in [196]).

When Mosmann et al. [16] described the Th1/Th2 paradigm in 1986, Th2 responses were considered to counterbalance the inflammatory consequences of Th1 mediated immunity. Today it is well understood, that the lineage decision between Th1 and Th2 cells is complex, with cross-regulation between the two subsets (reviewed in [197, 198]). GATA3 represses the IL-12-STAT4-IFNγ pathway of Th1 differentiation through several mechanisms, while T-bet directly inhibits GATA3 [192, 199, 200]. T-bet deficient mice developed multiple physiological and inflammatory features characteristic of asthma [201]. Both UC and CD patient material was analysed to investigate this Th1/Th2 paradigm, however it remained

controversial whether these IBD subtypes are characterised by unique $CD4^+$ T cell differentiation profiles [17, 19, 202–204]. Li et al. [205] isolated $CD4^+$ T cells from the lamina propria of UC and CD intestinal biopsies to analyse T cell phenotype and function. CD biopsies were characterised by a higher prevalence of IFNγ or T-bet expressing Th1 skewed cells and decreased IL-13^+ or $GATA3^+$ $CD4^+$ T cells compared to UC. However, the Th2 signature in UC patients is supported by few studies and a genetic host susceptibility still needs to be determined by GWAS.

1.9.3 Th17 cells

$CD4^+$ T cells differentiate into Th17 cells in response to extracellular microbes and fungi and are largely located at barrier sites, such as the skin, lung or intestine. IL-6 and transforming growth factor (TGF) β induce Th17 differentiation, in the absence of IL-4 and IL-12, through the recruitment of STAT3 and retinoic acid receptor-related orphan nuclear receptor (ROR) γt (reviewed in [173]). RORγt expression is necessary for Th17 differentiation, though not sufficient, and Th17 differentiation is dependent on the cooperation with multiple other transcription factors, including STAT3 [206–210]. Mice deficient in TF STAT3 and RORγt, show reduced Th17 cell numbers, indicating the important role of these transcription factors in maintaining the Th17 phenotype. Th17 cells were characterized by the production of IL-17A, IL-17F, and IL-22 as signature cytokines, which promote the development and recruitment of neutrophils and enhanced epithelial barrier function [211–214]. Th17 cells were also potent producers of IL-21, which can act as an autocrine growth factor, although its production is not unique to this Th cell type [215–217].

Th17 express the IL-23R and IL-23 was originally thought to be essential for Th17 cell differentiation. However, subsequent studies have shown that IL-23 is dispensable for Th17 cell differentiation, but critical for cell survival and the reinforcement of pathogenic effector potential [218–220]. Depending on the surrounding cytokine milieu, Th17 cells can either produce IFNγ or IL-10, with IL-1β

or IL-2 driving these pro- or anti-inflammatory responses [221]. Th17 differentiation also experiences cross-regulation, it is induced by TGF-β and IL-6 signalling but can be inhibited by IFNγ or IL-4 which instead convert towards Th1 or Th2 differentiation, respectively. In addition, TGF-β is necessary for Th17 and Treg differentiation, with the presence or absence of IL-6 either inducing Th17 or Treg differentiation, respectively (reviewed in [222]). TGF-β also drives the expression of the TF forkhead box P3 (FoxP3) [61, 223]. This dichotomy in the generation of Th17 and Treg cells plays an important role in balancing intestinal homeostasis.

Th17 cells have been implicated in the pathogenesis of IBD. Increased levels of IL-17 and IL-23 were detected in colon biopsies of IBD patients [21, 224]. Single nucleotide polymorphisms in the *IL-23R* gene were associated with the susceptibility to IBD [42]. In addition, GWAS studies identified strong links between IBD and multiple Th17 pathways, with risk alleles in Th17 associated genes, such as *CARD9*, *IL12B*, *STAT3*, *RORC*, *IL23R*, and *CCR6* [225, 226]. These findings are supported by experimental mouse models. Mice lacking the IL-23p19 subunit, unique to the IL-23 cytokine, show reduced intestinal inflammation [26, 227, 228]. In addition, adoptive transfer of RoRγt- deficient T cells into RAG knock out mice, failed to produce Th17 cytokines and did not induce colitis [229].

1.9.4 Treg cells

Treg cells are critical in maintaining immune tolerance and inhibit uncontrolled innate and adaptive immune responses to both self and foreign antigens. Studies performed in the early 1970s indicated the presence of a suppressive T cell subset developing in the thymus, as thymectomised mice developed tissue damage in multiple organs, including the ovaries, thyroid and testes [230–232]. These studies established the existence of both potentially pathogenic self reactive T cells and regulatory T cells, which are required for the prevention of autoimmunity [232]. These findings were supported by later studies, in which adoptively transferred naïve CD45RB^{hi} CD4^{+} T cells induced severe inflammation in multiple organs in

athymic rats, which was ameliorated by co-transfer of CD45RB^{lo} CD4^{+} T cells [233]. Nowadays, Treg cells are characterised by the expression of the high-affinity IL-2Rα chain, CD25 [234] and the transcription factor FoxP3 [235], and are important for maintaining immune homeostasis and preventing autoimmune and inflammatory diseases, including IBD (reviewed in [236]).

The master transcriptional regulator, FoxP3 is essential for Treg development and function. The *FoxP3* gene was identified as the defective gene in Scurfy mice. Scurfy is an X-linked recessive disorder, which is lethal in male mice within their first month of life as a result of a systemic autoimmune disease characterised by hyper-proliferative CD4^{+} T cells and increased production of pro-inflammatory cytokines [237]. These symptoms paralleled the clinical manifestations observed in the human disorder IPEX (immune dysregulation, polyendocrinopathy, enteropathy, X-linked syndrome), where patients were shown to carry loss of function mutations in the *FoxP3* gene [238, 239].

IL-2 is another critical molecule for Treg function. Mice lacking IL-2, the α-chain of the IL-2 receptor (IL-2Rα) or the β-chain of the IL-2 receptor (IL-2Rβ) spontaneously develop hyperproliferation and -activation of peripheral T cells with autoimmune components (such as hemolytic anemia and multi-organ autoimmune disease) and hyperreactivity to commensal microbes. These mice showed a greatly reduced number of CD4^{+} CD25^{+} T cells (reviewed in [240]). In addition, mice lacking CD25 (IL-2Rα chain) develop lethal disease, with similar symptoms as IL-2 deficient mice. CD25 deficient patients develop symptoms, which are indistinguishable from IPEX, and show defective IL-10 expression by CD4 T cells [241]. These findings indicate, that IL-2 plays an important role in controlling peripheral T cell tolerance.

Several mechanisms of Treg mediated suppression have been described. Treg cells produce immunosuppressive cytokines, such as IL-10 and TGFβ. These

cytokines were shown to contribute to the suppression of intestinal inflammation in Treg depleted mice [242]. Treg cells expressing both IL-10 and Foxp3 were found in the large intestinal lamina propria but not in the spleen [243, 244]. In addition, Treg cells were described to mediate cell contact dependent suppression and functional modification or killing of APCs. Cell-contact dependent inhibition of effector immune responses can be achieved by increased expression of inhibitory molecules on the cell surface. Several surface markers enriched on Foxp3$^+$ Treg, including CTLA-4, GITR, OX-40, ICOS and PD-1, have been shown to promote their regulatory function and survival. Interaction with these surface molecules can directly modulate the effector cell or alternatively downmodulate APC functions, thereby inhibiting effector cell activation (reviewed in [245]).

CTLA-4 expressing Tregs can bind to CD80 and/or CD86 expressed by activated CD4 T cells with a higher affinity than CD28, thereby inhibiting the binding of CD80/CD86 to CD28 (reviewed in [246]). CTLA-4 expressing Tregs were also described to interact with CD80/CD86 expressed by DCs, thereby activating indoleamine 2,3-dioxygenase (IDO). IDO metabolises the essential amino acid tryptophan, which reduces the amounts of free tryptophan and was associated with decreased activation of T cells (reviewed in [245]). Therefore, CTLA-4-CD80/86 interaction can have both cell autonomous and indirect inhibitory effects on T cell activation. The co-inhibitory molecule PD-1 expressed by activated CD4 T cells binds to PD-L1 and PD-L2, expressed by hematopoietic and non-hematopoietic cells. PD-1 signalling recruits the phosphatase SHP2, which mainly dephosphorylates the signalling cascade downstream of CD28. PD-1 is therefore considered a repressor of the PI3K-AKT pathway important in TCR signalling and suppresses IL-2 production (reviewed in [247, 248]).

FoxP3$^+$ CD4$^+$ T cells are present in all organs in the body, and constitute around 10 % of the total CD4$^+$ T cells. In contrast, in the intestinal lamina propria they make up around 30 % in the colonic lamina propria and around 20 % in

the small intestinal lamina propria (reviewed in [249]). Several murine studies show the development of intestinal inflammation upon disruption of regulatory T cell pathways, particularly in response to intestinal microbiota (reviewed in [250]). Indeed, it was shown that Treg cell numbers in the colonic lamina propria were decreased in germ-free and antibiotic-treated mice compared to wild type mice, highlighting the importance of intestinal microbiota in the accumulation and function of colonic Treg cells [251–254]. In contrast, Treg cell numbers in the small intestinal lamina propria were unchanged or increased in germ-free mice compared to specific pathogen-free (SPF) mice [251, 252]. Kim and colleagues [255] showed, that germ-free mice fed an elemental diet devoid of dietary antigens had severely reduced Treg cell numbers in the small intestinal lamina propria, suggesting that majority of small intestinal Treg cells are induced by dietary antigens. These studies highlight, that intestinal Treg cells express a unique set of TCRs specific for intestinal antigens, to maintain tolerance to both food antigens and commensal microbiota.

Treg cell development

In vivo data suggest, that Treg cells comprise two developmentally different subsets: thymus-derived, also known as natural, Tregs (tTregs or nTreg) and peripherally derived Tregs (pTregs). The thymus is the primary site of T cell development. $CD4^+$ $CD25^+$ tTregs differentiate from double-negative $CD4^-$ $CD8^-$ thymocytes, undergoing TCR rearrangement to generate $CD4^+$ $CD8^+$ T cells. These double positive thymocytes undergo positive selection in the thymus cortex. They interact with self peptide presented by $MHCII^+$ cortical epithelial cells. If they show a high enough affinity, they receive survival signals and migrate into the thymus medulla to undergo negative selection. Here, self antigen is presented on MHC class II molecules expressed by APCs, in the presence of co-stimulatory molecules, and if the interaction with the antigen is too strong, the double-positive thymocytes undergo apoptosis. Precursors that show high affinity to self-peptide subsequently

develop into $CD4^+$ single-positive thymocytes, giving rise to $CD4^+$ $CD25^+$ Treg cells. After exiting the thymus, a fraction of these tTregs home to the gastrointestinal tract, where they promote tolerance to dietary antigens and intestinal microbiota (reviewed in [256]). It seems plausible that the tTreg functions are further shaped by the intestinal environment at these tissue sites.

PTregs are differentiated de novo from naïve $CD4^+$ T cells at peripheral sites upon TCR engagement, in the presence of IL-2 and TGFβ [257, 258]. The gastrointestinal tract is the location of peripheral Treg cell induction. Naïve $CD4^+$ $FoxP3^-$ T cells exit the thymus and migrate to the gut, where they encounter microbiota and dietary antigens, inducing the conversion to Treg cells. The microbiota can provide bacterial antigens and a TGFβ-rich environment, which supports the expansions and differentiation of peripheral Treg cells in the gut compared to secondary lymphoid organs [259]. TGFβ synergises with retinoic acid, a vitamin A metabolite produced by $CD103^+$ DCs, to supports peripheral Treg cell development in the intestine [260, 261].

Definitive markers to reliably differentiate tTregs and pTregs have not been identified, the TF Helios and the cell surface receptor Neuropilin-1 have been proposed to be preferentially expressed by tTregs [253, 262, 263], but these results remain controversial [264]. Thus, it remains challenging to determine the relative contributions of tTreg and pTreg cells to the Treg population in different tissues and inflammatory settings. Furthermore, mouse studies identified three unique, conserved non-coding sequences (CNS 1-3), intronic enhancers of the *FoxP3* gene locus, defining the size, composition and stability of the Treg cell pool [265, 266]. CNS3 and CNS1 were specifically relevant for thymic and peripherally-induced Treg cells, respectively [265]. Using $FoxP3^{\Delta CNS1}$-deficient mice, studies showed that mice exhibited deficiencies in pTreg cells in GALT and MLN compared to littermates. In addition, they developed pronounced Th2-type driven inflammation of the lung and gastrointestinal tract [265, 267]. These studies provided key evidence that pTreg

cells have a distinct, essential function in maintaining homeostasis at mucosal sites.

Finally, FoxP3$^+$ Treg cells can adapt to their surrounding microenvironment by co-expressing transcription factors RoRγt and GATA3, associated with Th17 and Th2 immune functions respectively. FoxP3$^+$ RoRγt$^+$ Treg cells were located in the normal intestine of both mice and humans [210, 268, 269], and it is not clear whether these double-expressors represent a Th17- or Treg-precursor cell or a fully differentiated FoxP3$^+$ Treg cells transitioning to Th17 cells in response to pro-inflammatory cytokines. Studies have shown that FoxP3$^+$ RORγt$^+$ Treg cells residing in the intestine are important in controlling intestinal Th1/Th2/Th17 effector responses [270, 271]. In addition, FoxP3$^+$ Treg cells can acquire Th2 effector features and were shown to express the TF GATA3. Deletion of Treg cell specific GATA3 results in a spontaneous inflammatory disorder in mice [272]. Treg cells were also shown to acquire Th1 effector functions when cultured in Th1 polarising cytokine conditions *in vitro* [273]. This plasticity might enable Treg cells to adapt to changing tissue environments.

1.9.5 Intestinal epithelial lymphocytes

IELs reside within the intestinal epithelium, where they are uniquely located at the interface of the host and the outside environment. They contribute to tissue homeostasis and protect the integrity of the epithelial barrier. IELs include several subsets, such as TCR$\gamma\delta^+$, CD8$\alpha\alpha^+$ and CD8$\alpha\beta^+$ T cells. IELs can be divided into two main subtypes. The natural IELs comprise TCR$\alpha\beta^+$ and TCR$\gamma\delta^+$ T cells, which can express CD8$\alpha\alpha$ but do not express CD4$^-$ or CD8$^-$. These natural IELs develop in the thymus, in the presence of self-antigen and subsequently acquire their activated phenotype. The small intestinal IELs include a large proportion of TCR$\gamma\delta^+$ cells expressing CD8, which can be up to 60 % [274, 275].

Induced IELs consist of CD4$^+$ and CD8$\alpha\beta^+$ TCR$\alpha\beta^+$ T cells, which often co-express CD8$\alpha\alpha$. They develop from naïve T cells, which are conventionally selected

in the thymus and acquire their activated phenotype and functional differentiation post-thymically in response to peripheral antigens (reviewed in [276]). These antigens are often presented by retinoic acid-synthesising αEβ7 integrin-positive DCs in the Peyer's patches. This interaction upregulates the expression of $\alpha 4\beta 7$ integrin by induced IELs, allowing them to migrate to the intestinal epithelium after trafficking through thoracic duct lymph and blood [277]. IELs, especially in the small intestine, express CD8$\alpha\alpha$ homodimers, which are induced upon activation [278, 279]. CD8$\alpha\alpha$ binds to the thymus leukaemia antigen (TLA), a non-classical MHC class I molecule expressed by small intestinal epithelial cells [280, 281]. TLA does not bind antigens [282] and is therefore not a classical antigen-presenting molecule. Instead, TLA functions to sequester and redirect CD8$\alpha\alpha$ away from the TCR, leading to negative signalling in IELs [283]. CD8$\alpha\alpha$ can be co-expressed with CD4 or CD8$\alpha\beta$ by TCR$\alpha\beta$ IELs, though a large proportion expressed CD8$\alpha\alpha$ alone. $CD4^+$ IELs represent a small fraction of the total IEL compartment, especially in the small intestine [284].

Induced IELs are modulated by non-self antigen encountered in the periphery. Early in life, the induced IEL fraction in the intestine is low but increases steadily with age in response to microbial antigen exposure [285–287]. The gradual accumulation of induced IELs at the intestinal barrier might reflect the maturation of the mucosal immune system in response to exogenous antigens encountered throughout life. In contrast, natural IELs develop in the thymus, and are the first type of antigen-experienced T cells residing in the intestine, even before birth [288]. The natural IEL population remains constant through life and therefore represents a smaller fraction of the IEL population at later stages in life, when induced IEL populations increase.

IEL effector functions can either be beneficial or pathogenic. IELs preserve the epithelium and restore tissue integrity after injury. The primary role of natural IELs might be the maintenance of epithelium integrity. Studies have shown that

natural TCR$\gamma\delta^+$ IELs have the ability to repair the epithelium [289, 290] and control the intestinal epithelial growth and turnover [291]. Induced IELs were also shown to exhibit protective functions. Antigen-specific, cytotoxic CD8$\alpha\beta^+$ IELs contribute to the elimination of multiple infectious agents, such as lymphocytic choriomeningitis virus (LCMV) [292], rotavirus [293] and Toxoplasma gondii [294]. CD4$^+$ induced IELs can upregulate the homodimer CD8$\alpha\alpha$ and adopt a cytotoxic yet regulatory phenotype. These CD4$^+$ CD8$\alpha\alpha^+$ IELs remain MHC class II restricted and might be able to detect antigen presented on MHC class II molecules presented on IECs. It was shown, that CD4$^+$ CD8$\alpha\alpha^+$ IELs can suppress Th1-induced intestinal inflammation in an IL-10-dependent manner, a process dependent on the NF-κB-GATA3-axis [295]. Therefore, IEL effector functions range from cytotoxic granule release to effector cytokine expression, such as IFNγ, IL-2, IL-4, IL-10 or IL-17 [292, 296, 297].

Multiple studies indicated a correlation between natural TCR$\gamma\delta^+$ IEL cell numbers in the intestinal mucosa and disease severity in IBD patients [298–300]. Mouse studies also showed that TCR$\gamma\delta^+$ IELs promote intestinal inflammation, suggesting a pro-inflammatory role for natural TCR$\gamma\delta^+$ IELs [301–303]. Induced CD8$\alpha\beta^+$ TCR$\alpha\beta^+$ IELs have been implicated to play a pro-inflammatory role in coeliac disease. They were shown to cause severe villous atrophy by interacting with MHC class I polypeptide-related sequence (MIC) antigens, expressed by IECs in patients with active disease, through the NK lineage receptor NKG2D [304, 305]. In addition, the cytokine IL-15, expressed by enterocytes, triggered cytotoxic responses by induced CD8$\alpha\beta^+$ IELS through the NKG2D signalling pathway[304]. In conclusion, IELs are at the interface between the innate and adaptive immune response and play an important part in recognising and eliminating infected IECs, as well as aiding repair of the mucosa after inflammatory damage.

1.10 Host T cell-microbial cross talk

Commensal bacteria serve many functions for the host, including digestion of food and out-competing pathogens for food and niche space. The microbiota educates the local and systemic immune response and promotes gut health. This favourable host-microbial cross talk was shown in germ-free mice, which exhibit multiple immunological defects (reviewed in [306]). Perturbation of the microbiota trough antibiotic treatment or bacterial strain reconstitution show the critical role of distinct bacteria in the maintenance of intestinal homeostasis [307–309]. Multiple T cell subsets are able to respond to microbial antigens, including $CD4^+$ and $CD8^+$ T cells or natural killer T cells. We will focus our discussion on the important role of bacteria in promoting the beneficial differentiation of $CD4^+$ T cells in the intestine.

The development of TCR transgenic (tg) mouse models enabled us to track microbiota-specific T cells and help us understand the diversity of $CD4^+$ T cell responses elicited through the recognition of distinct commensal antigens. TCR transgenic mice carry T cells that express a TCR of known antigen specificity and the usage of these mice allow us to understand microbe-T cell interactions and can show us that commensal-specific T cell phenotypes are highly contextual.

The microbiota shape the $CD4^+$ T cell compartment and colonisation of germ-free mice with minimal bacteria communities induced Treg cell development, and both Th1 and Th17 cell development in Treg cell defective TCR tg SMARTA mice. These findings highlight the balance between these opposing pro- and anti-inflammatory responses, which are dependent on the microenvironment [252]. Germ-free mice were shown to carry low Th17 cell numbers, which are normally enriched in the small intestine [310], and fewer Treg cells in the colon [251]. Treg cell numbers were unchanged in the small intestine of germ-free mice, suggesting dietary antigens induce Treg cell development at this tissue site [255].

The majority of Th17 responses in the intestine are thought to be induced by commensals. Ivanov et al [65] showed that the colonisation of the murine ileum with a single commensal microbe, *Segmented filamentous bacterium* (SFB), is sufficient to induce the expansion of Th17 cells, producing IL-17 and IL-22 in the lamina propria. Subsequent studies showed, that the attachment of SFB to IECs is the important signal for Th17 induction [311]. SFB has not been identified as a human commensal, but an equivalent bacterium, *Bifidobacterium adolescentis*, has been identified in the human microbiota, which closely associates with IECs and induces a Th17 response in the small intestine of monocolonised germ free mice [312].

Akkermansia muciniphila is a mucin-degrading commensal bacteria and present in the human microbiota. It has been associated with a favourable outcome in cancer patients undergoing immune checkpoint inhibitor treatment targeting the PD-1/PDL-1 axis [313]. The protective mechanism is likely to be mediated through an IFNγ producing Th1 anti-tumour response against *A. muciniphila* [313]. Adoptive transfer of *A. muciniphila*-specific naïve CD4 T cells into colonised gnotobiotic hosts induces IgG1 antibodies and antigen-specific T cell responses in mice. *A. muciniphila*-specific CD4 T cells showed a T follicular helper (Tfh) cell phenotype and were localised to the Peyer's patches and the MLNs, with very few cells found in the lamina propria of the small and large intestine [314]. In SPF mice the majority of transferred *A. muciniphila*-specific naïve CD4 T cells also adopt a Tfh phenotype, however greater numbers were detected in the lamina propria, with some adopting a Th1 or Th17 pro-inflammatory phenotype [314]. Thus, T cell responses towards *A. muciniphila* appear to be context dependent.

Treg cells in the intestine express a unique TCR repertoire that is mainly reactive to microbial antigens and play an important role in maintaining tolerance towards microbial and food antigens [315]. Of interest, if T cells expressing these commensal-reactive TCRs fail to differentiate into Tregs under pro-inflammatory conditions, they can differentiate into effector T cells instead and induce colitis [315].

This study showed that the differentiation of naïve T cells, with TCR specificity to foreign commensals, into the Treg-cell lineage may be critical in preventing the generation of colitogenic T effector cells. However, it did not address how commensal bacteria shape colonic Treg cell responses. A later study of the same group adoptively transferred naïve commensal-reactive tg T cells, expressing the previously identified colonic Treg TCRs, to study the kinetics of peripheral Treg development in normal hosts. Donor TCR tg T cells were located in MLN as soon as 2 days after transfer. Treg cell differentiation was dependent on Notch2-dependent DCs and independent of TGFβ [316]. However, both studies were based on the analysis of Treg cells expressing TCRs specific to multiple bacterial antigens.

Both the Hsieh and Littman groups investigated the pathobiont nature of *Helicobacter* spp. using TCR tg T cells and established that the T cell responses towards *Helicobacter* are highly context dependent. A distinct pool of Treg cells are induced during homeostatic conditions, while experimental colitis drives effector T cell responses in response to *H. hepaticus* colonisation [317, 318]. The Littman group generated a *Helicobacter*-specific TCR tg cell line by identifying TCR sequences from colitogenic IL-23R–GFP$^+$ T cells that were specific for a *H. hepaticus* unique protein, containing two immunodominant epitopes [318]. This TCR tg mouse model is therefore only reactive to a distinct peptide sequence found on *H. hepaticus* and allows the investigation of *H. hepaticus* specific CD4 T cell responses during homeostasis and intestinal inflammation. In conclusion, these studies highlight the ability of pathobionts to induce the differentiation of colonic Tregs, which maintain tolerance towards non-self antigens. The use of antigen-specific tg mouse models allow us to investigate how the differentiation of bacterial-specific T cells is influenced by the tissue microenvironment, with tolerogenic responses favoured during homeostasis, while pro-inflammatory responses predominated during inflammation. They further provide a tool to investigate the role of IEC MHC class II expression in shaping these antigen-specific CD4 T cell responses to maintain homeostasis.

1.11 Aims of the thesis

IECs have many immunological functions and there has been increasing interest in their ability to express MHC class II molecules, which can directly interact with CD4 T cells. The expression of IEC MHC class II appears to be influenced by distinct environmental signals. Small intestinal IECs constitutively express MHC class II and upregulate its expression during inflammatory conditions. In contrast, colonic IECs do not express MHC class II at homeostasis but upregulate its expression during intestinal inflammation. As IECs are uniquely located at the interface between host and microbiota, it seems plausible that IECs take up luminal antigens, derived from food or microbiota, and present them on MHC class II molecules to CD4 T cells residing in the intestinal mucosa. Previous studies have reported that microbe-specific CD4 T cells can adapt pathogenic or homeostatic responses depending on the environmental context. However, it is currently unclear whether MHC class II expression by IECs shapes these different CD4 T cell phenotypes and functions in the intestine.

We therefore aim to understand whether IECs can function as non-conventional antigen presenting cells and whether the location of MHC class II expressing IECs along the length of the gastrointestinal tract influences their ability to modulate CD4 T cell phenotypes and functions, potentially reflecting the changing microenvironment of the tissue.

The specific aims of this thesis are:

1. To determine whether IECs possess key features to function as non-conventional antigen presenting cells.

2. To investigate the involvement of IEC MHC class II expression in the protection against colonic pathogens or chemically induced colitis.

3. To determine the role of MHC class II expression by small intestinal IECs during homeostasis.

4. To analyse the role of IEC MHC class II expression in modulating microbe-reactive CD4 T cell phenotypes and functions.

2
Materials and Methods

2.1 Mice

H2-Ab1$^{fl/fl}$ mice were bought from JAX laboratory (B6.129X1-H2-Ab1tm1Koni/J) [319]. H2-Ab1$^{fl/fl}$ mice were crossed to B6.Cg-tg(VIL-1-cre)997Gum/J mice [320] bought from JAX laboratory to generate H2-Ab1^{VC} and H2-Ab1$^{fl/fl}$ mice. HH7-2tg TCR transgenic mice were provided by Dan R. Littman (New York). HH7-2tg mice were crossed in-house to B6.Foxp3^{hCD2}IL-10^{GFP} mice [321, 322] to generate HH7-2tgIL10GFP mice. The strains were maintained in accredited animal facilities at the University of Oxford, UK. Mice were bred under specific pathogen-free (SPF) conditions and routinely screened for pathogens and *Helicobacter* species. All experiments were performed in accordance with the UK Scientific Procedures Act of 1986 and under a Project License (PPL) authorised by the UK Home Office Animal Procedures Committee and approved by the Sir William Dunn School of Pathology Local Ethical Review Committee.

Mice were bred hemizygous for the Cre allele, resulting in H2-Ab1$^{fl/fl}$ Cre-negative and H2-Ab1$^{fl/fl}$ Cre-positive littermates. Age- and sex-matched littermates were used and co-housed throughout the experiment. Mice were analysed at 6-12 weeks for the large intestinal work and at 12-15 weeks for the small intestinal work.

2.2 Genotyping

Ear tissue samples were digested overnight at 56 °C in lysis buffer (5 mM EDTA, 100 mM Tris-HCl, 0.2 % SDS, 200 mM NaCl and 0.2 mg/ml proteinase K (Bioline)). DNA was precipitated from the digested supernatants with isopropanol. After washing with 70 % ethanol, the dried DNA pellet was resuspended in 200 µl of MilliQ water. PCR reactions were carried out in a total volume of 15 µl using Taq polymerase (0.07 U/µl, Invitrogen), PCR buffer (1x, Bioline), $MgCl_2$ solution (2 mM, Bioline), dNTP mix (0.2 mM, Sigma), primers (0.5 µM) and 1.5 µl of DNA samples.

Primer sequences are listed below:

Primer Cre1 F: AGGTTCGTTCACTCATGGA

Primer Cre2 R: TCGACCAGTTTAGTTACCC

Control Fabpi F: CCTCCGGAGAGCAGCGATTAAAAGTGTCAG

Control Fabpi R: TAGAGCTTTGCCACATCACAGGTCATTCAG

The Cre PCR was performed under the following conditions:

1. 94 °C, 4 min
2. 94 °C, 30 s
3. 60 °C, 30 s
4. 72 °C, 1 min
5. 30 cycles from step 2
6. 72 °C, 5 min
7. Hold at 4 °C

10 µl of the sample was run on a 1.5 % agarose gel. Band sizes are 250 bp for the Cre band and 480 bp for the internal control (Fabpi) band.

2.3 Bacterial culture

2.3.1 *Citrobacter rodentium*

The nalidixic acid resistant *Citrobacter rodentium* (*C. rodentium*) (ICC169, kind gift from Dr. Gad Frankel, Imperial College, London, UK) strain was used for this thesis. *C. rodentium* was grown on Luria-Bertani (LB) agar plates (supplemented with nalidixic acid, 50 µg/ml) overnight (ON) at 37 °C. A single colony was transferred to Luria-Bertani broth supplemented with nalidixic acid (50 µg/ml, BD-Biosciences) and grown ON at 37 °C shaking to stationary phase. The following day, the culture was diluted to an optical density (OD) of 0.1 at OD_{600} and grown to log phase, OD_{600} of around 1. Bacteria were harvested by centrifugation and resuspended in sterile PBS for *in vivo* use.

2.3.2 *Helicobacter hepaticus*

Helicobacter hepaticus (*H. hepaticus*) (NCI-Frederick isolate 1A) [67] was cultured on blood agar plates supplemented with trimethoprim (5 µg/ml), vancomycin (10 µg/ml) and polymyxin B (2.5 IU/ml) (TVP, Oxoid) under microaerophilic conditions (10 % CO2, 10 % H2, 80 % N2) at 37 °C in CampyPak jars (Oxoid). After 2 d *H. hepaticus* was expanded as a liquid culture in tryptic soy broth containing both TVP and 10 % FCS in vented Erlenmeyer flasks under a microaerophilic atmosphere, shaking at 170 rpm at 37 °C to stationary phase. The liquid culture was split daily and inoculated at OD_{600} 0.1. The culture was grown to log phase, OD_{600} of around 1, before bacteria was harvested by centrifugation. The bacteria were resuspended in sterile PBS for *in vivo* infection.

2.4 *In vivo* models

2.4.1 *H. hepaticus* models

H. hepaticus model

H. hepaticus was cultured as described in section 2.3.2. *H. hepaticus* infection was induced by infecting mice intragastrically (i.g.) with 10^8 colony forming

units (CFU) *H. hepaticus* on two or three consecutive days. Mice were sacrificed at the indicated time points.

H. hepaticus and anti-IL-10R model

H. hepaticus was cultured as described in section 2.3.2. Chronic colitis was induced by infecting mice intragastrically (i.g.) with 10^8 CFU *H. hepaticus* on two or three consecutive days and injecting intraperitoneally (i.p.) 1 mg of mAb anti-IL-10R (clone 1B1.2) weekly, for the durations indicated. For the resolution of chronic inflammation experiments mice were left untreated for three or four weeks (as indicated) after chronic inflammation was induced with *H. hepaticus* and anti-IL-10R as described before. Mice were sacrificed at the indicated time points.

Resolution of *H. hepaticus* and anti-IL-10R model

Chronic colitis was induced for four weeks as described in section 2.4.1. Mice were subsequently left untreated for three weeks to allow for the resolution of intestinal inflammation. Mice were sacrificed after a total of seven weeks.

2.4.2 *C. rodentium* model

C. rodentium was cultured as described in section 2.3.1. Mice were infected i.g. with 10^9 CFU *C. rodentium*. Mouse weight was monitored every day during the infection and mice were euthanized if weight loss exceeded 20 % of their initial body weight. Mice were sacrificed at the indicated time points.

2.4.3 Chronic DSS model

During each dextran sulfate sodium (DSS) cycle, mice received 1.5 % DSS in their drinking water for five days. Afterwards mice were administered normal drinking water for 14 days. This DSS cycle was repeated for a total of three times. The mouse weight was monitored every day during this period unless mice regained their initial weight from before the start of each cycle. Mice were euthanized if weight loss exceeded 20 % of their initial body weight.

2.5 Assessment of intestinal and systemic inflammation

2.5.1 Quantification of *C. rodentium* colonization

To measure tissue adherent *C. rodentium* levels of *C. rodentium* infected mice different tissues (spleen, liver, colon, caecum) and caecal contents were isolated. Tissues were weighed and homogenised in 600 µl of sterile PBS using glass beads in a FASTPREP-24 (MP) for 40 s at 6.5 m/s. Caecal contents were vortexed and centrifuged at 1000 g for 1 min. Both the lysate and the caecal content supernatants were serially diluted in PBS and the different dilutions plated on nalidixic acid (50 µg/ml) LB agar plates. The LB agar plates were incubated at 37 °C ON before CFUs were counted. The number of colonies were normalised to the weight of the tissue or caecal content to generate CFU/mg.

2.5.2 Histological assessment

To assess colonic disease, colonic tissue sections were isolated and rinsed in PBS/0.1 % BSA. The caecum was opened longitudinally, rinsed in PBS/0.1 % BSA and placed on a blotting paper. All tissues were fixed in buffered 10 % formalin for more than 24 h and then changed into 70 % ethanol. The tissue was paraffin wax embedded and 4 µm sections were stained with haematoxylin and eosin (H& E). Inflammation was scored semi-quantitatively by two researchers in a blinded fashion. The scoring system for *C. rodentium* induced colitis is outlined in table 2.1, for *H. hepaticus* + anti-IL-10R induced colitis in table 2.2 and for chronic DSS induced colitis in table 2.3.

The proximal, mid and distal colon scores were averaged to obtain the overall colon score ranging from 0 to 12 for *H. hepaticus*. The caecum was scored separately.

The mid and distal colon scores were averaged to obtain the overall colon score ranging from and 0 to 15 for *C. rodentium* induced colitis. The caecum was scored

separately.

The mid and distal colon scores were averaged to obtain the overall colon score ranging from and 0 to 52 for chronic DSS induced colitis [83].

A	Epithelial markers					
	Score	Hyperplasia	and/or	Goblet Cell Depletion	and/or	Damage
	0	None		None		None
	1	Mild (1.5x)		Mild (25 %)		Mild
	2	Moderate (2-3x)		Marked (25-50 %)		Marked
	3	Severe (>3x)		Substantial (>50 %)		Substantial
B	Inflammation in lamina propria					
	Score	Criteria				
	0	None - few leukocytes				
	1	Mild - some increase in leukocytes at tips of crypt OR many lymphoid follicles				
	2	Moderate - marked infiltrate (broadening of the crypt)				
	3	Severe - dense infiltrate throughout				
C	Submucosal markers					
	Score	Edema	and/or	Infiltration	and/or	Follicle
	0	None	and/or	None	and/or	None
	1	Mild	and/or	Mild	and/or	Enlarged
	2	Marked	or	Marked		-
	3	Marked	and	Marked		-
D	Area affected					
	Score	% of section				
	0	None				
	1	Up to 25 %				
	2	25-50 %				
	3	>50 %				
E	Markers of severe inflammation					
	Score	Bleeding	and/or	Crypt abscesses	and/or	Necrosis/ Ulceration
	0	None		None		None
	1	Some		Few		None
	2	Marked		Many		Few/Small
	3	-		-		Large/Many

Table 2.1: Histological scoring of *C. rodentium* induced colitis

A	Epithelial markers					
	Score	Hyperplasia	and/or	Goblet Cell Depletion	and/or	Damage
	0	None		None		None
	1	Mild (1.5x)		Mild (25 %)		Mild
	2	Moderate (2-3x)		Marked (25-50 %)		Marked
	3	Severe (>3x)		Substantial (>50 %)		Substantial

B	Inflammation in lamina propria	
	Score	Criteria
	0	None - few leukocytes
	1	Mild - some increase in leukocytes at tips of crypt OR many lymphoid follicles
	2	Moderate - marked infiltrate (broadening of the crypt)
	3	Severe - dense infiltrate throughout

C	Area affected	
	Score	% of section
	0	None
	1	Up to 25 %
	2	25-50 %
	3	>50 %

D	Markers of severe inflammation	
	Score	Criteria
	0	None
	1	Submucosal inflammation OR Few crypt abscesses (<5)
	2	Submucosal inflammation AND Few crypt abscesses (<5)
	2	Many crypt abscesses (<5) OR Extensive submucosal inflammation OR Crypt branching
	3	Many crypt abscesses (<5) AND Extensive submucosal inflammation / Crypt branching
	3	Ulceration OR Extensive fibrosis

Table 2.2: Histological scoring of *H. hepaticus* + anti-IL-10R induced colitis

A	Inflammation	
	Score	Criteria
	0	None
	1	Slight
	2	Moderate
	3	Severe
B	Extent	
	Score	Criteria
	0	None
	1	Mucosa
	2	Mucosa and Submucosa
	3	Transmural
C	Crypt damage	
	Score	Criteria
	0	None
	1	Basal 1/2 damaged
	2	Basal 2/3 damaged
	3	Only surface epithelium intact
	4	Entire crypt and epithelium lost
D	Hyperplasia	
	Score	Criteria
	0	No proliferation
	1	Hyperplasia
	2	Metaplasia without crypt depletion
	3	Metaplasia with crypt depletion
E	Area affected (x each item)	
	Multiply by	% of section
	1	0-25 %
	2	26-50 %
	3	51-75 %
	4	76-100 %

Table 2.3: Histological scoring of chronic DSS induced colitis

2.6 Cell isolation, enrichment and sorting

2.6.1 Isolation of spleen and lymph node cells

Cells were isolated from the organs by mashing the tissue through a 100 µM nylon mesh. All centrifugation steps were carried out at 1500 rpm for 5 min. Cells were washed in PBS/0.1 % BSA. Red blood cells were lysed with ACK lysis buffer (10 mM $KHCO_3$, 150 mM NH_4Cl, 0.1 mM Na_2.EDTA, pH 7.2-7.4) for 3 min at RT. Cells were washed with PBS/0.1 % BSA and filtered through a 70 µM cell strainer. Cells were resuspended in PBS/0.1 % BSA for further use.

2.6.2 Isolation of colonic lamina propria lymphocytes

The colon was cut open longitudinally and the luminal content was removed. The colon tissue was cut into smaller pieces of around 0.5 cm and placed in ice cold PBS/0.1 % BSA. The supernatant was removed and around 20 ml prewarmed (37 °C) RPMI 1640/5 % FCS supplemented with 5 mM ethylenediaminetetraacetic acid (EDTA) (Gibco, UK) was added. Tubes were subjected to orbital shaking for 20 min at 37 °C and 180 rpm. This washing step was performed for a total of 2 times and if intestinal epithelial cells (IECs) or intestinal epithelial lymphocytes (IELs) were analysed those washes were used for further processing described in 2.6.4 and 2.6.3. Next, the EDTA activity was neutralised by adding around 20 ml of RPMI 1640/5 % FCS containing 15 mM HEPES (4-(2-hydroxyethyl)-1-piperazineethanesulfonic acid) to the tissue pieces and shaking it for 15 min at 37 °C and 180 rpm. The tissue pieces were then digested in 10 ml pre-warmed RPMI 1640/5 % FCS containing 0.4 mg/ml type VIII collagenase (Sigma Aldrich, UK) and 40 µg/ml DNase I (Roche, UK) for 45 - 60 min at 37 °C, 180 rpm. Supernatants were filtered through a 70 µM nylon mesh and the collagenase activity neutralised by adding EDTA at 5 mM. After centrifugation the cells were resuspended in 3 ml P30 solution (30 % Percoll (GE, Amersham, UK) in PBS). 3 ml P75 (75 % Percoll in PBS) were overlayed with 4 ml P40 (40 % Percoll in RPMI 1640) and then with 3 ml P30 containing the cells to create a three-layered discontinuous gradient. Or 3 ml P75 were overlayed

with 3 ml P37.5 (37.5 % Percoll in RPMI 1640) containing the cells to create a two-layered discontinuous gradient. Gradients were centrifuged for 20 min at 1800 rpm with minimal acceleration and no brake at RT. Leukocytes were isolated from the P40/P75 or P37.5/P75 interface. Cells were washed with PBS/0.1 % BSA and resuspended in ice-cold PBS/0.1 % BSA.

2.6.3 Isolation of colonic intestinal epithelial lymphocytes

The EDTA washes from 2.6.2 were filtered through a 100 µM cell strainer and topped up to 50 ml with RPMI 1640/10 % FCS and 15 mM HEPES. Cells were centrifuged at 1500 rpm for 5 min at 4 °C. The cell pellet was resuspended in 3 ml P30 solution. To create a three-layered discontinuous gradient 3 ml P75 were overlayed with 4 ml P40 and then 3 ml P30 containing the cells. Gradients were centrifuged for 20 min at 1800 rpm with minimal acceleration and no brake at RT. Intestinal epithelial leukocytes (IELs) were isolated from the P40/P75 interface. After washing with PBS/0.1 % BSA, cells were resuspended in ice-cold PBS/0.1 % BSA.

2.6.4 Isolation of colonic intestinal epithelial cells

The EDTA washes from 2.6.2 were filtered through a 100 µM cell strainer and topped up with RPMI 1640/10 % FCS and 15 mM HEPES. Cells were centrifuged at 1500 rpm for 5 min at 4 °C. The supernatant was carefully removed and the cell pellet divided into two tubes. Cells were centrifuged at 3000 rpm for 10 min at 4 °C. For RNA samples the cell pellet was resuspended in RLT buffer supplemented with beta mercaptoethanol (βMe) and stored at −20 °C until further use. For flow cytometry analysis the cell pellet was trypsinised with TrypLE for around 5 min at RT. After adding RPMI 1640/10 % FCS and 15 mM HEPES cells were centrifuged again and cells used for staining.

2.6.5 Isolation of small intestinal lamina propria lymphocytes

The Peyer's patches were removed from the small intestine (SI) with scissors. The SI was cut open longitudinally and washed in PBS/0.1 % BSA. If the duodenum,

jejunum and ileum were analysed separately the SI was laid out in a Z-shape and was divided into 3 equal parts. These 3 parts were further cut into 3-4 cm pieces. The tissue was incubated in RPMI 1640/5 % BSA supplemented with 5 mM EDTA for 20 min while shaking at 37 °C. To remove IELs and IECs, the tissue was added to RPMI 1640 supplemented with 5 mM EDTA and shaken vigorously for 30 s. The supernatant was removed and the shaking process repeated for a total of 3 times while the tissue pieces start turning pink. The tissue pieces were cut finely with scissors and digested in 20 mL of digestion medium (RPMI 1640/5 % FCS, 0.4 mg/ml type VIII collagenase, 40 µg/ml DNase I) for around 25 min at 180 rpm and 37 °C. Cells were filtered through a 70 µM cell strainer and topped up with 20 ml of PBS/0.1 % BSA containing 5 mM EDTA. Undigested tissue pieces were mashed through the filter with a 3 ml syringe plunger using the rubber end. Cells were centrifuged at 1500 rpm for 5 min and resuspended in 4 ml P37.5. Cells were centrifuged at 1800 rpm for 5 min at 4 °C. The supernatant was aspirated and the cell pellet washed with PBS/0.1 % BSA before being resuspended in ice-cold PBS/0.1 % BSA.

2.6.6 Isolation of small intestinal intestinal epithelial cells and intestinal epithelial lymphocytes

The Peyer's patches were removed from the SI with scissors and the SI opened longitudinally. If duodenum, jejunum and ileum were analysed separately the SI was laid out in a Z-shape and cut into 3 equal parts. The 3 tissue pieces were cut into around 4 cm large pieces and washed 3 times with gut wash buffer (HBSS supplemented with 2 % FCS, 1:50 HEPES, 1:100 Gluta-Max, 1:100 NaPyruvate, 1:100 Pen/Strep). Afterwards the tissue was cut into around 5 mm pieces and incubated in 10 ml of gut wash buffer containing 2 mM DTT at 37 °C and 200 rpm for 10 min. After vigorously shaking the tube 15 times, the supernatant was filtered through a 100 µM nylon mesh and the tissue transferred into a new tube containing 10 ml of gut wash buffer supplemented with 5 mM EDTA. The tissue was incubated for 7 min at 37 °C at 200 rpm. After vigorously shaking the tube 15 times the supernatant was filtered through a 100 µM cell strainer and the supernatant kept

on ice. The tissue was used for a repeated EDTA wash and the tissue shaken 25 times after the incubation time. The supernatant was filtered as mentioned before and the two supernatant fractions combined. The cell solution was spun down at 1000 rpm for 5 min and the cell pellet washed with DMEM media. If SI LPLs were needed the tissue pieces were digested as described in section 2.6.5. The IEC and IEL containing cell pellet was digested with 10 ml of DMEM supplemented with 0.1 U/ml Dispase and 0.1 mg/ml DNAase I at 180 rpm and 37 °C for 8 min. The digestion was stopped with 2.5 % DMEM buffer. After centrifugation at 1000 rpm for 5 min, cells were washed once with 2.5 % DMEM buffer. The cells were resuspended in ice-cold PBS/0.1 % BSA.

2.7 Flow cytometry

2.7.1 Surface staining

Cells were isolated as described in section 2.6. With the CasyCounter cell numbers were determined and approximately 5×10^6 cells were plated in a 96-well U- bottom plate. Cells were centrifuged at 1500 rpm for 5 min. Cell pellets were resuspended in 100 µl PBS/0.1 % BSA containing 1:200 FcR block and 1:1000 live dead stain and incubated for 20 min at 4 °C. After washing cells twice with PBS/0.1 % BSA, cell pellets were resuspended in 50 µl PBS/0.1 % BSA containing surface antibodies (see table 2.4) for 30 min at 4 °C in the dark. Cells were washed twice with PBS/0.1 % BSA and fixed in 200 µl of FoxP3 Fixation/Permeabilization buffer for 30 min at RT. Cells were washed in PBS/0.1 % BSA and either analysed or stained intracellular. Dead cells were excluded using the fixable viability dye eFluor-780.

Samples were acquired on the BD LSRFortessa and BD LSRII flow cytometers (Becton Dickinson) using FACSDiva software (BD Biosciences). Absolute cell numbers were calculated by adding CountBright beads (Life Technologies) to each sample before acquisition on the flow cytometer. The data was analysed using FlowJo10 (Tree Star, Inc).

2.7.2 Restimulation for cytokine production

Cells were restimulated in a 96-well U-bottom plate for 3 h at 37 °C 5 % CO_2 in 200 µl RPMI 1640/10 % FCS containing 100 U/ml penicillin/streptomycin, 2 mM L-glutamine and 0.05 mM 2-mercaptoethanol, supplemented with 0.1 µg ml^{-1} Phorbol 12-myristate 13-acetate (PMA), 1 µg ml^{-1} ionomycin and 10 µg ml^{-1} Brefeldin A. Cells were washed in RPMI 1640 and centrifuged at 1500 rpm for 5 min. Cells were stained as described below.

Or cells were restimulated for 3.5 h at 37 °C 5 % CO_2 in 200 µl RPMI 1640/10 % FCS containing penicillin/streptomycin, GlutaMax, 2-mercaptoethanol, sodium pyruvate and HEPESs supplemented with 0.1 µg/ml PMA, 1 µg/ml ionomycin and 1:1000 Golgiplug and Golgistop. Cells were washed in RPMI 1640, centrifuged at 1500 rpm for 5 min and stained as described below.

2.7.3 Intracellular cytokine staining

After surface staining was performed as described in section 2.7.1, cells were either stored ON in PBS/0.1 % BSA at 4 °C in the dark and processed the following day or immediately washed, fixed and permeabilised using the BD Cytofix/Cytoperm kit, according to the manufacturer's instructions. Cells were centrifuged at 1500 rpm for 5 min, resuspended in 50 µl staining buffer containing intracellular antibodies (see table 2.4) for 1 h at 4 °C in the dark. Cells were washed in staining buffer, subsequently in PBS/0.1 % BSA and resuspended in PBS/0.1 % BSA for flow cytometry analysis.

2.7.4 Intracellular transcription factor staining

After surface staining was performed as described in section 2.7.1, cells were either stored ON in PBS/0.1 % BSA at 4 °C in the dark and processed the following day or immediately washed with 1x FoxP3 permeabilization buffer (eBioscience) containing 2 % rat serum. Cells were centrifuged at 1500 rpm for 5 min, resuspended in 100 µl 1X FoxP3 permeabilization buffer containing 2 % rat serum and incubated

for 1 h. Afterwards cells were incubated in 50 µl 1X FoxP3 permeabilization buffer containing antibodies at the indicated dilutions (see table 2.4) for 45 min at 4 °C in the dark. Cells were washed in 1X FoxP3 permeabilization buffer, subsequently in PBS/0.1 % BSA and resuspended in PBS/0.1 % BSA for flow cytometry analysis.

2.7.5 Fluorescence activated cell sorting and adoptive transfer of HH7-2tg CD4 T cells

A spleen from a donor mouse was removed and the spleen mashed with a sterile syringe on a 70 µm cell strainer. The cells were resuspended in sterile PBS/EDTA/BSA and centrifuged at 1500 rpm for 5 min. The cell pellet was resuspended in 1 ml ACK lysis buffer and incubated for 3 min. Cells were washed in PBS/EDTA/BSA and centrifuged at 1500 rpm for 5 min. The staining of cells was performed in 100 µl staining buffer per 10 million cells. The staining buffer, containing all antibodies of interest (see table 2.5), was diluted in sterile PBS/EDTA/BSA and cells were stained for 30 min at 4 °C in a 50 ml canonical tube. Afterwards, 50 ml of sterile PBS/EDTA/BSA was added and the cells centrifuged at 1500 rpm for 5 min. Cells were counted and cell concentration adjusted to 20 000 000 cell/ml. Naïve HH7-2tg or HH7-2tgIL10GFP CD4 T cells were sorted as single, live, CD11c-/CD11b-/B220-, CD45+, CD4+, CD25-, $CD44^{lo}CD62L^{hi}$, TCRVb6+ on the Aria II (BD Bioscience) sorter. FACS sorted HH7-2tgIL10GFP CD4 T cells were resuspended in 200 µl sterile PBS and intravenously injected into *H. hepaticus* colonised recipient mice via the tail vein. 2000 or 20000 naïve donor HH7-2tg CD4 T cells were injected for flow cytometric analysis, as indicated. FACS sorted HH7-2tg CD4 T cells were used for co-culture experiments.

2.8 Quantification of cytokine levels

Supernatants from tissue explants and organoid cultures were collected and cytokine levels measured by enzyme-linked immunosorbent assay (ELISA). All cytokines were measured with DuoSet ELISAs (R&D) and the assay performed according to the manufacturer instruction. 3,3',5,5'-Tetramethylbenzidine (TMB) (eBioscience) was

Surface marker	Clone
CD45.1	A20
CD45.2	104
CD45	30-F11
cd4	GK1.5; RM 4-5
CD8a	53-6.7
CD8b	H57-597
TCRgd	GL3
TCRb	H57-597
hCD2	TS1/8
CD44	IM7
CD62L	MEL-14
PD-1	29F.1A12
PD-L1	10F.9G2
MHCII	M5/114.15.2
EpCAM	G8.8
CD11c	N418
CD11b	M1/70
B220	RA3-6B2
Siglec F	E50-2440
Ly6C	HK1.4
Ly6G	1A8
F4/80	BM8
CD3	145-2C11
CD19	6D5
CD138	281-2
ICOS	C398.4.A
CCR6	29-2L17
CD152	UC10-4B9

Intracellular marker	Clone
T-bet	4B10
Gata3	TWAJ
FoxP3	FJK-16S
RoRgt	Q31-378
IFNg	XMG1.2
IL-17a	TC11-18H10.1
TNFa	MP6-XT22
IL-10	JES5-16E3

Table 2.4: List of antibodies used in this study

Antibody	Clone
GFP	
CD11c	N418
CD11b	M1/70
B220	RA3-6B2
CD62L	Mel-14
CD44	IM7
CD25	Ebio3c7
TCRVbeta6	RR4-7
CD4	RM 4-5
CD45	30-F11
L/D	

Table 2.5: HH7-2tg CD4 T cell FACS panel

used as a substrate and the reaction was stopped using 2 M H_2SO_4. The cytokine levels of organ explants were normalized to the input tissue weight.

2.9 Gene expression analysis

2.9.1 Tissue processing for RNA isolation

Snap frozen tissue was homogenized with glass beads in 350 µl RLT buffer, containing beta-mercaptoethanol (βMe), for 40 s at 6.5 m/s in a FASTPREP-24 (MP). The samples were used for subsequent RNA isolation or stored at −80 °C for future RNA isolation.

2.9.2 Organoid processing for RNA isolation

Two organoid containing wells of a 24-well plate were washed with PBS and the organoids resuspended in 350 µl RLT buffer, supplemented with βMe. Samples were stored either stored at −80 °C or processed immediately.

2.9.3 RNA isolation and quantitative PCR (qPCR)

RNA was prepared using the RNeasy Mini Kit (Qiagen) according to the manufacturer's protocol. 0.8-2 µg of RNA was reversed transcribed using the SuperScript III Reverse Transcriptase Kit (Fisher Scientific) and oligo-dT primers (Sigma)

according to the manufacturer's protocol. cDNAs were diluted 1:5 and 4 µl were used in a final reaction volume of 20 µl. Samples were run in duplicates and TaqMan Gene expression array probes (Applied Biosystems) and the qPCR Mastermix (Eurogentec) were used. Quantitative real-time PCR was performed on the StepOnePlus Real-Time PCR System (Applied Biosystems) with the cycling conditions recommended by the manufacturer. Expression levels were calculated using the $2^{-\delta Ct}$ method and values were normalized to Hprt (hypoxanthine phosphoribosyl transferase- housekeeping gene).

2.10 Intestinal 3D organoid culture

2.10.1 Isolation of primary intestinal epithelial cells and culturing of intestinal epithelial 3D organoids

Epithelial crypts were isolated and cultured as organoids following methods established by Sato et al. [111]. Briefly, the colonic tissue was harvested from H2-Ab1$^{fl/fl}$ and H2-Ab1^{VC} mice, cut into small pieces and washed extensively in ice cold PBS. The tissue was then incubated with 2 mM EDTA in PBS for 90 min at 4 °C while rocking gently. The tissue was vigorously resuspended in PBS/10 % FCS and the SN containing the crypt fraction filtered through a 100 µm cell strainer and centrifuged. Crypts were embedded in 20 µl of matrigel/well (Corning) and seeded into a 24-well plate. The matrigel was left to polymerize for 15 min at 37 °C with the plate flipped upside down. Thereafter 400 µl per well of complete conditioned medium (Ad-DF+++) was added [Advanced Dulbecco's Modified Eagle Medium (DMEM)/F12 supplemented with 1 % P/S, 10 mM HEPES, 1X GlutaMax, 50 ng/ml EGF, 1× N2, 1× B27 (all from Invitrogen), 1 mM N-acetylcysteine (NAC), 10 µM RhoK-inhibitor (Y-27632 dihydrochloride monohydrate) (both from Sigma), a 1:5 dilution of Wnt3A and Noggin, and a 1:10 dilution of R-spondin-1]. The medium was changed every other day and organoids were expanded over around three passages before they were used for experiments.

Supplements	Purpose
Matrigel (laminin-rich)	Laminin (α1 and α2) is enriched at the crypt base. Provides 3D matrix [323].
Epidermal growth factor (EGF)	Supports intestinal proliferation [324].
Noggin	Induces an expansion of crypt numbers. Negative regulator of Bone morphogenetic protein (BMP). BMP pathway functions as a negative regulator of crypts [325, 326].
Wnt-3A	Required for crypt proliferation and stem cell maintenance [327, 328].
R-spondin	Wnt agonist. Potentiates Wnt signalling [329].
Rock-inhibitor (Y27632)	Prevent dissociation-induced apoptosis [330].
N-acetyl-l-cysteine (NAC) (dispensable)	ROS quencher
B27	Antioxidant cocktail, vitamin A, insulin [331].
N2 (dispensable)	Human transferrin, (holo), insulin recombinant full chain, progesterone, putrescine, selenite [331].

Table 2.6: Media supplements to support colonic organoid growth *ex vivo*.

Wnt3A and R-spondin-1 were produced by recombinant murine Wnt3A L cells (ATCC CRL-2647) and RspoI-Fc HEK 293T cells (kind gift from Dr. Calvin Kuo, Stanford, United States). Noggin was produced by recombinant murine Nog-Fc Hek 293T cells (kind gift from Dr. Gjis van den Brink, Amsterdam, Netherlands). Cells were incubated in Ad-DF+++ medium [Advanced DMEM/F12 supplemented with 10 mM HEPES and 1x GlutaMax], supernatants of these cells then harvested and sterile filtered. The concentration of the recombinant protein of each batch was compared to previously tested batches with optimal protein levels via a spotblot (Noggin and R-spondin-1) or a beta-catenin stabilisation assay (Wnt3A). The purpose of each media supplement is listed in Table 2.6.

2.10.2 Cytokine stimulation of intestinal 3D organoids

Organoids were treated with the indicated stimuli for the indicated amount of time. Organoids were further used for gene expression or flow cytometry analysis, described in 2.9 and 2.7 respectively. For immunofluorescent staining of stimulated

and unstimulated organoids, the organoids were split 1:2 and seeded in 20 µl matrigel/well on a round glass coverslip into 24-well plates. The matrigel was left to polymerize for 10 min at 37 °C without flipping the plate and 400 µl/well Ad-DF+++ medium added. Organoids were treated with the indicated stimuli for 16 h and stained the following day as described in section 2.11.3.

2.10.3 Organoid co-culture with HH7-2tg CD4 T cells

Pre-treatment HH7-2tg CD4 T cells

Round-bottom 96-well plates were pre-coated with 5 µg/ml anti-CD3 in PBS at 37 °C for 2 h. HH7-2tg CD4 T cells were FACS sorted as described in section 2.7.5. HH7-2tg CD4 T cells were seeded at 500 000 cell/ml at 200 µl per well in complete RPMI medium (10 % FBS, 1:100 Pen/Strep, 1:100 HEPES, 1:100 GlutaMax, 1:100 Na-Pyruvate, 50 μM β-Me), containing 2 µg/ml anti-CD28. Cells were incubated for three days at 37 °C and 5 % CO_2. Next, cells were transferred into fresh complete RPMI medium and into a new round-bottom 96-well plate, with 5 ng/ml recombinant murine IL-2 supplemented, but without anti-CD3/anti-CD28, and rested for two days at 37 °C and 5 % CO_2. At the end, dead cells were removed using the Miltenyi dead/cell removal kit following the manufacturer's instructions.

Pre-treatment colonic organoids

Organoids were grown as described above. When organoids reached their passaging state, organoids were disrupted using TrypLE Express and mechanic force for around 1 min. Organoid fragments were filtered through a 100 µm strainer and spun down at 1200 rpm for 5 min. Organoids were seeded at 1:1 dilution into matrigel and grown for 36 h at 37 °C and 5 % CO_2 in Ad-DF++ medium before they were treated with 20 ng/ml recombinant murine IFNγ in Ad-DF+++ medium for 16 h at 37 °C and 5 % CO_2. IFNγ containing medium was removed and organoids were peptide-pulsed with 1 µg/ml *H. hepaticus* peptide HH_1713 (Genscript) in Ad-DF++ medium for 2 h at 37 °C and 5 % CO_2. Next, organoids were isolated from the matrigel by

incubating them for 30 min at 4 °C in Corning Cell Recovery Solution. Organoids were washed in PBS and then used for the co-culture.

Colonic organoid and HH7-2tg CD4 T cell co-culture

100 000 HH7-2tg CD4 T cells were combined with organoids isolated from 2 dense wells of a 24 well plate. 1/3 of the cell-organoid mix was resuspended with 2/3 of a collagen/matrigel mix (50 % PureColl; 25 % matrigel; 1 % MEM; 0.375 % sodium bicarbonate, 1 µg/ml recombinant murine CCL19). 30 µl of this final cell-collagen mix was seeded into each well of a 24-well plate and 500 µl Ad-DF+++ medium were added per well, containing 5 ng/ml recombinant murine IL-2 and IL-7. Depending on the co-culture condition, 1 µg/ml *H. hepaticus* peptide HH_1713 and/or anti-mouse MHC class II (5 µg/ml, clone M5/114.15.2) was added. The co-culture was incubated at 37 °C and 5 % CO_2 for three days without media change. If cytokine production of HH7-2tg CD4 T cells was assessed, the coculture was incubated with Ad-DF+++ medium, containing 1:1000 GolgiPlug and 1:1000 GolgiStop for 4 h at 37 °C and 5 % CO_2 at the end of the three day co-culture period. HH7-2tg CD4 T cells were isolated by removing the supernatant and incubating the collagen/matrigel mix with 100 U/ml Collagenase VII in PBS for 1 h at 37 °C and 5 % CO_2. HH7-2tg CD4 T cells were subsequently stained for flow cytometric analysis. Supernatants were kept for quantification of cytokine levels.

2.11 Fluorescence microscopy

2.11.1 Fluorescence microscopy of paraffin embedded tissue

Paraffin-embedded sections were deparaffinised in xylene and rehydrated with ethanol. Antigen retrieval was performed with 10 mM citrate buffer (pH 6). Slides were blocked with PBS containing 5 % BSA and 10 % normal goat serum (NGS) for 1 h at RT in a moist chamber. Primary antibodies were added in PBS containing 5 % BSA and 10 % NGS for 1 h at RT. Slides were washed three times in PBS and subsequently stained with the secondary Abs in PBS with 5 % BSA and 10 %

NGS for 30 min at RT. After washing three times, the slides were incubated with DAPI (1:10000, Sigma-Aldrich) in PBS. After a further three washes the slides were mounted with ProLong Gold Antifade Mountant (Fisher Scientific). Images were acquired with the Olympus Fluoview FV1000 confocal microscope and the Olympus Fluoview Software (Olympus, Tokyo, Japan).

2.11.2 Fluorescence microscopy of OCT embedded tissue

Slides containing 7 µm thick OCT sections were thawed and dried at RT for several minutes. Slides were washed with PBS and permeabilised for 30 min with PBS, containing 0.5 % saponin and 10 % serum. Slides are subsequently incubated for 1 h at RT with antibodies in 5 %BSA/PBS. The following antibodies were used: anti-CD3 (1:100, ab5690, Abcam), anti-MHCII (1:100, clone M5/114.15.2) and anti-Ecadherin (1:100, clone 36/E-CADHERIN). Slides were washed with PBS and subsequently incubated with secondary antibodies for 30 min at RT in the dark. The following secondary antibodies were used: goat anti-rat 647 (1:400), goat anti-mouse 488 (1:400) and goat anti-rabbit 555 (1:400) (all lifetechnologies). Slides were washed with PBS and incubated with DAPI (1:10000, Sigma-Aldrich) in PBS. After a further three washes the slides were mounted with ProLong Gold Antifade Mountant (Fisher Scientific). Whole colon "swiss roll" images were collected at a 10x magnification on a Zeiss LSM 880 confocal microscope (Zeiss, Germany).

2.11.3 Fluorescence microscopy of organoids

For immunofluorescent staining of the organoids, the organoids were washed with PBS and fixed with 2 % paraformaldehyde for 10 min at RT. Organoids were washed with PBS and subsequently incubated with 100 % methanol at −20 °C for 10 min. Organoids were washed with PBS and blocked with PBS containing 5 % BSA, 10 % goat-serum and 0.5 % saponin for 30 min at RT. Organoids were stained with antibodies in PBS containing 5 % goat-serum and 0.5 % saponina for 1 h at RT. After washing in PBS, organoids were incubated with DAPI (1:10000, Sigma-Aldrich) in PBS. After final washes in PBS, organoids were mounted with ProLong Gold

Antifade Mountant (Fisher Scientific) on a cover slide. Images were acquired with the Olympus Fluoview FV1000 confocal microscope and the Olympus Fluoview Software (Olympus, Tokyo, Japan).

2.12 Statistics

Statistical significance between two *in vivo* treatment groups was calculated using the non-parametric Mann-Whitney test. Except for weight curves where p-values were determined by two-way ANOVA multiple comparisons test with Sidak's correction. Correlation analysis were performed using Spearman's correlation analysis. If cell populations isolated from multiple tissue sites from the same animal were compared, statistical significance was determined by Friedman test, with Dunn's multiple comparisons.

Statistical significance between multiple *in vitro* treatment groups was calculated using repeated measure mixed-effects analysis with Tukey's multiple comparisons test, with a single pooled variance.

Statistical analysis was performed using GraphPad Prism 9 (GraphPad Software, US). Differences were considered statistically significant when p: *$p<0.05$; **$p<0.001$; ***$p<0.0001$; ****$p<0.00001$.

3

Colonic IECs have the machinery to function as non-conventional antigen presenting cells

Contents

3.1 Introduction 65
3.2 Results 70
3.2.1 MHC class II deficiency of IECs in H2-Ab1^{VC} mice . . . 70
3.2.2 MHC class II mRNA is expressed by cIECs 72
3.2.3 MHC class II protein is expressed by cIECs 77
3.2.4 IECs can take up and process antigen 80
3.2.5 MHC class II deletion in IECs of H2-Ab1^{VC} mice is not totally efficient 83
3.2.6 Lack of MHC class II expression by cIECs does not result in intestinal pathology at steady state 85
3.3 Discussion 92

3.1 Introduction

DCs, macrophages and B cells constitutively express MHC class II and are considered conventional APCs. However, in recent years more and more cell types have been proposed to present antigens on MHC class II molecules to CD4$^+$ T cells. These range from haematopoietic cell types, such as mast cells, basophils and eosinophils,

to non-haematopoietic cell types located in the periphery, such as endothelial cells or epithelial cells (reviewed in [332]). A *bona fide* APC is characterised by a set of key properties that allows the activation of naïve T cells. The activation of naïve T cells by APCs needs three key signals. First, the cognate antigen presented on a MHC class II molecule is recognised by its specific TCR expressed by CD4 T cells. This initial T cell activation is sustained by a second co-stimulatory or co-inhibitory signal provided by APCs, which promotes the survival and expansion of the T cells [333]. Finally, the third signal is received in the form of cytokines, provided by APCs and other surrounding cells, which direct the differentiation into different effector and regulatory T cell subsets (see section 1.9 and reviewed in [334]).

APCs are expressing a variety of co-stimulatory and co-inhibitory molecules and the nature of the signal influences the T cell response, either promoting or inhibiting T cell activation, differentiation and function. Co-stimulatory molecules include CD80/CD86, expressed by APCs, which binds to CD28 expressed by T cells, as well as CD40-CD40L, OX40-OX40L and ICOS-ICOS-L (reviewed in [335]). CD40 is ubiquitously expressed by immune cells, such as B cells or DCs, and non-immune cells, such as epithelial cells (reviewed in [336]). CD40L is primarily expressed by activated CD4 T cells and interaction with CD40 regulates the costimulatory activity of APCs by inducing the expression of CD80 and CD86, ICAM1 and HLA-DR [336, 337]. In addition, CD40-CD40L interaction induces the production of IL-12 by DCs, which is important in the polarisation of Th1 cells [336]. Conversely, co-inhibitory signals suppress T cell activation and function. These include PD-1, CTLA-4 and LAG3 (reviewed in [338]).

If T cells are activated through their TCR but do not receive co-stimulatory signals, they enter an inactive state known as anergy (reviewed in [339]). Conflicting results have been generated to test whether IECs express co-stimulatory or co-inhibitory signals (see section 1.8). At steady state and under inflammatory conditions, mRNA expression of both co-stimulatory and co-inhibitory molecules

appears to be present in IECs. However, detection of surface expression of those molecules was inconsistent across different studies and when detected, these molecules were expressed at low levels and mainly present in inflamed intestinal tissue (see section 1.8, [132, 165–168]).

As described in section 1.9, the intestinal T cell populations mainly consists of activated T cells. These differ in their activation requirement from naïve T cells. If they encounter their specific antigen, it triggers their effector functions and this process is less dependent on co-stimulation. These characteristics of activated T cells would allow IECs to modulate activated T cell effector functions, without the need of co-stimulatory molecule expression. In addition, to their expression of all the necessary antigen-processing machinery as well as their expression of co-stimulatory molecules and cytokines, APCs tune their response by being able to recognise and respond to danger-associated and pathogen-associated signals. For example, DCs express pattern recognition receptors (PRRs) that mediate their activation in response to pathogens.

Intestinal epithelial cells (IECs) are uniquely located at the interface between the host immune system and the intestinal lumen, rich in food and microbial antigens. The epithelium provides a physical barrier, which prevents the microbiota from penetrating the intestinal mucosa and thereby minimises the exposure of the intestinal immune system to luminal antigens. An efficient crosstalk between the host and the gut microbiota results in a hyporesponsive state towards the resident microbiota, maintaining homeostasis. IECs might regulate the adaptive immune response to luminal antigens through their MHC class II expression.

IECs were shown to express MHC class II molecules [127–130], which could allow them to function as non-conventional APCs. Human siIECs constitutively express MHC class II molecules [128, 130–133] whereas cIECs do not express MHC class II molecules at steady state [340]. At both tissue sites IECs upregulate MHC class II

expression in response to inflammation. It was shown, that the pro-inflammatory cytokine IFNγ induced the surface expression of MHC class II molecules, as well as Ii and HLA-DM, on human colonic IEC-like cell lines [139]. In addition, these human colonic IEC-like cell lines processed and presented antigen from their apical surface, but only when high concentrations of antigen were present [139]. Mimicking pro-inflammatory conditions, the transfection of human colonic IEC-like cell lines with CIITA allowed IECs to take up and process antigen from both the apical and basolateral membranes [140].

The physical epithelial barrier is further strengthened by inducible mechanisms that are activated following the recognition of DAMPS and PAMPs by IECs. IECs express a variety of different PRRs to respond to such signals, and TLR signalling was shown to maintain barrier function [104, 105]. The ability of IECs to recognise and respond to DAMPs and PAMPS combined with their ability to express MHC class II, puts them in a unique position to relay environmental cues to the adaptive immune system in the gut. The recognition of microbial components via TLRs might lead to the induction of MHC class II expression by IECs. We therefore hypothesised that IECs can function as non-conventional antigen-presenting cells and modulate $CD4^+$ T cell phenotype and function. Previous studies have determined that cIECs do not constitutively express MHC class II and upregulate its expression in response to intestinal inflammation. The lack of MHC class II expression by cIECs at colonic homeostasis raised the question whether chronic, low grade, systemic inflammation experienced in ageing [341] might induce MHC class II expression by cIECs, which influences intestinal homeostasis. A recent mouse study showed that the intestinal permeability increased with age due to age-related microbial dysbiosis [342]. Microbial antigens were able to pass the epithelial barrier of aged mice and entered the blood stream, where they provoke systemic inflammation, characterised by increased IL-6 serum levels. In contrast, aged germ-free mice did not experience age-associated inflammation. However, their colonisation with microbiota from conventional old mice induced systemic inflammation [342]. This study suggests

that aged mice experience a dysfunctional crosstalk between the microbiota and the immune system. We therefore hypothesised that MHC class II expression by large intestinal IECs is upregulated in aged mice and plays an important role in maintaining tolerance in the large intestine. In addition, we want to understand whether IECs possess the requirements to function as non-conventional APCs.

In order to study the specific role of epithelial MHC class II expression in modulating CD4 T cell functions, we generated mice that are selectively deficient in MHC class II expression in IECs. The murine MHC class II genes are located in the region of the H2 complex on chromosome 17, which was historically called the "I" region. The H2 complex produces two classical MHC class II molecule, I-A and I-E, consisting of both an α- and β-chain. Inbred mouse strains have unique sets of H2 alleles, termed H2 haplotypes. C57BL mice have the H2 haplotype I-Ab [343], as they carry a mutation in the E_α gene promoter which inhibits the synthesis and expression of the E_α-protein [344, 345]. As a result, we only had to knock out H2-Ab1 expression for our functional studies. This was achieved by crossing a transgenic strain in which *H2-Ab1* is flanked by loxP recombination sites (H2-Ab1$^{fl/fl}$) [319] with another transgenic strain expressing the Cre recombinase under the control of the epithelial cell-specific promoter Villin (Villin-Cre) [320]. IEC-specific MHC class II deficient mice will be referred to as H2-Ab1^{VC}, and their MHC class II sufficient litter mate controls will be referred to as H2-Ab1$^{fl/fl}$. To exclude any potential microbiota differences, littermate controls were used throughout these studies. In addition, we utilised the organoid system and generated H2-Ab1$^{fl/fl}$ and H2-Ab1^{VC} 3D organoids. It enabled us to functionally assess IEC responses to activating stimuli *in vitro*.

The main objectives of this chapter are:

1. To generate mice that selectively lacked MHC class II expression by IECs for functional analysis.

2. To define the stimuli inducing MHC class II expression by IECs.

3. To explore the ability of IECs to take up and process antigen.

4. To investigate the role of MHC class II expression by large intestinal IECs in the maintenance of intestinal homeostasis in aged mice.

3.2 Results

3.2.1 MHC class II deficiency of IECs in H2-Ab1^{VC} mice

To study the role of antigen presentation by IECs we crossed transgenic mouse lines to facilitate Villin-Cre mediated deletion of the H2-Ab1 gene, generating H2-Ab1^{VC} mice that lack MHC class II expression specifically in IECs (see section 2.1). To confirm that H2-Ab1^{VC} mice were deficient in IEC MHC class II expression, we isolated IECs from the small intestine as well as the caecum. Although MHCII^{+} IECs were evident in H2-Ab1$^{fl/fl}$ mice, especially in the SI, both small intestinal IECs (siIECs) and caecal IECs (cmIECs) isolated from H2-Ab1^{VC} mice completely lacked MHC class II expression (Figure 3.1 A and B, respectively). Representative FACS plots are shown in Figure 3.1 C. These results indicate that the Villin-Cre mediated deletion of H2-Ab1 was successful in siIECs and cmIECs of H2-Ab1^{VC} mice.

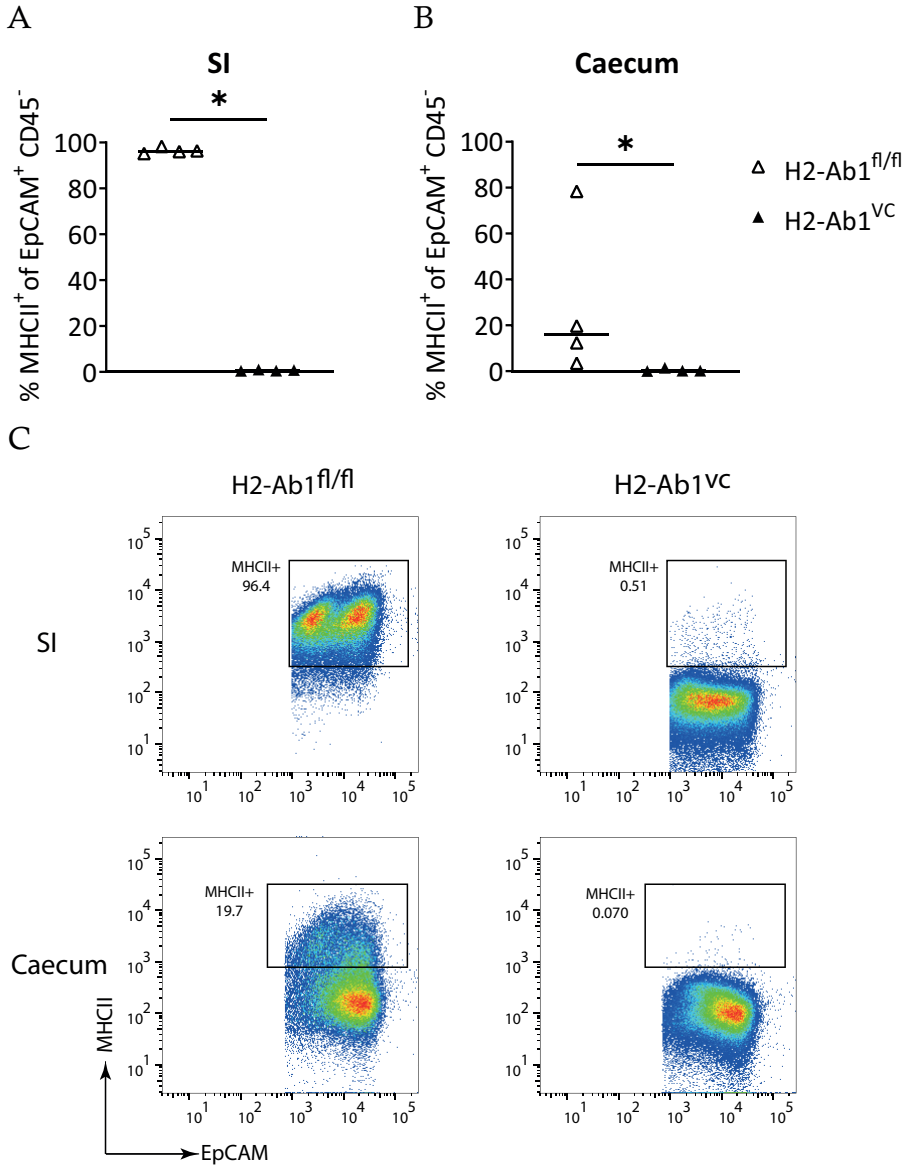


Figure 3.1: Successful deletion of MHC class II expression by IECs in H2-Ab1^{VC} mice. MHC class II expression by siIECs (A) and cmIECs (B) was analysed by flow cytometry. (C) Representative FACS plots of MHC class II^{+} IECs are shown. Symbols denote group median. Statistical significance between the groups was determined by Mann-Whitney test. P-value summary: *p<0.05. Data from one experiment with total mouse numbers per group as follows; n=4 H2-Ab1^{VC} and n=4 H2-Ab1$^{fl/fl}$ littermates.

3.2.2 MHC class II mRNA is expressed by cIECs

As IEC MHC II expression was greatly reduced in the LI relative to the SI (see Figure 3.1), we next tested whether stimulation with cytokine or TLR ligands could induce MHC class II mRNA expression by primary colonic IECs. To this end, we established both H2-Ab1^{VC} and H2-Ab1$^{fl/fl}$ cIEC organoids *ex vivo* (see Methods section 2.10). These organoids were stimulated with a range of cytokines linked to intestinal inflammation and expression of MHC class II was assessed by RTqPCR. These cytokine include IFNγ, IL-22, IL-17, TNFα, IL-13, IL-18, IFNλ2, IFNβ, IL-1α, IL-6 and IL-25. As described previously [137], IFNγ treatment led to the upregulation of MHC class II mRNA levels in cIECs of H2-Ab1$^{fl/fl}$ mice (Figure 3.2 A). Some lower level of MHC class II expression was observed in IFNγ treated cIECs of H2-Ab1^{VC} mice, which might reflect inefficient Villin-Cre mediated deletion of MHC class II in some ISCs (Figure 3.2 A and further discussed in Chapter 3.2.5). The other cytokines tested did not induce MHC class II expression by cIECs (Figure 3.2 A). CIITA regulates MHC class II expression in IECs [346] and IFNγ stimulation led to a marked increase in CIITA mRNA levels in both H2-Ab1$^{fl/fl}$ and H2-Ab1^{VC} cIECs (Figure 3.2 B). These results indicate that IFNγ is a potent inducer of MHC class II expression by primary IECs, that is likely driven by increased CIITA expression.

To explore this further, we investigated the kinetics of CIITA and MHC class II expression by cIECs. *Ex vivo* cIEC organoids were treated with IFNγ for the indicated times and expression levels were analysed by RTqPCR. MHC class II mRNA expression by cIECs barely increased over the first 5 h of IFNγ treatment, but was increased after 6 h and was expressed at high levels after 8 h (Figure 3.3 A). In contrast, CIITA mRNA expression by cIECs increased within the first hour of IFNγ treatment, was highly upregulated after 2 h and plateaued at very high levels after 4 h (Figure 3.3 B). Together, these results show that IFNγ stimulation highly upregulates CIITA mRNA expression prior to MHC class II mRNA expression in

cIECs.

IECs can sense potential harmful pathogens through different pattern recognition receptors (PRRs), including Toll-like receptors (TLRs) [104, 105]. PGN-SA is a peptidoglycan preparation from the Gram-positive bacterium *Staphylococcus aureus* and is known to be a TLR2 ligand. Pam3CSK4 is a synthetic triacylated lipopeptide and a TLR1/2 ligand. However, stimulation of colonic H2-Ab1$^{fl/fl}$ and H2-Ab1^{VC} organoids with these TLR1/2 ligands did not lead to the induction of MHC class II or CIITA expression by cIECs (Figure 3.4 A and B, respectively). We also tested stimulation with the synthetic TLR3 agonist poly(I:C) and the TLR4 agonist lipopolysaccharide (LPS), however, we did not detect any upregulation of MHC class II and CIITA expression levels in cIECs of H2-Ab1$^{fl/fl}$ or H2-Ab1^{VC} organoids (Figure 3.4 C-F). Similarly, stimulation with the TLR9 agonist CpG, or with the TL4/TLR5 agonist combination of LPS and flagellin, did not induce MHC class II expression by cIECs (Figure 3.4 G). Finally, we also found that muramyl dipeptide (MDP), the minimal bioactive peptidoglycan motif recognised by the intracelullar sensor nucleotide-binding oligomerization domain 2 (NOD2), did not induce MHC class II expression by cIECs (Figure 3.4 G). Overall, these results indicate that the TLR and NOD2 ligands we tested in this study could not induce MHC class II and CIITA expression in primary cIECs.

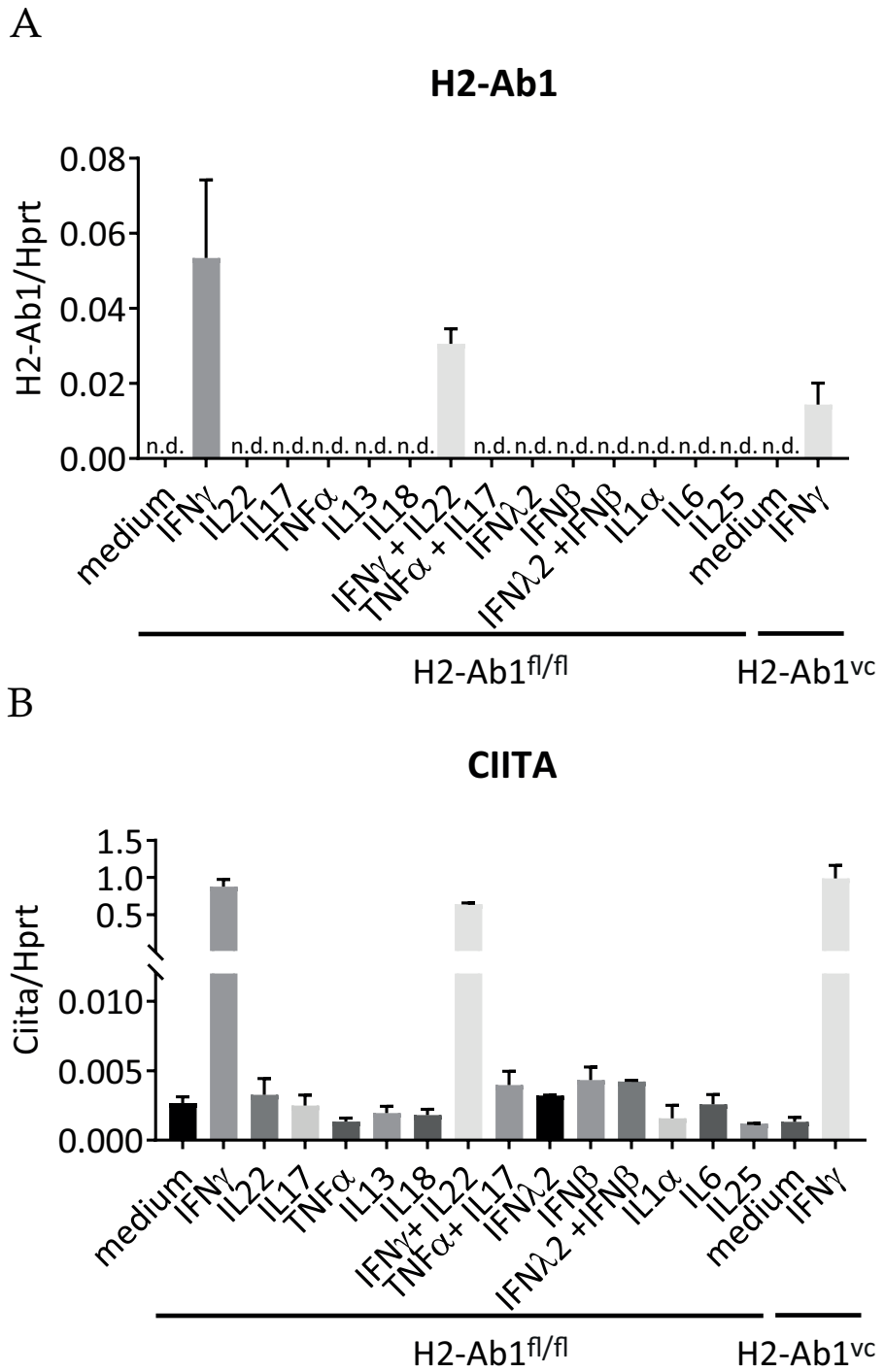


Figure 3.2: IFNγ is a potent inducer of MHC class II and CIITA mRNA expression in cIEC organoids. H2-Ab1^{VC} and H2-Ab1$^{fl/fl}$ cIEC organoids were stimulated with the indicated cytokines for 16 h and MHC class II and CIITA mRNA levels analysed by RT-qPCR. MHC class II (A) and CIITA (B) mRNA expression levels. Bars denote mean (± SD) as a relative to the respective Hprt mRNA levels. Cytokines were used at 20 ng/ml. Data from one of two independent experiments with two technical replicates run in duplicates, expect for the IFNγ stimulation of H2-Ab1^{VC} organoids, which were four technical replicates run in duplicates.

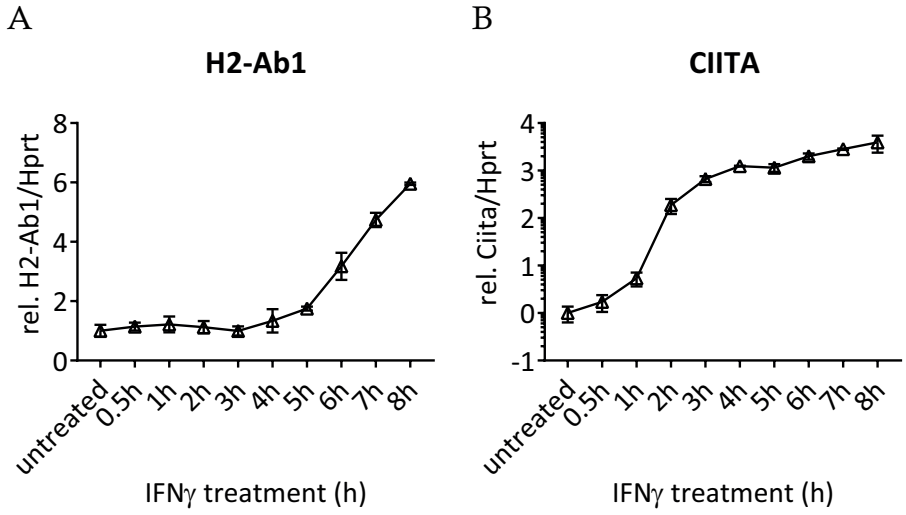


Figure 3.3: MHC class II mRNA expression levels by cIECs can be robustly detected after 6 h **of IFN**γ**.** H2-Ab1^{VC} and H2-Ab1$^{fl/fl}$ colonic organoids were stimulated with IFNγ (20 ng/ml) for the indicated time and mRNA expression levels determined by RT-qPCR. MHC class II (A) and CIITA (B) mRNA expression levels by cIECs after IFNγ stimulation. Symbols denote mean ($\pm$ SD). Data from one experiment with two technical replicates run in duplicates per sample.

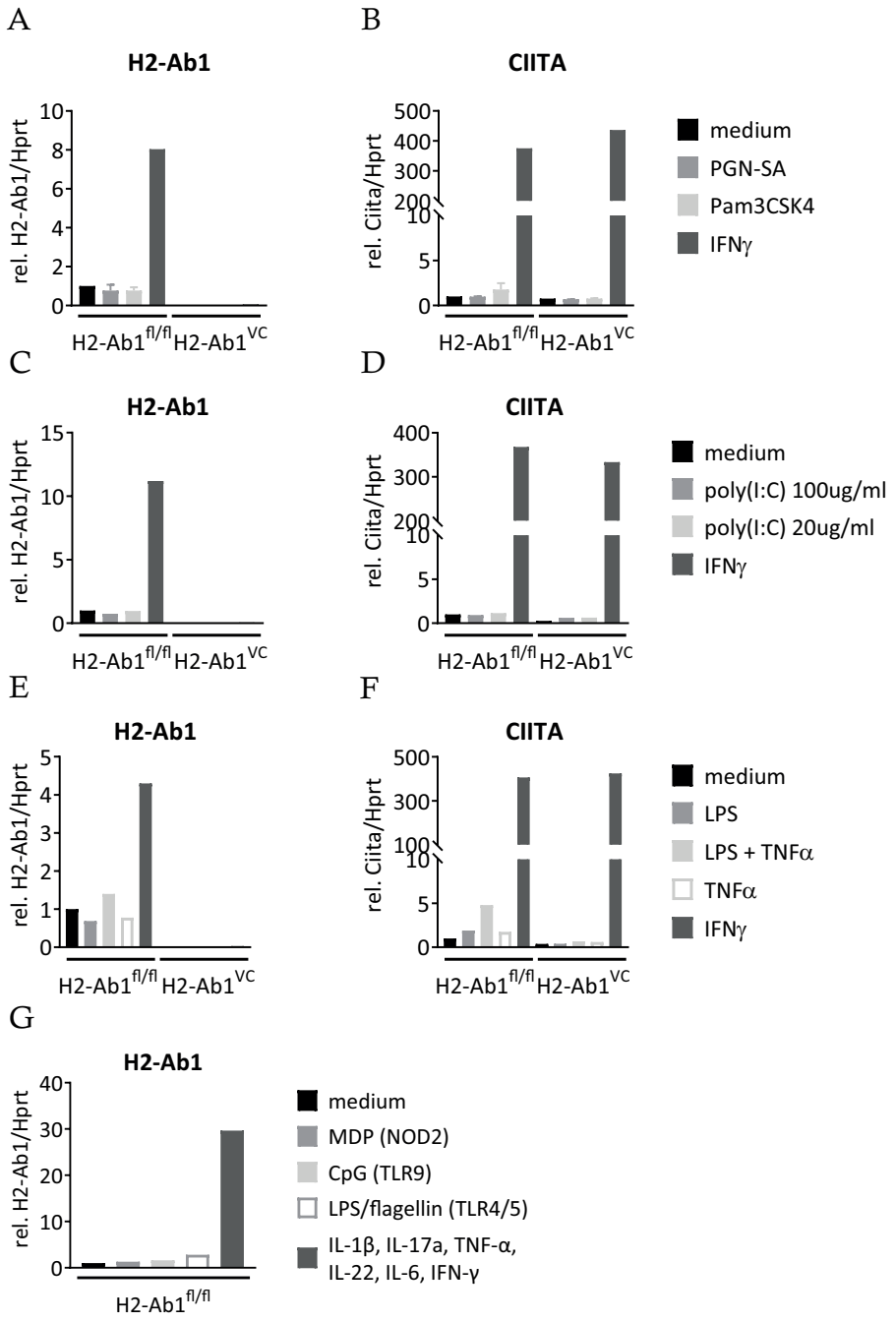


Figure 3.4: Selected TLR and NOD2 ligands do not induce MHC class II mRNA expression in H2-Ab1^{VC} and H2-Ab1$^{fl/fl}$ colonic organoids. H2-Ab1^{VC} and H2-Ab1$^{fl/fl}$ colonic organoids were stimulated with the indicated TLR and NOD2 ligands. MHC class II (A) and CIITA (B) mRNA levels after TLR1/2 stimulation. MHC class II (C) and CIITA (D) mRNA levels after TLR3 stimulation. MHC class II (E) and CIITA (F) mRNA levels after TLR4 stimulation. (G) MHC class II mRNA levels after TLR4/5, TLR9 and NOD2 stimulation. The mean of two technical replicates is depicted. Expression levels are normalized to Hprt and expressed relative to the medium control. Data from one experiment. Note: Stimulations in (G) were performed by Dr. Elizabeth Mann, Kennedy Institute of Rheumatology, University of Oxford.

3.2.3 MHC class II protein is expressed by cIECs

To confirm MHC class II expression at protein level, we analysed MHC class II expression on primary cIECs by flow cytometry. H2-Ab1$^{fl/fl}$ and H2-Ab1^{VC} cIEC organoids were stimulated with IFNγ for the indicated time. Extracellular MHC class II protein expression was undetectable until around 8 h of IFNγ treatment, when very low levels were observed in H2-Ab1$^{fl/fl}$ cIECs (Figure 3.5). However, after 16 h of IFNγ treatment around 60 % of H2-Ab1$^{fl/fl}$ cIECs expressed MHC class II on their surface (Figure 3.5). As expected, we did not detect any MHC class II protein expression in H2-Ab1^{VC} cIEC organoids (Figure 3.5). Thus, most primary cIECs expressed MHC class II protein after 16 h of IFNγ stimulation and this period was used in subsequent experiments.

Next, we assessed the localisation of the MHC class II protein in H2-Ab1$^{fl/fl}$ and H2-Ab1^{VC} colonic organoids following stimulation with IFNγ. The organoids were probed with DAPI, and stained with anti-E-cadherin and anti-MHCII antibodies for immuno-fluorescent microscopy. After IFNγ stimulation, MHC class II protein was readily detectable at the basolateral and apical membrane as well as intracellularly in the H2-Ab1$^{fl/fl}$ colonic organoids (Figure 3.6). As expected, IFNγ treated H2-Ab1^{VC} organoids generally did not express detectable MHC class II protein (Figure 3.6). However, on rare occasions, we did detect isolated IEC crypts which still expressed MHC class II protein, indicating that the Villin-Cre mediated deletion of MHC class II is not 100 % efficient (see section 3.2.5). These results highlight that cIECs express MHC class II protein after IFNγ stimulation and that the protein is localised not only at the apical but also at the basolateral membrane. This allows for the potential interaction of CD4$^+$ Th cells residing in the lamina propria and CD4$^+$ IELs, located in the intestinal epithelial layer, with peptides presented on MHC class II molecules by IECs.

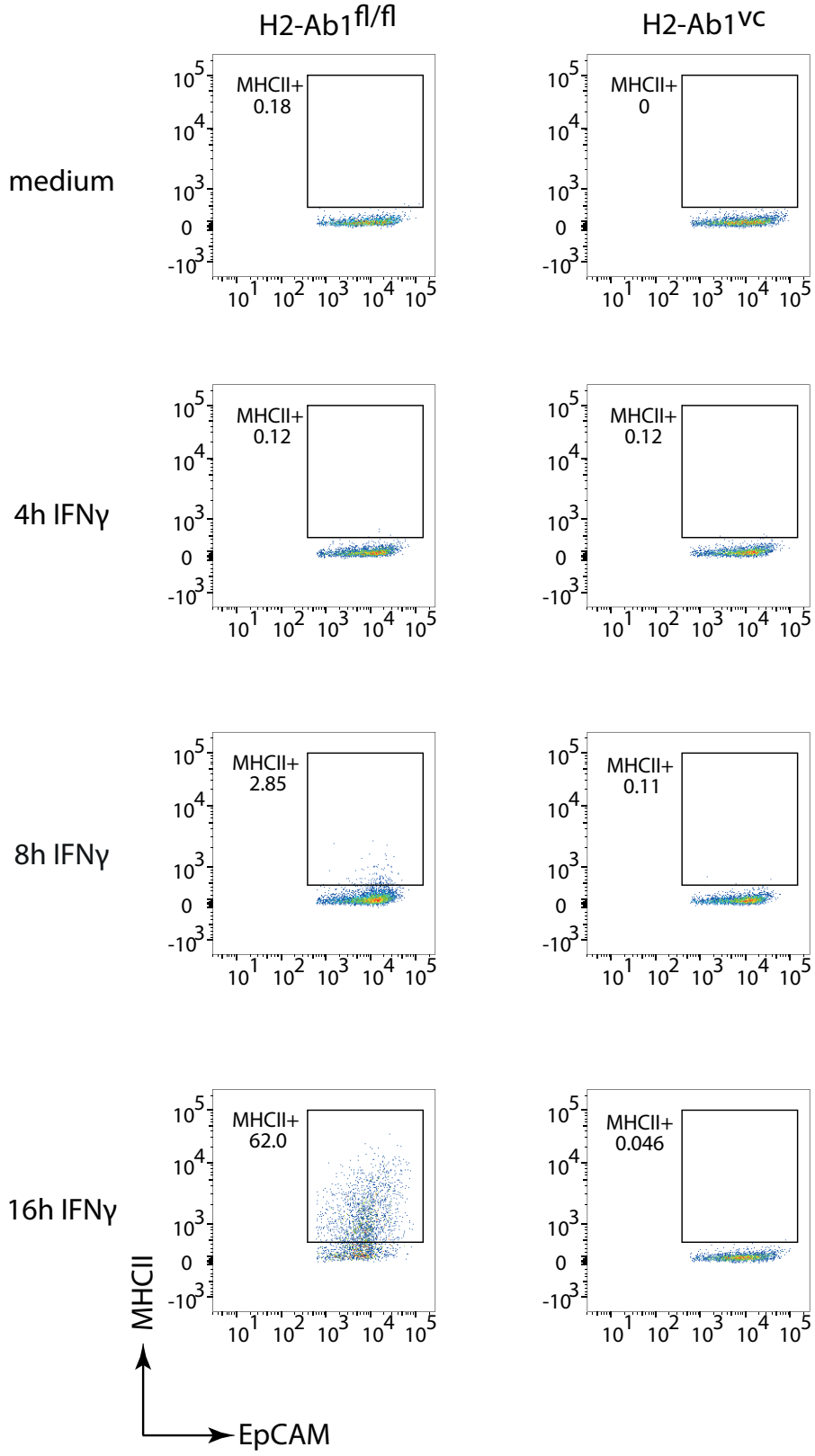


Figure 3.5: MHC class II protein expression can be robustly detected after 16 h of IFNγ treatment. H2-Ab1^{VC} and H2-Ab1$^{fl/fl}$ colonic organoids were stimulated with IFNγ (20 ng/ml) for the indicated time and protein expression levels determined by flow cytometry. Data from one experiment with two technical replicates per sample.

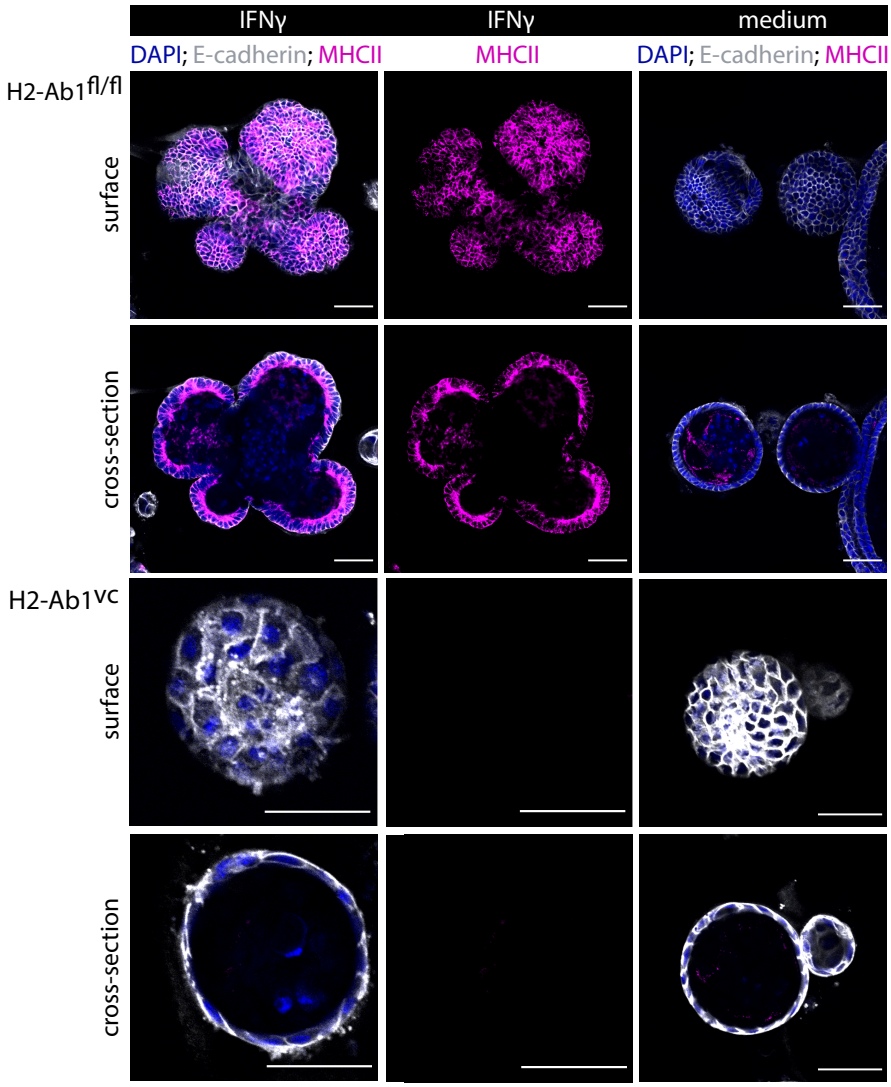


Figure 3.6: MHC class II protein is located at the cell surface and intracellular in H2-Ab1$^{fl/fl}$ cIECs after IFNγ treatment. H2-Ab1^{VC} and H2-Ab1$^{fl/fl}$ colonic organoids were stimulated with IFNγ (20 ng/ml) for 16 h and MHC class II protein localisation was assessed by immuno-fluorescent imaging. Organoids were stained for MHC class II (magenta), E-cadherin (grey) and DAPI (blue). Bar= 50 μm. Representative images of one of three independent experiments.

3.2.4 IECs can take up and process antigen

A prerequisite to function as an APCs is the ability to take up and process antigen prior to its presentation via the MHC class II molecule on the cell surface. To assess their protein uptake and processing capacity *ex vivo* cIEC organoids were cultured with DQ™ Ovalbumin for the indicated time. DQ™ Ovalbumin is a conjugate of ovalbumin labelled with the BODIPY FL dye, and while the molecule is intact the fluorescent signal is self-quenched. Following uptake and proteolytic degradation in the cell, the self-quenching capacity is lost and a bright green fluorescent signal can be detected by flow cytometry [347, 348] (Figure 3.7 A).

We chose the incubation with DQ™ Ovalbumin for 3 h at 4 °C as our experimental reference, as the protein uptake and processing capacity of cells is greatly reduced at these low temperatures. We detected a significant increase in the relative median fluorescent intensity (MFI) of DQ™ Ovalbumin after 2 h incubation at 37 °C in H2-Ab1$^{fl/fl}$ cIECs (Figure 3.7 B). This increase doubled after 3 h incubation at 37 °C (Figure 3.7 B).

Next, we used BMDCs, as professional APCs, to compare their protein uptake and processing capacity to cIECs. In addition, we treated our cIEC organoids with IFNγ for 16 h prior to DQ™ Ovalbumin incubation to determine whether IFNγ stimulation influences the protein uptake and processing ability. After 1 h of DQ™ Ovalbumin incubation at 37 °C BMDCs exhibited significantly higher MFI levels which further increased after 2 h or 3 h incubation (Figure 3.7 C). In contrast, cIEC organoids showed a tendency towards modestly increased MFI levels after 3 h incubation at 37 °C, which was significant after IFNγ treatment (Figure 3.7 C). Overall, the MFI of cIEC organoids was around 15 x lower than the MFI of BMDCs after 3 h incubation with DQ™ Ovalbumin at 37 °C (Figure 3.7 C). However, it must be noted that BMDCs took up high amounts of DQ™ Ovalbumin during the 3 h incubation at 4 °C (Figure 3.7 C and D). Therefore, when assessing the relative MFI, BMDCs showed a significant increase of around 3.5 x after 3 h incubation

at 37 °C, whereas IFNγ treated cIEC showed a significant increase of around 2 x (Figure 3.7 D). Taken together, these results show that cIECs can take up and process protein, although to a much lower extent than BMDCs.

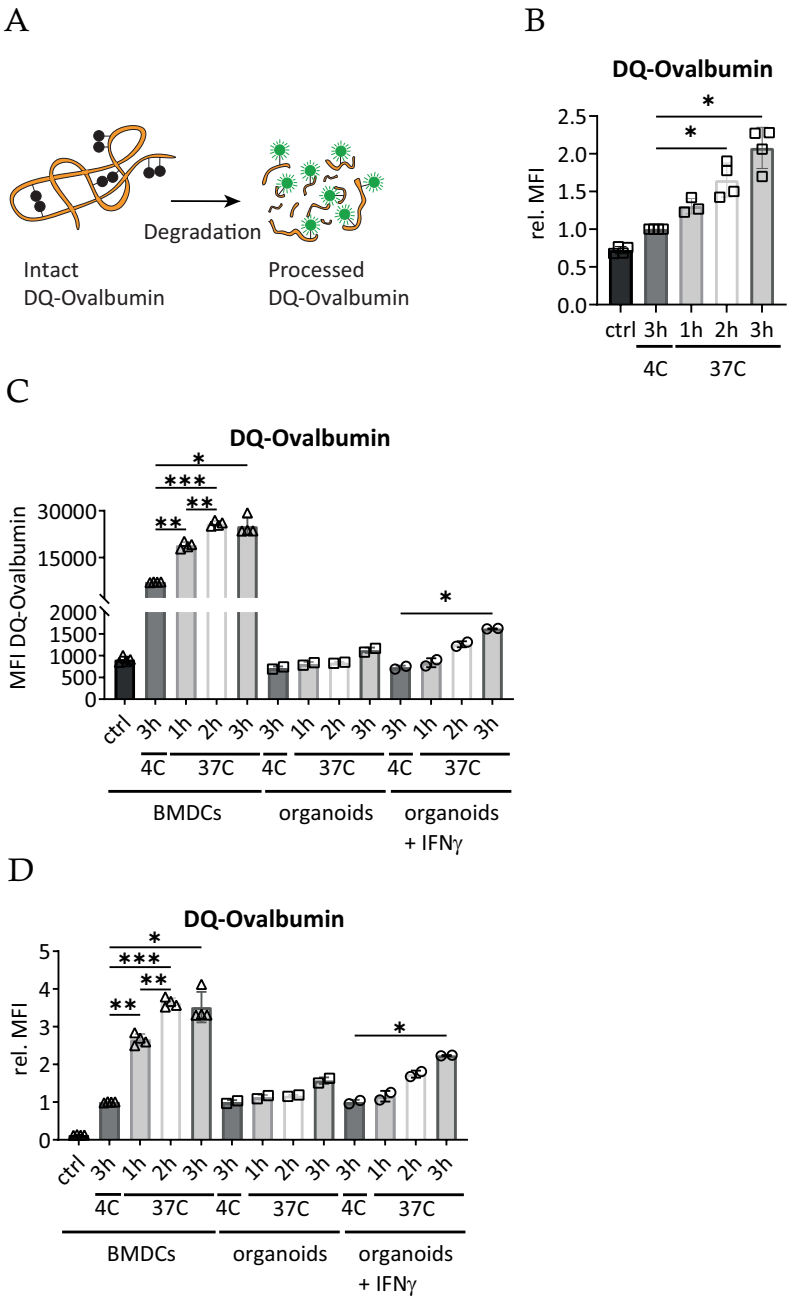


Figure 3.7: CIECs can take up and process protein. H2-Ab1$^{fl/fl}$ cIEC organoids and BMDCs were incubated with DQ™ Ovalbumin for the indicated time and median fluorescent intensity assessed by flow cytometry. Where indicated, organoids were stimulated with IFNγ (20 ng/ml) for 16 h prior to DQ™ Ovalbumin incubation. (A) Schematic of DQ™ Ovalbumin properties. (B) Relative MFI was assessed at indicated times of cIEC organoids. Bars denote group mean (± SD) as a relative to 3 h incubation at 4 °C. (C) MFI of BMDCs and cIECs organoids. Bars denote group mean (± SD). (D) Relative MFI of BMDCs and cIECs organoids. Bars denote mean (± SEM) as a relative to 3 h incubation at 4 °C. Statistical significance between the groups was determined by Mann-Whitney test (B) or mixed-effects analysis with Geisser-Greenhouse correction and Tukey's multiple comparisons test (C and D). (B) Data from four pooled independent experiments with two technical replicates each. P-value summary: *p<0.05; **p<0.01; ***p<0.001. (C and D) Representative data of one of two independent experiments with four technical replicates for BMDC values and two technical replicates for cIEC values.

3.2.5 MHC class II deletion in IECs of H2-Ab1^{VC} mice is not totally efficient

To examine the efficiency of MHC class II deletion in colonic IECs we performed immuno-fluorescent staining on IFNγ stimulated *ex vivo* colonic organoids of H2-Ab1^{VC} mice. The organoids were probed with DAPI, and stained with anti-E-cadherin and anti-MHCII antibodies for immuno-fluorescent microscopy. On rare occasions, we did observe MHC class II positive intestinal crypts after IFNγ stimulation (Figure 3.8 A).

To further assess the efficiency of Villin-Cre mediated deletion of MHC class II expression by cIECs *in vivo*, we performed immuno-fluorescent staining on OCT embedded caecal tissue sections obtained from H2-Ab1^{VC} mice colonised with *Helicobactr hepaticus*. For this purpose we rolled the entire caecum into a swiss roll and cut cross sections, which were used for immuno-fluorescent staining. The swiss roll sections were probed with DAPI, anti-E-cadherin and anti-MHCII antibodies for immuno-fluorescent microscopy. Again, we observed MHC class II expressing crypts on rare occasions (Figure 3.8 B). Within the whole cross section of this one area of the swiss roll we detected one MHC class II expressing crypt, suggesting that inefficient Villin-Cre mediated deletion of MHC class II occurs in less than 1 % of intestinal crypts. In summary, these data indicate that Villin-Cre mediated deletion of MHC class II expression is not 100 % efficient and that there are rare intestinal crypts expressing MHC class II *in vivo* and in our *ex vivo* organoid experiments.

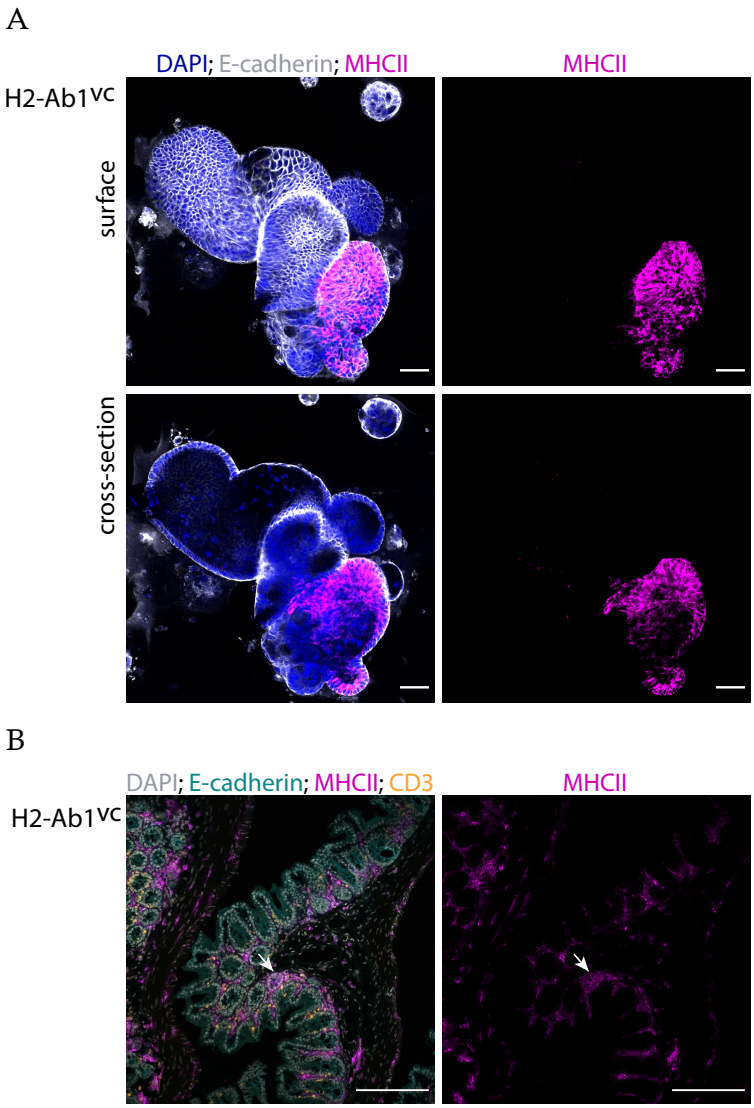


Figure 3.8: MHC class II$^+$ intestinal crypts are present on rare occassions in H2-Ab1$^{fl/fl}$ cIECs. (A) H2-Ab1^{VC} were stimulated with IFNγ (20 ng/ml) for 16 h and MHC class II protein localisation was assessed by immuno-fluorescent imaging. Organoids were stained for MHC class II (magenta), E-cadherin (grey) and DAPI (blue). Bar=50 μm. Representative image of one of three independent experiments. (B) H2-Ab1^{VC} mice were orally infected with 10^8 CFU *H. hepaticus* on three consecutive days. Mice were sacrificed at two weeks post infection. Swiss rolls from the caecum were prepared and MHC class II protein localisation was assessed by immuno-fluorescent imaging. The caecal tissue was stained for MHC class II (magenta), CD3 (orange), E-cadherin (cyan) and DAPI (grey). Bar=200 μm. Representative image of two mice from one experiment.

3.2.6 Lack of MHC class II expression by cIECs does not result in intestinal pathology at steady state

To investigate whether loss of MHC class II expression in IECs lead to spontaneous intestinal inflammation over time, we analysed two independent cohorts of H2-Ab1$^{fl/fl}$ and H2-Ab1^{VC} littermates after around a year of co-housing.

First, we investigated whether MHC class II deletion led to overt systemic inflammation but did not detect any significant differences in spleen weights between H2-Ab1$^{fl/fl}$ and H2-Ab1^{VC} littermates (data not shown). To investigate the impact of IEC MHC class II expression on intestinal homoeostasis, colonic and caecal tissues were paraffin-embedded, sectioned and stained with H&E. Histological analysis of the whole colon did not show any development of intestinal pathology (Figure 3.9 A). We did however detect a significant but slight increase in histopathology scores for the caecum of H2-Ab1^{VC} mice compared to H2-Ab1$^{fl/fl}$ littermates (Figure 3.9 B). This increased score was driven by increased cell infiltration into the caecal tissue, as illustrated in the representative histology images in Figure 3.9 C.

To assess whether MHC class II expression by cIECs regulates intestinal and systemic Th cell frequencies, we compared colonic lamina propria (cLP) and MLN CD4$^+$ Th cell frequencies of aged H2-Ab1$^{fl/fl}$ and H2-Ab1^{VC} littermates. We found significantly increased CD4$^+$ Th cell frequencies and total numbers in the LP of H2-Ab1^{VC} mice compared to H2-Ab1$^{fl/fl}$ littermates (Figure 3.10 A and B, respectively). In contrast, CD4$^+$ Th cell frequencies in MLNs were comparable (data not shown). In addition, analysis of Treg frequencies in the LP and MLNs did not reveal any significant differences between the two groups (Figure 3.10 C, and data not shown). To investigate possible differences in inflammatory cytokine production, leukocytes from the LP and MLNs were restimulated with PMA and ionomycin. We found that the frequencies of both LP and MLN CD4$^+$ T cells secreting IFNγ, TNFα and IL-17A did not differ between H2-Ab1^{VC} and H2-Ab1$^{fl/fl}$ littermates (Figure 3.11 A-C, and data not shown). Thus, lack of MHC class II expression by cIECs led to

increased infiltration and/or accumulation of $CD4^+$ Th cells into the LP but did not modulate their pro-inflammatory cytokine production.

We also investigated whether deletion of MHC class II expression by IECs influenced MHC class II expression by professional APCs. We therefore assessed $B220^+$ and $CD11c^+$ cells for their MHC class I and II expression in the MLNs by flow cytometry (Figure 3.12 A and Figure 3.13 A). $B220^+$ cell frequencies (Figure 3.12 A) as well as MHC class I and II frequencies (Figure 3.12 B and C, respectively) were comparable between H2-$Ab1^{VC}$ and H2-$Ab1^{fl/fl}$ littermates. We also observed comparable $CD11c^+$ cell frequencies between H2-$Ab1^{fl/fl}$ and H2-$Ab1^{VC}$ littermates (Figure 3.13 B). $MHCI^+$ $CD11c^+$ cell frequencies were comparable, in contrast to $MHCII^+$ $CD11c^+$ cell frequencies, which showed a significant reduction in H2-$Ab1^{VC}$ mice compared to H2-$Ab1^{fl/fl}$ littermates (Figure 3.13 B and C, respectively). Together, these observations indicate that lack of MHC class II expression by cIECs leads to a reduction in $MHCII^+$ $CD11c^+$ cells in the MLNs.

Thus, ablation of MHC lass II expression in cIECs led to increased $CD4^+$ T cell frequencies in the cLP, but not to the spontaneous development of colonic intestinal pathology. In contrast, increased cell infiltration was detected in the caecum of H2-$Ab1^{VC}$ mice compared to H2-$Ab1^{fl/fl}$ littermates, which caused a significantly increased but low histopathological score. Therefore, lack of MHC class II expression by cIECs does not lead to the spontaneous development of severe caecal or colonic intestinal pathology.

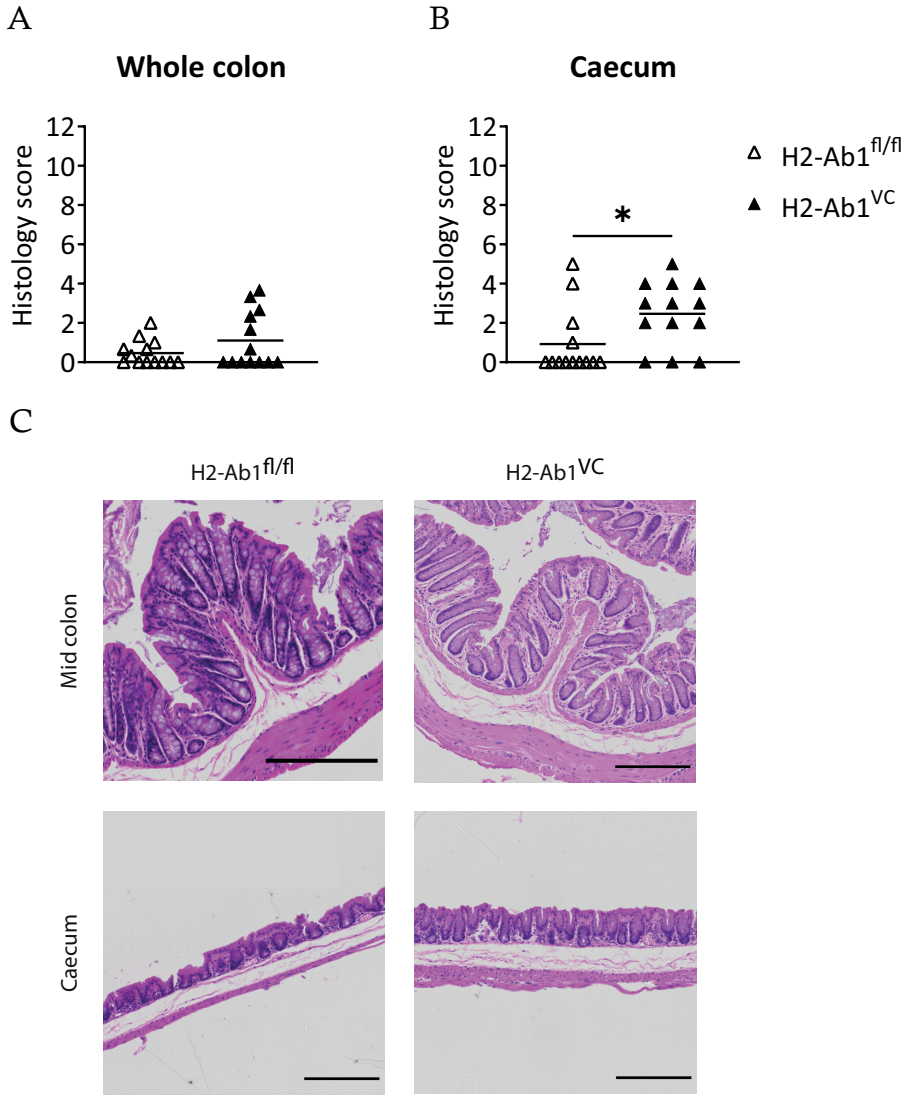


Figure 3.9: H2-Ab1^{VC} mice show low but significantly increased histopathology scores in the caecum. H2-Ab1^{VC} and H2-Ab1$^{fl/fl}$ mice were co-housed for around 11 to 12 months. Symbols denote individual histopathology scores of the whole colon (A) and caecum (B). Horizontal bars indicate group medians. Statistical significance between the groups was determined by Mann-Whitney test. P-value summary: *p<0.05. (C) Representative images of H&E stainings. Scale bars, 200 μm. Data from two pooled independent experiments with total mouse numbers per group as follows; n=11 H2-Ab1^{VC} and n=13 H2-Ab1$^{fl/fl}$ littermates.

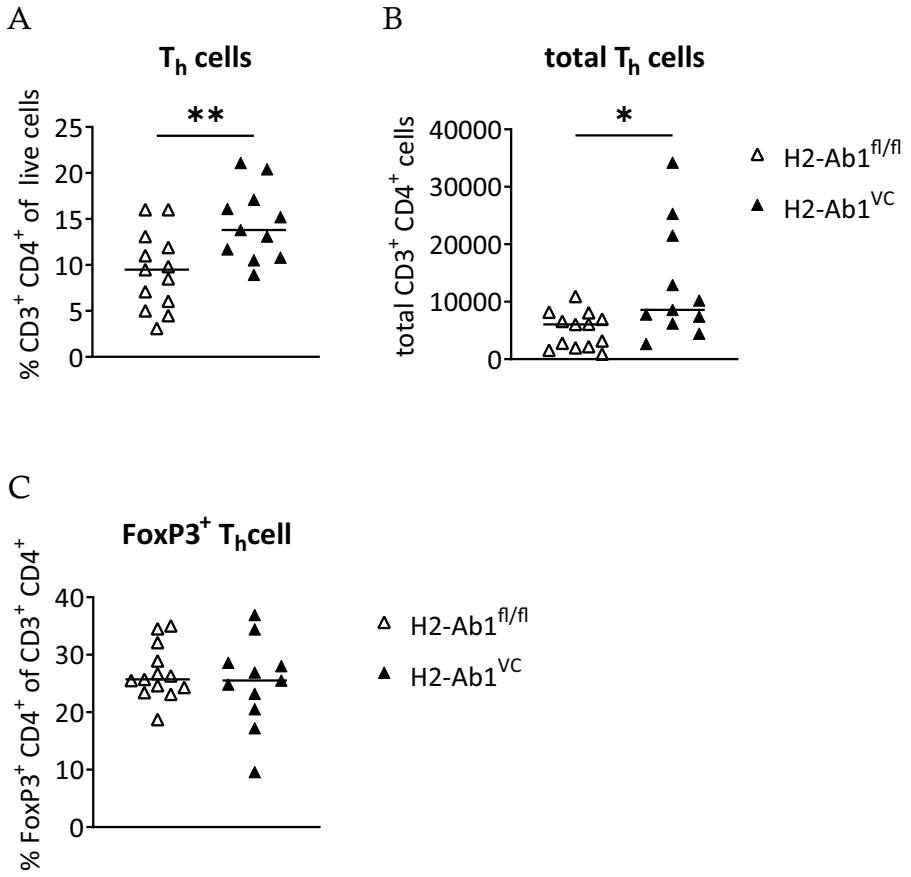


Figure 3.10: Increased Th cell frequencies and numbers in the colonic lamina propria of aged H2-Ab1^{VC} mice. H2-Ab1^{VC} and H2-Ab1$^{fl/fl}$ mice were co-housed for around 11 to 12 months. Symbols denote $CD4^+$ T cell frequencies (A) and numbers (B) as well as $FoxP3^+$ $CD4^+$ T cell frequencies (C) in the cLP of H2-Ab1^{VC} and H2-Ab1$^{fl/fl}$ littermates. Horizontal bars indicate group medians. Statistical significance between the groups was determined by Mann-Whitney test. P-value summary: *$p<0.05$; **$p<0.01$. Data from two pooled independent experiments with total mouse numbers per group as follows; n=11 H2-Ab1^{VC} and n=13 H2-Ab1$^{fl/fl}$ littermates.

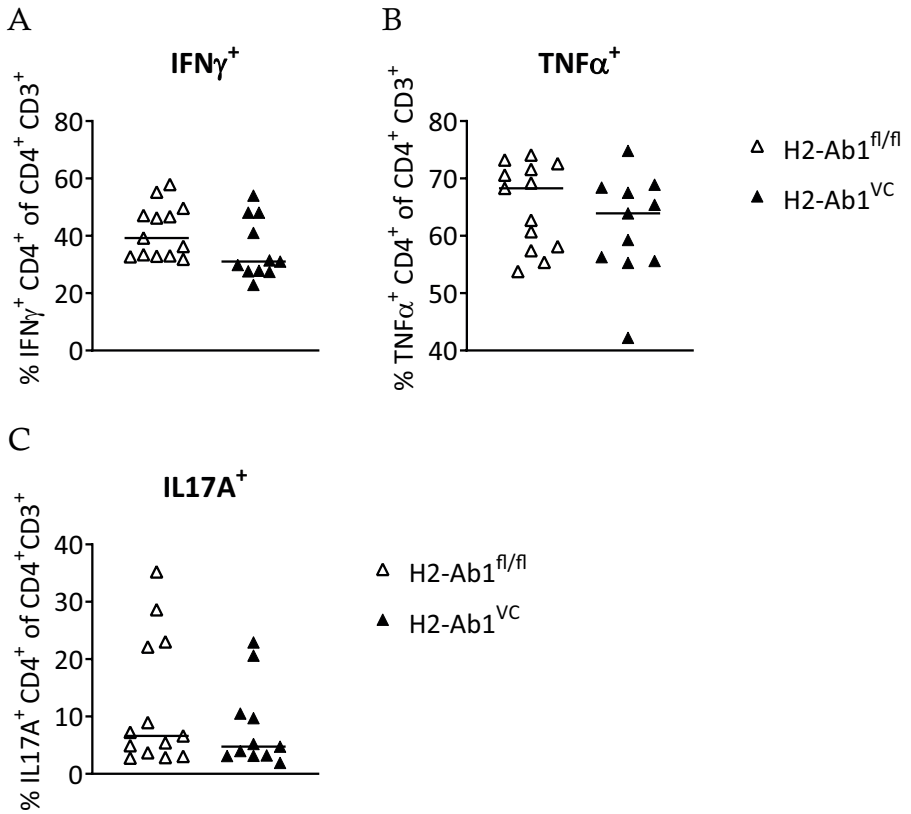


Figure 3.11: Comparable effector cytokine expression by colonic lamina propria CD4$^+$ T cells in aged H2-Ab1^{VC} and H2-Ab1$^{fl/fl}$ littermates. H2-Ab1^{VC} and H2-Ab1$^{fl/fl}$ mice were co-housed for around 11 to 12 months. Symbols denote IFNγ^+ (A), TNFα^+ (B) and IL-17A$^+$ (C) CD4$^+$ T cell frequencies in the cLP of H2-Ab1^{VC} and H2-Ab1$^{fl/fl}$ littermates. Horizontal bars indicate group medians. Statistical significance between the groups was determined by Mann-Whitney test. Data from two pooled independent experiments with total mouse numbers per group as follows; n=11 H2-Ab1^{VC} and n=13 H2-Ab1$^{fl/fl}$ littermates.

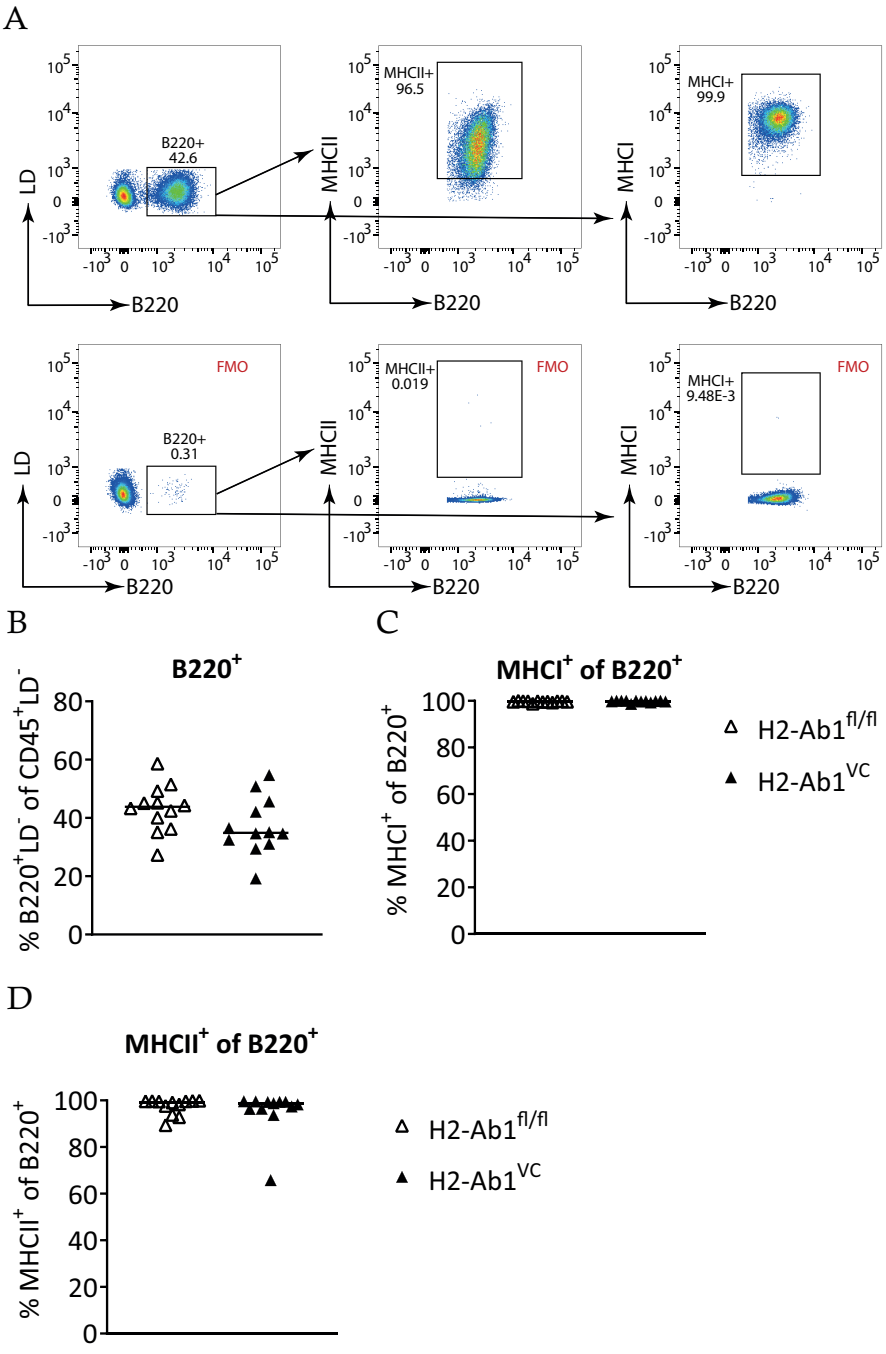


Figure 3.12: Lack of MHC class II expression by cIECs does not impact MHC class I and II expression by B220$^+$ cells in MLNs. H2-Ab1^{VC} and H2-Ab1$^{fl/fl}$ mice were co-housed for around 11 to 12 months and MHC class I and II expression by B220$^+$ cells in the MLNs analysed by flow cytometry (A). Symbols denote B220$^+$ cell frequencies (A) as well as MHC class I (B) and MHC class II frequencies (C) by B220$^+$ cells. Horizontal bars indicate group medians. Statistical significance between the groups was determined by Mann-Whitney test. Data from two pooled independent experiments with total mouse numbers per group as follows; n=11 H2-Ab1^{VC} and n=13 H2-Ab1$^{fl/fl}$ littermates.

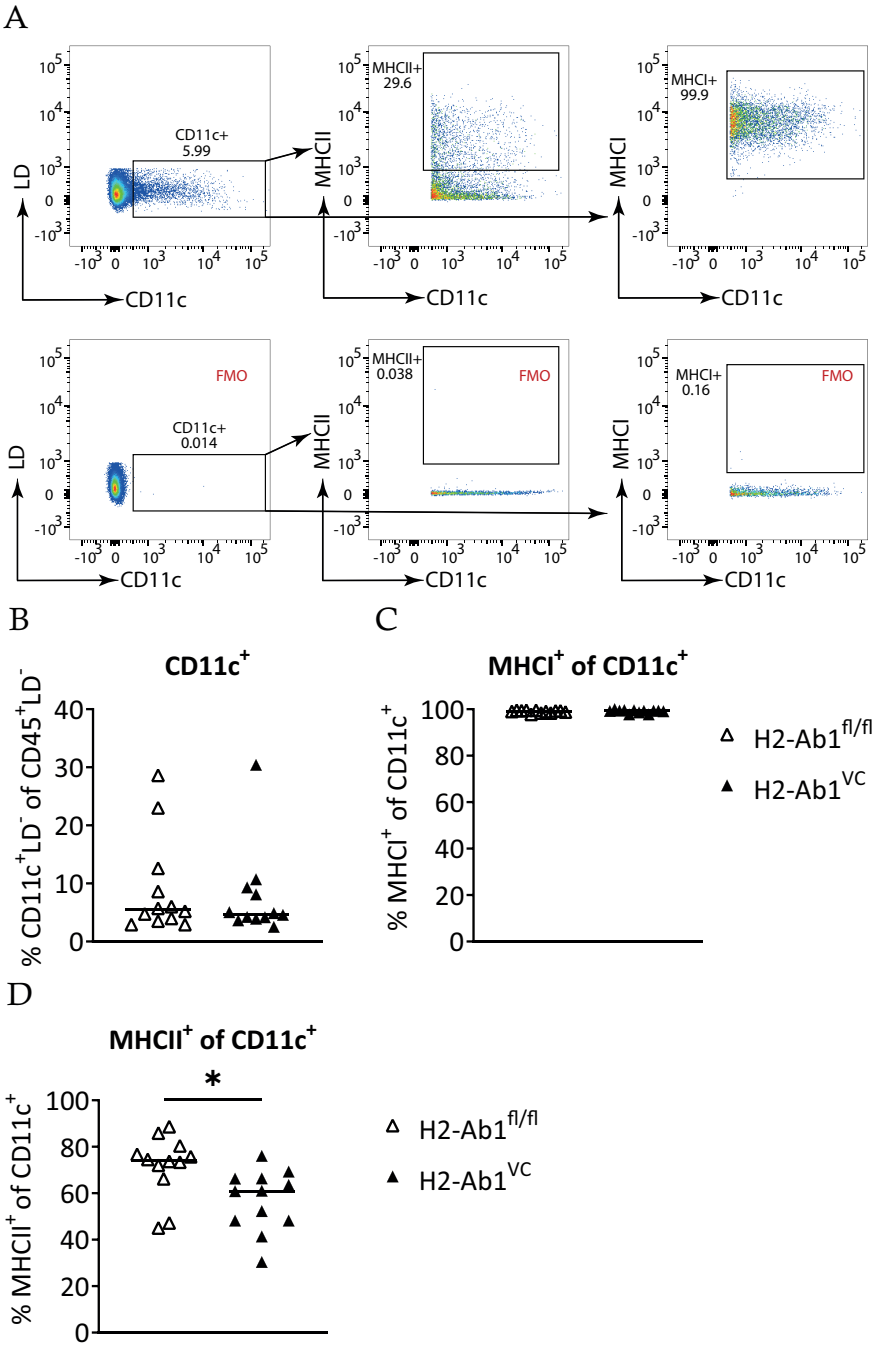


Figure 3.13: Reduced MHCII$^+$ CD11c$^+$ frequencies in the MLNs of aged H2-Ab1^{VC} mice. H2-Ab1^{VC} and H2-Ab1$^{fl/fl}$ mice were co-housed for around 11 to 12 months and MHC class I and II expression by CD11c$^+$ cells in the MLNs analysed by flow cytometry (A). Symbols denote CD11c$^+$ cell frequencies (A) as well as MHC class I (B) and MHC class II frequencies (C) by CD11c$^+$ cells. Horizontal bars indicate group medians. Statistical significance between the groups was determined by Mann-Whitney test. P-value summary: *p<0.05. Data from two pooled independent experiments with total mouse numbers per group as follows; n=11 H2-Ab1^{VC} and n=13 H2-Ab1$^{fl/fl}$ littermates.

3.3 Discussion

It is currently not known whether colonic IECs can function as non-conventional antigen presenting cells, thereby conveying environmental signals to the adaptive immune response to maintain intestinal homeostasis. In particular, it is unclear whether colonic IECs have the machinery to provide an activating signal to CD4 T cells through TCR signalling upon peptide:MHC class II molecule recognition. Previous work has demonstrated that MHC class II can be expressed by IECs, and MHC class II expression by IECs is likely to be dependent on the local microenvironment surrounding the IEC. Murine small intestinal IECs constitutively express MHC class II at steady state and upregulate its expression during intestinal inflammation [134], whereas murine colonic IECs lack MHC class II expression during homeostasis but also increase its expression during intestinal inflammation [137]. This raises the question whether different stimuli can induce MHC class II expression by IECs. The intestinal epithelium is exposed to different gradients along the length of the gastrointestinal tract. For example, siIECs are in contact with a high amount of food antigens but low amount of microbiota antigens, while this is inverted for colonic IECs (reviewed in [3]).

Our focus on the role of epithelial MHC class II expression was further motivated by studies showing MHC class II expression by IECs in IBD patients [135, 136, 138]. Human siIECs were described to constitutively express high levels of IEC MHC class II, especially at the tip of the villus [128, 130–133]. In contrast, MHC class II expression by human cIECs is absent under steady state condition [340]. Under inflammatory conditions, MHC class II is upregulated in both human small intestinal and colonic IECs [131, 135, 136, 138], which raises the question whether MHC class II expression by IECs modulates inflammatory CD4 T cell responses. Before we investigated the functional consequences of MHC class II expression by IECs, we first wanted to determine whether IECs have the machinery to function as non-conventional APCs. To this end, we established colonic organoids from H2-Ab1$^{fl/fl}$ and H2-Ab1^{VC} mice and assessed the potential of different cytokines

linked to intestinal inflammation to induce MHC class II expression in IECs. Here, we report that IFNγ is a potent inducer of IEC MHC class II expression in H2-Ab1$^{fl/fl}$ colonic organoids. In addition, IFNγ activated the expression of CIITA, the co-transactivator of MHC class II expression that regulates MHC class II expression in IECs.

CIITA is a highly specific and essential transactivator of MHC class II genes (reviewed in [349]). In non-haematopoietic cells, including IECs, CIITA expression is regulated by the pIV promoter, which is activated by IFNγ [346]. We therefore wanted to determine the temporal dynamics of CIITA and MHC class II expression in response to IFNγ stimulation in primary IECs and detected a rapid induction of CIITA mRNA expression within the first hour of IFNγ stimulation. The induction of CIITA expression preceded the activation of MHC class II mRNA expression, which is efficiently upregulated after 8 h of IFNγ stimulation. MHC class II protein expression was readily detectable after 16 h of IFNγ stimulation. These findings support the notion, that CIITA expression is rapidly induced upon IFNγ stimulation and that the transactivator in turn activates MHC class II mRNA expression in IECs. Waldburger et al [346] generated pIV knockout mice, which exhibited a selective loss of IFNγ-induced MHC class II expression by non-haematopoietic cells, highlighting CIITA as the key transactivator of MHC class II expression. In multiple other non-haematopoietic cell types, the ability to inhibit CIITA-dependent MHC class II expression has been linked to TGFβ [350], IL-1β [351] as well as the pathogens *chlamydia* [352] and *cytomegalovirus* [353, 354]. In addition, IFNγ induced CIITA expression in mouse microglia cells was shown to be inhibited by IL-4 and IL-10, though the molecular mechanism is not clear [355]. However, it remains to be determined, whether IFNγ-mediated MHC class II expression can be suppressed in IECs.

IECs can recognise components of microbes through TLRs and TLR signalling into epithelial cells allows IECs to adjust its innate immune responses towards

tolerogenic and inflammatory components of the gut microbiota. Importantly, innate immune responses of IECs are thought to be important in mediating the crosstalk between the gut microbiota and the host immune system. Polymorphisms in some of these receptors have been linked to increased incidence or pathogenesis of CD [356–358]. In addition, multiple studies suggest that TLR signalling in IECs plays a critical role in sensing and responding to microbial antigens [359–361]. The ability of IECs to sense microbial components and to express MHC class II raised the question whether TLR signalling in IECs could induce MHC class II expression by colonic IECs. We therefore stimulated colonic organoids with ligands for TLR1, TLR2, TLR3, TLR4, TLR5 or TLR9 and NOD2 but none of these ligands were able to induce MHC class II mRNA expression in primary cIECs.

At steady state, IFNγ production by small intestinal lamina propria lymphocytes is induced by IL-12 (mainly produced by macrophages) [137]. The microbiota has been proposed to induce MHC class II expression by siIECs, which is supported by the findings that antibiotic treatment of mice reduced both IL-12 levels and MHC class II expression by siIECs and by the absence of epithelial MHC class II expression in germ-free mice [137, 141]. Consistent with a requirement for microbial sensing, siIECs of MyD88-/- TRIF-/- mice do not express MHC class II at steady state or during inflammation [1, 137]. We used colonic primary IECs, but not small intestinal IECs, to test the ability of different TLR stimuli to induce MHC class II expression and differences in TLR expression between small intestinal and colonic IECs has been described. Price et al [107] reported the expression of TLR1, TLR2, TLR3, TLR4, and TLR5 (but not TLR9) in colonic IECs, and also in colonic organoids. In their hands, colonic organoids responded robustly to TLR2 and TLR5 agonists, but not to TRL3 or TLR4 stimulation [107]. However, this study did not investigate MHC class II expression in response to the TLR agonists tested [107]. All TLRs used in our study signal at least partially through MyD88, expect TLR3, which signals through the adaptor TRIF. They therefore use the same adaptor proteins for their signal transduction, which were described to induce MHC class

II expression in siIECs [137]. Lack of IEC MHC class II induction by the tested TLR ligands either suggests that they are indeed not able to induce MHC class II expression in colonic primary IECs. Or, it could also be possible that the TLRs are post-transcriptionally regulated or that the downstream signalling of TLRs is regulated by additional mechanisms to prevent overreaction of IECs towards the microbiota.

The following paragraph is my own work and has been published [1].

Whether IFNγ is the sole inducer of MHC class II expression on IECs is not entirely clear, particularly as MHC class II molecules were detected on siIECs in mice lacking IFNγR, highlighting potential IFNγ independent induction mechanisms [362]. However, expression of Ii and CIITA mRNA was low in IFNγR-deficient IEC [362], which might suggest reduced antigen presentation capabilities. In addition, a subsequent study reported that IFNγR-/- mice did not express MHC class II on IECs, which supports the importance of IFNγ as a critical inducer [137]. Different environmental factors of the IFNγ-/- mice in the different studies, such as diet and microbiota, might have contributed to these conflicting results. Indeed, the food antigen gliadin was shown to increase MHC class II expression by siIECs in coeliac disease [142, 143] and withdrawal of the antigen resulted in reduced siIEC MHC class II levels [131, 144]. However, the effects of gliadin are likely to have been indirect, as it can drive activation of IFNγ-secreting T cells that drive inflammation [363]. Cells which potentially release IFNγ in the intestine include innate lymphoid cells 1 (ILC1) [364], natural killer cells (NK) [137], natural killer T cells (NKT) [137], $\gamma\delta$ T cells [365], as well as conventional T cells ($CD4^+$ and $CD8^+$ T cells) [137]. During both homeostasis and inflammation, mice lacking adaptive and innate lymphocyte populations (Rag2-/- IL-2rg-/-) completely lacked MHC class II expression on siIECs, whereas those lacking conventional T cells only (Rag2-/-) showed reduced levels of MHC class II on siIECs [137]. Thus, it appears that both innate and adaptive lymphocytes contribute to IFNγ-dependent

induction of MHC class II on siIECs at steady state.

In order to present peptide on MHC class II molecules, which can be recognised by the adaptive immune system, IECs need to be able to take up and process peptides and load them onto MHC class II molecules. To assess the ability of primary cIECs to acquire and process antigen we used DQ™ Ovalbumin, which allows the monitoring of intracellular trafficking and processing of ovalbumin in living cells. Here, we show that primary cIECs are able to take up and process protein within 3 h, which was increased if colonic organoids were pre-stimulated with IFNγ. We used BMDCs as a professional APC comparison in our experiment and detected a rapid uptake of larger amounts of ovalbumin by BMDCs, which was evident already after 1 h and increased further within the next 2 h. Unsurprisingly, DCs are superior to IECs in their ability to take up and process peptides. Immature DCs are thought to acquire the majority of proteins through the internalisation of extracellular material through a non-specific process called macropinocytosis (reviewed in [366]). In addition to non-specific antigen uptake, APCs express several cell surface receptors that enable the uptake of antigen through clathrin-mediated endocytosis [160]. B cells mostly rely on receptor-mediated endocytosis for their antigen acquisition and show little macropinocytic activity [160]. The final and important process, through which APCs (especially DCs and macrophages) can take up antigen is phagocytosis, an endocytic process, which is initiated by the binding of opsonised particles to certain receptors on the surface of the phagocyte. This is followed by actin-dependent membrane reorganization around the particle, eventually forming an intracellular vesicle containing the ingested material [160, 162]. IECs have been described to endocytose entire commensals under inflammatory conditions or dysbiosis [367]. In addition, SFB has been shown to transfer antigens into IECs via an adhesion-directed endocytosis pathway at steady state, which contributed to the generation of both commensal-specific CD4 T cell responses and commensal-specific homeostatic Th17 cells [368]. These findings highlight, that

IECs can sample commensal antigens.

Conventional APCs can migrate through the tissue to sample their environment and acquire foreign antigen through the processes described above. In contrast, IECs are stationary and structurally polarized – their apical surface faces the intestinal lumen, while they are in contact with the lamina propria through their basolateral membrane. In our study we used 3D colonic organoids to assess the ability of primary cIECs to take up and process proteins. In this setting, cIECs will acquire protein from their basolateral membrane. It seems plausible that IECs show varying abilities to take up antigen from either the apical or basolateral membrane. Indeed, Hershberg et al [139] showed that, without additional activation, human colonic IEC-like cell lines were able to process and present antigen from their apical surface, but only in the presence of high concentrations of antigen[139]. A subsequent study from the same group determined, that transfection of a human colonic IEC-like cell line with CIITA, allowed IECs to take up and process antigen from both the basolateral and apical membrane [140]. Of interest, pre-stimulation of our 3D colonic organoids with IFNγ also increased the uptake and processing of ovalbumin, highlighting the ability of IECs to increasingly sample antigen from the lamina propria in inflammatory conditions. The increased sampling capacity of IECs during intestinal inflammation could be especially important for the restoration of homeostasis as it allows the adaptive immune system to react both to dysbiosis and inflammatory cues from the mucosa. Further studies could use 2D organoids to assess the ability of primary cIECs to acquire antigen from the apical membrane, which is in contact with microbial antigens *in vivo*.

In addition, our colonic organoids were grown in media supporting the maintenance of ISC rather than differentiated IECs. It could be possible that differentiated IECs are better equipped to take up and process antigen as they are located at the upper part of the colonic crypt and therefore in closer proximity to the microbiota. However, Biton et al [134] FACS-sorted EpCAM$^+$ siIECs, containing Lgr5$^+$ ISC, and assessed their antigen uptake and processing capacity with DQ™ Ovalbumin.

They detected that mainly ISC within the EpCAM$^+$ IECs were able to process the extracellular protein. These findings allow the suggestion that IECs are be able to present both self- and environmental-peptides, to inform the adaptive immune system not only about microbial communities but also about the health status of the host.

Our results show that primary cIECs are able to take up and process antigen, however it does not address whether IECs possess the molecular machinery to load the processed peptides onto the MHC class II molecule to be presented at the cell surface. Previous work of our own group (unpublished data) and other studies have shown that IECs do express important molecules of the MHC class II presentation pathway. It was demonstrated that in the presence of IFNγ, human colonic IEC-like cell lines express MHC class II, as well as Ii and HLA-DM on their cell surface [139]. This highlights that IECs express important molecules of the antigen processing pathway, an important feature of antigen presenting cells. In Chapter 6 we will address the question whether IECs can functionally present peptide to antigen-specific CD4 T cells.

The term inflammaging describes the chronic, sterile, low-grade inflammation, which is thought to contribute to the pathogenesis of age-related diseases (reviewed in [369]). Both self and non-self stimuli induce inflammaging, such as pathogens, endogenous cell debris and dysfunctional molecules, nutrients and gut microbiota [369]. These signals are recognised by distinct receptors and activate the innate immune response. We hypothesised that ageing leads to changes in the intestinal tissue and immune system and that the low-grade inflammation associated with ageing would lead to the induction of MHC class II expression by IECs. We therefore wanted to assess the importance of MHC class II expression by IECs in maintaining immune tolerance in aged mice. Here we report, that aged mice lacking IEC MHC class II expression experience increased infiltration of cells into the caecal but not the colonic mucosa, as assessed by histology. When we isolated LPL from the colon

we detected increased frequencies and numbers of $CD4^+$ T cells in mice lacking IEC MHC class II expression. This was however not reflected in changed $FoxP3^+$ $CD4^+$ T cells.

Age-related differences in the gut microbiota composition were observed in centenarians (100 years old) compared to younger adults (30 years old on average) and older humans (70 years old). The gut microbiota of centenarians showed a low diversity in its microbial composition. It was characterised by changes in the relative proportions of Firmicutes subpopulation, with a decrease in the *Clostridium* cluster XIVa and an increase in *Bacilli*. In addition, their gut microbiota is enriched in Proteobacteria, a group of facultative anaerobes containing bacteria defined as pathobionts [370, 371]. It is therefore possible that ageing is associated with an increase in pathobiont abundance. These opportunistic pro-inflammatory bacteria are thought to induce pro-inflammatory immune responses and if regulatory pathways are impaired in aged individuals, can lead to intestinal inflammation. *H. hepaticus* belongs to the Proteobacteria and has been described as a pathobiont. Future studies could colonise H2-$Ab1^{VC}$ mice with *H. hepaticus* and let them age. This could aid in understanding the role of IEC MHC class II expression in aiding the cross-talk between microbial communities and the adaptive immune system. Thus, in aged individuals environmental factors increasingly activate innate and adaptive immune responses. As IECs participate in the cross talk between the microbiota and immune cells, antigen presentation might be a critical mechanisms in modulating CD4 T cell responses and thereby intestinal homeostasis.

Colonic IECs do not express MHC class II expression at steady state [340] but caecal IECs do (see Figure 3.1 and [372]). It would therefore be possible that caecal IECs express MHC class II in aged mice, possibly even at higher levels than in younger mice. However, we did not measure MHC class II expression by cIECs in our aged mice. If we were to repeat these experiments, we would compare IEC MHC class II expression of aged versus young mice, in addition to assessing IEC

MHC class II in H2-Ab1$^{fl/fl}$ versus H2-Ab1^{VC} mice. In aged mice, IEC MHC class II deficiency could results in the impairment of the instruction of the adaptive immune system, potentially leading to the accumulation of immune cells in the caecal mucosa. However, we did not assess the specific cell type accumulating in caecal LP of our histology sections, so they could also be innate immune cells and further immuno-fluorescent imaging could shed light on the exact cell type. We did not detect increased accumulation of cells in colonic histological tissue sections of aged H2-Ab1^{VC} mice, but obtained increased CD4 T cell numbers from the colonic lamina propria of aged H2-Ab1^{VC} mice. Again, further studies could assess the colonic histological sections for the presence of CD4 T cells, to investigate whether the increased CD4 T cell numbers isolated from the cLP are also detectable in the colonic tissue sections of H2-Ab1^{VC} mice.

In addition, we assessed whether IEC MHC class II expression influenced CD4 T cell functions. We did not detect changes in the pro-inflammatory cytokine production of TNFα, IFNγ and IL-17A by CD4^{+} T cells of H2-Ab1$^{fl/fl}$ and H2-Ab1^{VC} mice. This suggests, that the pro-inflammatory cytokine production by CD4 T cells was not impaired in aged mice. It would be interesting to assess the overall tissue cytokine levels, to determine whether the ageing process resulted in increased pro-inflammatory cytokine levels in the intestinal tissue. It was described that inflammaging is associated with higher levels of IL-6, and epidemiologic studies of older adults assessed serum IL-6 levels and found that the age-associated increase in IL-6 was low to moderate and robustly associated with incident disease, disability and mortality (reviewed in [373]). It would therefore be interesting to assess IFNγ levels in the intestinal tissue of H2-Ab1$^{fl/fl}$ and H2-Ab1^{VC} mice, as activation of CD4 T cells through the recognition of the peptide:MHC class II complex on IECs could induce tolerogenic responses and thereby maintain tolerance. As we saw an accumulation of CD4 T cells in the colonic lamina propria of H2-Ab1^{VC} mice but no differences in their pro-inflammatory cytokine production, it would also be plausible that CD4 T cells of H2-Ab1$^{fl/fl}$ and H2-Ab1^{VC} mice produce comparable levels of

cytokines but that the increase in cell number within the mucosa of H2-Ab1^{VC} mice results in an increased absolute amount of cytokines released into the tissue and thereby negatively influence intestinal homeostasis.

When we assessed the MHC class II expression by CD11c^{+} cells in MLNs, we detected a small reduction in MHC class II expression in H2-Ab1^{VC} compared to H2-Ab1$^{fl/fl}$ litter mates. Stephens et al [374] reported that small intestinal CD11c^{+} mononuclear phagocytes (MNP) of H2-Ab1^{VC} mice showed a marked reduction in MHC class II expression, highlighting the possibility of MNPs to acquire MHC class II molecules from siIECs. It was further shown that the MHC class II molecules could be acquired both by cell-contact-dependent and cell-contact-independent mechanisms. The lack of siIEC MHC class II expression caused a reduction of Helios^{-} microbial-responsive Tregs, suggesting that MHC class II expression by IECs is important in maintaining microbiota-induced Tregs [374]. This highlights, that next to direct interaction with CD4 T cells, MHC class II expressing IECs could potentially transmit peptide:MHC class II complexes to MNP by exosomes, trogocytosis or efferocytosis (phagocytosis of dying IECs) [375].

Stephens et al [374] also showed that loss of MHC class II expression by IECs influenced T cell-dependent antibody responses. They detected a more even distribution of Ig clonotypes in H2-Ab1^{VC} mice than in H2-Ab1$^{fl/fl}$ littermate controls, which were dominated by a single clone. The Ig repertoire of H2-Ab1^{VC} mice showed a decreased proportion of IgA, suggesting they produce less high-affinity IgA toward intestinal microbes. This might impair the ability of the adaptive immune system to respond adequately to the microbial communities.

Altogether, we were able to show that IFNγ is a potent inducer of MHC class II expression in IECs. In addition, IECs take up and process antigen, thereby possessing an important prerequisite to function as non-conventional antigen presenting cells. In the context of ageing, where chronic inflammation can trigger MHC class II

upregulation, MHC class II on IECs protects from inflammatory cell infiltration. These results support future work to study the adaptive immune response in the context of MHC class II sufficient and deficient IECs. We do not propose that IECs replace professional APCs, rather that IEC MHC class II expression modulate the phenotype and function of already activated CD4 T cells within the mucosa.

4

Role of MHC class II expression by small intestinal IECs

Contents

4.1 Introduction 103
4.2 Results 105
4.2.1 MHC class II is increasingly expressed by IECs along the small intestinal tract 105
4.2.2 MHC class II expression by siIECs is important for CD8$\alpha\alpha^+$ CD4$^+$ IEL homeostasis 108
4.3 Discussion 114

4.1 Introduction

In Chapter 3, we showed that IECs have some of the key features to function as non-conventional APCs. We additionally described that the lack of IEC MHC class II expression resulted in increased CD4 T cell frequencies and numbers in the colonic lamina propria of aged mice, suggesting the potential of IECs to modulate CD4 T cell phenotype and function via MHC class II expression. Next, we turned to the small intestine to investigate the role of siIEC MHC class II expression in maintaining intestinal homeostasis. In contrast to the colon, siIECs constitutively express MHC class II at steady state, both in humans and mice [128, 130–134]. Similar to cIECs,

MHC class II expression by siIECs is upregulated under inflammatory conditions [134, 137]. MHC class II expression by siIECs was shown to play a key role in experimental GvHD [137]. GvHD is mediated by mature donor T cells responses initiated upon recognition of host alloantigens, which cause severe inflammation in several tissues, especially the small intestine [376]. Koyama and colleagues [137] used mice deficient in IEC MHC class II expression and found that antigen presentation by siIECs activated donor $CD4^+$ T cells, which caused GvHD-induced lethality *in vivo* [137]. MHC class II expression by siIECS was induced by the IL-12-IFNγ-cytokine axis, and it was shown that the IFNγ response by LPLs was driven by IL-12 secretion from myeloid cells [137]. Therapeutic targeting of this pathway by blockade of IL-12/23p40 led to decreased lethality [137]. MHC class II expression by siIECs is driven by the microbiota, as germ-free mice lacked IEC MHC class II expression [137]. Microbiota is thought to induce epithelial MHC class II expression via TLRs, as mice lacking the TLR adaptors MyD88 and TRIF, lacked MHC class II expression [137, 377]. The role of the microbiota in inducing MHC class II expression in siIECs, was supported by studies, showing that antibiotic treatment of mice was accompanied by a reduction in siIEC MHC class II expression [377].

The ability of the microbiota to induce MHC class II expression on siIECs was further shown to be dependent on the feeding rhythm, which resulted in a diurnal MHC class II expression pattern of siIECs [372]. The diurnal expression pattern of MHC class II expression by siIECs was lost in germ free mice or mice lacking core circadian clock genes. In addition, the diurnal expression pattern was shifted if mice were subjected to time-restricted feeding to either the dark or the light phase of a 24 h day cycle [372]. The dietary composition was shown to be an important driver of siIEC MHC class II expression, as a high fat diet (HFD) led to a marked reduction of MHC class II expression and loss of diurnal expression pattern [372].

The marked reduction of siIEC MHC class II expression caused by a HFD was shown to be mediated through the down-regulation of the PRRs TLR2 and NOD2, as well as IFNγ induced genes in ISCs [377]. Indeed, IFNγ levels were reduced in the intestinal tissue of HFD mice [377]. Two distinct ISC subsets were described to express high levels of MHC class II, both of which were highly proliferative and able to take up and process antigen [134].

The described studies highlight the intricate cross-talk between siIECs and the microbiota, which influences antigen presentation by siIECs. As highlighted above, siIEC MHC class II expression leads to the activation of CD4 T cell effector responses in the inflammatory setting of GvHD [137]. However, MHC class II expression was also described to support the IL-10 production of $CD4^+$ IELs [372]. IL-10^+ $CD4^+$ IELs contributed to epithelial barrier functions and H2-$Ab1^{VC}$ mice subjected to T-cell transfer colitis developed intestinal inflammation, associated with increase barrier permeability and reduced frequencies of IL-10^+ $CD4^+$ IELs [372]. These results suggest that siIEC MHC class II expression plays a protective role in T-cell transfer mediated colitis, in part mediated by tolerogenic responses by $CD4^+$ IELs.

We therefore wanted to investigate whether siIEC MHC class II expression plays an important role in the accumulation of $CD4^+$ IEL populations in the small intestine at steady state and whether it influences $CD4^+$ IEL functions.

4.2 Results

4.2.1 MHC class II is increasingly expressed by IECs along the small intestinal tract

In contrast to cIECs, siIECs express MHC class II at steady state and we wanted to investigate whether loss of MHC class II expression by siIECs modulates the $CD4^+$ T cells located in the intraepithelial compartment. As the tissue imprinting might differ along the small intestinal tract, we divided it into three equal sized sections for

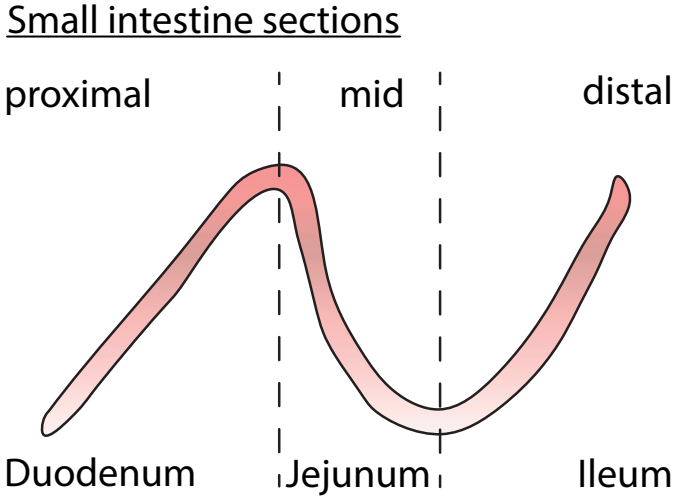


Figure 4.1: Schematic of small intestinal sections. Schematic of the small intestinal tract, which was divided into three equal sized tissue sections for subsequent analysis: duodenum (D), jejunum (J) and ileum (I).

our analysis. We named the proximal part duodenum (D), the middle part jejunum (J) and the distal part ileum (I) (see Figure 4.1). In humans, the duodenum is the first small part of the small intestine and approximately 25 cm long, so the separation used here does not adequately reflect the human small intestinal anatomy.

We first assessed MHC class II expression by siIECs along the small intestinal tract of H2-Ab1$^{fl/fl}$ mice by flow cytometry (Figure 4.2 A). We detected a gradual increase in MHCII$^+$ EpCAM$^+$ cell frequencies when moving from the duodenum (around 40 % MHCII$^+$ IECs) towards the ileum (80-90 % MHCII$^+$ IECs) (Figure 4.2 B). In addition, when analysing the MFI of MHCII$^+$ siIECs, we detected a 4- to 5-fold increase in MHC class II expression levels in the ileum compared to the duodenum of H2-Ab1$^{fl/fl}$ mice (Figure 4.2 C and D). However, no siIEC MHC class II expression was detected in H2-Ab1^{VC} mice (Figure 4.2 C and D). These results indicate that there is a gradient of increasing MHC class II expression by siIECs from the proximal to the distal area of the SI.

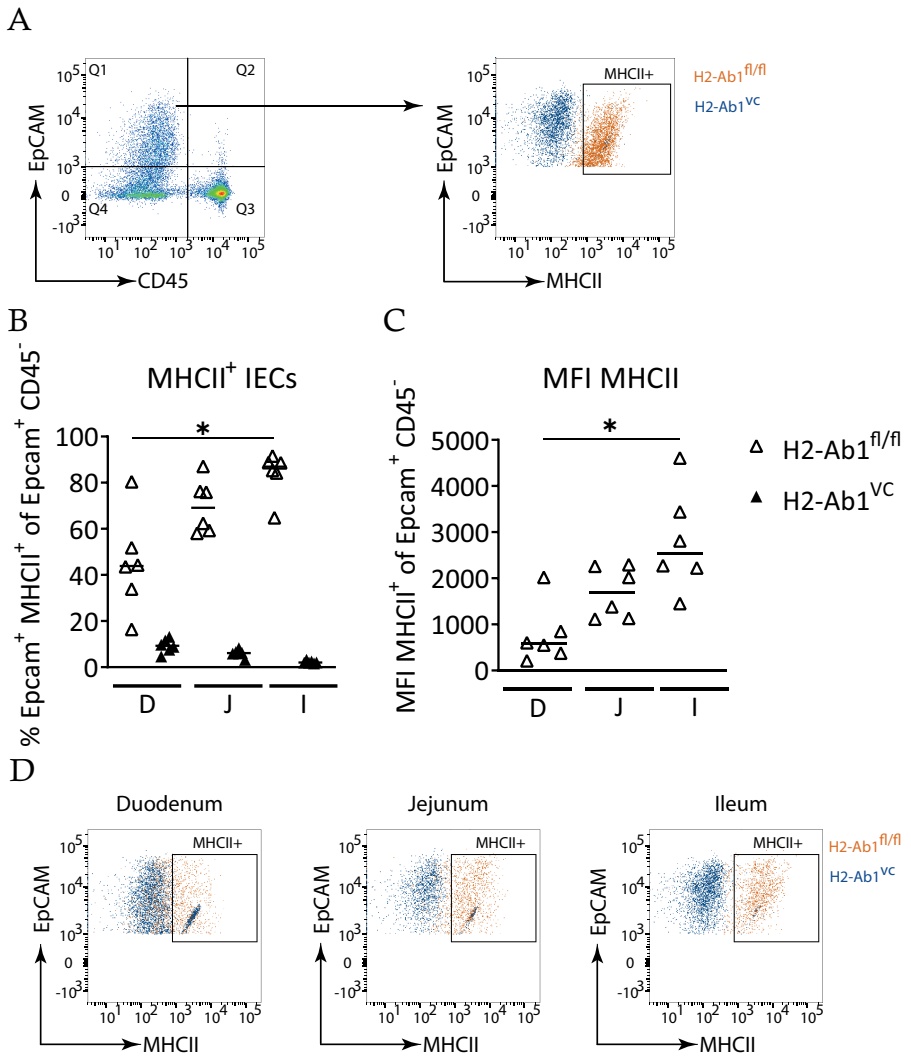


Figure 4.2: SiIECs show increased MHC class II expression in the distal area of the SI. (A) SiIECs were isolated from the duodenum (D), jejunum (J) and ileum (I) and analysed by flow cytometry. MHCII$^+$ EpCAM$^+$ siIEC frequencies (B) and MFI of MHCII$^+$ siIECs (C) were assessed. (D) Representative FACS plots of MHCII$^+$ IECs from the duodenum (left), jejunum (middle) and ileum (right). Horizontal bars indicate group medians. Statistical significance between the H2-Ab1$^{fl/fl}$ groups was determined by Friedman test, with Dunn's multiple comparisons. P-value summary: *p<0.05. Representative data from one of two independent experiments with total mouse numbers per group as follows; n=6 H2-Ab1^{VC} and n=6 H2-Ab1$^{f/fl}$ littermates. Mice were housed in the new SPF-B animal facility.

4.2.2 MHC class II expression by siIECs is important for CD8$\alpha\alpha^+$ CD4$^+$ IEL homeostasis

Next, we wanted to investigate whether antigen presentation by siIECs via MHC class II modulates CD4$^+$ IEL populations residing in the epithelial layer. We isolated IELs from the duodenum, jejunum and ileum of H2-Ab1$^{fl/fl}$ and H2-Ab1^{VC} littermates and assessed IEL subset frequencies by flow cytometry (Figure 4.3 A). Although we did not detect significant changes in the total CD4$^+$ TCRβ^+ IEL populations in the different sites of H2-Ab1$^{fl/fl}$ and H2-Ab1^{VC} littermates, there was a general trend towards reduced frequencies in the latter (Figure 4.3 B). Moreover, we detected a trend towards reduced CD8$\alpha\alpha^+$ CD4$^+$ IEL frequencies in the jejunum, alongside significantly reduced frequencies of this IEL subset in the ileum of H2-Ab1^{VC} mice compared to H2-Ab1$^{fl/fl}$ littermates (Figure 4.3 C). Consistent with this, we found significantly reduced CD8$\alpha\alpha^+$ CD4$^+$ IEL cell numbers in the ileum of H2-Ab1^{VC} mice compared to H2-Ab1$^{fl/fl}$ littermates (data not shown). In contrast, we observed that CD8$\alpha\beta^+$ CD4$^+$ IEL frequencies were low and comparable along the small intestinal tract of H2-Ab1$^{fl/fl}$ and H2-Ab1^{VC} littermates (Figure 4.3 D). Finally, we found that the reduction of CD8$\alpha\alpha^+$ CD4$^+$ IEL frequencies was counterbalanced by a significant increase in conventional CD8$^-$CD4$^+$ IEL frequencies in the ileum of H2-Ab1^{VC} mice compared to H2-Ab1$^{fl/fl}$ littermates (Figure 4.3 D). We did not observe any consistent changes in CD4$^-$ TCR$\gamma\delta^+$ or CD4$^-$ TCRβ^+ IEL populations between H2-Ab1^{VC} and H2-Ab1$^{fl/fl}$ littermates (data not shown). Taken together, these results show that MHC class II expression by siIECs is important for the maintenance of CD8$\alpha\alpha^+$ CD4$^+$ IELs in the ileum.

We then wanted to investigate whether MHC class II expression by siIECs modulates conventional CD8$^-$CD4$^+$ IEL subsets. We analysed GATA, FoxP3 and RoRγt expression and detected comparable GATA3$^+$ CD8textsuperscript-CD4$^+$ IEL frequencies along the small intestinal tract of H2-Ab1$^{fl/fl}$ and H2-Ab1^{VC} littermates (Figure 4.4 A). However, we detected significantly increased frequencies of FoxP3$^+$ CD8$^-$CD4$^+$ IEL and of RoRγt$^+$ CD8$^-$CD4$^+$ IEL in the ileum of H2-Ab1^{VC} mice

compared to H2-Ab1$^{fl/fl}$ littermates (Figure 4.4 B and C). Further analyses of FoxP3^{+} RoRγt^{-}, FoxP3^{+} RoRγt^{+} and FoxP3^{-} RoRγt^{+} subsets within the conventional CD8^{-}CD4^{+} IEL population revealed trends towrds increased frequencies of all three subsets in the ileum of H2-Ab1^{VC} mice, which reached statisitical significance for the FoxP3^{-} RoRγt^{+} subset (Figure 4.4 D-F). Overall, these data indicate that MHC class II expression by siIECs in the ileum plays an important role in limiting FoxP3 and RoRγt expression by conventional CD8^{-}CD4^{+} IELs.

As CD8$\alpha\alpha^{+}$ IEL cell frequencies and cell numbers were low in H2-Ab1^{VC} mice it was challenging to analyse potential differences in subsets of these cells in H2-Ab1^{VC} compared to H2-Ab1$^{fl/fl}$ littermates. We therefore FACS sorted 2000 CD8$\alpha\alpha^{+}$ and conventional CD8^{-}CD4^{+} IELs from H2-Ab1^{VC} and H2-Ab1$^{fl/fl}$ littermates and assessed their expression of lineage associated transcription factors and effector molecules by RT-qPCR. We detected a trend towards higher Runx3 mRNA expression in CD8$\alpha\alpha^{+}$ CD4^{+} IELs compared to conventional CD8^{-}CD4^{+} IELs (Figure 4.5 A). In addition, it appeared that CD8$\alpha\alpha^{+}$ IELs in H2-Ab1^{VC} mice expressed higher Runx3 mRNA levels than in H2-Ab1$^{fl/fl}$ littermates (Figure 4.5 A). Furthermore, we observed that T-bet expression levels were comparable between conventional CD8^{-}CD4^{+} IELs in both H2-Ab1^{VC} and H2-Ab1$^{fl/fl}$ littermates, although the CD8$\alpha\alpha^{+}$ IELs in H2-Ab1^{VC} mice trended towards higher T-bet expression (Figure 4.5 B). We also assessed CD8α expression levels to confirm our FACS sorting strategy and, as expected, found markedly higher expression levels in CD8$\alpha\alpha^{+}$ than in conventional CD8^{-}CD4^{+} IELs of H2-Ab1^{VC} and H2-Ab1$^{fl/fl}$ littermates (Figure 4.4 C). Lastly, we assessed expression levels of the effector molecule granzyme B and detected a trend towards higher granzyme B expression CD8$\alpha\alpha^{+}$ IELs compared to conventional CD4^{+} IELs in both H2-Ab1^{VC} and H2-Ab1$^{fl/fl}$ littermates (Figure 4.5 D). In summary, these findings confirm that CD8$\alpha\alpha^{+}$ IELs and conventional CD4^{+} IELs have distinct expression profiles. Although our results suggested that CD8$\alpha\alpha^{+}$ IELs in H2-Ab1^{VC} mice may express higher levels of Runx3, T-bet and granzyme B, the preliminary nature of these experiments means

that further confirmation is required.

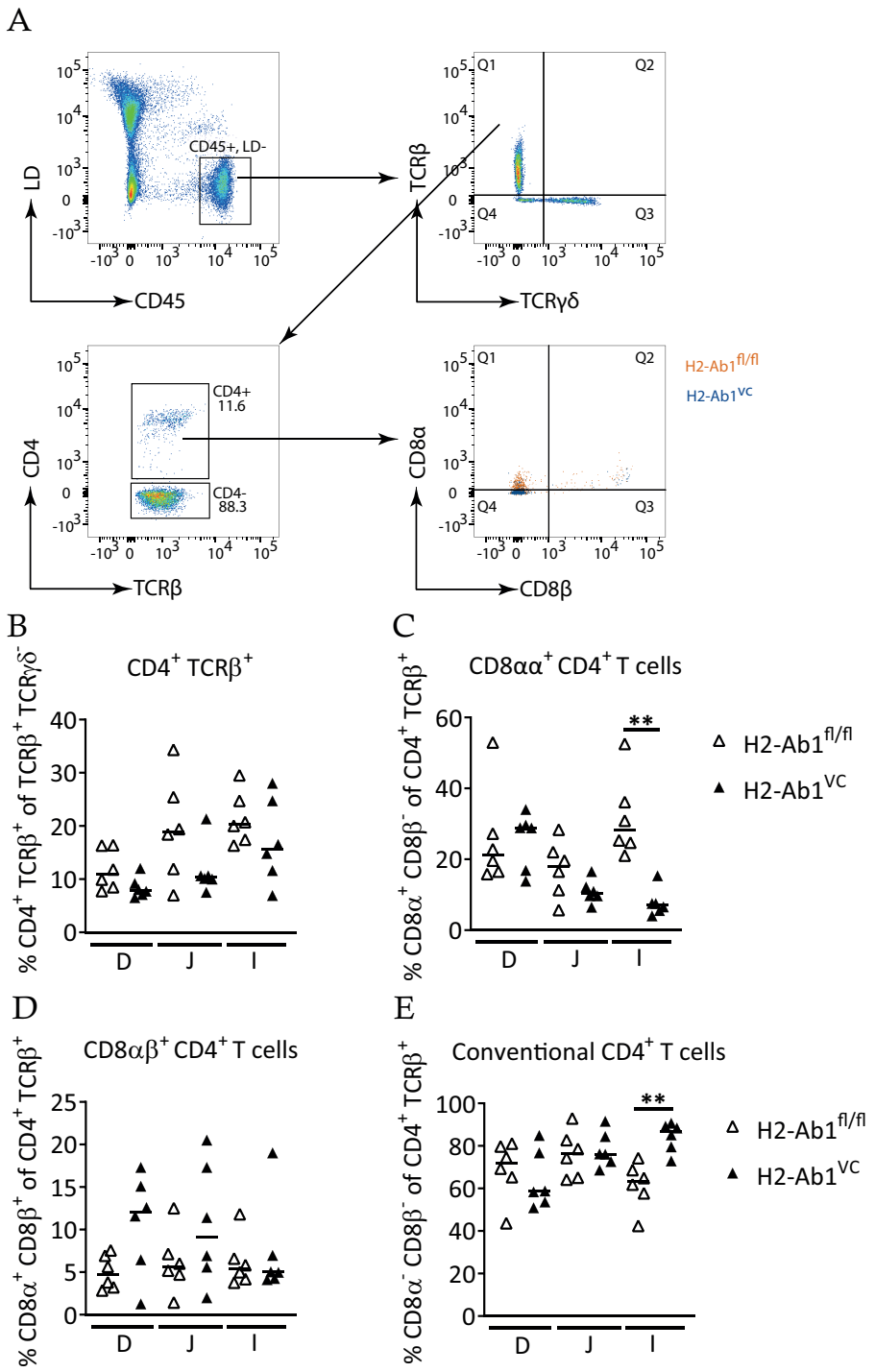


Figure 4.3: Significantly reduced CD8$\alpha\alpha^+$ CD4$^+$ IEL frequencies and increased conventional CD4$^+$ IEL frequencies in the ileum of H2-Ab1^{VC} mice. (A) SiIELs were isolated from the duodenum (D), jejunum (J) and ileum (I) and analysed by flow cytometry. Symbols denote CD4$^+$ (B), CD8$\alpha\alpha^+$ (C), CD8$\alpha\beta^+$ (D) and CD8$\alpha\beta^-$ (E) IEL frequencies. Horizontal bars indicate group medians. Statistical significance between the groups was determined by Mann-Whitney test. P-value summary: **p<0.01. Representative data from one of two independent experiments with total mouse numbers per group as follows; n=6 H2-Ab1^{VC} and n=6 H2-Ab1$^{f/fl}$ littermates. Mice were housed in the new SPF-B animal facility.

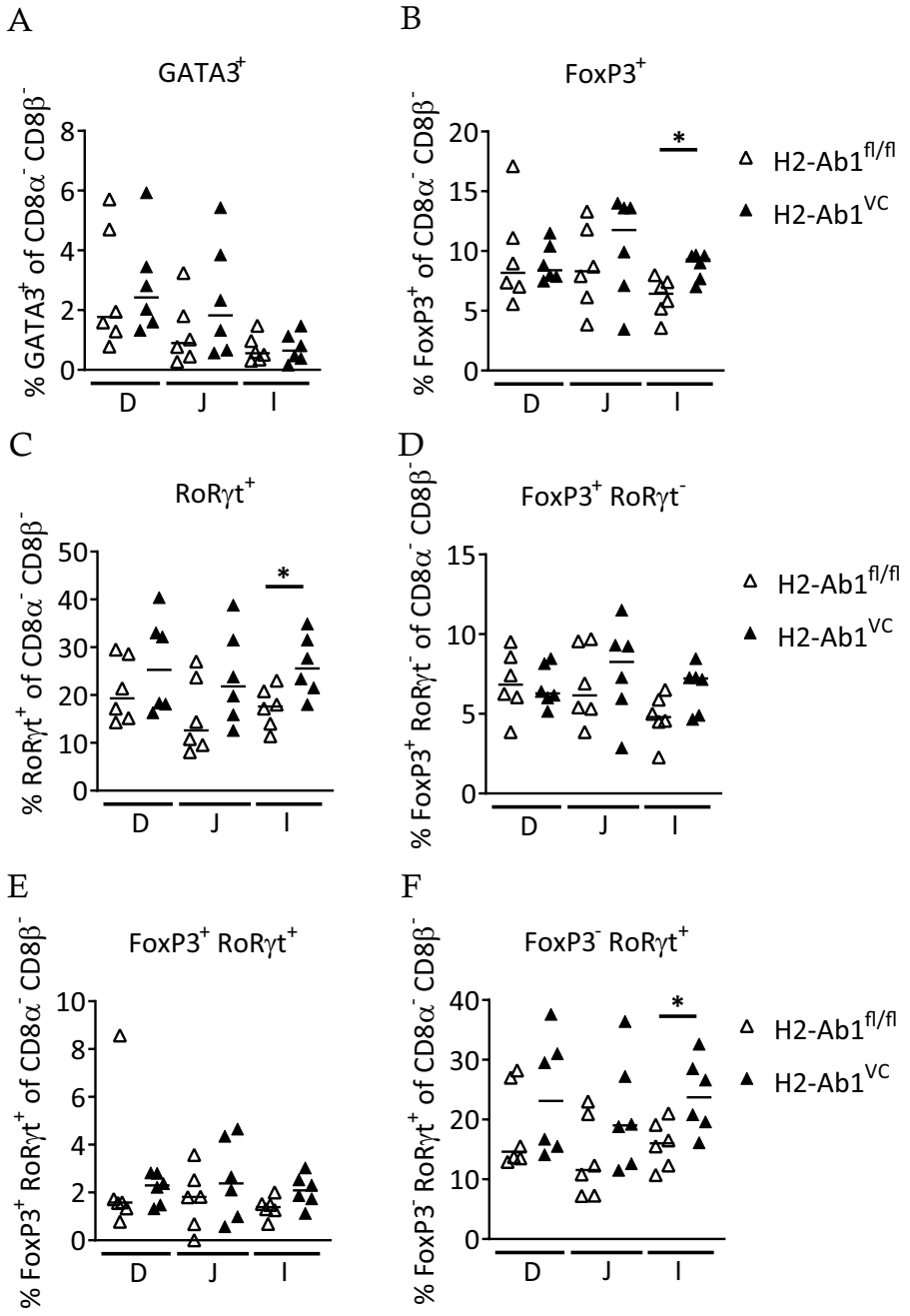


Figure 4.4: Increased FoxP3 and RoRγt expression by conventional CD4$^+$ IELs in the ileum of H2-Ab1^{VC} mice. Conventional CD4$^+$ IELs were isolated from the duodenum (D), jejunum (J) and ileum (I) and transcription factor expression analysed by flow cytometry. Symbols denote GATA3$^+$ (A), FoxP3$^+$ (B), RoRγt$^+$ (C) as well as FoxP3$^+$ RoRγt$^-$ (D), FoxP3$^+$ RoRγt$^+$ (E) and FoxP3$^-$ RoRγt$^+$ (F) conventional CD4$^+$ IEL frequencies. Horizontal bars indicate group medians. Statistical significance between the groups was determined by Mann-Whitney test. P-value summary: *$p<0.05$. Representative data from one of two independent experiments with total mouse numbers per group as follows; n=6 H2-Ab1^{VC} and n=6 H2-Ab1$^{f/fl}$ littermates. Mice were housed in the new SPF-B animal facility.

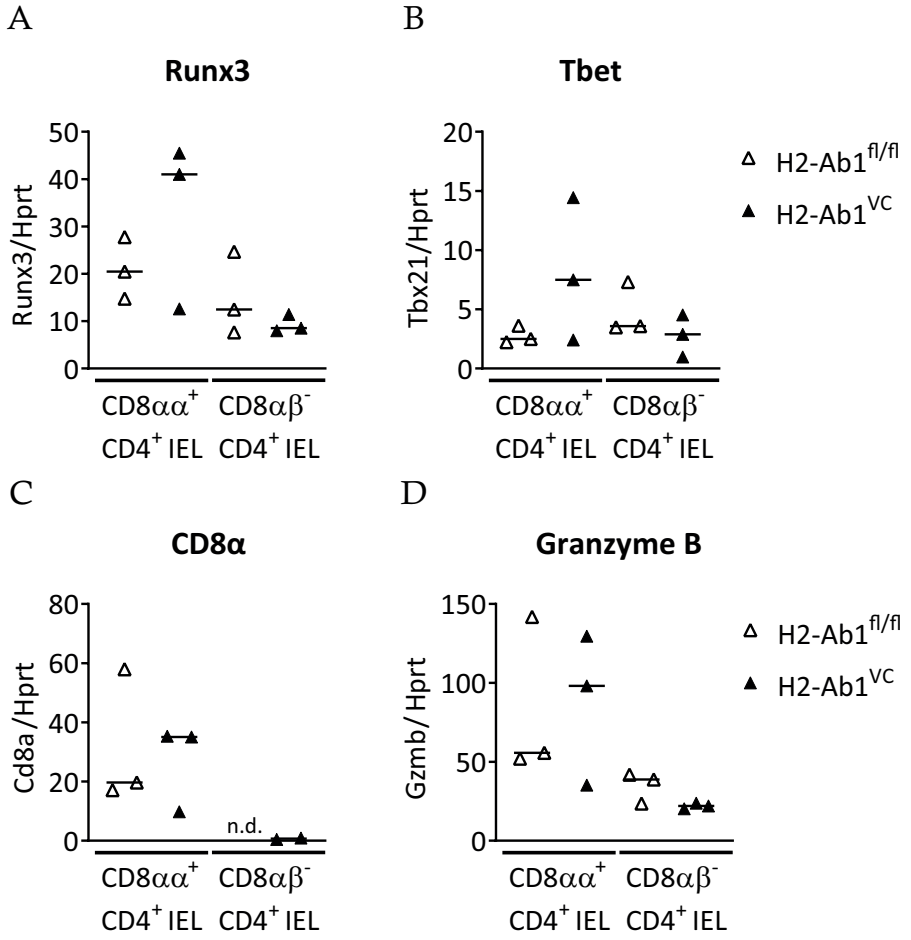


Figure 4.5: Effector function analysis of CD8$\alpha\alpha^+$ and conventional CD4$^+$ IELs in the ileum. 2000 CD8$\alpha\alpha^+$ and conventional CD4$^+$ IELs were FACS sorted and RNA was isolated. Runx3 (A), T-bet (B), CD8α (C) and granzyme B (D) mRNA expression levels were measured by RT-qPCR. Gene induction was normalised to the house-keeping gene Hprt. RT-qPCR experiments were performed in technical duplicates. N.d.; not detectable. Data from one experiment with total mouse numbers per group as follows; n=3 H2-Ab1^{VC} and n=3 H2-Ab1$^{f/fl}$ littermates. Mice were housed in the new SPF-B animal facility.

4.3 Discussion

The SI microbiota plays a central role in inducing siIEC MHC class II expression, which is partly mediated through the recognition of microbial antigens via IEC PRRs. MHC class II expression by siIECs follows a diurnal rhythm, which is influenced by diet composition and rhythmicity. This dynamic cross-talk between the host and the microbiota allows the host do adapt its immune responses to an anticipated increase in luminal antigens [372].

Here, we report that MHC class II expression by siIECs increases from the proximal to the distal area of the small intestine. This was both reflected in increased frequencies of $MHCII^+$ IECs and increased MHC class II MFI. This increase in MHC class II expression by siIECs from the proximal to the distal area of the small intestine was either confirmed [137, 378] or contradicted [372] by different studies. These discrepancies in the siIEC MHC class II gradient could be due to differences in the murine microbial communities or dietary compositions at the different animal facilities. Indeed, it was shown that distinct commensals can induce or suppress siIEC MHC class II expression [372]. *Akkermansia*, Lachnospiraceae and SFB belonged to the siIEC MHC class II "inducers" and are mucosa-associated bacteria which actively attach to siIEC, while *Lactobacillus Murinus* belonged to the "suppressors" [372]. The attachment of SFB to siIECs subsequently leads to cell division control protein 42 homolog (CDC42)-mediated microbial adhesion triggered endocytosis [368]. CDC42-deficiency resulted in the loss of diurnal siIEC MHC class II expression pattern, as well as a depletion of MHC class II "inducer" bacteria, such as SFB and *Akkermansia* [372]. These results suggest, that CDC42-mediated endocytosis contributes to siIEC MHC class II expression.

We further assessed the impact of siIEC MHC class II expression on $CD4^+$ IEL populations. Here, we report that loss of IEC MHC class II expression in the ileum resulted in a near loss of the $CD8\alpha\alpha^+$ $CD4^+$ IEL population. This loss was counter-balanced by an increase in conventional $CD4^+$ IELs in the ileum of H2-$Ab1^{VC}$

mice. Interestingly, these conventional $CD4^+$ IELs showed increased expression of the TF FoxP3 or RoRγt in H2-$Ab1^{VC}$ compared to H2-$Ab1^{fl/fl}$ littermate controls.

These findings are in accordance with multiple studies, which also reported that loss of siIEC MHC class II expression results in the marked reduction of $CD8\alpha\alpha^+$ $CD4^+$ IELs [378, 379]. Bilate et al [379] showed that TCR signalling and antigen presentation by siIECs are required for $CD8\alpha\alpha^+$ $CD4^+$ IEL differentiation in the epithelium. However, TCR signalling was not critical for $CD8\alpha\alpha^+$ $CD4^+$ IEL maintenance in the epithelial niche [379]. They further showed that both Treg and Teff cells migrate into the intestinal epithelium and can differentiate into $CD8\alpha\alpha^+$ $CD4^+$ IELs [379]. Terminally differentiated $CD8\alpha\alpha^+$ $CD4^+$ IELs showed reduced TCR diversity, suggesting that their differentiation process favours certain TCR specificities, possibly mediated by IEC antigen presentation. $CD8\alpha\alpha^+$ $CD4^+$ IELs shared TCR specificities with Treg and Teff cells, implicating a lineage relationship between them [379]. Indeed, multiple studies revealed that $CD8\alpha\alpha^+$ $CD4^+$ IELs originate from conventional $CD4^+$ T cells [380–382].

This lineage relationship could explain, why we see an increase in conventional $CD4^+$ IELs expressing increased FoxP3 or RoRγt. The lack of siIEC MHC class II expression could result in an accumulation of conventional $CD4^+$ IELs, unable to further differentiate into $CD8\alpha\alpha^+$ $CD4^+$ IELs. And as $CD8\alpha\alpha^+$ $CD4^+$ IEL were shown to develop from both Treg and Teff cells [379], this could result in the increased FoxP3 and RoRγt expression we detected in our study.

While $CD8\alpha\alpha^+$ $CD4^+$ IEL maintenance was not critically dependent on TCR signalling, a small fraction of its population re-engaged their TCR, suggesting that their functions can be modulated by siIEC MHC class II expression [379]. The analysis of the effector functions of $CD8\alpha\alpha^+$ $CD4^+$ IELs shown in this chapter is preliminary data that needs to be confirmed and further characterised in future experiments. It revealed that the remaining $CD8\alpha\alpha^+$ $CD4^+$ IELs of H2-$Ab1^{VC}$

mice showed a trend towards increased TF Runx3 and T-bet expression as well as granzyme B expression. This could suggest that the CD8$\alpha\alpha^+$ CD4$^+$ IEL population in a MHC class II sufficient host consists of two cell subsets with distinct effector functions. The first one being dependent on siIEC MHC class II expression for its differentiation, exerting tolerogenic effector functions, while the second one differentiates independent of epithelial antigen presentation and exerting more pro-inflammatory functions. Single-cell RNAseq experiments could reveal whether CD8$\alpha\alpha^+$ CD4$^+$ IELs consist of two functionally distinct cell clusters.

The differentiation of CD8$\alpha\alpha^+$ CD4$^+$ IELs from conventional CD4$^+$ T cells [380–383] is mediated by changes in TF expression. Conventional CD4$^+$ and CD8$^+$ T cells maintain their lineage through the expression of T helper–inducing POZ/Krüppel-like factor (ThPOK) and runt-related transcription factor 3 (Runx3), respectively. Upon reaching the intestinal epithelium, CD4$^+$ T cells reactivate the CD8$^+$ lineage program, through up-regulation of Runx3 and down-regulation of ThPOK expression, which allows them to express the homodimer CD8$\alpha\alpha$ in the epithelium [380–382]. CD8$\alpha\alpha$ binds to the non-classical MHC class I molecule TLA, expressed by siIECs [280, 281]. It was later shown, that the TF T-bet is a critical regulator of CD8$\alpha\alpha^+$ CD4$^+$ IEL differentiation, as it induces Runx3 and inhibits ThPOK expression [384]. This process was supported by T-bet-inducing cytokines, such as IFNγ, IL-27, TGFβ and RA [384].

It was further shown, that microbiota-induced IFNγ drives PD-L1 expression by siIECs and that lack of siIEC PD-L1 expression resulted in the loss of CD8$\alpha\alpha^+$ CD4$^+$ IEL differentiation [378]. These findings highlight that siIECs act as critical non-conventional APCs for the differentiation of CD8$\alpha\alpha^+$ CD4$^+$ IEL by providing both TCR stimulation and co-inhibitory signalling. Future studies could investigate the PD-L1 expression along the length of the small intestine, to assess whether the frequency of PD-L1$^+$ IECs increases from the duodenum towards the ileum and

thereby follows the pattern of siIEC MHC class II expression.

The microbiota is required for the differentiation of CD8$\alpha\alpha^+$ CD4$^+$ IELs, as germ-free mice lack CD8$\alpha\alpha^+$ CD4$^+$ IELs [380, 382]. The commensal *Lactobacillus reuteri* was identified to promote the differentiation of CD8$\alpha\alpha^+$ CD4$^+$ IELs, through the supply of indole derivatives of dietary tryptophan to the host [383]. Despite multiple studies investigating CD8$\alpha\alpha^+$ CD4$^+$ IEL differentiation requirements, their functions are currently not fully understood. As CD8$\alpha\alpha^+$ CD4$^+$ IEL TCR specificity is restricted [379], it seems likely that a distinct set of antigens presented by siIECs mediates its differentiation and function. In addition, previous studies propose that the CD8$\alpha\alpha$ homodimer acts as a TCR co-repressor, which reduces the antigen sensitivity of the TCR (reviewed in [385]). This might suggest that CD8$\alpha\alpha^+$ CD4$^+$ IELs require an increased minimum signal strength for its restimulation (reviewed in [385]). As IELs reside in the intestinal epithelium, they are part of the first line defence against invading pathogens. Future studies could investigate the functional consequences caused by the loss of CD8$\alpha\alpha^+$ CD4$^+$ IELs by assessing their importance in the clearance of enteric viruses. Enteric viruses, such as rotavirus [386] or adenovirus [387], can directly infect IECs, thereby initiating robust innate and adaptive immune responses (reviewed in [388]), which could be supported by IEC antigen presentation. In addition, one could use the parasite Cryptosporidium tyzzeri [389], which also directly infects siIECs. These infectious agents could provide the siIECs with a unique pool of antigens that could initiate CD8$\alpha\alpha^+$ CD4$^+$ IEL functions. Studying CD4$^+$ IEL responses of H2-Ab1^{VC} mice and littermate controls towards these infectious agents could provide further insights into the role of IEC antigen presentation in controlling enteric infections.

These results highlight that MHC class II expression by siIECs is critical for the differentiation of CD8$\alpha\alpha^+$ CD4$^+$ IELs in the intestinal epithelium. Here, we have shown that siIECs can act as non-conventional APC for specific subset of CD4$^+$ IELs, namely CD8$\alpha\alpha^+$ CD4$^+$ IELs.

5

Role of MHC class II expression by colonic IECs during intestinal inflammation

Contents

5.1 Introduction 118
5.2 Results 123
5.2.1 MHC class II expression on cIECs does not impact acute intestinal inflammation triggered by *Citrobacter rodentium* infection 123
5.2.2 MHC class II deficiency by cIECs does not influence chronic intestinal inflammation 129
5.2.3 MHC class II expression by cIECs is potentially important during the resolution of chronic intestinal inflammation 138
5.2.4 MHC class II expression by cIECs does not influence intestinal inflammation induced by chronic DSS treatment 156
5.3 Discussion 166

5.1 Introduction

In the intestine the microbiota is separated from the host by a single layer of epithelial cells. This intimate relationship led to the development of a vast array of reciprocal interactions. This complex and dynamic crosstalk between the microbiota and the immune system is important during health and inflammation and is in part

mediated by IECs.

Despite the finding that IECs express MHC class II, it is currently not clear how IEC MHC class II expression contributes to intestinal homeostasis. Multiple studies report that during inflammatory conditions both human and murine small intestinal and colonic IECs upregulate MHC class II. This was detected in the immune-mediated disorders IBD, coeliac disease and GvHD, as well as during intestinal infections with *Salmonella enterica* or *Heligmosomoides polygyrus* [131, 134–138]. However, it is still unclear whether MHC class II expression by IECs induces pro- or anti-inflammatory responses in CD4 T cells.

The localisation of MHC class II molecules within IECs from endoscopic biopsies differs between healthy individuals and IBD patients [133, 147]. In inflamed samples of CD and UC patients, the expression of MHC class II molecules increased at the basolateral membrane and decreased in multi-vesicular bodies (MVB), which are part of the endosomal pathway, compared to healthy controls [147]. These observations support the hypothesis that MHC class II molecules get redistributed from MVB to the basolateral membrane during intestinal inflammation and that this could enable IECs to present antigen to $CD4^+$ T cells in the mucosa during inflammatory conditions. Conflicting results exist about the functional outcomes of these TCR-peptide:MHC class II interactions *in vivo*. And it is currently not clear whether IEC MHC class II expression enhances pro- or anti-inflammatory responses. Several studies have suggested a regulatory function of IEC MHC class II expression. It was shown that the expression of autoantigen by IECs resulted in the expansion of antigen-specific $CD4^+$ $FoxP3^+$ Treg cells in the intestinal mucosa [390]. A further study abolished MHC class II expression in all non-haematopoietic cells, including IECs, through the deletion of the pIV promoter of the CIITA gene [391]. This resulted in more severe chronic T-cell-mediated colitis, which was associated with an increase in T-bet expression in the colon and reduced Treg cell proportions

in the epithelium [391]. Another study described increased susceptibility to *C. rodentium* infection in mice lacking IEC MHC class II expression [392].

These findings are opposed to reports describing that IEC MHC class II expression activates T effector cells. The co-culture of primary cIECs, isolated from IBD patients, with autologous or allogeneic healthy peripheral blood T cells stimulated CD4 T cell proliferation and IFNγ secretion compared to healthy controls. This process was inhibited by blocking MHC class II [136]. It was further reported, that the co-culture of IFNγ-pretreated murine siIECs induced IFNγ secretion by $CD4^+$ IELs, but not by LPLs [393]. In addition, a recent study detected a slight protection from DSS-induced and T cell transfer colitis in mice lacking MHC class II expression [392]. These findings contrast with a previous study, which generated tg mice expressing the I-A^b MHC class II molecule either in DCs (CD11c-promoter) or IECs (fatty acid binding promoter) [394]. They found that only MHC class II expression by DCs, but not IEC MHC class II expression, was sufficient in inducing severe intestinal pathology following adoptive transfer of $CD4^+$ T cells into Rag2-/- mice. However, the expression of only I-A^b restricts the repertoire of presentable antigen by APCs. The seemingly incompatible conclusions of these studies about the ability of IEC MHC class II expression to induce tolerogenic or pro-inflammatory CD4 T cell responses might reflect distinct environmental features of the different experimental models of intestinal inflammation and could suggest that IEC MHC class II expression induce either pro- or anti-inflammatory CD4 T cell responses depending on the tissue context.

To assess the ability of IECs to modulate CD4 T cell phenotypes and functions and how this interaction contributes to the maintenance of intestinal homeostasis, we used multiple murine models of colitis. These included bacterial infections as well as chemical disruption of the intestinal epithelium (also see section 1.3).

C. rodentium infection is a well characterised model of acute intestinal infection and inflammation [50]. *C. rodentium* is able to colonise both the caecum and the

colon of mice. The infection peaks after around one week and remains steady until around 12 d pi, after which the clearance phase is initiated by the host and bacterial shedding decreases rapidly. We have chosen to investigate the role of cIEC MHC class II expression at 14 d, as we hypothesised that MHC class II expression by IECs is important in instructing CD4 T cell effector responses to mediate clearance and to re-establish intestinal homeostasis. *C. rodentium* infection is characterised by Th1 and even more potent Th17 responses [54, 61]. We hypothesised that mice deficient in IEC MHC class II expression show delayed clearance of *C. rodentium* infection and altered CD4 T cell effector responses.

H. hepaticus infection is a valuable model for investigating the role of Treg cells in maintaining intestinal tolerance. *H. hepaticus* can chronically colonise immunocompetent mice without causing intestinal inflammation, and host tolerance towards *H. hepaticus* is driven by IL-10 production. IL-10 is the key regulatory cytokine produced by Treg cells and mediates intestinal tolerance. IL-10 deficient mice develop spontaneous enterocolitis [395–397], which was associated with increased Th1 responses [396]. *H. hepaticus* colonisation of immunodeficient mice has been associated with the development of intestinal inflammation [68, 69]. Indeed, *H. hepaticus* colonisation of IL-10 deficient mice leads to the development of typhlocolitis [70, 71]. The induction of intestinal inflammation by *H. hepaticus* colonisation can be reproduced by concomitant blockade of IL-10R signalling using an anti-IL-10R antibody in wild-type C57BL mice [25]. In this model, the intestinal inflammation is driven by a type 1 cytokine response, including IL-12, TNFα and IFNγ [70, 72]. As described in Chapter 1, IFNγ is a potent inducer of MHC class II expression by IECs (see Figure 3.2). We therefore wanted to investigate whether IEC MHC class II expression plays an important part in mediating CD4 T cell effector responses.

As anti-IL-10R treatment blocks the regulatory circuits initiated by *H. hepaticus* colonisation, we would not be able to address the ability of IEC MHC class II expression in modulating Treg cell responses. We therefore adjusted the *H. hepaticus* + anti-IL-10R model in subsequent experiments, and stopped anti-IL-10R treatment

after the induction of intestinal inflammation. This allowed the degradation of the anti-IL-10R antibody and with that, the re-establishment of regulatory circuits leading to the resolution of intestinal inflammation. This allowed us to assess the importance of cIEC MHC class II expression in tissue regeneration and re-establishment of intestinal homeostasis.

Finally we used the chronic DSS model to address the importance of IEC MHC class II expression in wound healing and tissue regeneration. DSS is a chemical substance, which is toxic to IECs and causes disruption of the epithelial barrier. This allows the translocation of luminal antigen into the intestinal mucosa and leads to the rapid induction of acute intestinal inflammation. By using multiple cycles of DSS treatment it is possible to model the reoccurring episodes of chronic intestinal inflammation and mucosal healing experienced by IBD patients. The tissue regeneration of the acute DSS model (one cycle of DSS treatment) is driven by innate immune responses and characterised by a marked infiltration of neutrophils into the tissue [78, 80]. In this study, we used the chronic DSS model, induced by multiple cycles of DSS treatment, which is characterised by accumulation of T cells in the mucosa and changes in Th1/Th2 cytokine expression [83].

In this chapter, we aim to investigate whether CD4 T cell responses are influenced by IEC MHC class II expression during intestinal infection and inflammation triggered by *C. rodentium* or *H. hepaticus*, or following repeated cycles of DSS. We will investigate the CD4 T cell phenotypes and functions in both the epithelium and the lamina propria. We hypothesise that MHC class II expression by IECs induces regulatory T cell responses and is important for the maintenance and restoration of intestinal homeostasis.

5.2 Results

5.2.1 MHC class II expression on cIECs does not impact acute intestinal inflammation triggered by *Citrobacter rodentium* infection

Having confirmed the generation of IEC-specific MHC class II knock-out mice (H2-Ab1^{VC}), we wanted to investigate the role of IEC MHC class II expression during acute colitis triggered by bacterial infection. We therefore infected H2-Ab1^{VC} and H2-Ab1$^{fl/fl}$ littermate mice with *Citrobacter rodentium* (Figure 5.1 A), a Gram negative pathogen that causes transient, acute disease, and monitored key local and systemic disease parameters until sacrifice on day 14 post-infection.

First, we investigated whether *C. rodentium* infection led to the upregulation of MHC class II protein expression by cIECs. For this purpose, we isolated cIECs and assessed MHC class II protein expression by flow cytometry. Uninfected animals showed no cIEC MHC class II expression, whereas infected H2-Ab1$^{fl/fl}$ mice showed around 20 % MHCII^{+} cIECs. In contrast, infected H2-Ab1^{VC} littermates expressed negligible levels of cIEC MHC class II (Figure 5.2 A). MHC class I expression by cIECs was also upregulated from around 30 % at steady state to approximately 55 % to 60 % upon *C. rodentium* infection and these were comparable between H2-Ab1^{VC} and H2-Ab1$^{fl/fl}$ littermates (Figure 5.2 A). To verify that IEC targeted deletion of MHC class II did not influence MHC class II expression of professional APCs, we assessed MHC class II levels on CD11c^{+} and B220^{+} cells of *C. rodentium* infected H2-Ab1^{VC} and H2-Ab1$^{fl/fl}$ littermates and found that these were comparable (Figure 5.2 B and C, respectively). These results confirm the inflammation induced upregulation of MHC class II expression by cIECs in H2-Ab1$^{fl/fl}$ but not in H2-Ab1^{VC} mice during *C. rodentium* infection, and further verify the efficiency of Villin-Cre mediated deletion of the H2-Ab1 gene in cIECs in H2-Ab1^{VC} mice.

In addition, *C. rodentium* infection led to the development of splenomegaly that was comparable between H2-Ab1^{VC} and H2-Ab1$^{fl/fl}$ littermates Figure 5.1 B). We

also did not observe any significant differences in body weight loss between infected H2-Ab1^{VC} and H2-Ab1$^{fl/fl}$ mice throughout the course of the experiment (Figure 5.1 C). Thus, MHC class II expression by IECs does not impact *C. rodentium* infection driven weight loss.

We next assessed the role of MHC class II expression by cIECs in controlling pathogen burden during *C. rodentium* infection. We measured the tissue-adherent *C. rodentium*, as well as the lumenal, planktonic *C. rodentium* present in the caecal contents. We detected similar tissue adherent *C. rodentium* levels in the colon (Figure 5.3 A) and caecum (Figure 5.3 B) as well as planktonic *C. rodentium* in the caecal contents (Figure 5.3 C) of infected H2-Ab1^{VC} and H2-Ab1$^{fl/fl}$ littermates. In mice with impaired protective immunity, there may be marked systemic spread of *C. rodentium* to the spleen [57, 58]. However, the majority of infected mice did not show *C. rodentium* translocation to the spleen and where it occurred, *C. rodentium* burden was very low (Figure 5.3 D). Therefore, H2-Ab1^{VC} and H2-Ab1$^{fl/fl}$ littermates had similar *C. rodentium* colonisation levels in intestinal tissues and rarely had systemic translocation.

We next examined whether the loss of MHC class II expression by IECs influenced *C. rodentium* induced intestinal inflammation. Colon and caecum tissue samples were collected on day 14 post-infection, then formalin fixed and paraffin-embedded, then sectioned and stained with H&E to assess intestinal pathology in a semi-quantitative manner (see Table 2.1). We observed the induction of marked intestinal inflammation and the colonic and caecal histopathology scores were comparable between *C. rodentium* infected H2-Ab1^{VC} and H2-Ab1$^{fl/fl}$ littermates (Figure 5.4 A and B, respectively). Representative H&E sections are depicted in Figure 5.4 C. These findings indicate that intestinal pathology induced by *C. rodentium* infection is not affected by IEC MHC class II expression.

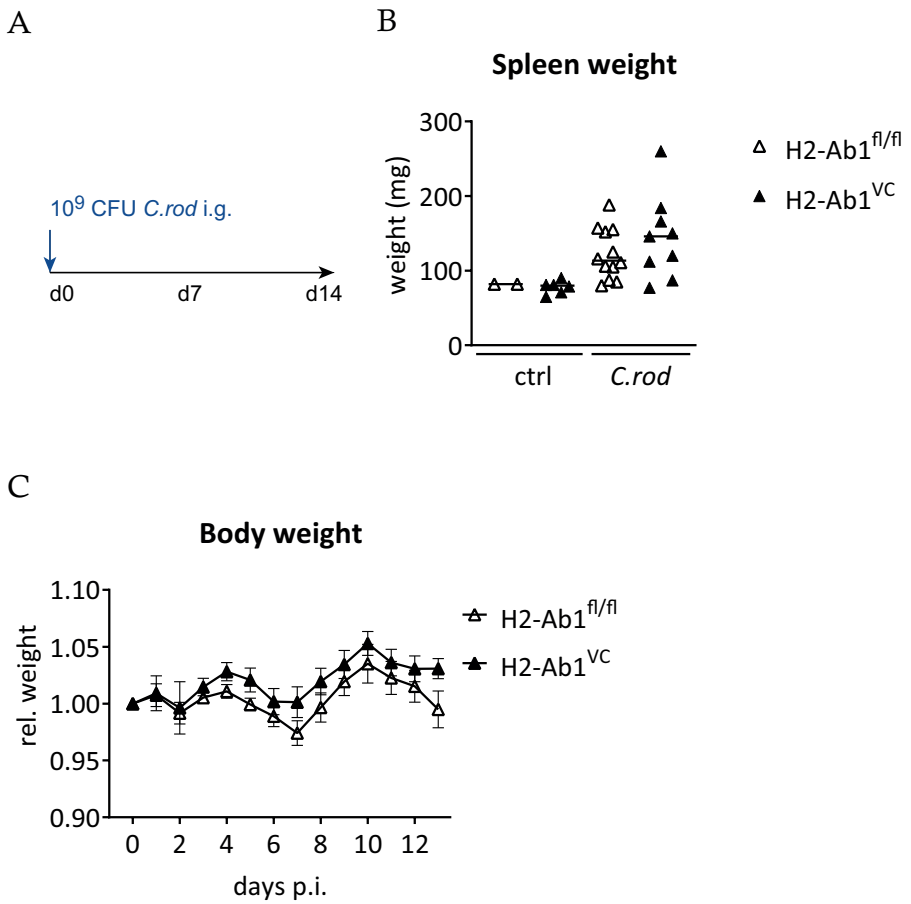


Figure 5.1: *C. rodentium* infected H2-Ab1^{VC} and H2-Ab1$^{fl/fl}$ mice show comparable body weight loss and similar spleen weight. H2-Ab1^{VC} and H2-Ab1$^{fl/fl}$ mice were orally infected with *C. rodentium* ($\sim 10^9$ CFU) and sacrificed at day 14 post infection. (A) Schematic of treatment protocol. (B) Spleen weight was assessed at day 14. Horizontal bars indicate group medians. (C) Mice were weighed daily until sacrifice. Symbols denote mean (± SEM) as a relative to the initial body weight. Statistical significance between the groups was determined by Mann-Whitney test (B) or two-way ANOVA multiple comparisons test with Sidak's correction (C). (B) Data from two pooled independent experiments with total mouse numbers per group as follows; n=9 H2-Ab1^{VC} and n=12 H2-Ab1$^{fl/fl}$ infected mice and n=6 H2-Ab1^{VC} and n=2 H2-Ab1$^{fl/fl}$ uninfected mice. (C) Representative data of one experiment of two independent experiments with five mice per group per time point.

Taken together, these results suggest that MHC class II expression by IECs does not play a pivotal role in controlling *C. rodentium* pathogenic burdens or associated intestinal inflammation.

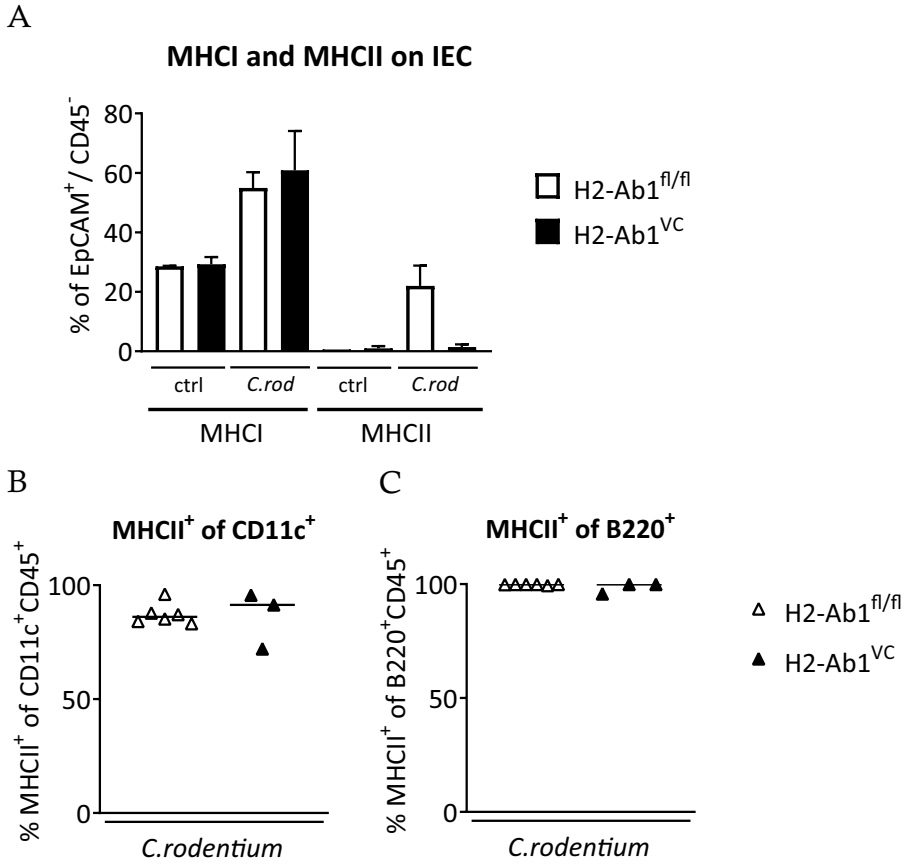


Figure 5.2: *C. rodentium* infection induces IEC MHC class II expression in H2-Ab1$^{fl/fl}$ mice. H2-Ab1^{VC} and H2-Ab1$^{fl/fl}$ mice were orally infected with *C. rodentium* ($\sim 10^9$ CFU) and sacrificed at day 14 post infection. (A) CIECs were isolated and analysed for MHC class I and II expression. Symbols denote mean ($\pm$ SD). (B) MHC class II expression of CD11c$^+$ cells was assessed in the MLNs. Horizontal bars indicate group medians. (C) MHC class II expression of B220$^+$ cells was assessed in the MLNs. Horizontal bars indicate group medians. Statistical significance between the groups was determined by the Mann-Whitney test. (A) Data from one experiment of n=4 H2-Ab1^{VC} and n=6 H2-Ab1$^{fl/fl}$ infected mice and n=2 H2-Ab1^{VC} and n=2 H2-Ab1$^{fl/fl}$ uninfected mice. (B and C) Data from one experiment of n=3 H2-Ab1^{VC} and n=6 H2-Ab1$^{fl/fl}$ infected mice.

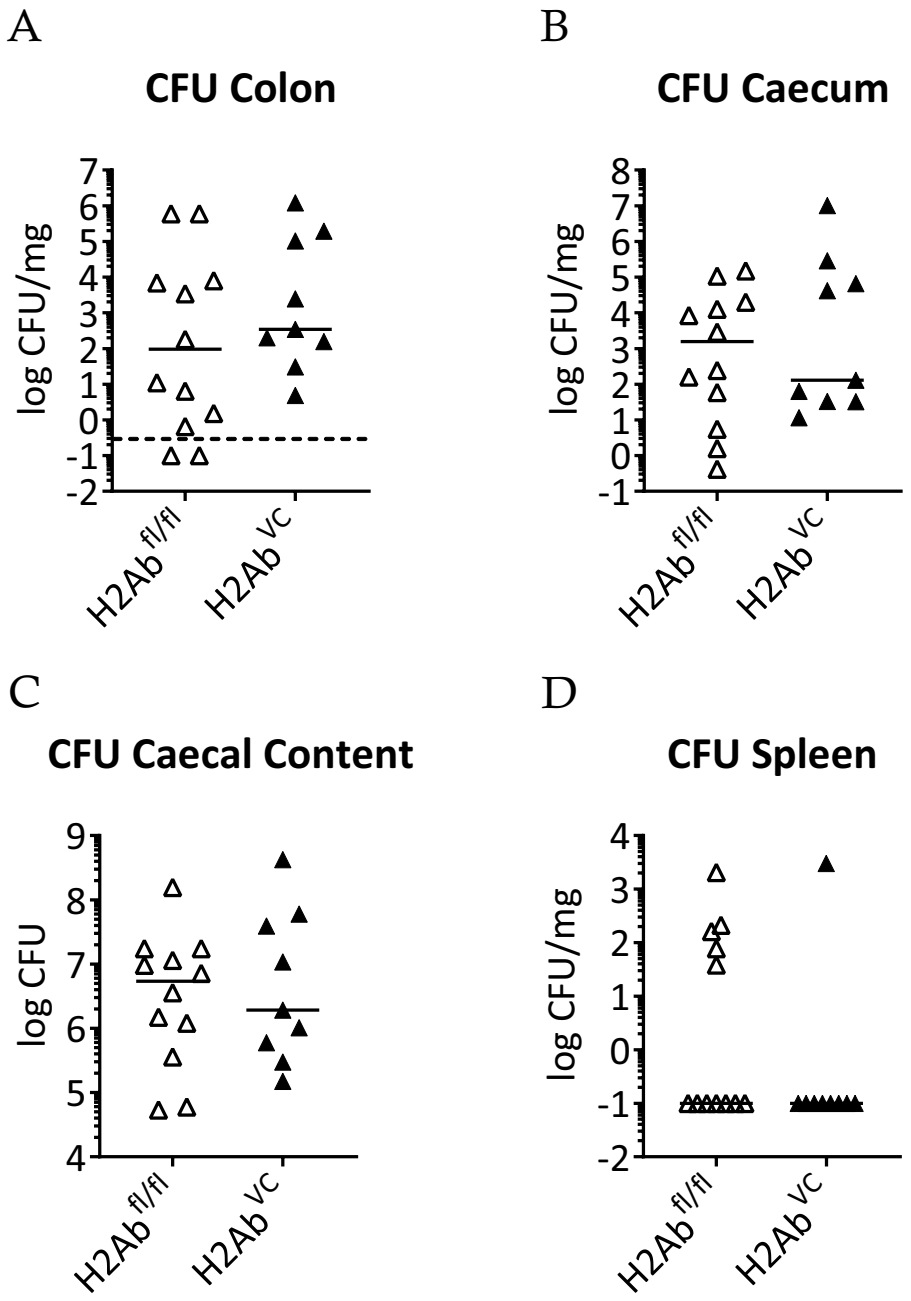


Figure 5.3: *C. rodentium* infected H2-Ab1^{VC} and H2-Ab1$^{fl/fl}$ mice show similar tissue adherent and planktonic bacteria in intestinal tissues and caecal contents. H2-Ab1^{VC} and H2-Ab1$^{fl/fl}$ mice were orally infected with *C. rodentium* ($\sim 10^9$ CFU) and sacrificed at day 14 post infection. Symbols denote tissue-adherent *C. rodentium* CFU in the colon (A) and caecum (B), planktonic *C. rodentium* CFU in the caecal content (C) as well as tissue-adherent *C. rodentium* CFU in the spleen (D). Horizontal bars indicate group medians. Dashed horizontal line depicts theoretical detection limit of assay. Statistical significance between the groups was determined by the Mann-Whitney test. Data from two pooled independent experiments of n=9 H2-Ab1^{VC} and n=12 H2-Ab1$^{fl/fl}$ infected mice.

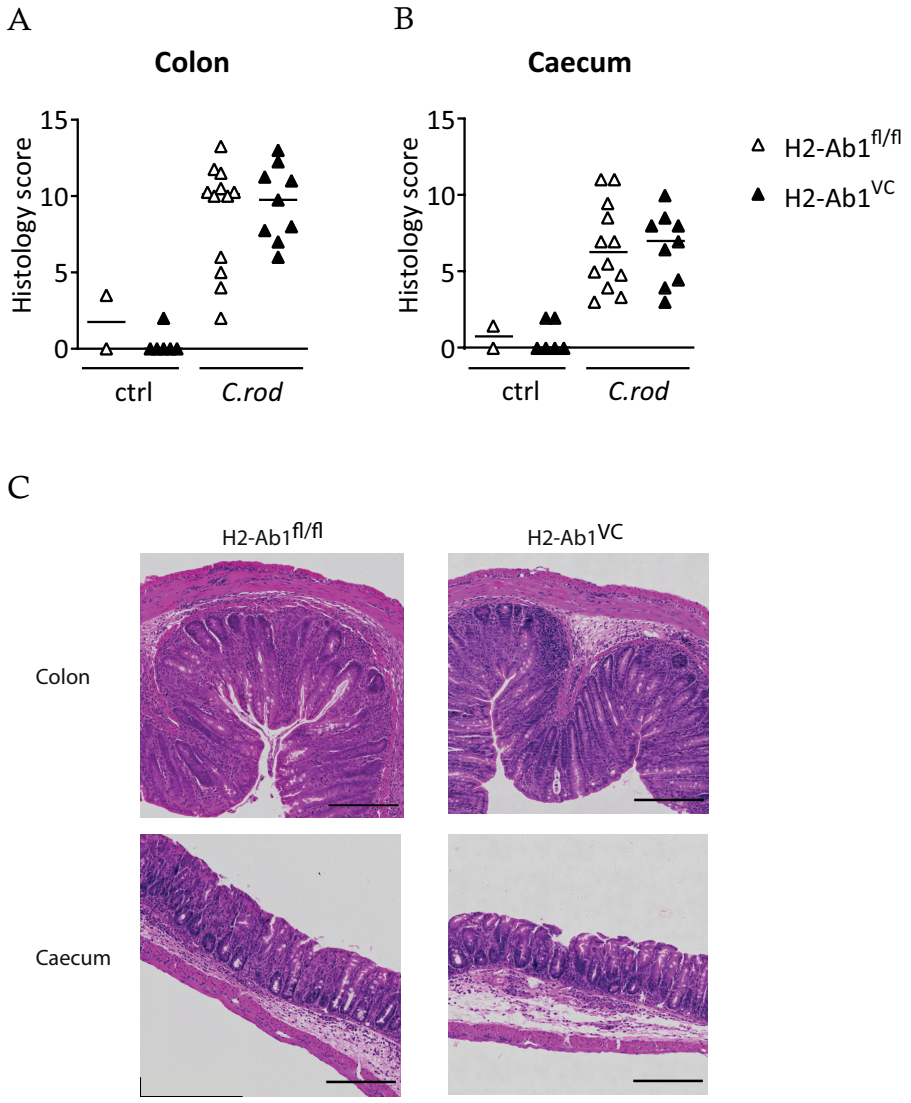


Figure 5.4: *C. rodentium* infected H2-Ab1^{VC} and H2-Ab1$^{fl/fl}$ mice exhibit comparable pathology. H2-Ab1^{VC} and H2-Ab1$^{fl/fl}$ mice were orally infected with *C. rodentium* ($\sim 10^9$ CFU) and sacrificed at day 14 post infection. Pathology scores in the colon (A) and caecum (B) as well as representative images depicting H&E stainings of colon and caecal sections (C). Symbols denote individual histopathological scores. Horizontal bars indicate group medians. Scale bars, 200 μm. Statistical significance between the groups was determined by the Mann-Whitney test. Data from two pooled experiments with total mouse numbers per group as follows; n=9 H2-Ab1^{VC} and n=12 H2-Ab1$^{fl/fl}$ infected mice and n=6 H2-Ab1^{VC} and n=2 H2-Ab1$^{fl/fl}$ uninfected mice.

5.2.2 MHC class II deficiency by cIECs does not influence chronic intestinal inflammation

We also wanted to investigate whether chronic intestinal inflammation was impacted by MHC class II expression on IECs. To test this we utilised the chronic intestinal inflammation model driven by the infection with *H. hepaticus* and concomitant administration of anti-IL-10R antibody (Figure 5.5 A) and analysed different disease parameters, with sacrifice on day 28 post-infection.

We first determined whether the chronic intestinal inflammation induced by *H. hepaticus* + anti-IL-10R treatment led to increased MHC class II expression by cIECs. Flow cytometric analyses demonstrated that MHC class II expression by cIECs was upregulated in *H. hepaticus* + anti-IL-10R treated H2-Ab1$^{fl/fl}$ mice compared to untreated controls (Figure 5.7 A). Importantly, *H. hepaticus* + anti-IL-10R treated H2-Ab1^{VC} mice did not show cIEC MHC class II expression (Figure 5.7 A). In contrast, MHC class I expression was elevated to a similar levels in cIECs of *H. hepaticus* + anti-IL-10R treated H2-Ab1^{VC} and H2-Ab1$^{fl/fl}$ littermates (Figure 5.7 A). To again verify that the Villin-Cre mediated deletion of MHC class II specifically targeted IECs, we isolated CD11c^{+} cells from the LPLs and assessed MHC class II expression by flow cytometry. Following *H. hepaticus* + anti-IL-10R treatment, we observed comparable increases in the proportions of MHC class II^{+} CD11c^{+} LPLs in H2-Ab1^{VC} and H2-Ab1$^{fl/fl}$ littermates (Figure 5.7 B).

We found that systemic inflammation, assessed by splenomegaly, was comparable between *H. hepaticus* + anti-IL-10R treated H2-Ab1^{VC} and H2-Ab1$^{fl/fl}$ littermates (Figure 5.5 B). Similarly, we did not detect any differences in body weight loss in *H. hepaticus* + anti-IL-10R treated H2-Ab1^{VC} and H2-Ab1$^{fl/fl}$ littermates (Figure 5.5 C).

We further determined whether the loss of MHC class II expression by IECs influences the severity of intestinal inflammation after *H. hepaticus* + anti-IL-10R treatment. Colonic and caecal tissue samples were formalin fixed, paraffin embedded, sectioned and stained with H&E and intestinal pathology assessed in a semi-quantitative manner (see Table 2.2). *H. hepaticus* + anti-IL-10R treatment induced marked intestinal inflammation but histopathology scores of the caecum and whole colon were equivalent between treated H2-Ab1^{VC} and H2-Ab1$^{fl/fl}$ littermates (Figure 5.6 A and B, respectively). Although *H. hepaticus* + anti-IL-10R treated H2-Ab1^{VC} mice showed a tendency towards increased intestinal inflammation in the proximal colon compared to H2-Ab1$^{fl/fl}$ littermates, this difference did not reach statistical significance (Figure 5.6 C). Representative images of the histopathology scores of the colon, caecum and proximal colon are depicted in Figure 5.6 D. Together, these observations indicate that the intestinal pathology associated with *H. hepaticus* + anti-IL-10R treatment was not significantly affected by IEC MHC class II expression.

To assess the impact of MHC class II expression by IECs on the CD4$^+$ T cell populations residing in the intestinal epithelial layer during chronic colitis, we isolated cIELs from *H. hepaticus* + anti-IL-10R treated H2-Ab1^{VC} and H2-Ab1$^{fl/fl}$ littermates (Figure 5.8 A). Flow cytometric analyses of the CD4$^+$ TCR$\gamma\delta^-$ IEL populations (Figure 5.8 B) revealed similar frequencies of CD8$\alpha\alpha^+$ CD4$^+$ IELs, CD8$\alpha\beta^+$ $^+$ CD4$^+$ IELs and conventional CD8$\alpha\beta^-$ CD4$^+$ IELs in the H2-Ab1^{VC} and H2-Ab1$^{fl/fl}$ littermates (Figure 5.8 C-E). In addition, CD4$^-$ TCR$\gamma\delta^+$ and CD4$^-$ TCR$\gamma\delta^-$ population frequencies were also comparable (data not shown). Therefore MHC class II expression by IECs does not appear to influence the recruitment and differentiation of cIELs in the intestinal epithelial layer during chronic intestinal inflammation.

As cIECs are in close contact with T cells residing both in the epithelial layer and in the lamina propria, we further investigated whether MHC class II expression

by cIECs influences Th cells in the lamina propria during chronic inflammation. We therefore isolated LPLs from the colon of *H. hepaticus* and anti-IL-10R treated H2-Ab1^{VC} and H2-Ab1$^{fl/fl}$ littermates and analysed them by flow cytometry (Figure 5.9 A). We observed similarly increased frequencies of CD4^{+} Th cells in treated compared to untreated H2-Ab1^{VC} and H2-Ab1$^{fl/fl}$ littermates (Figure 5.9 B). Further analysis of Th cell subsets revealed that although chronic intestinal inflammation caused a reduction in Treg (FoxP3^{+} RoRγ^{-}) and marked increase in Th17 (FoxP3^{-} RoRγ^{+}) Th cell frequencies in the LPL compartment, there were no significant differences between H2-Ab1^{VC} and H2-Ab1$^{fl/fl}$ mice (Figure 5.9 C-E). Overall, these data suggest that MHC class II expression by cIECs does not impact the differentiation and/or accumulation of Treg and Th17 cells during chronic intestinal inflammation.

To assess *H. hepaticus*-specific Th cell responses, LPLs were isolated from *H. hepaticus* + anti-IL-10R treated H2-Ab1^{VC} and H2-Ab1$^{fl/fl}$ littermates and restimulated *in vitro* with sHelAg and analysed by flow cytometry. Although sHelAg restimulation did not alter Th cell frequencies in LPLs(Figure 5.10 A), it did induce the production of IFNγ, IL-17 and TNFα by Th cells (Figure 5.10 B-D). However, the frequency of LPL Th cells expressing each of these effector cytokines was similar between *H. hepaticus* + anti-IL-10R treated H2-Ab1^{VC} and H2-Ab1$^{fl/fl}$ littermates (Figure 5.10 B-D). In contrast, Th cells isolated from the MLNs of the same mice did not show IFNγ, IL-17 and TNFα production after sHelAg restimulation (data not shown), whereas PMA/ionomycin restimulation resulted in comparable production of IFNγ, IL-17 and TNFα by Th cells in the LPLs and MLNs (data not shown). These observations highlight that LPL Th cells are highly enriched in *H. hepaticus*-specific Th cells. Overall, these results highlight that MHC class II expression by IECs does not influence the capability of *H. hepaticus*-specific LPL Th cells to produce IFNγ, IL-17 or TNFα during chronic intestinal inflammation.

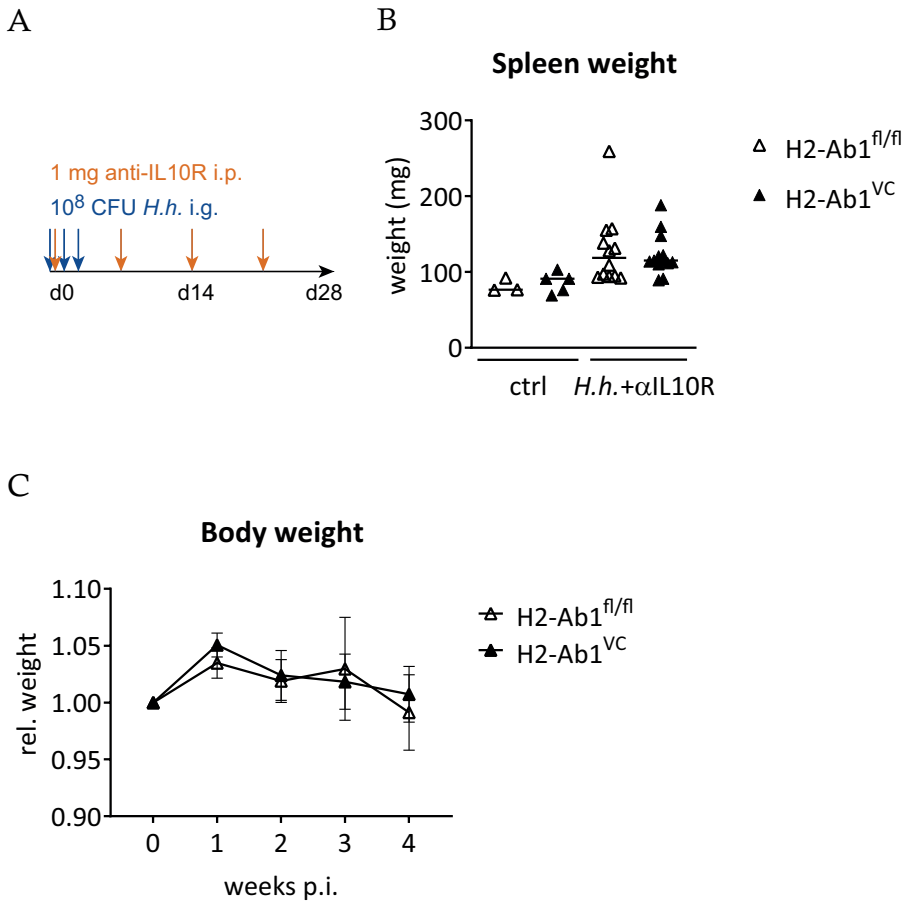


Figure 5.5: *H. hepaticus* + anti-IL-10R treated H2-Ab1^{VC} and H2-Ab1$^{fl/fl}$ mice show comparable body weight loss and similar spleen weight. H2-Ab1^{VC} and H2-Ab1$^{fl/fl}$ littermates were orally infected with 10^8 CFU *H. hepaticus* on three consecutive days and i.p. injected with 1 mg anti-IL-10R weekly. Mice were sacrificed at four weeks post infection. (A) Schematic of treatment protocol. (B) Spleen weight was assessed after four weeks. Horizontal bars indicate group medians. (C) Mice were weighed weekly until sacrifice. Symbols denote mean (± SEM) as a relative to the initial body weight. Statistical significance between the groups was determined by Mann-Whitney test (B) or two-way ANOVA multiple comparisons test with Sidak's correction (C). (B) Data from two pooled independent experiments with total mouse numbers per group as follows; n=13 H2-Ab1^{VC} and n=12 H2-Ab1$^{fl/fl}$ treated mice and n=5 H2-Ab1^{VC} and n=3 H2-Ab1$^{fl/fl}$ untreated mice. (C) Data of one experiment with six mice per group per time point.

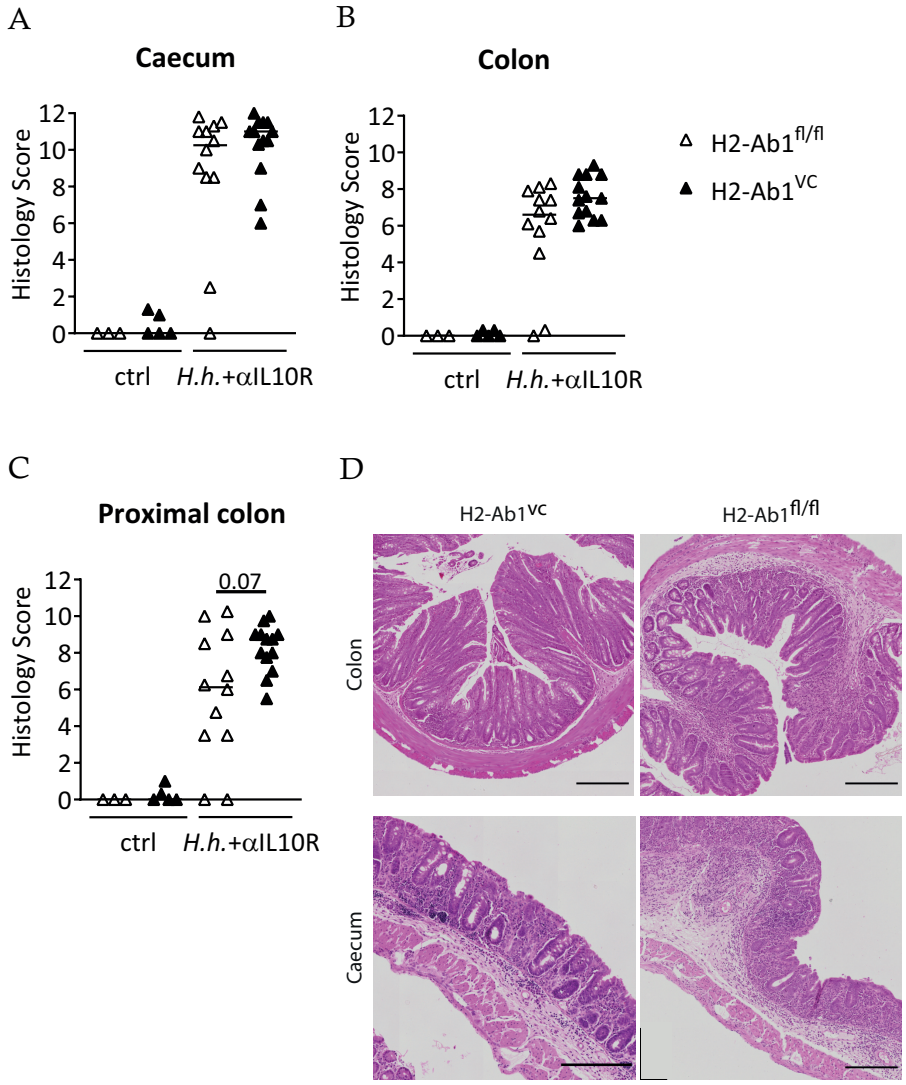


Figure 5.6: *H. hepaticus* + anti-IL-10R treated H2-Ab1^{VC} and H2-Ab1$^{fl/fl}$ mice show comparable histopathology scores. H2-Ab1^{VC} and H2-Ab1$^{fl/fl}$ littermates were orally infected with 10^8 CFU *H. hepaticus* on three consecutive days and i.p. injected with 1 mg anti-IL-10R weekly. Mice were sacrificed at four weeks post infection. Histopathology scores of the caecum (A), whole colon (B) and proximal colon (C). Horizontal bars indicate group medians. (D) Representative H&E sections of the colon from H2-Ab1^{VC} and H2-Ab1$^{fl/fl}$ littermates. Scale bars, 200 μm. Statistical significance between the groups was determined by Mann-Whitney test. Data from two pooled independent experiments with total mouse numbers per group as follows; n=13 H2-Ab1^{VC} and n=12 H2-Ab1$^{fl/fl}$ treated mice and n=5 H2-Ab1^{VC} and n=3 H2-Ab1$^{fl/fl}$ untreated mice.

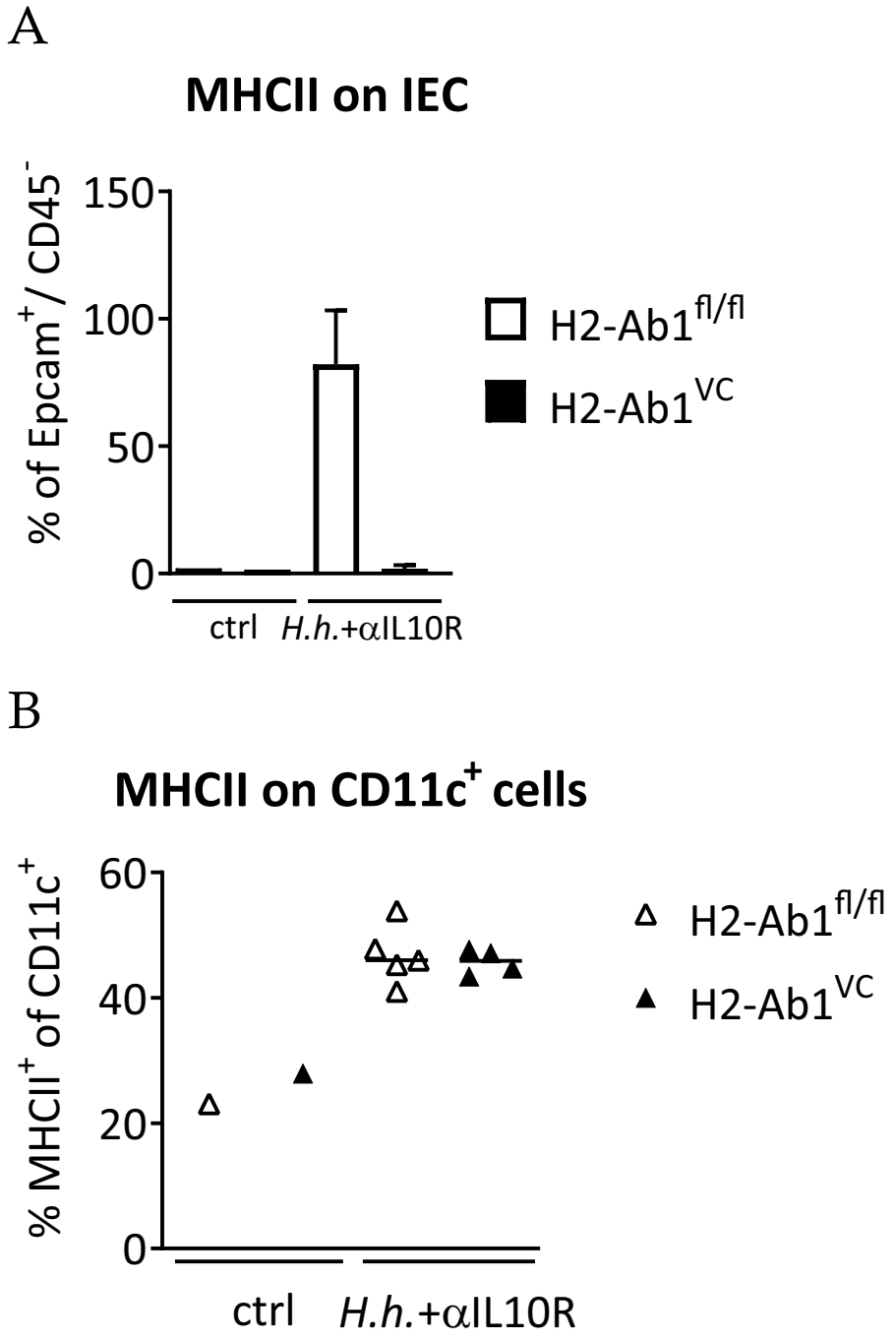


Figure 5.7: *H. hepaticus* + anti-IL-10R treatment induces MHC class II expression by cIECs in H2-Ab1$^{fl/fl}$ mice. H2-Ab1^{VC} and H2-Ab1$^{fl/fl}$ littermates were orally infected with 10^8 CFU *H. hepaticus* on three consecutive days and i.p. injected with 1 mg anti-IL-10R weekly. Mice were sacrificed at three weeks post infection. (A) MHC class I and II expression by cIECs of treated H2-Ab1^{VC} and H2-Ab1$^{fl/fl}$ littermates and untreated controls. Symbols denote mean (± SD). (B) MHC class II expression of CD11c$^+$ cells isolated from the lamina propria of *H. hepaticus* + anti-IL-10R treated H2-Ab1^{VC} and H2-Ab1$^{fl/fl}$ littermates and untreated controls. Horizontal bars indicate group medians. Statistical significance between the groups was determined by Mann-Whitney test. Data from one experiment with total mouse numbers per group as follows; n=4 H2-Ab1^{VC} and n=5 H2-Ab1$^{fl/fl}$ treated mice and n=1 H2-Ab1^{VC} and n=1 H2-Ab1$^{fl/fl}$ untreated mice.

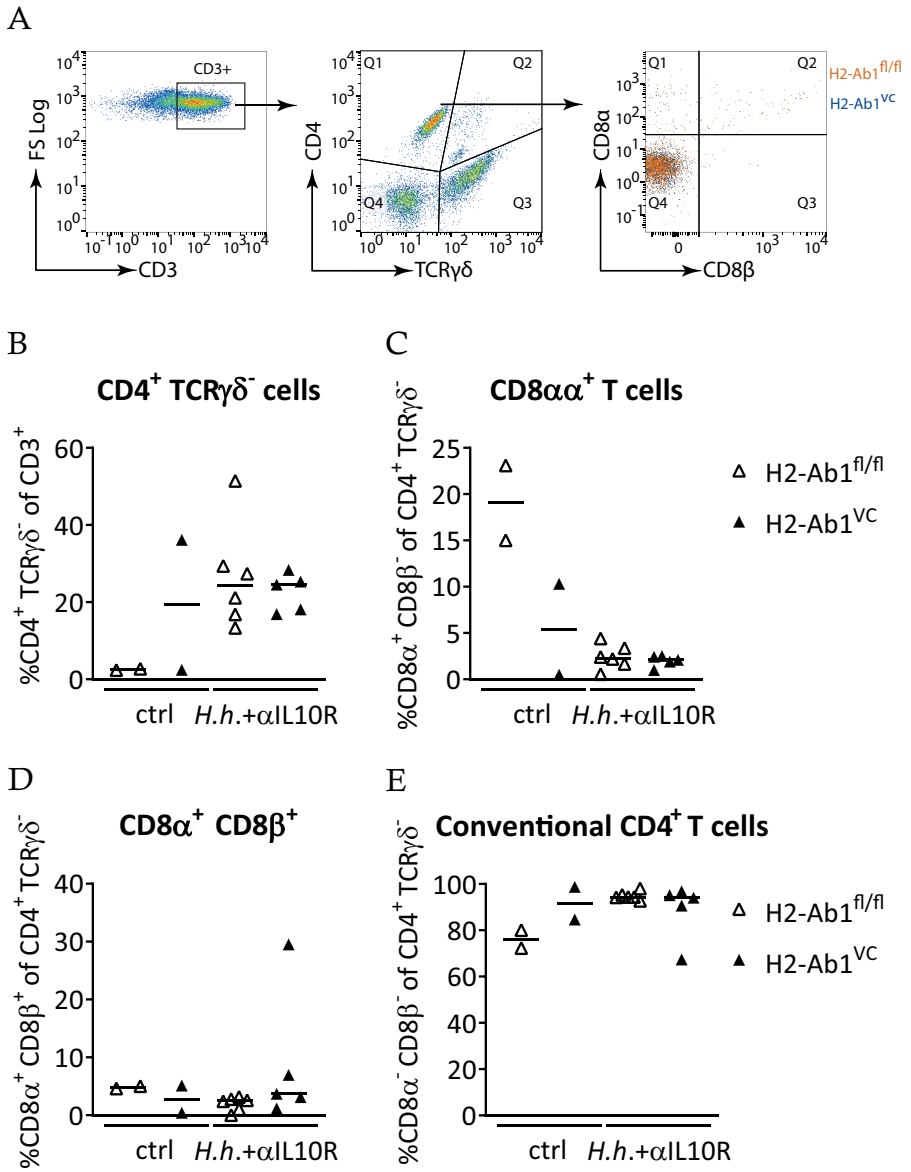


Figure 5.8: Colonic CD4$^+$ IEL frequencies of *H. hepaticus* + anti-IL-10R treated H2-Ab1^{VC} and H2-Ab1$^{fl/fl}$ mice are comparable. H2-Ab1^{VC} and H2-Ab1$^{fl/fl}$ littermates were orally infected with 10^8 CFU *H. hepaticus* on three consecutive days and i.p. injected with 1 mg anti-IL-10R weekly. Mice were sacrificed at four weeks post infection. (A) Schematic of FACS gating strategy. Frequencies of CD4$^+$ TCR$\gamma\delta^-$ IELs (B) as well as their daughter CD8α^+ CD8β^- (C), CD8α^+ CD8β^+ (D) and CD8α^- CD8β^- (E) subsets. Horizontal bars indicate group medians. Statistical significance between the groups was determined by Mann-Whitney test. Data from one experiments with total mouse numbers per group as follows; n=5 H2-Ab1^{VC} and n=6 H2-Ab1$^{fl/fl}$ treated mice and n=2 H2-Ab1^{VC} and n=2 H2-Ab1$^{fl/fl}$ untreated mice.

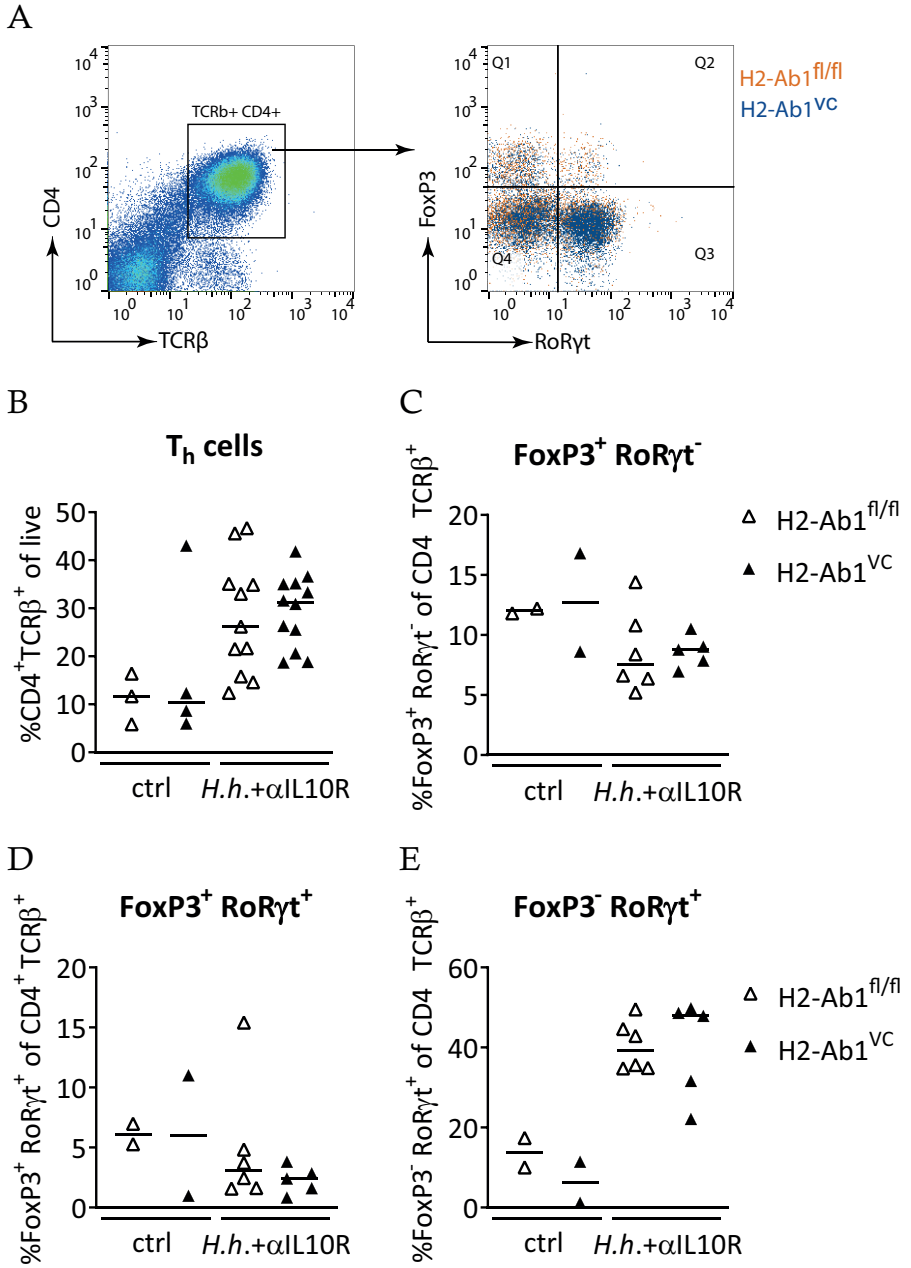


Figure 5.9: Lamina propria CD4$^+$ T cell frequencies of *H. hepaticus* + anti-IL-10R treated H2-Ab1^{VC} and H2-Ab1$^{fl/fl}$ mice are comparable. H2-Ab1^{VC} and H2-Ab1$^{fl/fl}$ littermates were orally infected with 10^8 CFU *H. hepaticus* on three consecutive days and i.p. injected with 1 mg anti-IL-10R weekly. Mice were sacrificed at four weeks post infection. (A) Schematic of FACS gating strategy. Frequencies of lamina propria CD4$^+$ TCRβ^+ T cells (B) and their daughter FoxP3$^+$ RoRγt$^-$ (C), FoxP3$^+$ RoRγt$^+$ (D) and FoxP3$^-$ RoRγt$^+$ (E) subsets. Horizontal bars indicate group medians. Statistical significance between the groups was determined by Mann-Whitney test. (B) Data from two pooled independent experiments with total mouse numbers per group as follows; n=12 H2-Ab1^{VC} and n=11 H2-Ab1$^{fl/fl}$ treated mice and n=4 H2-Ab1^{VC} and n=3 H2-Ab1$^{fl/fl}$ untreated mice. (C-E) Data from one experiment with total mouse numbers per group as follows; n=5 H2-Ab1^{VC} and n=6 H2-Ab1$^{fl/fl}$ treated mice and n=2 H2-Ab1^{VC} and n=2 H2-Ab1$^{fl/fl}$ untreated mice.

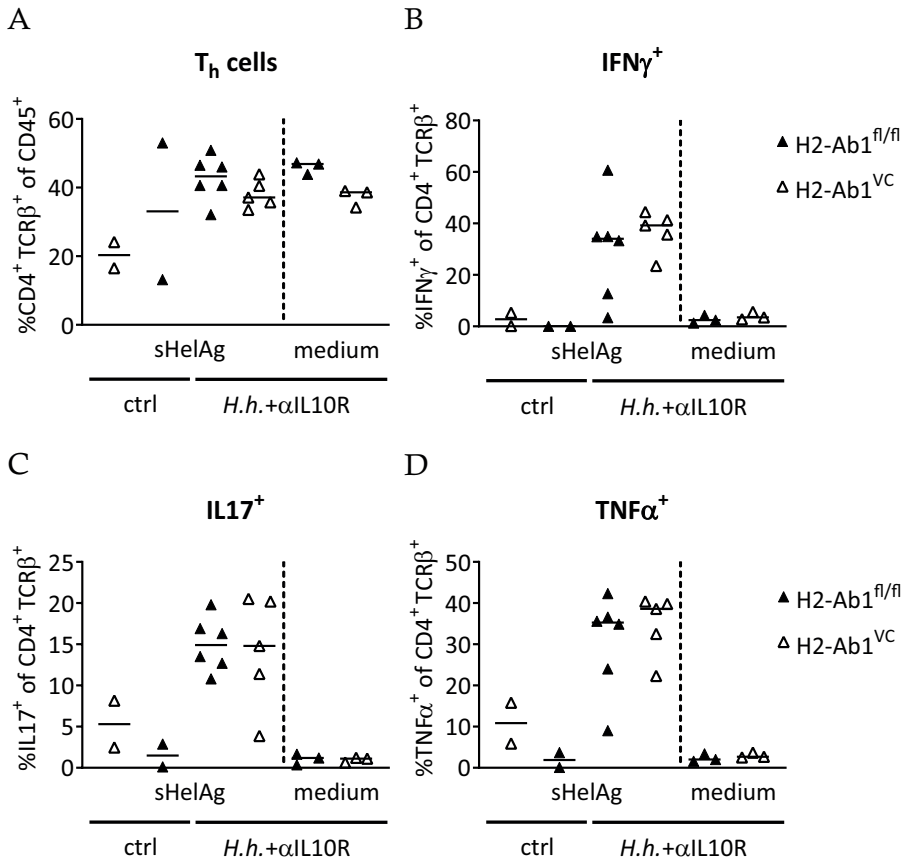


Figure 5.10: SHelAg treatment induced cytokine production by LPLs of *H. hepaticus* + anti-IL-10R treated H2-Ab1^{VC} and H2-Ab1$^{fl/fl}$ mice. H2-Ab1^{VC} and H2-Ab1$^{fl/fl}$ littermates were orally infected with 10^8 CFU *H. hepaticus* on three consecutive days and i.p. injected with 1 mg anti-IL-10R weekly. Mice were sacrificed at four weeks post infection. LPLs were isolated in restimulated with sHelAg ON. (A) Frequencies of CD4$^+$ TCRβ^+ T cells. Frequencies of IFNγ (B), IL-17 (C) and TNFα (D) producing CD4$^+$ T cells. Horizontal bars indicate group medians. Statistical significance between the groups was determined by Mann-Whitney test. (A-D) Data from one experiments with total mouse numbers per group as follows; n=5 H2-Ab1^{VC} and n=6 H2-Ab1$^{fl/fl}$ treated mice and n=2 H2-Ab1^{VC} and n=2 H2-Ab1$^{fl/fl}$ untreated mice.

5.2.3 MHC class II expression by cIECs is potentially important during the resolution of chronic intestinal inflammation

CD and UC are characterised by chronic intestinal inflammation and patients typically experience periods of mucosal inflammation and remission. As MHC class II expression by IECs is upregulated during intestinal inflammation, we wanted to investigate whether MHC class II expression by IECs is important during the resolution of intestinal inflammation. We therefore induced chronic intestinal inflammation using *H. hepaticus* + anti-IL-10R treatment for four weeks and then the anti-IL-10R treatment was stopped to enable the resolution of intestinal inflammation for a further three weeks (Figure 5.11 A).

At the end point of the experiment (d42), H2-Ab1^{VC} mice showed significantly reduced spleen weights when compared to H2-Ab1$^{fl/fl}$ mice, suggesting reduced systemic inflammation (Figure 5.11 B). However, we did not detect any significant differences in body weight between H2-Ab1$^{fl/fl}$ and H2-Ab1^{VC} mice at any point during this experiment (Figure 5.11 C).

We next investigated the impact of IEC MHC class II expression on the resolution of chronic intestinal inflammation at the end point of the experiment (d42). Colonic and caecal tissue was formalin fixed, paraffin embedded, sectioned and stained with H&E. Intestinal pathology was assessed in a semi-quantitative manner (see Table 2.2). We found that both H2-Ab1$^{fl/fl}$ and H2-Ab1^{VC} mice still exhibited marked and comparable caecal inflammation (Figure 5.12 A). However, we found that H2-Ab1^{VC} mice showed significantly higher levels of colonic inflammation when compared to H2-Ab1$^{fl/fl}$ littermates (Figure 5.12 B). This difference was particularly evident in the proximal colon, where significantly higher inflammation scores were recorded for H2-Ab1^{VC} mice compared to H2-Ab1$^{fl/fl}$ littermates (Figure 5.12 C). Representative pathology images are shown in Figure 5.12 D. Overall, these observations indicate that MHC class II expression by cIECs may have a role in supporting the resolution

of chronic intestinal inflammation in the colon.

As IECs are in close contact with IELs residing in the intestinal epithelial layer we examined whether lack of IEC MHC class II expression influenced the composition of differentiation of cIEL populations during the resolution of chronic intestinal inflammation. CIELs were isolated and analysed by flow cytometry (Figure 5.13 A). At the endpoint of the experiment (d42) we observed a trend towards increased frequencies of $CD4^+$ $TCR\gamma\delta^-$ IEL in both treated H2-$Ab1^{VC}$ and H2-$Ab1^{fl/fl}$ compared to untreated mice (Figure 5.13 B). However, further analysis of the $CD4^+$ $TCR\gamma\delta^-$ IEL population showed no differences in $CD8\alpha\alpha^+$ $CD4^+$, $CD8\alpha\beta^+$ $CD4^+$ or conventional $CD8\alpha\beta^-$ $CD4^+$ IEL subsets in treated H2-$Ab1^{fl/fl}$ versus H2-$Ab1^{VC}$ mice (Figure 5.13 C-E). Moreover, $CD4^-$ $TCR\gamma\delta^+$ and $CD4^-$ $TCR\gamma\delta^-$ IEL frequencies were unchanged (data not shown). Therefore, MHC class II expression by cIECs does not influence the composition of $CD4^+$ cIEL subsets in the intestinal epithelial layer during the resolution of chronic intestinal inflammation.

To further investigate the increased inflammation in H2-$Ab1^{VC}$ mice we assessed Treg and Th17 frequencies in colonic LPLs isolated from H2-$Ab1^{VC}$ and H2-$Ab1^{fl/fl}$ littermates by flow cytometry at the end point of the experiment (d42) (Figure 5.14 A). We found increased Th cell frequencies in the LPL of treated versus untreated mice, but did not detect significant differences between treated H2-$Ab1^{VC}$ and H2-$Ab1^{fl/fl}$ littermates (Figure 5.14 B). Additional analysis of Th cells subset revealed no significant differences in $FoxP3^+$ $RoR\gamma t^-$ or $FoxP3^-$ $RoR\gamma t^+$ subsets between *H. hepaticus* and anti-IL-10R treated H2-$Ab1^{VC}$ and H2-$Ab1^{fl/fl}$ mice, and although there was a trend towards reduced frequencies of $FoxP3^+$ $RoR\gamma t^+$ cells in H2-$Ab1^{VC}$mice, this difference did not reach statistical significance (Figure 5.14 C-E). These results suggest the lack of cIEC MHC class II expression did not influence Treg and Th17 cell proportions in the colonic lamina propria during the resolution of chronic intestinal inflammation.

We next assessed whether the sustained inflammation in treated H2-Ab1^{VC} mice might be driven by changes in cytokine and antimicrobial peptide (AMP) production, or proliferation and stemness status of the IEC. We therefore analysed colonic tissue lysates from H2-Ab1$^{fl/fl}$ and H2-Ab1^{VC} mice at the end point of the experiment (d42). We detected comparable levels of the cytokines IL-17A and IL-10 in colon tissues of H2-Ab1$^{fl/fl}$ and H2-Ab1^{VC} littermates (Figure 5.15 A and B, respectively). Although IL-22 expression levels were slightly increased in treated H2-Ab1^{VC} mice relative to those in H2-Ab1$^{fl/fl}$ mice, we detected a large range of intra-group variation (Figure 5.15 C).

Next, we assessed expression of selected AMP and the antimicrobial lectin RegIIIγ in colonic tissue samples at the experimental end point (d42). Although we found elevated expression of S100A8, RegIIIγ and NOS2 compared to untreated controls, we did not detect any significant differences between H2-Ab1$^{fl/fl}$ and H2-Ab1^{VC} mice (Figure 5.15 D-F). There was a tendency towards higher S100A8 expression by H2-Ab1^{VC} mice compared to H2-Ab1$^{fl/fl}$ littermates, but this did not reach statistical significance (Figure 5.15 E). Amphiregulin is encoded by the Areg gene and promotes tissue repair upon injury. We also detected increased Areg expression levels in colonic tissue samples at the experimental end point (d42), but these were comparable in H2-Ab1$^{fl/fl}$ and H2-Ab1^{VC} mice (Figure 5.15 G).

We also assessed potential differences in cell proliferation and 'stemness' within the colonic tissue samples at the experimental end point (d42), by measuring expression of Ki67 and Lgr5, respectively (Figure 5.15 H and I, respectively). We found no difference in Ki67 expression (Figure 5.15 H) and saw reduced Lgr5 expression (Figure 5.15 I) during the resolution phase of chronic intestinal inflammation, when compared to steady state. However, again we did not detect any significant changes between treated H2-Ab1$^{fl/fl}$ and H2-Ab1^{VC} mice. Taken together, these results highlight that IEC MHC class II expression did not influence the expression of cytokines IL-17A, IL-10 and IL-22 and did not modulate AMP expression. Furthermore, it did not influence cell proliferation and the stemness

status of the colonic tissue.

Naïve intestinal Th cells are primed by APCs in the MLNs before they differentiate and migrate into the peripheral tissue. We therefore assessed their cytokine production at the experimental end point (d42).We found significantly increased frequencies of TNFα^+ and IFNγ^+ CD4$^+$ Th cells in the MLNs of treated H2-Ab1^{VC} mice compared to treated H2-Ab1$^{fl/fl}$ littermates (Figure 5.16 A and C, and B and D, respectively). In contrast, the frequencies of IL-17A$^+$ CD4$^+$ Th cells in the MLNs of H2-Ab1$^{fl/fl}$ and H2-Ab1^{VC} littermates were comparable (data not shown). This upregulation of pro-inflammatory cytokine production was restricted to the MLNs as we did not detect significant changes in TNFα, IFNγ and IL-17A expression levels by Th cells in the lamina propria (data not shown).

Midway through my DPhil studies, my supervisor relocated to the University of Glasgow and I joined Fiona Powrie's group at the Kennedy Institute, University of Oxford. Thenceforward, my mouse colonies were housed at the new SPF-B animal facility. Although both animal facilities were SPF, we wanted to validate whether the delayed resolution of chronic inflammation in H2-Ab1^{VC} mice was conserved across both animal facilities, SPF-A and SPF-B. In addition, as the Powrie group had established that peak chronic intestinal inflammation occurred at three weeks post *H. hepaticus* + anti-IL-10R treatment in their SPF-B facility, we adjusted our treatment protocol to three weeks for induction of chronic intestinal inflammation and four weeks of resolution phase (Figure 5.17 A). Under these conditions, at the experimental endpoint (d42), we detected comparable spleen weights in H2-Ab1$^{fl/fl}$ and H2-Ab1^{VC} littermates (Figure 5.11 B). These results contrast with those in Figure 5.11 B, suggesting that the reduction in spleen weight initially observed in H2-Ab1^{VC} mice during the resolution of chronic intestinal inflammation was not conserved across multiple animal facilities.

We next assessed whether the delay in the resolution of intestinal inflammation in H2-Ab1^{VC} mice could still be detected in the new SPF-B animal facility. Assessment of caecal pathology at the experimental endpoint (d42), revealed comparable levels of intestinal inflammation in H2-Ab1$^{fl/fl}$ and H2-Ab1^{VC} mice (Figure 5.18 A), although the pathology scores were lower when compared to those observed in the old SPF-A animal facility (Figure 5.12 A). Similar observations were made regarding colon pathology, with comparable levels of colonic inflammation found in H2-Ab1^{VC} and H2-Ab1$^{fl/fl}$ mice in the new SPF-B animal facility (Figure 5.18 B and C), in contrast to higher pathology scores in H2-Ab1^{VC} mice in the old SPF-A animal facility (Figure 5.12 B and C). Representative pathology images are shown in Figure 5.18 D. In general, the intestinal pathology scores in both H2-Ab1^{VC} and H2-Ab1$^{fl/fl}$ mice housed in the new SPF-B animal facility were lower than those housed in the old SPF-A animal facility. However, these data suggest that lack of MHC class II expression by IECs did not impact the resolution of chronic intestinal inflammation in the new SPF-B animal facility.

At the experimental end point (d42), we also assessed MHC class II expression by cIECs and detected around 85 % MHC class II^{+} IECs in treated H2-Ab1$^{fl/fl}$ mice, whereas very few MHCII^{+} IECs were present in H2-Ab1$^{fl/fl}$ mice (Figure 5.19 A and B). Thus, during the resolution phase of chronic intestinal inflammation IECs still expressed high levels of MHC class II and had the potential to interact with CD4^{+} T cells.

We next assessed whether lack of MHC class II expression by IECs influenced colonic IEL populations during the resolution of intestinal inflammation (d42) in mice housed in the new SPF-B animal facility. We therefore isolated cIELs and analysed them by flow cytometry (Figure 5.20 A). Analysis of the total CD4^{+} TCR$\gamma\delta^{-}$ IEL population revealed significantly decreased frequencies in H2-Ab1^{VC} compared to H2-Ab1$^{fl/fl}$ mice (Figure 5.20 B). Analysis of the CD4^{+} TCR$\gamma\delta^{-}$ IEL subsets showed no significant differences in CD8$\alpha\alpha^{+}$ CD4^{+} and CD8$\alpha\beta^{+}$ CD4^{+} IEL

frequencies between H2-Ab1$^{fl/fl}$ and H2-Ab1^{VC} mice (Figure 5.20 C and D). Analysis of conventional CD8$\alpha\beta^-$ CD4$^+$ IELs revealed a strong tendency towards decreased frequencies in H2-Ab1^{VC} versus H2-Ab1$^{fl/fl}$ mice (Figure 5.20 E). We also found that, CD4$^-$ TCR$\gamma\delta^+$ and CD4$^-$ TCR$\gamma\delta^-$ IEL frequencies were unchanged (data not shown). Therefore lack of MHC class II expression by IECs led to reduced CD4$^+$ TCR$\gamma\delta^-$ IEL frequencies during the resolution of chronic intestinal inflammation.

Next, we assessed the Treg and Th17 frequencies in the colonic lamina propria during the resolution of intestinal inflammation (d42) in the mice housed in the new SPF-B animal facility (Figure 5.21 A). Assessment of the overall Th cell population showed comparable Th cell frequencies in H2-Ab1$^{fl/fl}$ and H2-Ab1^{VC} littermates (Figure 5.21 B). Additional analysis revealed similar frequencies of FoxP3$^+$, RoRγt$^+$ and FoxP3$^+$ RoRγ^+ Th cell subsets in H2-Ab1^{VC} and H2-Ab1$^{fl/fl}$ mice (Figure 5.21 C-E). Overall, these results show that IEC MHC class II expression did not influence the Treg and Th17 frequencies in the colonic lamina propria during the resolution of chronic intestinal inflammation in the new SPF-B animal facility.

Finally, we assessed TNFα and IFNγ expression levels by MLN Th cells during the resolution of intestinal inflammation (d42) in the mice housed in the new SPF-B animal facility. Th cell frequencies were comparable in the MLNs of H2-Ab1$^{fl/fl}$ and H2-Ab1^{VC} littermates (Figure 5.22 A) and the proportions of TNFα^+ and IFNγ^+ CD4$^+$ Th cells after PMA/ionomycin restimulation were comparable (Figure 5.22 B and C, respectively). Taken together, these data indicate that, in the mice housed in the new SPF-B animal facility, IEC MHC class II expression did not affect TNFα and IFNγ production by MLN Th cells during colitis resolution.

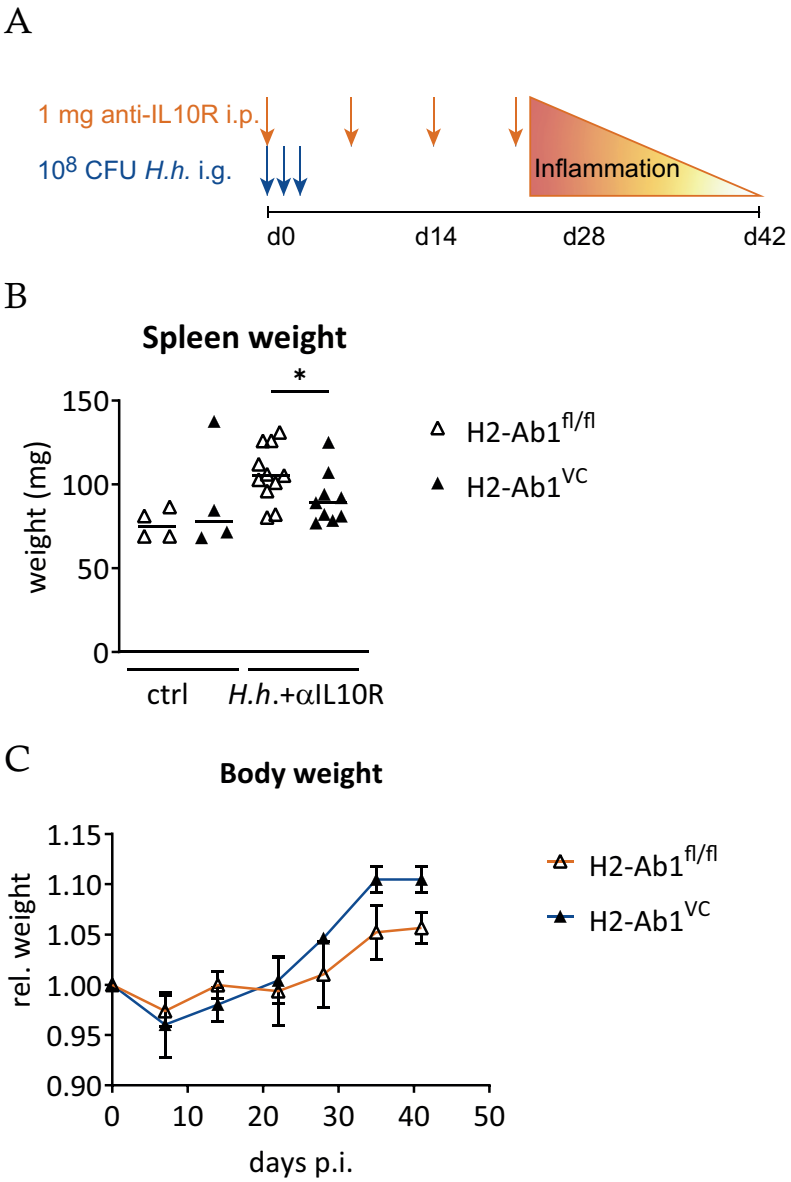


Figure 5.11: Reduced spleen weight but comparable body weight of H2-Ab1^{VC} mice during the resolution phase of *H. hepaticus* + anti-IL-10R treatment. H2-Ab1^{VC} and H2-Ab1$^{fl/fl}$ littermates were orally infected with 10^8 CFU *H. hepaticus* on three consecutive days and i.p. injected with 1 mg anti-IL-10R weekly for four weeks. Mice were sacrificed at seven weeks post infection. (A) Schematic of treatment protocol. (B) Spleen weight was assessed after seven weeks. Horizontal bars indicate group medians. (C) Mice were weighed at the indicated time points until sacrifice. Symbols denote mean (± SEM) as a relative to the initial body weight. Statistical significance between the groups was determined by Mann-Whitney test (B) or two-way ANOVA multiple comparisons test with Sidak's correction (C). P-value summary: *$p<0.05$. (B) Data from two pooled independent experiments with total mouse numbers per group as follows; n=9 H2-Ab1^{VC} and n=11 H2-Ab1$^{fl/fl}$ treated mice and n=4 H2-Ab1^{VC} and n=4 H2-Ab1$^{fl/fl}$ untreated mice. (C) Data of one experiment with n=3 H2-Ab1^{VC} and n=4 H2-Ab1$^{fl/fl}$ treated mice.

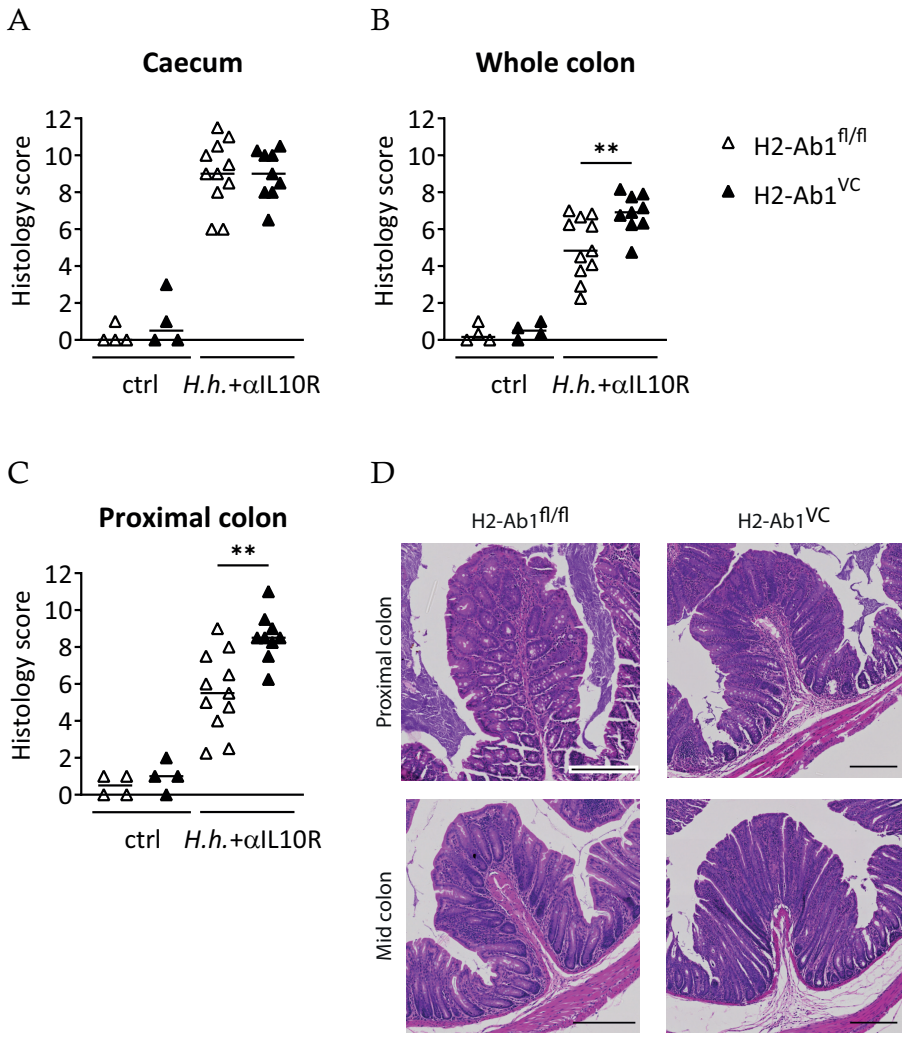


Figure 5.12: Delayed resolution of inflammation of *H. hepaticus* + anti-IL-10R treated H2-Ab1^{VC} mice. H2-Ab1^{VC} and H2-Ab1$^{fl/fl}$ littermates were orally infected with 10^8 CFU *H. hepaticus* on three consecutive days and i.p. injected with 1 mg anti-IL-10R weekly for four weeks. Mice were sacrificed at seven weeks post infection. Histopathology scores of the caecum (A), whole colon (B) and proximal colon (C). Horizontal bars indicate group medians. (D) Representative H&E sections of the colon from H2-Ab1^{VC} and H2-Ab1$^{fl/fl}$ littermates. Scale bars, 200 μm. Statistical significance between the groups was determined by Mann-Whitney test. P-value summary: *p<0.05; **p<0.001. Data from two pooled independent experiments with total mouse numbers per group as follows; n=9 H2-Ab1^{VC} and n=11 H2-Ab1$^{fl/fl}$ treated mice and n=4 H2-Ab1^{VC} and n=4 H2-Ab1$^{fl/fl}$ untreated mice.

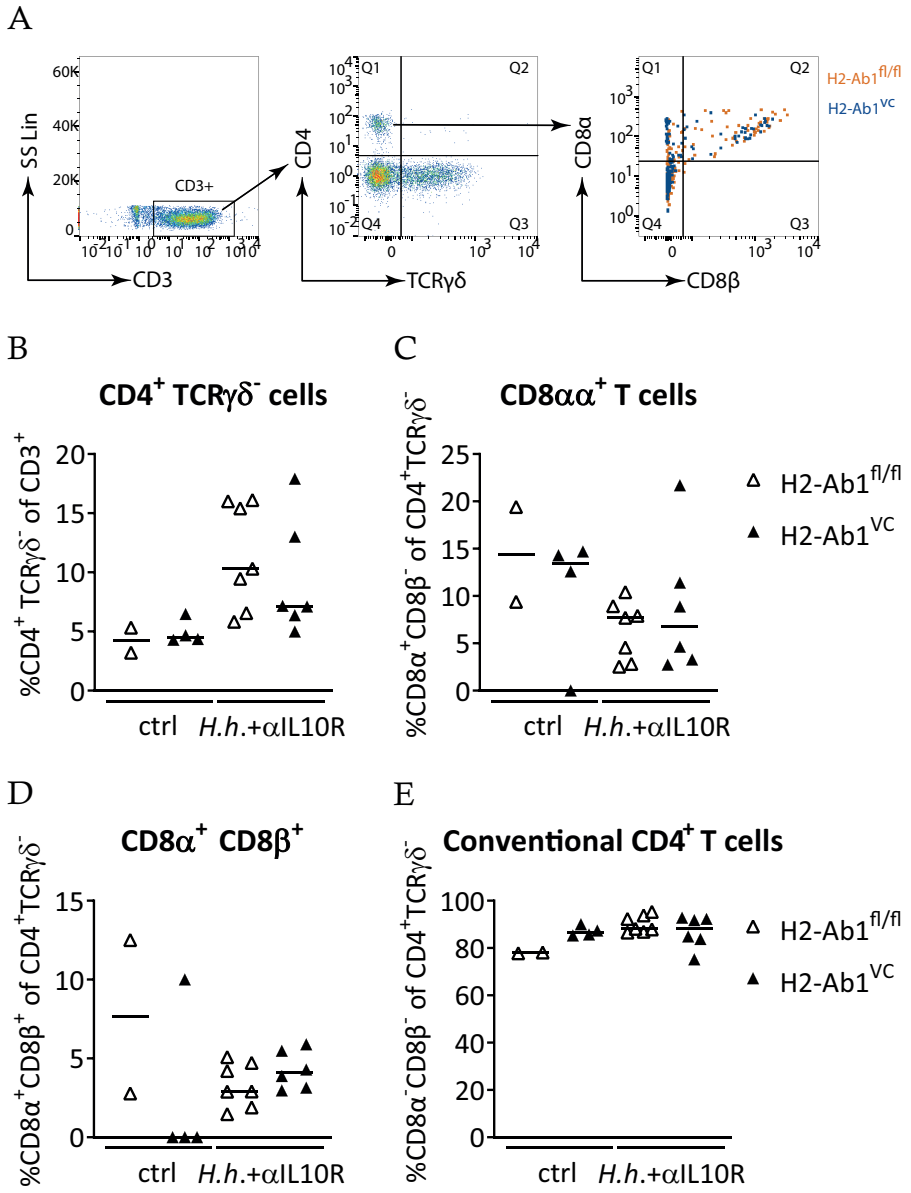


Figure 5.13: Comparable colonic CD4$^+$ IEL frequencies during the resolution of chronic inflammation. H2-Ab1^{VC} and H2-Ab1$^{fl/fl}$ littermates were orally infected with 10^8 CFU *H. hepaticus* on three consecutive days and i.p. injected with 1 mg anti-IL-10R weekly for four weeks. Mice were sacrificed at seven weeks post infection. (A) Schematic of FACS gating strategy. Frequencies of CD4$^+$ TCR$\gamma\delta^-$ IELs (B) as well as their daughter CD8α^+ CD8β^- (C), CD8α^+ CD8β^+ (D) and CD8α^- CD8β^- (E) subsets. Statistical significance between the groups was determined by Mann-Whitney test. (B-E) Data from one experiment with total mouse numbers per group as follows; n=6 H2-Ab1^{VC} and n=7 H2-Ab1$^{fl/fl}$ treated mice and n=3 H2-Ab1^{VC} and n=2 H2-Ab1$^{fl/fl}$ untreated mice.

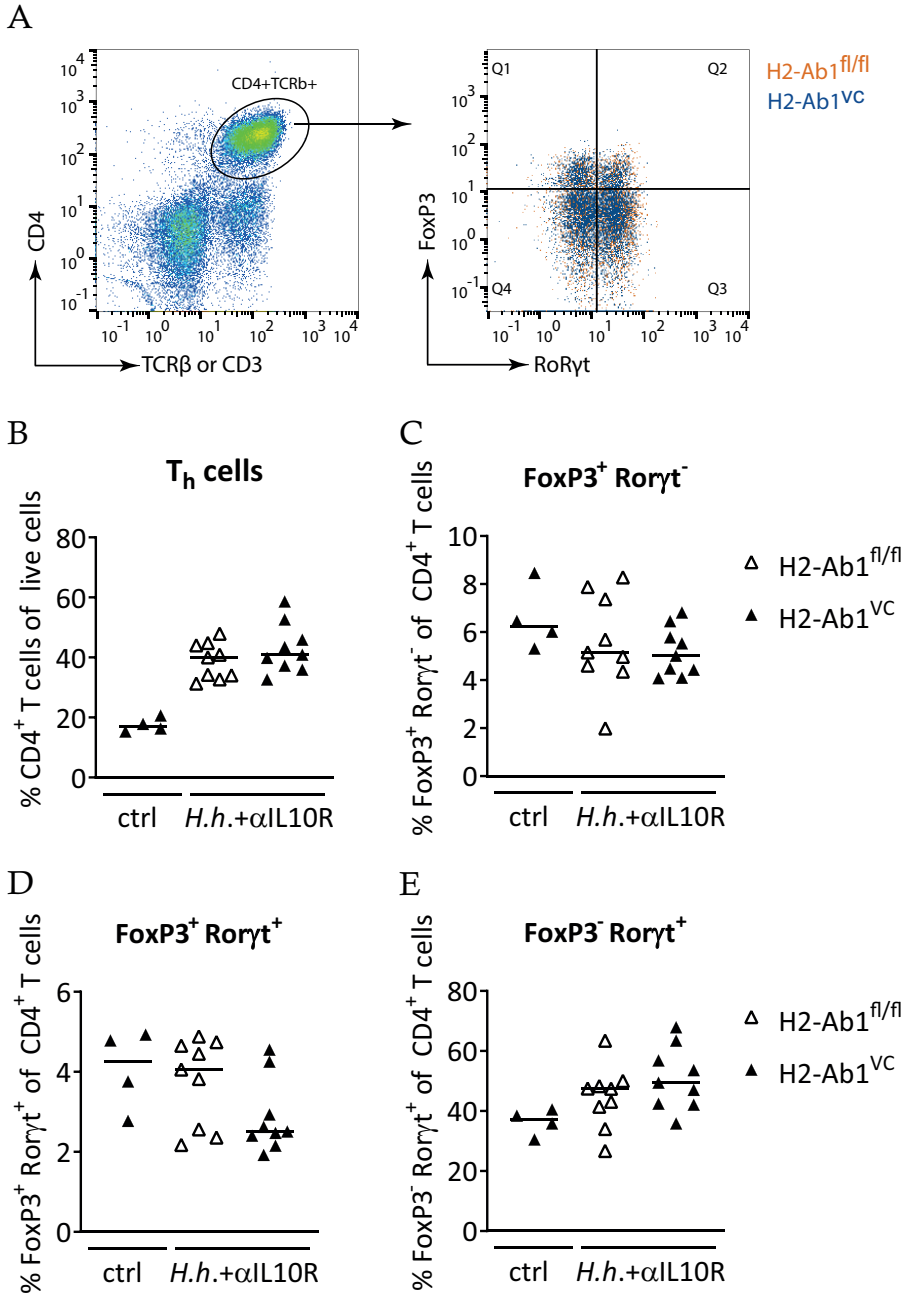


Figure 5.14: Comparable Treg and Th17 frequencies during the resolution of chronic inflammation between H2-Ab1^{VC} and H2-Ab1$^{fl/fl}$ littermates. H2-Ab1^{VC} and H2-Ab1$^{fl/fl}$ littermates were orally infected with 10^8 CFU *H. hepaticus* on three consecutive days and i.p. injected with 1 mg anti-IL-10R weekly for four weeks. Mice were sacrificed at seven weeks post infection. (A) Schematic of FACS gating strategy. Frequencies of CD4$^+$ TCRβ^+ T cells (B) and their daughter FoxP3$^+$ RoRγt$^-$ (C), FoxP3$^+$ RoRγt$^+$ (D) and FoxP3$^-$ RoRγt$^+$ (E) subsets. Horizontal bars indicate group medians. Statistical significance between the groups was determined by Mann-Whitney test. Statistical significance between the groups was determined by Mann-Whitney test. (B-E) Data from two pooled independent experiments with total mouse numbers per group as follows; n=9 H2-Ab1^{VC} and n=9 H2-Ab1$^{fl/fl}$ treated mice and n=4 H2-Ab1^{VC} untreated mice.

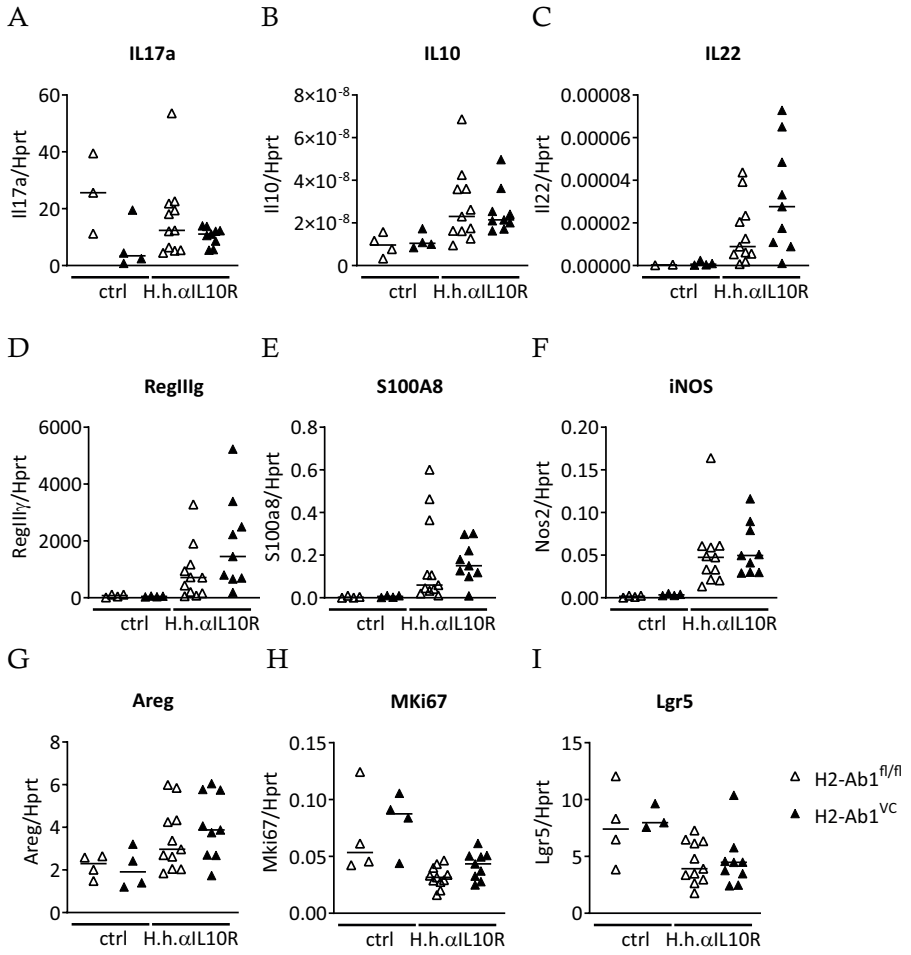


Figure 5.15: Comparable cytokine and AMP expression, as well as proliferation and stemness status in colonic tissue of H2-Ab1$^{fl/fl}$ and H2-Ab1^{VC} mice during resolution of chronic inflammation. H2-Ab1^{VC} and H2-Ab1$^{fl/fl}$ littermates were orally infected with 10^8 CFU *H. hepaticus* on three consecutive days and i.p. injected with 1 mg anti-IL-10R weekly for four weeks. Mice were sacrificed at seven weeks post infection. Colon tissue was isolated from H2-Ab1$^{fl/fl}$ and H2-Ab1^{VC} mice and cDNA prepared for RT-qPCR analysis. Symbols denote IL-17A (A), IL-10 (B), IL-22 (C), RegIIIγ (D), S100A8 (E), NOS2 (F), Areg (G), MKi67 (H) and Lgr5 (I) mRNA levels. Values were normalised to the housekeeping gene HPRT. Statistical significance between the groups was determined by Mann-Whitney test. Data from two pooled independent experiments with total mouse numbers per group as follows; n=9 H2-Ab1^{VC} and n=11 H2-Ab1$^{fl/fl}$ treated mice and n=4 H2-Ab1^{VC} and n=4 H2-Ab1$^{fl/fl}$ untreated mice.

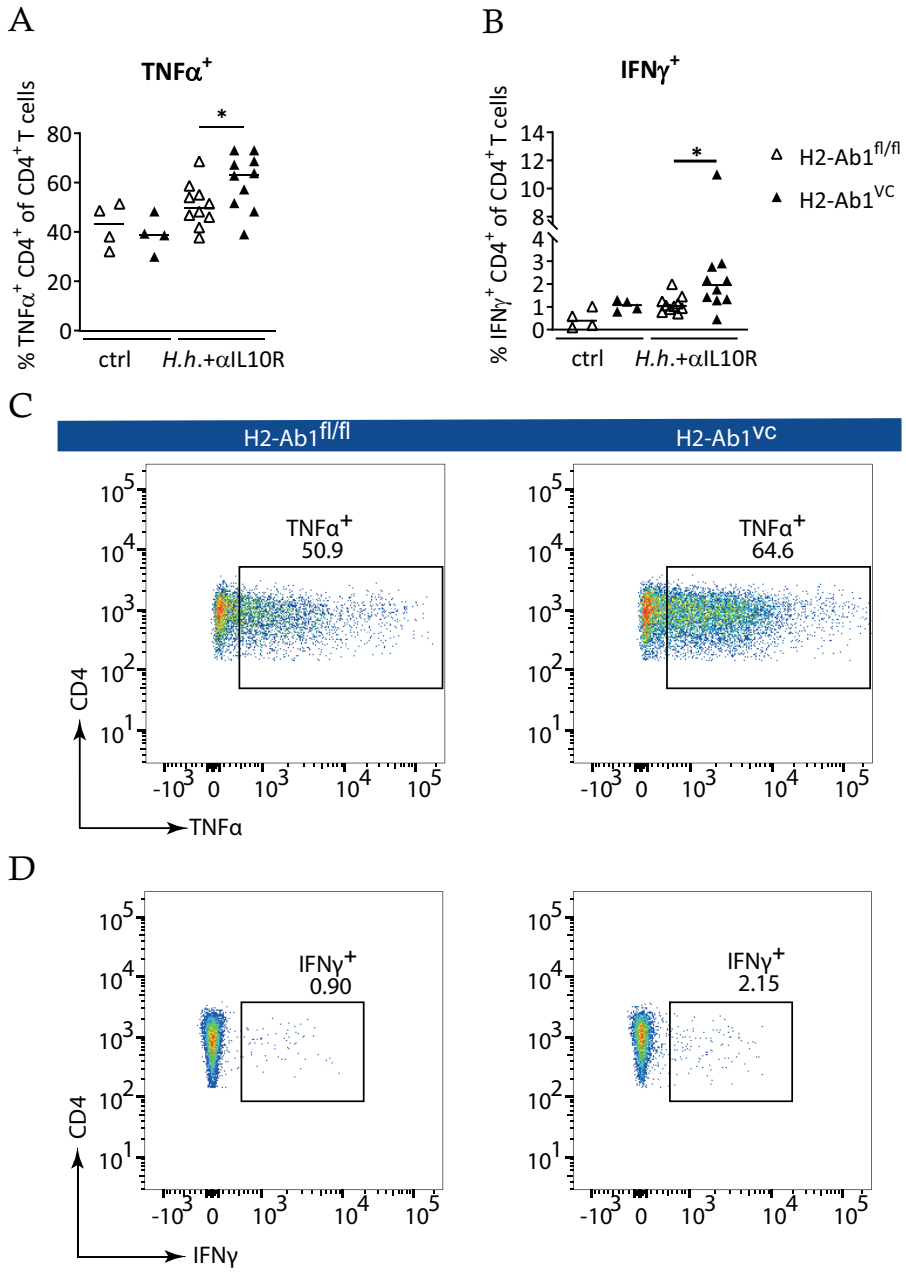


Figure 5.16: Increased TNFα and IFNγ production by MLN Th cells of H2-Ab1^{VC} mice during the resolution phase of *H. hepaticus* + anti-IL-10R treatment. H2-Ab1^{VC} and H2-Ab1$^{fl/fl}$ littermates were orally infected with 10^8 CFU *H. hepaticus* on three consecutive days and i.p. injected with 1 mg anti-IL-10R weekly for four weeks. Mice were sacrificed at seven weeks post infection. Frequencies of TNFα (A) and IFNγ (B) expression by CD4$^+$ T cells in the MLNs. Horizontal bars indicate group medians. Representative FACS plots of TNFα (C) and IFNγ (D) expressing CD4$^+$ T cells. Statistical significance between the groups was determined by Mann-Whitney test. P-value summary: *p<0.05. Data from two pooled independent experiments with total mouse numbers per group as follows; n=10 H2-Ab1^{VC} and n=10 H2-Ab1$^{fl/fl}$ treated mice and n=4 H2-Ab1^{VC} and n=4 H2-Ab1$^{fl/fl}$ untreated mice.

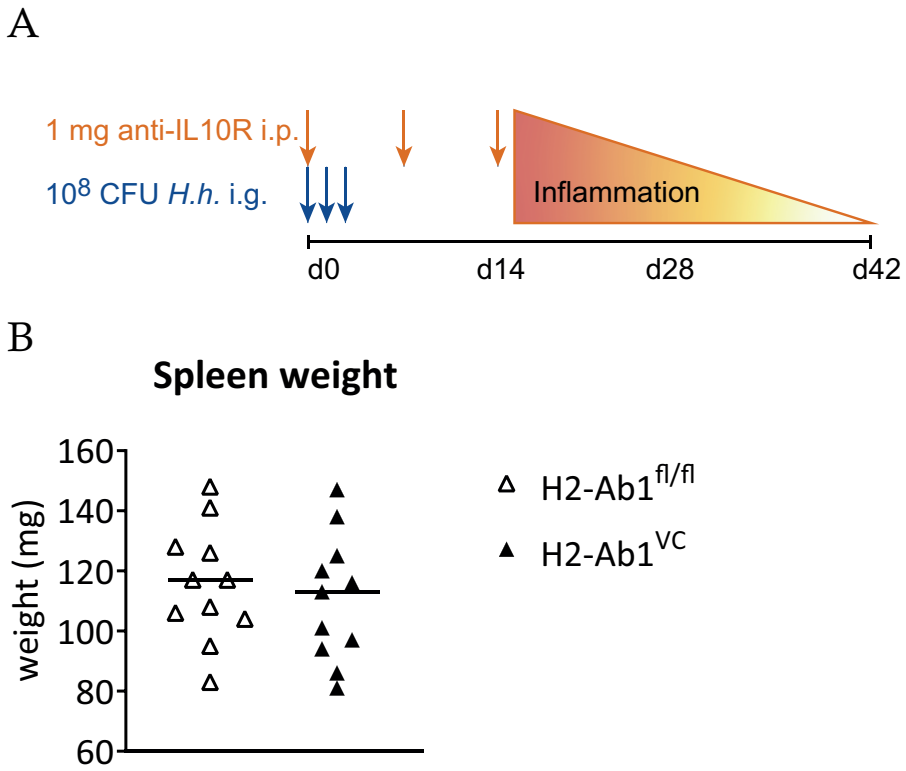


Figure 5.17: Comparable spleen weight during the resolution phase of *H. hepaticus* + anti-IL-10R treatment at the new SPF-B animal facility. H2-Ab1^{VC} and H2-Ab1$^{fl/fl}$ littermates were orally infected with 10^8 CFU *H. hepaticus* on three consecutive days and i.p. injected with 1 mg anti-IL-10R weekly for three weeks. Mice were sacrificed at seven weeks post infection. (A) Schematic of treatment protocol. (B) Spleen weight was assessed after seven weeks. Horizontal bars indicate group medians. Statistical significance between the groups was determined by Mann-Whitney test. Data from one experiment with total mouse numbers per group as follows; n=11 H2-Ab1^{VC} and n=11 H2-Ab1$^{fl/fl}$ treated mice. Mice were housed in the new SPF-B animal facility.

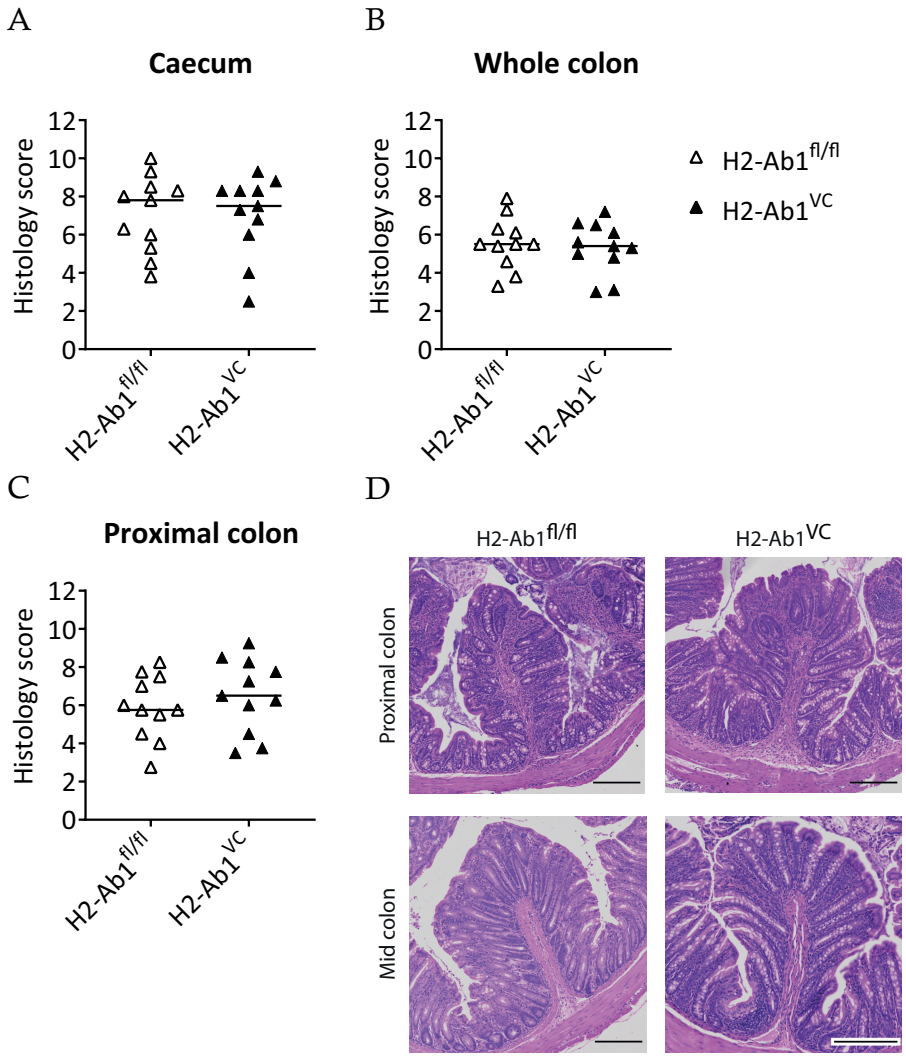


Figure 5.18: Comparable resolution of inflammation of *H. hepaticus* + anti-IL-10R treated H2-Ab1^{VC} mice in new SPF-B animal facility. H2-Ab1^{VC} and H2-Ab1$^{fl/fl}$ littermates were orally infected with 10^8 CFU *H. hepaticus* on three consecutive days and i.p. injected with 1 mg anti-IL-10R weekly for three weeks. Mice were sacrificed at seven weeks post infection. Histopathology scores of the caecum (A), whole colon (B) and proximal colon (C). Horizontal bars indicate group medians. (D) Representative H&E sections of the colon from H2-Ab1^{VC} and H2-Ab1$^{fl/fl}$ littermates. Scale bars, 200 μm. Statistical significance between the groups was determined by Mann-Whitney test. Data from one experiment with total mouse numbers per group as follows; n=11 H2-Ab1^{VC} and n=11 H2-Ab1$^{fl/fl}$ treated mice. Mice were housed in the new SPF-B animal facility.

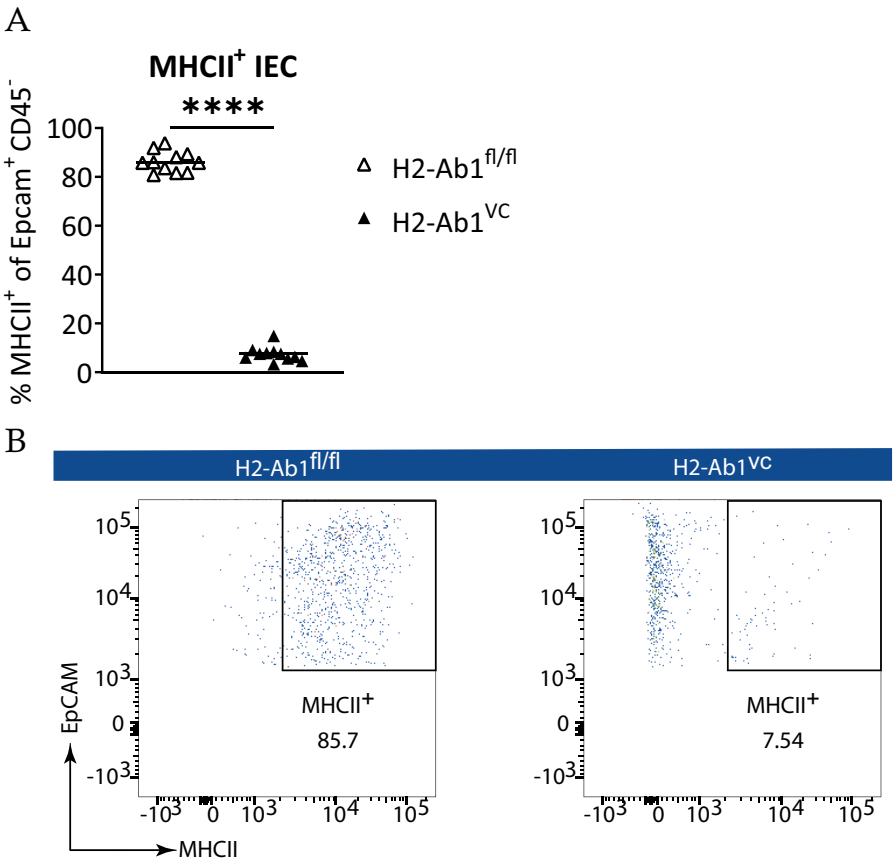


Figure 5.19: Upregulated MHC class II expression by cIECs during the resolution of inflammation of *H. hepaticus* + anti-IL-10R treated H2-Ab1$^{fl/fl}$ mice. H2-Ab1^{VC} and H2-Ab1$^{fl/fl}$ littermates were orally infected with 10^8 CFU *H. hepaticus* on three consecutive days and i.p. injected with 1 mg anti-IL-10R weekly for three weeks. Mice were sacrificed at seven weeks post infection. MHC class II expression of EpCAM$^+$ (A) and CD45$^+$ (B) cells. Horizontal bars indicate group medians. Representative FACS plots of MHC class II expressing EpCAM$^+$ (C) and CD45$^+$ (D) cells. Statistical significance between the groups was determined by Mann-Whitney test. P-value summary: **p<0.001; ****p<0.00001.Data from one experiment with total mouse numbers per group as follows; n=11 H2-Ab1^{VC} and n=11 H2-Ab1$^{fl/fl}$ treated mice. Mice were housed in the new SPF-B animal facility.

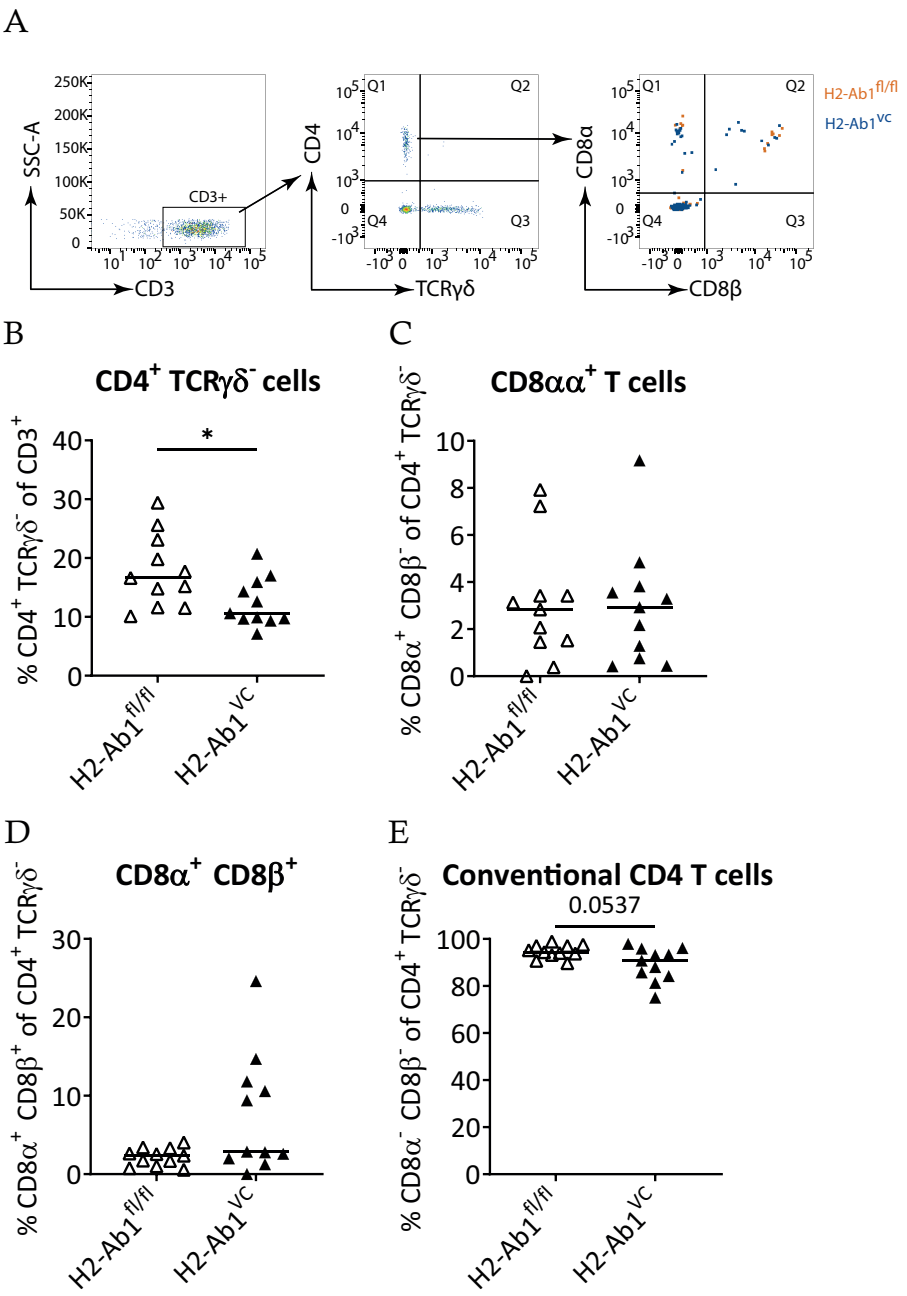


Figure 5.20: Reduced colonic CD4$^+$ IEL frequencies in H2-Ab1^{VC} mice during the resolution of chronic inflammation in the new SPF-B animal facility. H2-Ab1^{VC} and H2-Ab1$^{fl/fl}$ littermates were orally infected with 10^8 CFU *H. hepaticus* on three consecutive days and i.p. injected with 1 mg anti-IL-10R weekly for three weeks. Mice were sacrificed at seven weeks post infection. (A) Schematic of FACS gating strategy. Frequencies of CD4$^+$ TCR$\gamma\delta^-$ IELs (B) as well as their daughter CD8α^+ CD8β^- (C), CD8α^+ CD8β^+ (D) and CD8α^- CD8β^- (E) subsets. Statistical significance between the groups was determined by Mann-Whitney test. P-value summary: *p<0.05. Data from one experiment with total mouse numbers per group as follows; n=11 H2-Ab1^{VC} and n=11 H2-Ab1$^{fl/fl}$ treated mice. Mice were housed in the new SPF-B animal facility.

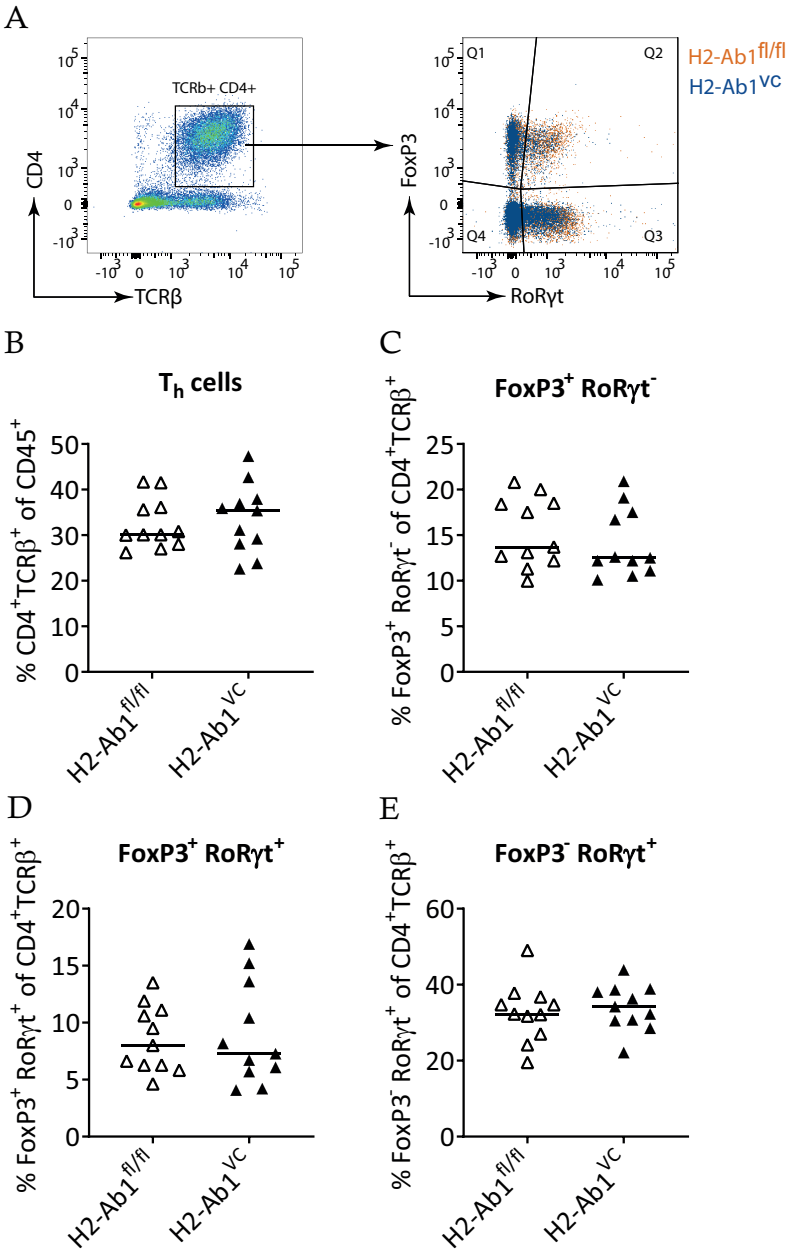


Figure 5.21: Comparable Treg and Th17 frequencies during the resolution of chronic inflammation between H2-Ab1^{VC} and H2-Ab1$^{fl/fl}$ littermates in the new SPF-B animal facility. H2-Ab1^{VC} and H2-Ab1$^{fl/fl}$ littermates were orally infected with 10^8 CFU *H. hepaticus* on three consecutive days and i.p. injected with 1 mg anti-IL-10R weekly for three weeks. Mice were sacrificed at seven weeks post infection. (A) Schematic of FACS gating strategy. Frequencies of CD4$^+$ TCRβ^+ T cells (B) and their daughter FoxP3$^+$ RoRγt$^-$ (C), FoxP3$^+$ RoRγt$^+$ (D) and FoxP3$^-$ RoRγt$^+$ (E) subsets. Horizontal bars indicate group medians. Statistical significance between the groups was determined by Mann-Whitney test. (B-E) Data from one experiment with total mouse numbers per group as follows; n=11 H2-Ab1^{VC} and n=11 H2-Ab1$^{fl/fl}$ treated mice. Mice were housed in the new SPF-B animal facility.

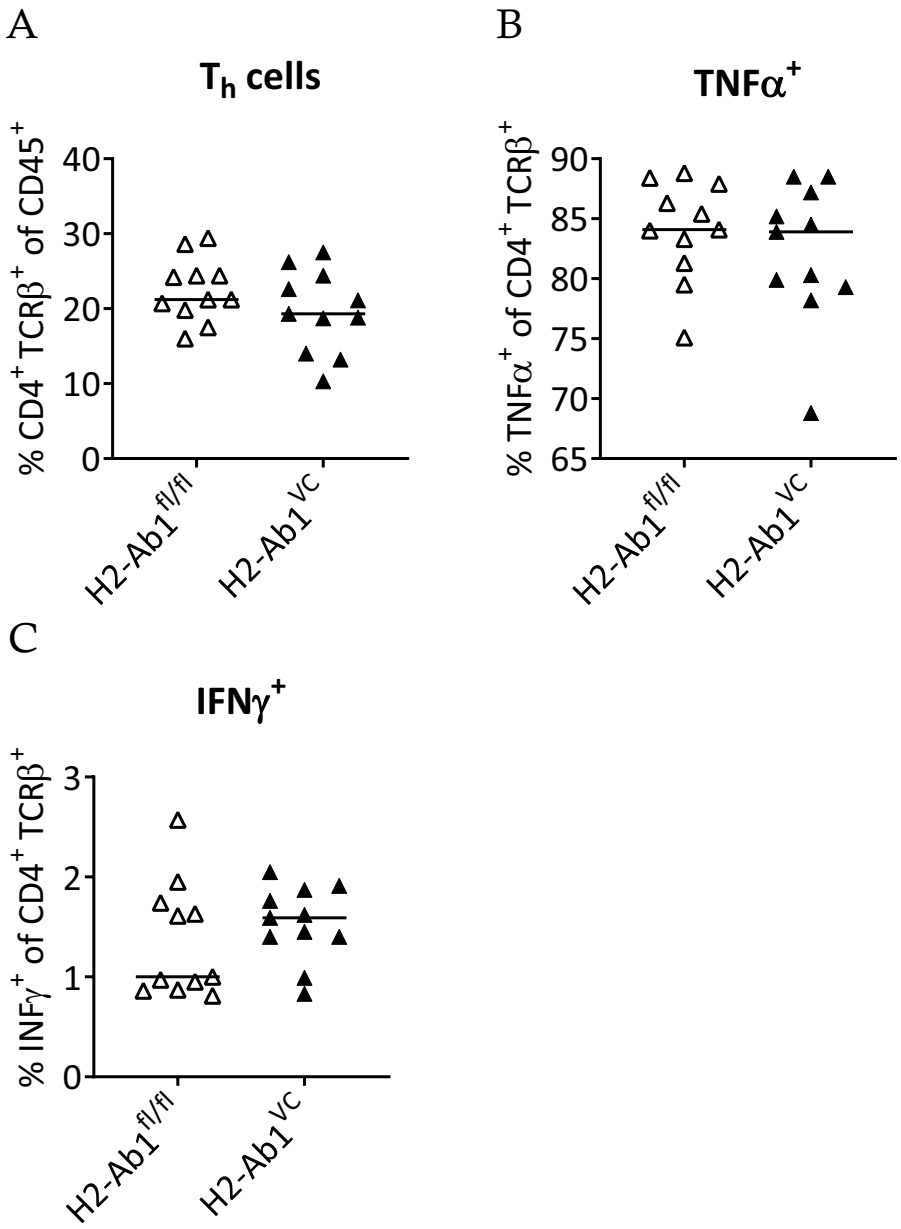


Figure 5.22: Comparable TNFα and IFNγ production by MLN Th cells of H2-Ab1^{VC} mice during the resolution phase of *H. hepaticus* + anti-IL-10R treatment in the new SPF-B animal facility. H2-Ab1^{VC} and H2-Ab1$^{fl/fl}$ littermates were orally infected with 10^8 CFU *H. hepaticus* on three consecutive days and i.p. injected with 1 mg anti-IL-10R weekly for three weeks. Mice were sacrificed at seven weeks post infection. Frequencies of CD4$^+$ T cells (A), as well as TNFα (B) and IFNγ (C) expression in the MLNs. Horizontal bars indicate group medians. Statistical significance between the groups was determined by Mann-Whitney test. Data from one experiment with total mouse numbers per group as follows; n=11 H2-Ab1^{VC} and n=11 H2-Ab1$^{fl/fl}$ treated mice. Mice were housed in the new SPF-B animal facility.

5.2.4 MHC class II expression by cIECs does not influence intestinal inflammation induced by chronic DSS treatment

We next wanted to use the chronic DSS model to mimic the long-lasting and relapsing nature of IBD in humans. We treated our mice with three cycles of 1.5 % DSS and terminated the experiment half way through the final recovery phase (d52) to assess the influence of IEC MHC class II expression on the resolution of chronic intestinal inflammation (Figure 5.23 A). We performed two independent experiments, which will be colour coded throughout the subsequent figures.

First, we determined the impact of chronic DSS treatment on MHC class II expression by cIECs. Flow cytometric analysis showed that cIECs expressed MHC class II in H2-Ab1$^{fl/fl}$ mice but not in H2-Ab1^{vc} mice. One mouse in the H2-Ab1^{vc} group showed insufficient MHC class II deletion in IECs (Figure 5.24 A and C). Importantly, these differences in MHC class II expression were not seen in CD45$^+$ cells in the epithelial washes. Here, we detected comparable MHC class II$^+$ CD45$^+$ cell frequencies between H2-Ab1$^{fl/fl}$ and H2-Ab1^{vc} mice (Figure 5.24 B and D). These data highlight that cIECs of H2-Ab1$^{fl/fl}$ mice express MHC class II during chronic DSS treatment and that the MHC class II expression by CD45$^+$ cells was not affected by Villin-Cre mediated deletion of MHC class II expression.

DSS treatment results in epithelial damage and mice develop colonic inflammation, which is evidenced by colon length shortening and body weight loss. As a measure of gross pathology, we assessed colon length, and although we detected a tendency towards decreased colon length in H2-Ab1^{VC} compared to H2-Ab1$^{fl/fl}$ mice in the first experiment, this was not observed in the second experiment (Figure 5.23 B). As an indication for systemic inflammation we assessed spleen weights. Although spleen weights were generally comparable between H2-Ab1$^{fl/fl}$ and H2-Ab1^{VC} mice (Figure 5.23 C), there was a trend towards reduced spleen weights in H2-Ab1^{VC} mice in the second experiment (Figure 5.23 C). When we assessed the body weight

of the animals we were able to detect a drop in body weight after each cycle of DSS treatment, which recovered during the water cycles. However, the body weights were very similar between H2-Ab1$^{fl/fl}$ and H2-Ab1^{VC} mice throughout the experiment (Figure 5.23 D). Body weights of both experiments were taken on slightly different days throughout the experiment and therefore not combined for this analysis. These results suggest that MHC class II expression by cIECs has little impact on systemic inflammation, colon length as well as body weight loss during chronic DSS treatment.

We further assessed the impact of cIEC MHC class II expression on the disease severity of chronic DSS colitis. Colonic tissue was formalin fixed, paraffin embedded, sectioned and stained with H&E. Intestinal pathology was assessed in a semi-quantitative manner by Dr. Mathilde Pohin (Kennedy Institute of Rheumatology, University of Oxford) (see Table 2.3). Chronic DSS treatment did induce intestinal inflammation but histology scores of the mid and distal colon were comparable between treated H2-Ab1$^{fl/fl}$ and H2-Ab1^{VC} littermates (Figure 5.25 A and B, respectively). Representative images of the histopathology scores of the mid and distal colon are depicted in Figure 5.25 C. In conclusion, the intestinal pathology caused by chronic DSS treatment was not significantly affected by cIEC MHC class II expression.

We next investigated whether loss of MHC class II expression by cIECs influences myleoid cell populations in the colonic lamina propria by flow cytometry (Figure 5.26). We detected a significant reduction in CD11b^{-} CD11c^{+} MHCII^{+} DCs in H2-Ab1^{VC} mice compared to H2-Ab1$^{fl/fl}$ littermates. However this reduction was only evident when both experiments were combined for the statistical analysis and not for each independent experiment (Figure 5.27 A). We did however detect significantly reduced CD11b^{-} CD11c^{+} MHCII^{+} DC cell numbers in the first DSS experiment (Figure 5.28 A). H2-Ab1^{VC} and H2-Ab1$^{fl/fl}$ mice showed comparable neutrophil, eosinophil and monocyte frequencies (Figure 5.27 B-D), with overall higher neutrophil frequencies in the second DSS experiment and higher eosinophil

frequencies in the first DSS experiment (Figure 5.27 B and C, respectively). The analysis of inflammatory monocytes showed a tendency towards reduced frequencies in H2-Ab1^{VC} mice in the first DSS experiment but this data did not repeat in the second DSS experiment (Figure 5.27 E). When analysing the inflammatory monocyte cell numbers we detected significantly reduced cell numbers in H2-Ab1^{VC} mice compared to H2-Ab1$^{fl/fl}$ littermates in the first DSS experiment (Figure 5.28 B). The analysis of macrophages and CD11c^{+} CD11b^{+} DCs showed comparable frequencies between H2-Ab1^{VC} and H2-Ab1$^{fl/fl}$ mice (Figure 5.27 F and G). We did however detect significantly reduced cell numbers for both macrophages and CD11c^{+} CD11b^{+} DCs in H2-Ab1^{VC} compared to H2-Ab1$^{fl/fl}$ mice (Figure 5.28 C and D). Overall these results show that the changes in myeloid cell frequencies and numbers varied between the two chronic DSS experiments.

We then wanted to investigate whether MHC class II deletion in cIECs influenced Treg and Th17 frequencies in the colonic lamina propria of chronic DSS mice. We therefore isolated Th cells from the colonic lamina propria and analysed Treg and Th17 populations by flow cytometry (Figure 5.29 A). We found that chronic DSS treated H2-Ab1$^{fl/fl}$ and H2-Ab1^{VC} littermates exhibited comparable Th cell frequencies (Figure 5.29 B). Moreover, we assessed FoxP3 and RoRγt frequencies of Th cells but did not detect major differences (Figure 5.29 C-E). Furthermore, we did not detect significant changes in GATA3 expression by Th cells (data not shown). Analysis of the Th cell population in the spleen and MLNs of H2-Ab1^{VC} and H2-Ab1$^{fl/fl}$ littermates showed comparable FoxP3, GATA3 and RoRγt frequencies (data not shown). Taken together, these results highlight that epithelial MHC class II expression during chronic DSS treatment does not influence the frequencies of overall Th cells and specifically of Treg and Th17 cells.

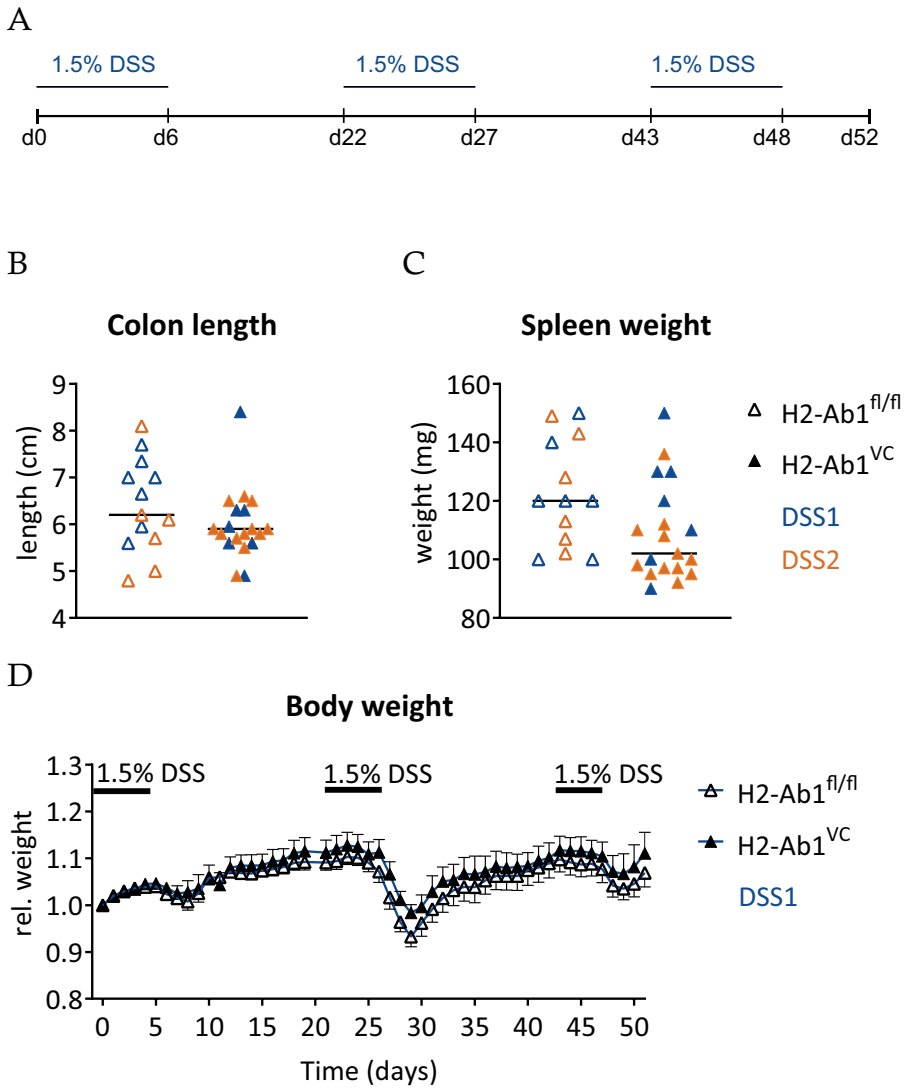


Figure 5.23: MHC II expression on IECs does not affect recovery from chronic DSS colitis. H2-Ab1^{VC} and H2-Ab1$^{fl/fl}$ littermates were subjected to three cycles of DSS treatment. Mice were sacrificed at day 52. (A) Schematic of treatment protocol. Colon length (B) and spleen weight (C) was assessed at day 52. Horizontal bars indicate group medians. (D) Mice were weighed at the indicated time points until sacrifice. Symbols denote mean (± SEM) as a relative to the initial body weight. H2-Ab1^{VC} mice show the upper error bar and H2-Ab1$^{fl/fl}$ mice show the lower error bar. Statistical significance between the groups was determined by Mann-Whitney test (B and C) or two-way ANOVA multiple comparisons test with Sidak's correction (D). (B and C) Data from two pooled independent experiments with total mouse numbers per group as follows; n=19 H2-Ab1^{VC} and n=13 H2-Ab1$^{fl/fl}$ treated mice. (D) Representative data from one of two independent experiments with total mouse numbers per group as follows; n=7 H2-Ab1^{VC} and n=7 H2-Ab1$^{fl/fl}$ treated mice. Mice were housed in the new SPF-B animal facility.

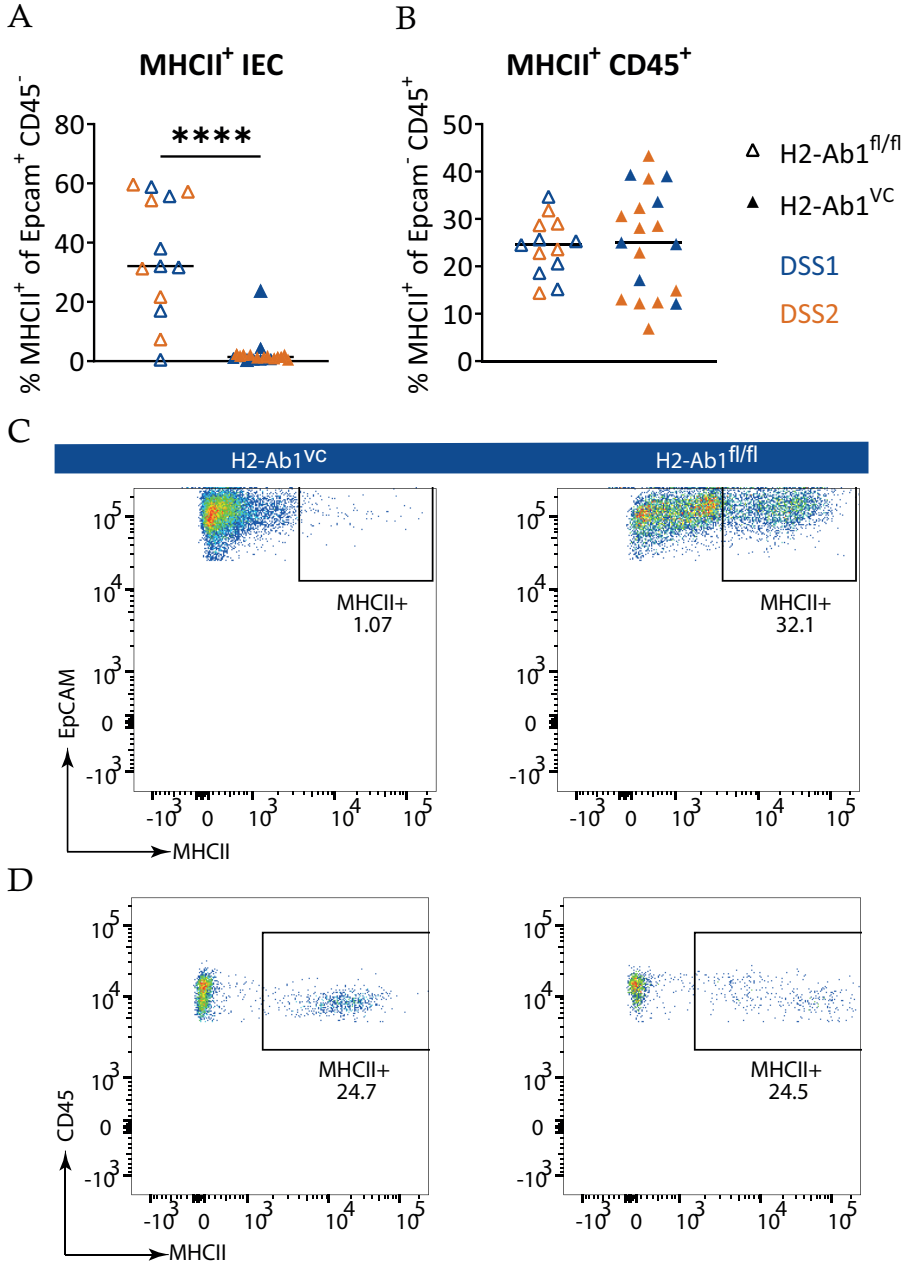


Figure 5.24: IECs express MHC class II during chronic DSS treatment in H2-Ab1$^{fl/fl}$ mice. H2-Ab1^{VC} and H2-Ab1$^{fl/fl}$ littermates were subjected to three cycles of DSS treatment. Mice were sacrificed at day 52. MHC class II expression of IECs (A) and CD45^{+} cells (B) was assessed at day 52. Horizontal bars indicate group medians. Representative FACS plots of MHC class II^{+} IECs (C) and CD45^{+} cells (D) of H2-Ab1^{VC} and H2-Ab1$^{fl/fl}$ mice are depicted. Statistical significance between the groups was determined by Mann-Whitney test (A and B). P-value summary: ****p<0.0001. Data from two pooled independent experiments with total mouse numbers per group as follows; n=19 H2-Ab1^{VC} and n=13 H2-Ab1$^{fl/fl}$ treated mice. Mice were housed in the new SPF-B animal facility.

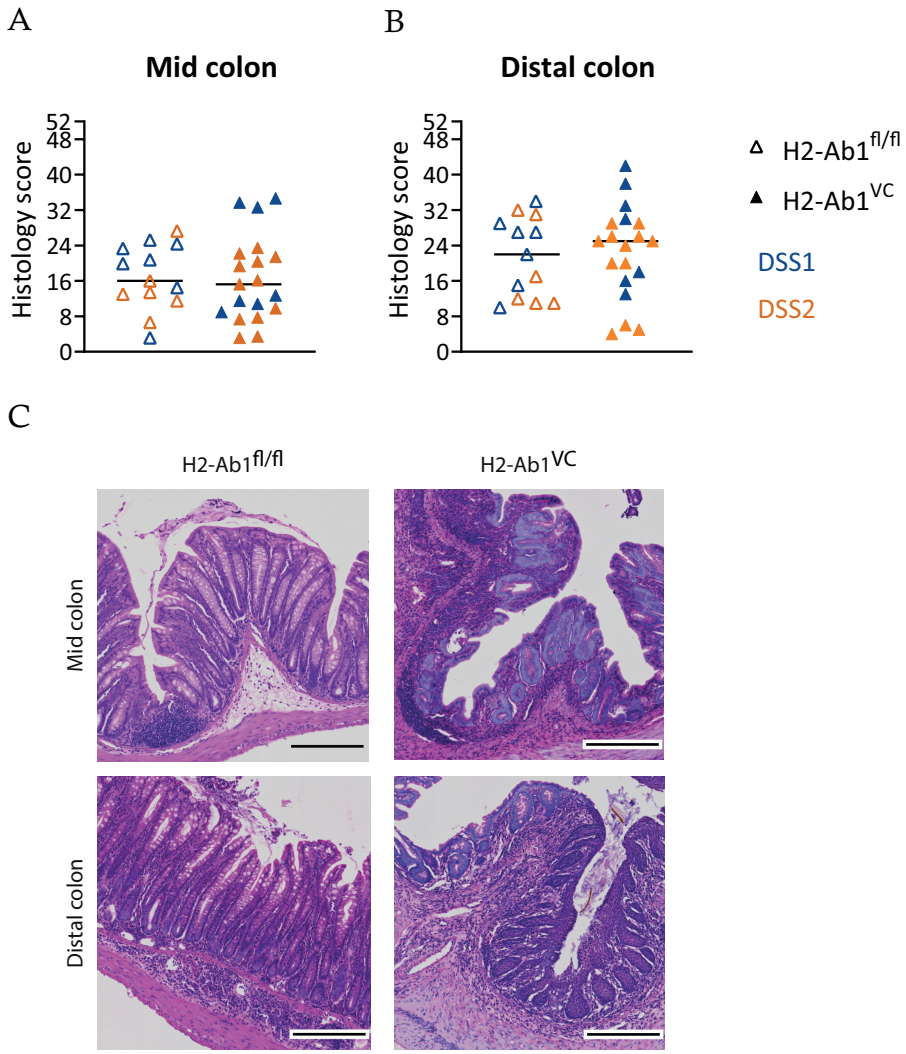


Figure 5.25: Histopathology scores of colonic sections of chronic DSS treated H2-Ab1$^{fl/fl}$ and Ab1^{VC} mice. H2-Ab1^{VC} and H2-Ab1$^{fl/fl}$ littermates were subjected to three cycles of DSS treatment. Mice were sacrificed at day 52. Histopathology scores of the (A) mid and (B) distal colon. Horizontal bars indicate group medians. (C) Representative H&E sections of the mid and distal colon of H2-Ab1^{VC} and H2-Ab1$^{fl/fl}$ mice. Scale bars, 200 μm. Statistical significance between the groups was determined by Mann-Whitney test (A and B). Data from two pooled independent experiments with total mouse numbers per group as follows; n=19 H2-Ab1^{VC} and n=13 H2-Ab1$^{fl/fl}$ treated mice. Mice were housed in the new SPF-B animal facility. Note: Chronic DSS histology slides were scored by Dr. Mathilde Pohin, Kennedy Institute of Rheumatology, University of Oxford.

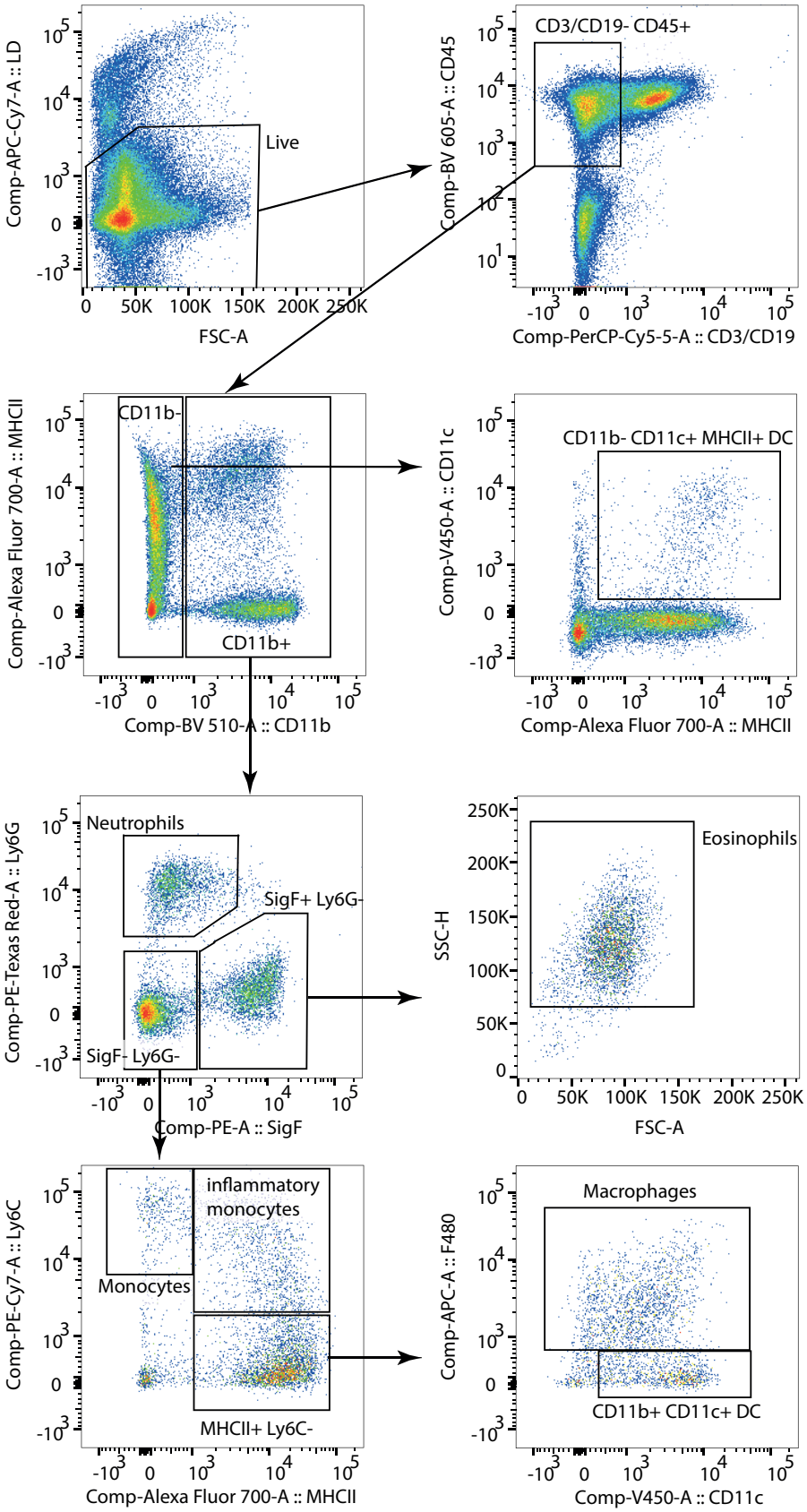


Figure 5.26: Myeloid gating strategy for chronic DSS. Schematic of FACS gating strategy for myeloid cell populations isolated from the colonic lamina propria.

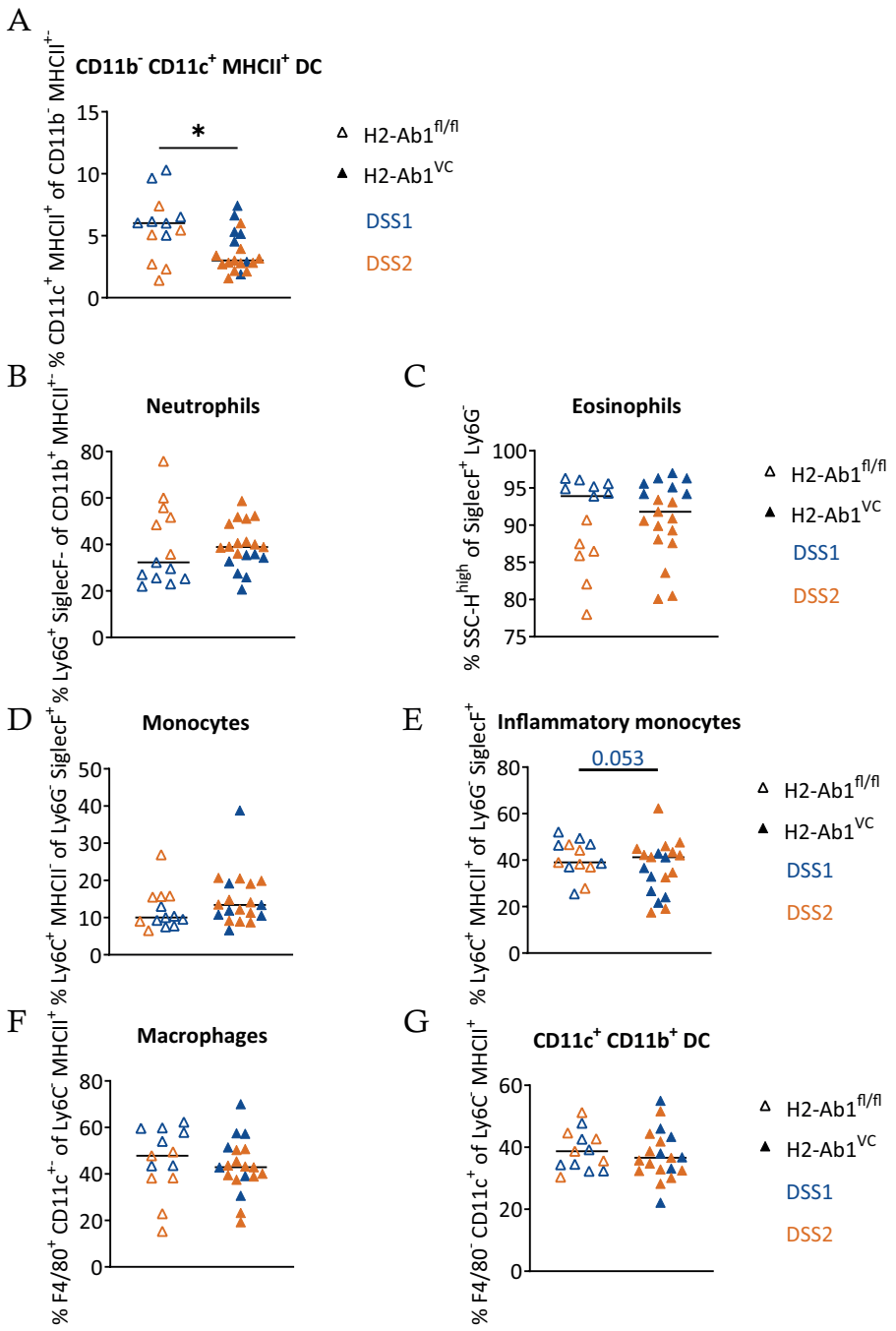


Figure 5.27: Comparable myeloid cell populations during chronic DSS treatment in H2-Ab1^{VC} and H2-Ab1$^{fl/fl}$ mice. H2-Ab1^{VC} and H2-Ab1$^{fl/fl}$ littermates were subjected to three cycles of DSS treatment. Mice were sacrificed at day 52. Frequencies of CD11b^{-} CD11c^{+} MHCII^{+} DCs (A), neutrophils (B), eosinophils (C), monocytes (D), inflammatory monocytes (E), macrophages (F) and CD11c^{+} CD11b^{+} DCs (G). Horizontal bars indicate group medians of pooled experiments. Statistical significance of the combined experiments as well as of each separate experiments was determined by Mann-Whitney test. The colour of the significance symbols indicates which test was significant; black for combined experiments; blue for the DSS1 experiment. P-value summary: *p<0.05. (A-G) Data from two pooled independent experiments with total mouse numbers per group as follows; n=19 H2-Ab1^{VC} and n=13 H2-Ab1$^{fl/fl}$ treated mice. Mice were housed in the new SPF-B animal facility.

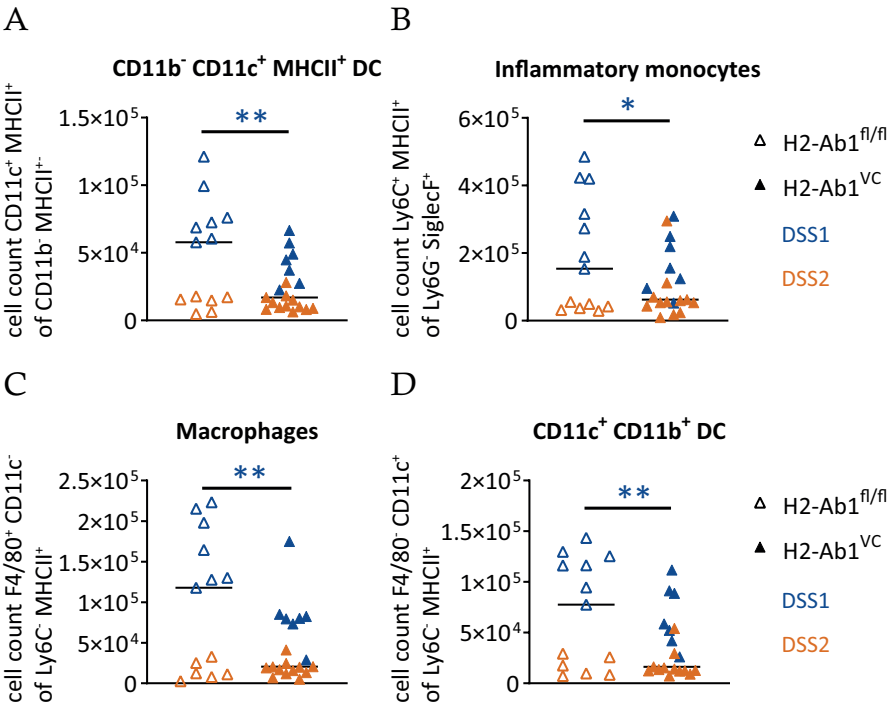


Figure 5.28: Reduced cell numbers in distinct myeloid populations in H2-Ab1^{VC} mice detected in the first chronic DSS experiment. H2-Ab1^{VC} and H2-Ab1$^{fl/fl}$ littermates were subjected to three cycles of DSS treatment. Mice were sacrificed at day 52. Cell numbers of CD11b^{-} CD11c^{+} MHCII^{+} DCs (A), inflammatory monocytes (B), macrophages (C) and CD11c^{+} CD11b^{+} DCs (D). Horizontal bars indicate group medians of pooled experiments. Statistical significance of the combined experiments as well as of each separate experiments was determined by Mann-Whitney test. The colour of the significance symbols indicates which test was significant; blue for the DSS1 experiment. P-value summary: *p<0.05; **p<0.001. (A-D) Data from two pooled independent experiments with total mouse numbers per group as follows; n=19 H2-Ab1^{VC} and n=13 H2-Ab1$^{fl/fl}$ treated mice. Mice were housed in the new SPF-B animal facility.

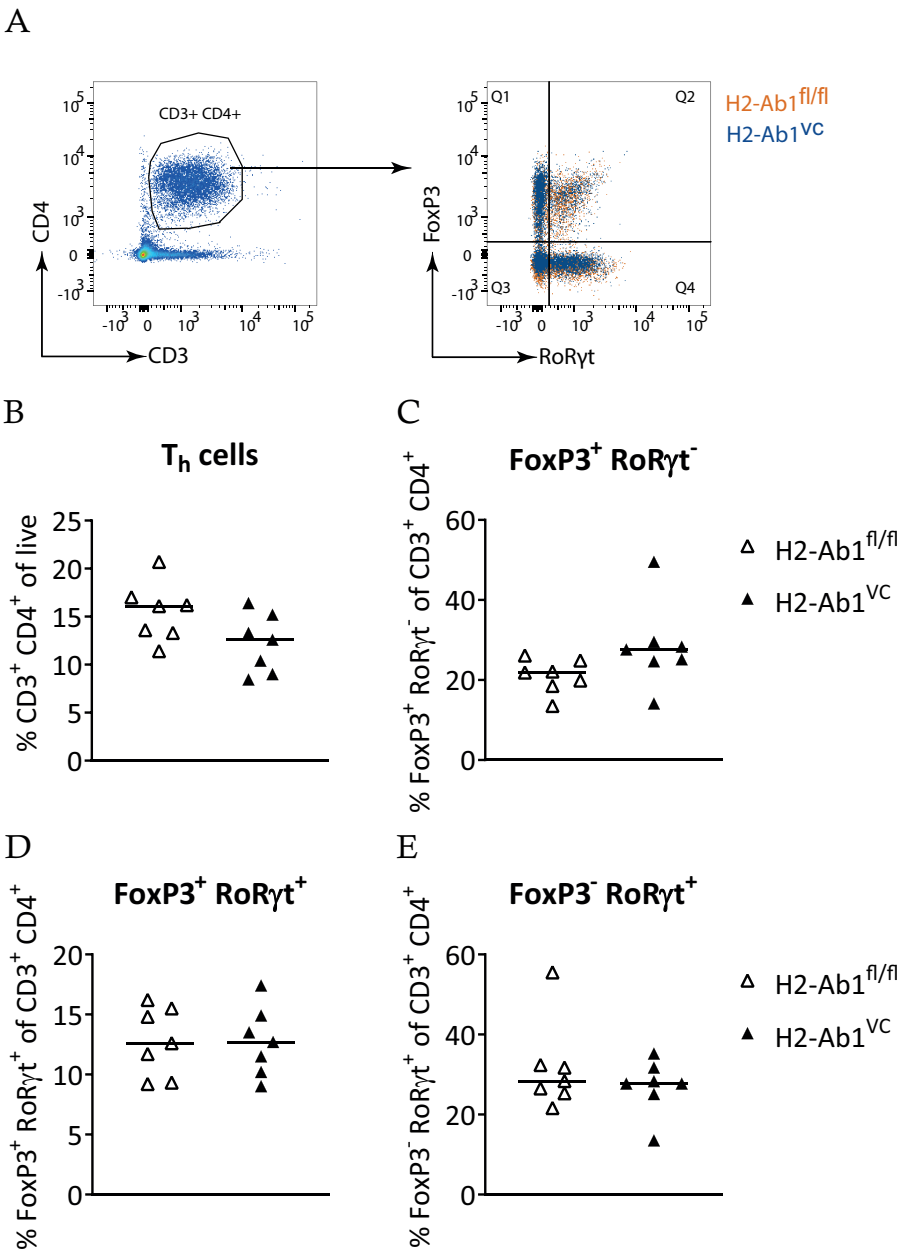


Figure 5.29: Comparable Treg and Th17 frequencies during chronic DSS treatment of H2-Ab1^{VC} and H2-Ab1$^{fl/fl}$ littermates. H2-Ab1^{VC} and H2-Ab1$^{fl/fl}$ littermates were subjected to three cycles of DSS treatment. Mice were sacrificed at day 52. (A) Schematic of FACS gating strategy. Frequencies of CD4$^+$ TCRβ^+ T cells (B) and their daughter FoxP3$^+$ RoRγt$^-$ (C), FoxP3$^+$ RoRγt$^+$ (D) and FoxP3$^-$ RoRγt$^+$ (E) subsets. Horizontal bars indicate group medians. Statistical significance between the groups was determined by Mann-Whitney test. (B-E) Data from one experiment with total mouse numbers per group as follows; n=7 H2-Ab1^{VC} and n=7 H2-Ab1$^{fl/fl}$ treated mice. Mice were housed in the new SPF-B animal facility.

5.3 Discussion

In this chapter we used bacterial- and chemical-induced colitis models, each driven by different disease mechanisms (see section 1.3) and affecting different locations of the colon. *H. helicobacter*-induced colitis mainly causes inflammation in the caecum and proximal colon, whereas *C. rodentium*- or DSS-induced colitis drive intestinal inflammation most severely in the distal colon. Therefore, we were able to assess the role of MHC class II expression across the length of the colon.

To study the role of MHC class II expression by cIECs in controlling *C. rodentium* infection, we selectively deleted MHC class II within IECs, using a Cre-lox genetic approach. Here, we report that *C. rodentium* infection upregulated MHC class II expression by IECs in H2-Ab1$^{fl/fl}$ but not H2-Ab1^{VC} mice. However, both H2-Ab1$^{fl/fl}$ and H2-Ab1^{VC} mice cleared *C. rodentium* infection and harboured comparable levels of *C. rodentium* in their intestinal tissue and caecal content. In addition, we did not observe drastic changes in histopathology or in the spleen mass between the different mouse genotypes during *C. rodentium* infection. These data show, that epithelial MHC class II expression plays a negligible role in clearing *C. rodentium* infection in the large intestine.

C. rodentium infection induced MHC class II expression by IECs in our experiments, so there was the potential of antigen presentation by cIEC influencing *C. rodentium* infection. It was recently shown, that *C. rodentium* depends on T3SS effector networks to inhibit the host immune response, including IEC MHC class II expression, towards its colonisation [398]. Of interest, a *C. rodentium* strain lacking 10 effector molecules involved in the modulation of innate immune responses in IECs (CRi9) resulted in an increased IFNγ response, which induced the expression of proteins involved in MHC class II processing and presentation by IECs [398]. These findings highlight that *C. rodentium* specifically targets inflammatory responses of IECs to support its colonisation. Future studies could be performed with the CRi9 *C. rodentium* strain, to ensure an intensified induction of cIEC MHC class

II expression, which could result in increased CD4 T cell effector responses. In addition, it is possible that by pooling the whole colon for our cIEC MHC class II expression analysis, we diluted regional differences in cIEC MHC class II expression. As the primary colonisation site of *C. rodentium* is the distal colon, it seems plausible that higher MHC class II expression levels are to be expected in this tissue region. Further studies should assess the *C. rodentium* colonisation levels of H2-Ab1^{VC} and H2-Ab1$^{fl/fl}$ littermates throughout the course of *C. rodentium* infection. This would give further information of *C. rodentium* colonisation levels at peak inflammation and whether H2-Ab1^{VC} and H2-Ab1$^{fl/fl}$ littermates show comparable clearance of *C. rodentium* on day 14 post infection.

Our data stand in contrast to a recent study by Jamwal and colleagues [392], who proposed that MHC class II expression by cIECs is important in limiting *C. rodentium*-induced colitis. In their study, loss of IEC MHC class II expression resulted in marked body weight loss, which resulted in the death of 50 % of H2-Ab1^{VC} mice by day 15 following *C. rodentium* infection, as they reached humane endpoint. The authors repeated the *C. rodentium* infection and assessed intestinal pathology and bacterial loads at day 9 (before the onset of marked body weight reduction). They described more severe colonic inflammation in H2-Ab1^{VC} mice compared to littermate controls [392]. Increased intestinal pathology was not due to differences in AMP or IL-22, IL-17A and IL-6 production, cytokines associated with Th17 responses [392]. It was further shown that increased colitis in H2-Ab1^{VC} mice was associated with an impaired induction of high affinity secretory IgA [392]. These results contradict previous studies showing that mice lacking secretory IgA do not die of *C. rodentium* infection [59] and that clearance of *C. rodentium* rather depends on B cells and IgG [59, 399]. We also did not detect any lethality of H2-Ab1^{VC} mice following *C. rodentium* infection. Another study assessed the role of IEC MHC class II expression in modulating small intestinal B cell receptor repertoires at steady state [374]. Lack of IEC MHC class II expression was associated with a more even distribution of Ig clonotypes compared to littermate controls, which

experienced a stronger clonal selection and had fewer clones [374]. In addition, they showed higher IgG and IgA levels in the feces of H2-Ab1^{VC} mice, but less IgA bound intestinal bacteria. These differences were lost when H2-Ab1^{VC} mice were crossed to TCRβ-/- mice, suggesting that IEC MHC class II expression influences T cell-dependent antibody responses [374].

Multiple factors can contribute to these opposing findings by Jamwal and colleagues [392] and our own study. For example, the differences could be driven by *C. rodentium* strain differences as they used the *C. rodentium* DBS100 strain, whereas we used the *C. rodentium* ICC169 strain. However, both DBS100 and ICC168 strains were obtained from the original *C. rodentium* stock of Barthold's group [400, 401]. The strain ICC169 we used in our study, is a spontaneous naladixic acid resistant derivative of ICC168 and is described to have a similar virulence as ICC168 [401]. So it seems unlikely that strain differences caused the observed differences in disease severity. Further, they performed a different infection protocol, which includes an antibiotic treatment of the mice with metronidazole four days before *C. rodentium* infection, after which mice are switched back onto water for one day before they are infected with *C. rodentium*. In contrast, our treatment protocol does not include the use of antibiotics, as we want to avoid changes in the microbiota caused by the antibiotic treatment (see Methods section 2.4.2). This could suggest that additional environmental variables could have contributed to the different disease outcome, such as the microbiota.

Next, we assessed the role of cIEC MHC class II expression in controlling *H. hepaticus* + anti-IL-10-R induced colitis. Here, we report that *H. hepaticus* + anti-IL-10-R treatment induced the upregulation of cIEC MHC class II expression in H2-Ab1$^{fl/fl}$ mice. Both H2-Ab1$^{fl/fl}$ and H2-Ab1^{VC} mice showed comparable histopathology in the caecum and whole colon, but we detected a trend towards increased pathology in the proximal colon of H2-Ab1^{VC} mice. When we assessed the impact of epithelial MHC class II expression on the accumulation of CD4^{+}

IELs, we did not observe drastic changes in the $CD4^+$ IEL composition, with the majority of them being conventional $CD4^+$ IELs. In addition, we did not observe drastic changes in any of the immune cell populations analysed or in spleen weight between the different mice genotypes. These data show, that epithelial MHC class II expression plays a negligible role in *H. hepaticus* + anti-IL-10-R induced colitis.

It is described that both microbial and host factors can drive the development of intestinal inflammation [6, 402]. *H. hepaticus* can chronically colonise wild type mice and has been referred to as pathobiont, due to its ability to induce pathogenic T cell responses during anti-IL-10R treatment. Mice colonised with *H. hepaticus* and treated with anti-IL-10R develop intestinal inflammation, which is characterised by increased IFNγ and IL-17 production in the intestinal tissue and the MLNs [70, 72]. It is now clear that the inflammatory processes are driven by IL-23, as mice lacking IL-23 were resistant to colitis development [25, 228]. A study performed by Xu and colleagues [318] used a novel *H. hepaticus* TCR tg mouse model to track the phenotypes of *H. hepaticus*-specific T cells in wild-type and immunodeficient mice. They showed that *H. hepaticus*-specific T cells in the caecal patch adopted a Tfh phenotype, whereas *H. hepaticus* colonisation induces the development of peripherally-induced RoRγt Treg cells in the large intestinal lamina propria at steady state [318]. In contrast, *H. hepaticus* colonisation of IL-10-/- deficient mice predominantly induced pro-inflammatory Th17 cells, which had Th1-like features. These *H. hepaticus*-induced Treg responses were shown to depend on the TF c-MAF [318]. These results show, that *H. hepaticus*-specific T cells adopt a regulatory phenotype in the colonic tissue at steady state but can acquire pro-inflammatory functions during intestinal inflammation. In addition, they acquire a Tfh phenotype in secondary lymphoid structures. These different phenotypes develop despite being activated by the same antigen specific TCR, which suggests that extrinsic signals mediate these differentiation processes. How *H. hepaticus* induces regulatory T cell responses during homeostasis in the tissue but not in lymphoid sites is currently

not understood.

In our experiments, we did not detect changes in peripherally-induced Treg cell proportions. However, this Treg pool consists of Treg cells with a variety of TCR specificities, including *H. hepaticus*-specific Treg cells. Therefore, we can not draw any conclusions about potential changes in microbe-specific Treg cell proportions driven by IEC MHC class II expression. As this colitis model is driven by increased IFNγ and IL-17 production in the intestinal tissue, it would be informative if additional studies would characterise tissue-specific pro-inflammatory cytokine levels, such as IL-12, IFNγ or TNFα, to assess whether MHC class II expression by cIECs might be important in modulating effector CD4 T cell responses. However, we did not detect marked changes in histopathology between H2-Ab1^{VC} and H2-Ab1$^{fl/fl}$ mice, so these changes are unlikely to influence disease outcome. Of note, we did detect a slight trend towards increased disease pathology in the proximal colon of H2-Ab1^{VC} mice. Both the caecum and the proximal colon are the primary site of *H. hepaticus* colonisation, so it could be possible that we washed out potential differences in the CD4 T cell response by using the entire colon for our LPL isolation and analysis. Future studies could separate the proximal colon from the mid and distal colon and analyse the effect of MHC class II expression on CD4 T cell phenotypes and functions within the proximal colon area. In addition, it would be important to assess the *H. hepaticus* colonisation levels of H2-Ab1^{VC} and H2-Ab1$^{fl/fl}$ littermates in the caecal content throughout the course of infection, as differences in *H. hepaticus* colonisation levels might impact CD4 T cell effector functions.

The treatment with anti-IL-10R inhibited regulatory circuits initiated by the host to maintain tolerance towards *H. hepaticus*, which leads to the induction of intestinal inflammation. Next, we hypothesised that MHC class II expression by cIECs is important in modulating Treg cell responses and thereby maintenance of intestinal homeostasis. To investigate whether IEC MHC class II expression

is therefore important in the resolution of intestinal inflammation, we induced intestinal inflammation by anti-IL-10R treatment of *H. hepaticus* colonised but subsequently stopped anti-IL-10R treatment to allow the resolution of intestinal inflammation and the re-establishment of regulatory circuits. Here we report, that lack of epithelial MHC class II expression resulted in increased disease severity in the colon, especially the proximal colon, of H2-Ab1^{VC} mice. The lack of IEC MHC class II expression did not influence the proportions of CD4^{+} IELs. In addition, we did not observe drastic changes in the Treg cell populations analysed as well the AMP and cytokine expression, or proliferation and stemness status of the tissue between the different mice genotypes. However, we did measure reduced spleen mass in H2-Ab1^{VC} mice compared to littermate controls and the increased disease pathology was accompanied by increased production of IFNγ and TNFα by CD4 T cells in MLNs. These results highlight an important role of MHC class II expression by cIECs in the resolution of intestinal inflammation. This phenotype presented in mice housed at the old SPF-A animal facility. However, when we repeated this experiment with mice housed at the new SPF-B animal facility this phenotype was lost.

The loss of the disease phenotype in mice housed at the new SPF-B animal facility, highlights the importance of the microbiota in driving disease severity. It seems plausible, that changes in the microbiota composition resulted in the different disease outcome. However, we did not perform comparative microbial composition analysis of intestinal tissue and/or faeces, so this explanation remains speculative. Multiple studies reported the importance of microbial antigens from both commensals and pathogens in triggering IL-10 production, an important cytokine for the resolution of intestinal inflammation (reviewed in [403]). It is also important to note, that we used slightly different disease protocols between the different institutes. The Powrie group had established that peak chronic intestinal inflammation occurred at three weeks post *H. hepaticus* + anti-IL-10R treatment in their facility. Therefore, we adjusted our treatment protocol from four to three

weeks for induction of chronic intestinal inflammation, and from three to four weeks of resolution phase, to maintain the seven weeks disease course. These changes in the treatment protocol could have resulted in the progression of the tissue regeneration progress in H2-Ab1^{VC} mice, levelling up with their littermates. This would suggest that IEC MHC class II expression is important in the initial phase of wound healing and tissue repair. Future work would aim to investigate the *H. hepaticus*-specific CD4 T cell responses during the resolution of intestinal inflammation. We ourselves performed initial studies of HH7-2tg CD4 T cell adoptive transfer at the beginning of the resolution model, but were unable to retain HH7-2tg CD4 T cells after seven weeks (data not shown), indicating that the Th17 cells, induced during intestinal inflammation, are not maintained during the resolution phase in both mice genotypes, even though *H. hepaticus* colonisation persists. Future work could adoptively transfer HH7-2tg CD4 T cells at a later time point during the infection course, to assess whether MHC class II expression by IECs might influence HH7-2tg CD4 T cell phenotypes during the resolution phase of intestinal inflammation.

Next, we used the chronic DSS model to investigate the role of IEC MHC class II expression in the tissue regeneration during chronic, reoccurring inflammation. Here, we report that chronic DSS treatment induced MHC class II expression by cIECs. Both H2-Ab1$^{fl/fl}$ and H2-Ab1^{VC} mice showed comparable histopathology in the caecum and colon and we did not detect marked differences in body weight loss, colon length or spleen weight. Further, we did not detect consistent changes in myeloid cell populations between experimental repeats. In addition, the immune cell populations analysed were comparable between H2-Ab1$^{fl/fl}$ and H2-Ab1^{VC} mice. These findings suggest that MHC class II expression by cIEC is not important in the tissue regeneration after chronic DSS treatment.

Previous studies have used the acute model of DSS-induced colitis in H2-Ab1$^{fl/fl}$ and H2-Ab1^{VC} mice and found conflicting results [374, 392]. Jamwal and colleagues [392] first investigated the role of cIEC MHC class II expression in acute mucosal

injury and therefore treated mice with 3 % DSS for seven days, without a water cycle [392]. Analysis on day seven revealed that lack of cIEC MHC class II expression led to a slight protection from acute DSS-induced colitis, which was reflected in a reduced colon length/weight ratio. However, histopathology scores were comparable between the mice genotypes [392]. Lack of cIEC MHC class II expression was accompanied by a reduction in IL-6 expression in the colonic tissue [392]. They next assessed whether IEC MHC class II expression is important in the tissue regeneration phase after acute mucosal injury. They therefore included a two week recovery period after DSS treatment and showed a slightly improved recovery from colitis and decreased IL-1β, IFNγ and TNFα expression in the colonic tissue of H2-Ab1$^{\mathrm{VC}}$ mice.

These results are in contrast with a study performed by Stephens and colleagues [374]. They assessed the role of IEC MHC class II expression in an acute model of DSS-induced colitis and treated mice for six days prior to their analysis, without a water cycle. They found that lack of cIEC MHC class II expression resulted in increased intestinal inflammation and decreased RoRγt^{+} Helios^{-} Treg cells in the MLNs [374]. RoRγt^{+} Helios^{-} Treg cells have been demonstrated to be important for the maintenance of intestinal homeostasis [404]. These findings suggest that a reduction in peripherally induced Helios^{-} Treg cells might result in hyperresponsiveness to microbial antigens, resulting in increased intestinal inflammation in H2-Ab1$^{\mathrm{VC}}$ mice [374].

In this chapter we used both acute and chronic intestinal inflammation models to assess the role of antigen presentation by cIECs. In addition, we investigated the role of MHC class II expression by cIECs during the resolution of chronic intestinal inflammation. We assessed disease severities across these different models, which manifested in different parts of the large intestine, and did neither detect a protective nor exacerbating role of antigen presentation by cIEC. However, antigen presentation by cIECs might support the resolution of intestinal inflammation. Lack of IEC MHC class II expression did not affect the frequencies of Treg cells across the different studies and where assessed, CD4^{+} IEL populations did not

change. In summary, MHC class II expression by cIECs does not induce critical regulatory CD4 T cell responses for the maintenance of intestinal homeostasis during bacterial-induced and chemical-induced colitis. However, cIEC MHC class II expression might be important in the resolution of chronic intestinal inflammation.

6

The role of MHC class II expression by colonic and caecal IECs in modulating CD4 T cell responses to *H. hepaticus*

Contents

6.1 Introduction 175
6.2 Results 179
6.2.1 *H. hepaticus* specific CD4 T cell modulation by MHC class II expression by IECs *in vivo* 179
6.2.2 HH7-2tg CD4 T cells are activated and their effector functions modulated by colonic organoid MHC class II expression 192
6.3 Discussion 208

6.1 Introduction

We identified in chapter 5 the potential importance of antigen presentation by cIECs in the resolution of intestinal inflammation and re-establishment of intestinal homeostasis, with increased disease severity identified in the proximal colon when MHC class II expression by cIECs was lacking. The proximal colon is one of the major *H. hepaticus* colonisation sites. Our results in chapter 3 showed that cIECs possess critical features to function as a non-conventional APC and that lack of

cIEC MHC class II expression resulted in increased $CD4^+$ T cell frequencies and numbers in the colonic lamina propria and in cell infiltration into the caecal lamina propria during low-grade, chronic inflammation associated with ageing. The caecum is another important colonisation site of *H. hepaticus*. The data prompts further study of the importance of antigen presentation by colonic and caecal IECs in maintaining intestinal homeostasis, to understand how MHC class II expression by these IECs modulates the CD4 T cell phenotypes and responses at these tissue niches.

Conflicting results have been generated in regard to the impact of antigen presentation by IECs on the effector functions of CD4 T cells. Some studies showed that MHC class II expression by IECs induced tolerogenic CD4 T cell responses [390–392] while others reported an induction of pro-inflammatory CD4 T cell responses [136, 137, 392, 393]. These seemingly contradictory results might highlight the importance of additional tissue micro-environmental cues honing the CD4 T cell responses initiated by IEC MHC class II expression. Indeed, it has been shown that both antigen presentation and co-inhibitory molecule PD-L1 expression by siIECs are critical for the differentiation of $CD8\alpha\alpha^+$ $CD4^+$ IELs [378]. Whether IECs are able to provide co-stimulatory or co-inhibitory signals is a matter of ongoing debate. The protein expression of some of these signals is thought to be driven by tissue inflammation, with CD86 protein expression by cIECs detected in UC patients [165] and CD40 protein expression by colonic and ileal IECs in CD and UC patients [167], while other studies did not detect CD80/CD86 protein expression in cIECs of UC patients [168]. In addition, only low ICOS-L and PD-L1 protein expression by cIECs was detected in IBD patients [169].

In the small intestine it has been shown that the microbial community shapes MHC class II expression by siIECs, with MHC class II "inducing" and "suppressing" commensals being described [372], the presence of these commensals likely to be dependent on the dietary composition. Indeed, the diet was shown to be an important regulator of siIEC MHC class II expression, as a HFD resulted in the

loss of siIEC MHC class II expression [372, 377]. In addition, a HFD resulted in microbial dysbiosis with reduced bacterial diversity and *Helicobacter* was among the bacterial genera reduced under a HFD [377]. It was further shown that *Helicobacter* colonisation induces the expression of epithelial MHC class II expression [377]. This raises the question whether *Helicobacter* utilises the microbial host cross-talk to induce MHC class II expression by IECs, which allows the adaptive immune response to initiate its tolerogenic responses towards *Helicobacter* colonisation and sustains intestinal homeostasis.

The infection with *H. hepaticus* is an important model system to investigate the induction of Treg cells in the intestine. Tolerance towards *H. hepaticus* was shown to be dependent on the induction of IL-10 production, with the loss of IL-10 in IL-10 deficient mice resulting in the spontaneous development of enterocolitis [397]. The regulatory cytokine IL-10 being produced by Treg cells. This infection model highlights the important balance between regulatory and pro-inflammatory circuits to maintain intestinal homeostasis. It is currently not known, how *H. hepaticus* induces Treg cell responses in the intestinal tissue to maintain tolerance. A recent study utilised a novel *H. hepaticus* TCR tg mouse model and showed that the colonisation with *H. hepaticus* induced the differentiation of peripherally-induced RoRγt$^+$ FoxP3$^+$ Treg cells in the colonic lamina propria [318]. During inflammatory conditions, this differentiation shifted to a pro-inflammatory Th17 phenotype [318]. However, it is not known whether antigen presentation by large intestinal IECs influences the Treg cell responses in the tissue during *H. hepaticus* colonisation.

These studies highlight the importance of *H. hepaticus*-specific Treg cell responses in maintaining tolerance towards *H. hepaticus*. However, it is not clear whether *H. hepaticus*-specific CD4 T cells receive TCR signalling from large intestinal IECs and whether this shapes their regulatory responses. To address these questions we utilised the *H. hepaticus* TCR tg mouse model to be able to investigate phenotypic and functional changes in *H. hepaticus*-specific CD4 T cells induced by epithelial

antigen presentation. In addition, we used *H. hepaticus*-specific double reporter mice, which allowed the detection of IL-10 production via a GFP signal and the identification of FoxP3$^+$ Treg cells by the expression of the surface marker hCD2, which avoided the need for fixation and permeabilisation of the cells and thereby the destruction of the IL-10GFP signal (HH7-2tgIL10GFP).

In this chapter we aim to understand how antigen presentation by large intestinal IECs shapes the phenotypes and responses of *H. hepaticus*-reactive CD4 T cells *in vivo* and whether there are distinct differences in the caecum versus the colon. We further developed a novel organoid co-culture system with *H. hepaticus*-specific CD4 T cells, to be able to investigate the importance of IEC antigen presentation in a more reductionist manner. The co-culture system enables us to consistently upregulate MHC class II expression by colonic organoids and as the co-culture only consists of colonic organoids and CD4 T cells, we will be able to track changes in CD4 T cell phenotypes and responses exclusively in response to antigen presentation by IECs. We hypothesise that antigen presentation by large intestinal IECs modulates peripherally-induced Treg cell phenotypes and responses.

6.2 Results

6.2.1 *H. hepaticus* specific CD4 T cell modulation by MHC class II expression by IECs *in vivo*

We had previously observed that MHC class II expression by siIECs limits FoxP3 expression by siIELs. We therefore determined whether MHC class II expression by IECs would modulate the $CD4^+$ T cell responses in the large intestine compartments, the colon and caecum. To study the impact of epithelial MHC class II expression on IL-10 production and FoxP3 expression by $CD4^+$ T cells, we used HH7-2tg mice crossed to B6.Foxp3hCD2 IL-10GFP reporter mice (HH7-2tgIL10GFP). H2-$Ab1^{fl/fl}$ and H2-$Ab1^{VC}$ littermates were colonised with *H. hepaticus* and, seven days later, adoptively transferred with 2000 naïve congenic ($CD45.1^+$ $CD45.2^+$) HH7-2tgIL10GFP CD4 T cells. After a further ten days, we analysed HH7-2tgIL10GFP CD4 T cells from the IEL compartment, caecal lamina propria, and colon lamina propria unsing flow cytometry (Figure 6.1 A).

We also investigated whether *H. hepaticus* colonisation leads to the upregulation of MHC class II expression by IECs. We therefore isolated cmIECs and cIECs at 17 d post colonisation and assessed MHC class II expression by flow cytometry (Figure 6.2 A). We found that around 60 % H2-$Ab1^{fl/fl}$ cmIECs expressed MHC class II (Figure 6.2 B), while around 30 % cIECs expressed MHC class II (Figure 6.2 C). In addition, we analysed the IEL compartment of both the colon and the caecum and detected only sporadic HH7-2tgIL10GFP IELs at both sites (data not shown). These results indicate, that *H. hepaticus* colonisation leads to the upregulation of MHC class II expression by IECs in the colon and especially in the caecum. However, transferred HH7-2tgIL10GFP CD4 T cells did not accumulate efficiently in the epithelial layer of both H2-$Ab1^{fl/fl}$ and H2-$Ab1^{VC}$ mice, making it impossible to ascertain if MHC class II expression by colonic and caecal IECs is required for the migration or retention of microbe-specific T cells in the epithelial layer. The IEL compartment was examined in subsequent experiments, but because

of the absence of HH7-2tgIL10GFP CD4 T cells, the data will not be discussed.

We next examined the caecal LP and detected comparable HH7-2tgIL10GFP $CD4^+$ T cell frequencies in both H2-$Ab1^{fl/fl}$ and H2-$Ab1^{VC}$ littermates (Figure 6.3 A). We then investigated the impact of IEC MHC class II expression on their regulatory functions by assessing FoxP3 and IL-10 expression. Within the HH7-2tgIL10GFP $CD4^+$ T cell population, we detected significantly increased frequencies of IL-10^- $FoxP3^+$ cells (Figure 6.3 B and E) and of IL-10^+ $FoxP3^-$ cells in H2-$Ab1^{VC}$ versus H2-$Ab1^{fl/fl}$ recipients (Figure 6.3 B, D and E). Moreover, there was also a trend towards increased frequencies of IL-10^+ $FoxP3^+$ cells in H2-$Ab1^{VC}$ mice, although the difference did not reach statistical significance (Figure 6.3 C and E). Interestingly, the majority of IL-10 producing HH7-2tgIL10GFP CD4 T cells did not express FoxP3 (Figure 6.3 C and D). Overall, our results suggest that MHC II expression by local IECs limits the accumulation or expansion of *H. hepaticus*-specific $CD4^+$ Treg subsets in the caecal LP.

Next, we analysed HH7-2tgIL10GFP $CD4^+$ T cells from the colonic LP. Whilst transferred HH7-2tgIL10GFP $CD4^+$ T cells were able to migrate into the colonic lamina propria of both H2-$Ab1^{fl/fl}$ and H2-$Ab1^{VC}$ littermates (Figure 6.4 A), we found comparable frequencies of IL-10^+ $FoxP3^+$ and IL-10^+ $FoxP3^-$ cells (Figure 6.4 C-E). There was a modest trend towards increased frequencies of IL-10^- $FoxP3^+$, but this was not statistically significant (Figure 6.4 B and E). Thus, the IL-10 and FoxP3 expression by HH7-2tgIL10GFP CD4 T cells residing in the colonic LP was not greatly affected by absence of MHC class II expression of cIECs.

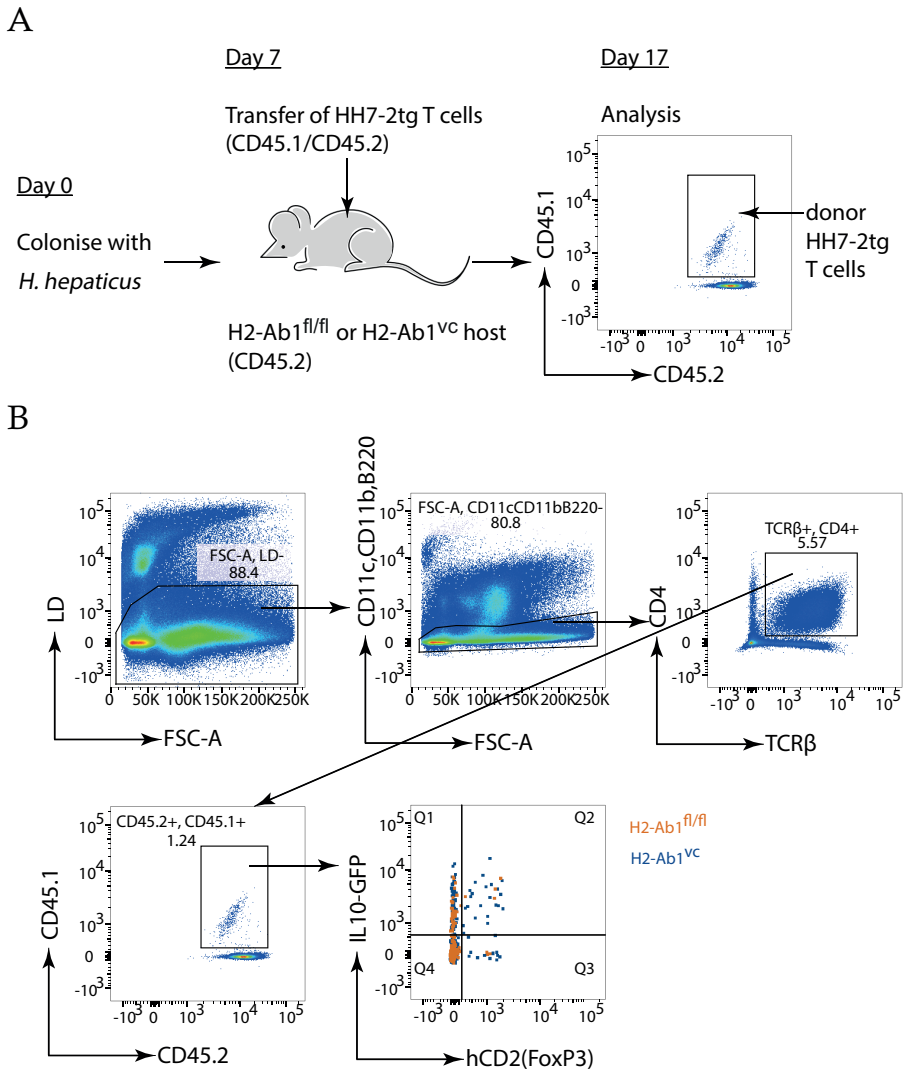


Figure 6.1: Experimental design of adoptive HH7-2tgIL10GFP CD4 T cell transfer. (A) FACS sorted naïve HH7-2tgIL10GFP CD4 T cells were adoptively transferred into *H. hepaticus* colonised H2-Ab1$^{fl/fl}$ and H2-Ab1^{VC} littermates. Mice were sacrificed 17 d post colonisation and tissues were analysed for the presence of HH7-2tgIL10GFP CD4 T cells by flow cytometry. (B) Gating strategy for flow cytometric analysis of HH7-2tgIL10GFP CD4 T cells in the caecal lamina propria.

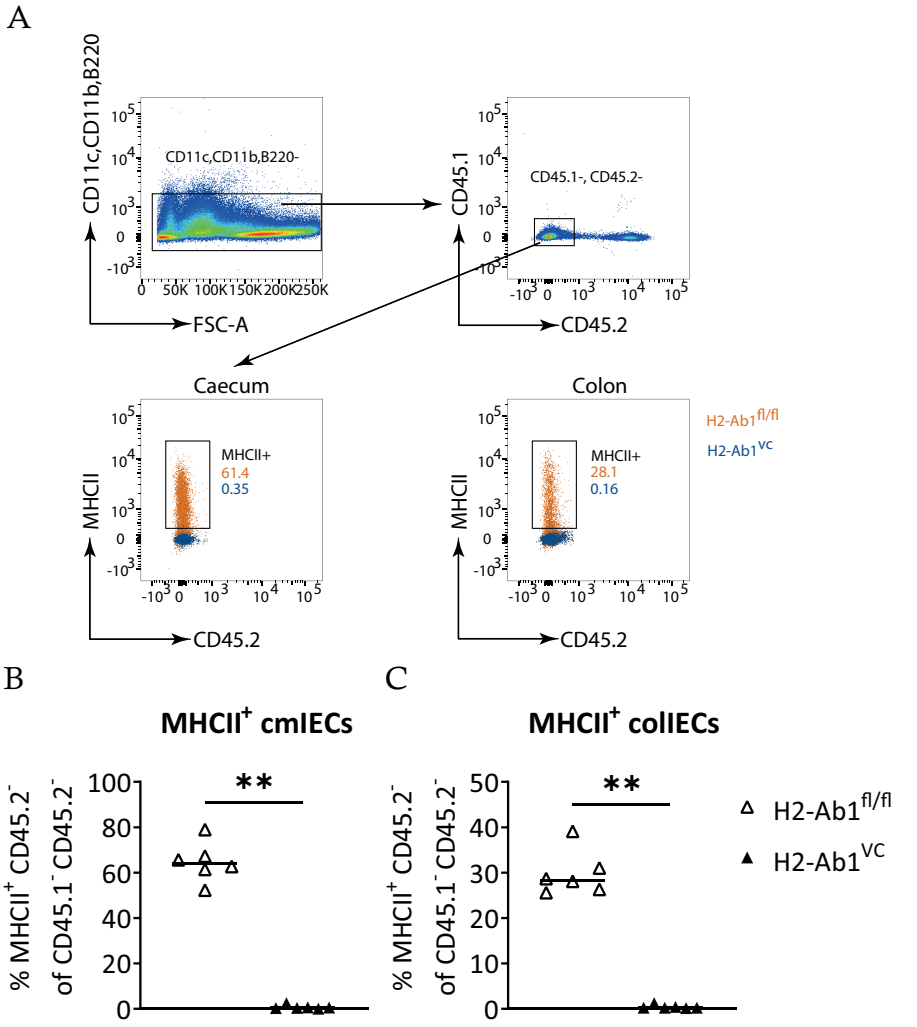


Figure 6.2: *H. hepaticus* colonisation induces MHC class II expression by IECs in the caecum and colon of H2-Ab1$^{fl/fl}$ mice. 2000 FACS sorted naïve HH7-2tgIL10GFP T cells were adoptively transferred into *H. hepaticus* colonised H2-Ab1$^{fl/fl}$ and H2-Ab1^{VC} littermates. Mice were sacrificed 17 d after colonisation and MHC class II expression by IECs assessed by flow cytometry. (A) Schematic of FACS gating strategy. Symbols denote MHC class II expression by caecal (B) and colonic (C) IECs of two pooled mice per sample. Horizontal bars indicate group medians. Statistical significance between the groups was determined by the Mann-Whitney test. P-value summary: **p<0.01. Data from one experiment with total mouse numbers per group as follows; n=6 H2-Ab1^{VC} and n=6 H2-Ab1$^{f/fl}$ littermates. Mice were housed in the new SPF-B animal facility.

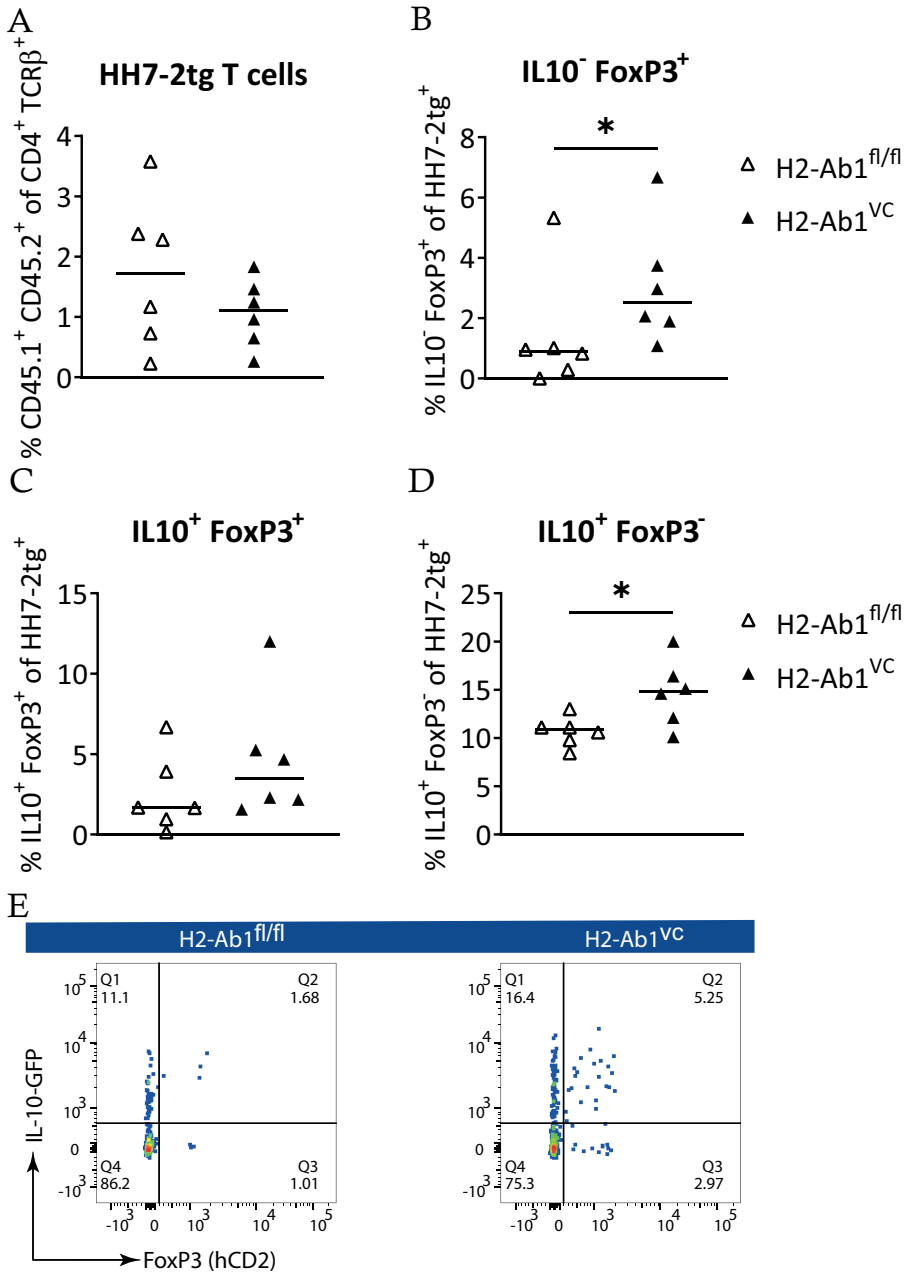


Figure 6.3: Increased IL-10 and FoxP3 expression by HH7-2tgIL10GFP CD4 T cells in the caecal lamina propria of H2-Ab1^{VC} mice. 2000 FACS sorted naïve HH7-2tgIL10GFP CD4 T cells were adoptively transferred into *H. hepaticus* colonised H2-Ab1$^{fl/fl}$ and H2-Ab1^{VC} littermates. Mice were sacrificed 17 d after colonisation and the presence of HH7-2tgIL10GFP CD4 T cells in the caecal lamina propria assessed by flow cytometry. Symbols denote frequencies of HH7-2tgIL10GFP CD4 T cells (A), IL-10$^-$ FoxP3$^+$ (B), IL-10$^+$ FoxP3$^+$ (C) and IL-10$^+$ FoxP3$^-$ (D) HH7-2tgIL10GFP CD4 T cells. (E) Representative FACS plots. Each symbol denotes two pooled mice. Horizontal bars indicate group medians. Statistical significance between the groups was determined by the Mann-Whitney test. P-value summary: *$p<0.05$. Data from one experiment with total mouse numbers per group as follows; n=6 H2-Ab1^{VC} and n=6 H2-Ab1$^{f/fl}$ littermates. Mice were housed in the new SPF-B animal facility.

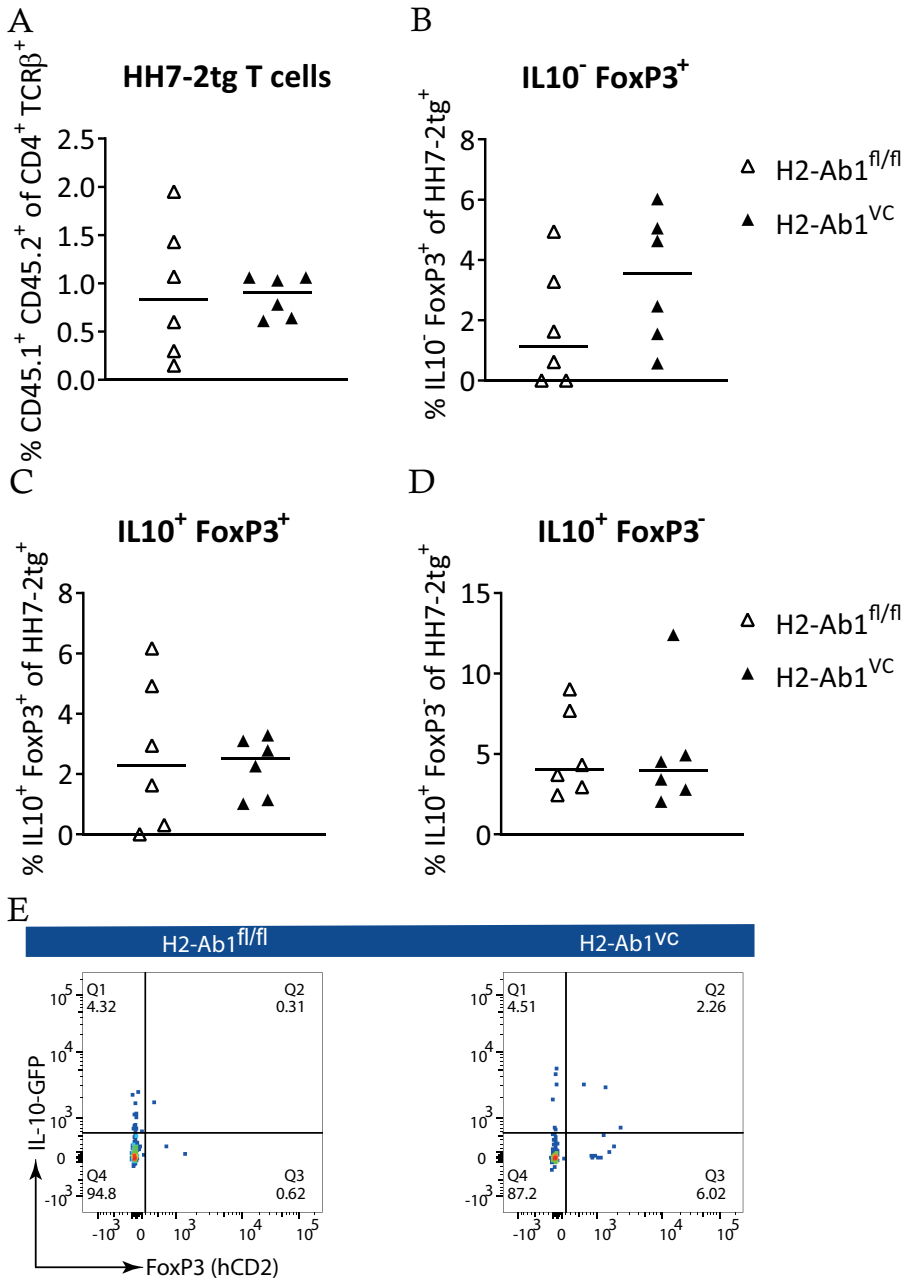


Figure 6.4: Comparable IL-10 and FoxP3 expression by HH7-2tgIL10GFP CD4 T cells in the colonic lamina propria of H2-Ab1^{VC} mice and H2-Ab1$^{fl/fl}$ littermates. 2000 FACS sorted naïve HH7-2tgIL10GFP CD4 T cells were adoptively transferred into *H. hepaticus* colonised H2-Ab1$^{fl/fl}$ and H2-Ab1^{VC} littermates. Mice were sacrificed 17 d after colonisation and the presence of HH7-2tgIL10GFP CD4 T cells in the colonic lamina propria assessed by flow cytometry. Symbols denote frequencies of HH7-2tgIL10GFP CD4 T cells (A), IL-10^{-} FoxP3^{+} (B), IL-10^{+} FoxP3^{+} (C) and IL-10^{+} FoxP3^{-} (D) HH7-2tgIL10GFP CD4 T cells. (E) Representative FACS plots. Each symbol denotes two pooled mice. Horizontal bars indicate group medians. Statistical significance between the groups was determined by the Mann-Whitney test. Data from one experiment with total mouse numbers per group as follows; n=6 H2-Ab1^{VC} and n=6 H2-Ab1$^{f/fl}$ littermates. Mice were housed in the new SPF-B animal facility.

We subsequently repeated the experiment but increased the adoptively transferred HH7-2tgIL-10-GFP CD4 T cell number from 2000 to 20000 to ensure sufficient HH7-2tgIL10GFP CD4 T cell recovery from the intestinal tissues without having to pool mice.

Consistent with previous results, we detected comparable presence of HH7-2tgIL10GFP CD4 T cells in the caecal and colonic LP between H2-Ab1$^{fl/fl}$ and H2-Ab1^{VC} recipients (Figure 6.5 A). However, in this experiment we observed comparable frequencies of IL-10^{-} FoxP3^{+}, IL-10^{+} FoxP3^{+} and IL-10^{+} FoxP3^{-} HH7-2tgIL10GFP CD4 T cells between H2-Ab1$^{fl/fl}$ and H2-Ab1^{VC} recipients at both tissue sites (Figure 6.5 B-D). This is in contrast to our previous observations where increased frequencies of FoxP3^{+} and IL-10^{+} HH7-2tg CD4^{+} T cells were present in the cecal LP of H2-Ab1^{VC} recipients (see Figure 6.3). Interestingly, we observed higher overall frequencies of IL-10 and FoxP3 expression by HH7-2tgIL10GFP CD4 T cells in the caecal LP in this experiment, compared to our previous experiment (around 2 x higher frequencies; compare Figure 6.5 to 6.3).

Having obtained different results regarding the induction of Treg cells and upregulation of IL-10 production by HH7-2tgIL10GFP CD4 T cells when IECs lack MHC class II expression, we hypothesised that differences in MHC class II expression levels by IECs results in different CD4 T cell phenotypes. It seems plausible, that MHC class II expression by IECs reflects the inflammation status of the tissue, with very low MHC class II expression during homeostasis and high MHC class II expression during inflammation. This could result in a spectrum of MHC class II expression levels by IECs depending on the tissue microenvironment, where low MHC class II expression by IECs modulates CD4 T cell phenotypes to a different extent than high MHC class II expression.

In this experiment, we also assessed MHC class II expression by IECs in the caecum and colon of *H. hepaticus* colonised H2-Ab1$^{fl/fl}$ and H2-Ab1^{VC} littermates

that had received 20000 HH7-2tgIL10GFP CD4$^+$ T cells. In H2-Ab1$^{fl/fl}$ recipients, we detected around 20 % MHCII$^+$ IECs in the caecum (Figure 6.6 A) and around 10 % MHCII$^+$ IECs in the colon (Figure 6.6 C), whereas there were virtually no MHCII$^+$ IECs found in the H2-Ab1^{VC} recipients. It is striking that expression of MHC class II by caecal and colon IECs in this experiment was around 3 X lower than in the previous experiment (see Figure 6.2).

The programmed death (PD)-1-PD-ligand (PD-L) 1 pathway was described to play an important role in regulating iTreg cell development and function [405]. PD-L1 is expressed by hematopoietic and non-hematopoietic cells and its expression by IECs is upregulated during intestinal inflammation [169, 406]. Therefore, CD4 T cells could potentially interact with MHC class II on IECs and additionally receive inhibitory signals through PD-1 and PD-L1 interaction. However, if IECs lack MHC class II expression, CD4 T cells will only receive signals via the PD-1 and PD-L1 pathway, which might favour the differentiation of FoxP3$^+$ HH7-2tgIL10GFP CD4 T cells. We therefore assessed PD-L1 expression by IECs in our second adoptive transfer experiment and observed a tendency towards increased frequencies of caecal (Figure 6.6 B) and colonic (Figure 6.6 D) PD-L1$^+$ IEC in H2-Ab1$^{fl/fl}$ mice compared to H2-Ab1^{VC} littermates. Taken together, these results show that *H. hepaticus* colonisation induces both MHC class II and PD-L1 expression by caecal and colonic IECs. Moreover, lack of MHC class II expression by caecal and colonic IECs appears to be accompanied by a reduction of epithelial PD-L1 expression.

To test whether MHC class II expression correlates with PD-L1 expression in IECs, we performed Spearman's correlation analyses and detected a very strong, positive and significant correlation between MHC class II and PD-L1 expression in both caecal and colonic IECs (Figure 6.7 A and B, respectively). Unfortunately, we did not assess PD-L1 expression levels by caecal and colonic IECs in the first adoptive transfer experiment, which showed high MHC class II expression by IECs (see Figures 6.2). Therefore, we cannot be certain whether IECs expressing high

MHC class II levels also express high PD-L1 levels.

Next, we investigated whether MHC class II expression by caecal and colonic IECs correlates with IL-10 production of HH7-2tgIL10GFP CD4 T cells. We included data of IL-10 producing HH7-2tgIL10GFP CD4 T cells and MHC class II expression by IECs of both adoptive transfer experiments into our Spearman's correlation analyses. We observed a moderate, negative correlation between IL-10 expression by HH7-2tgIL10GFP CD4 T cells and MHC class II expression by caecal and colonic IECs, which was however not significant (caecum: r=-0.5055; p=0.0812 and colon: r=-0.5220; p=0.0707, Figure 6.7 C and D, respectively). In addition, we performed Spearman's correlation analyses for FoxP3 expression by HH7-2tgIL10GFP CD4 T cells and MHC class II expression by caecal and colonic IECs. Again, we observed a moderate, negative correlation between FoxP3 expression by HH7-2tgIL10GFP CD4 T cells and MHC class II expression by caecal and colonic IECs, which was not significant (caecum: r=-0.4341; p=0.1405 and colon: r=-0.5309; p=0.0646, Figure 6.7 E and F, respectively). Altogether, these results suggests that there is a strong, positive relationship between MHC class II and PD-L1 expression by caecal and colonic IECs. An increase in MHC class II expression by caecal and colonic IECs appears to negatively influence IL-10 production and FoxP3 expression by HH7-2tgIL10GFP CD4 T cells, though more investigations will be needed to support this claim.

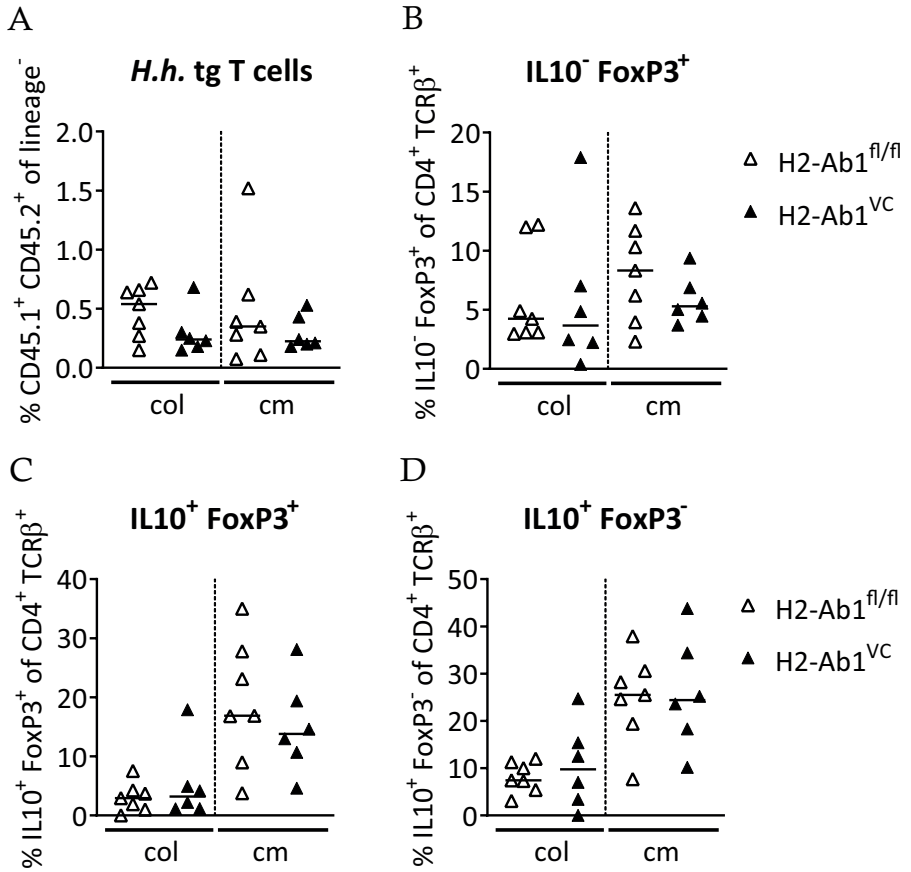


Figure 6.5: Comparable IL-10 and FoxP3 expression by HH7-2tgIL10GFP CD4 T cells in context of lower MHC class II expression by caecal IECs. 20000 FACS sorted naïve HH7-2tgIL10GFP CD4 T cells were adoptively transferred into *H. hepaticus* colonised H2-Ab1$^{fl/fl}$ and H2-Ab1^{VC} littermates. Mice were sacrificed 17 d after colonisation and HH7-2tgIL10GFP CD4 T cell presence in caecal lamina propria determined by flow cytometry. (A) Symbols denote HH7-2tgIL10GFP CD4 T cell frequencies in the caecal lamina propria. Frequencies of IL-10^{-} FoxP3^{+} (B), IL-10^{+} FoxP3^{+} (C) and IL-10^{+} FoxP3^{-} (D). Horizontal bars indicate group medians. Statistical significance between the groups was determined by the Mann-Whitney test. Data from one experiment with total mouse numbers per group as follows; n=6 H2-Ab1^{VC} and n=7 H2-Ab1$^{f/fl}$ littermates. Mice were housed in the new SPF-B animal facility.

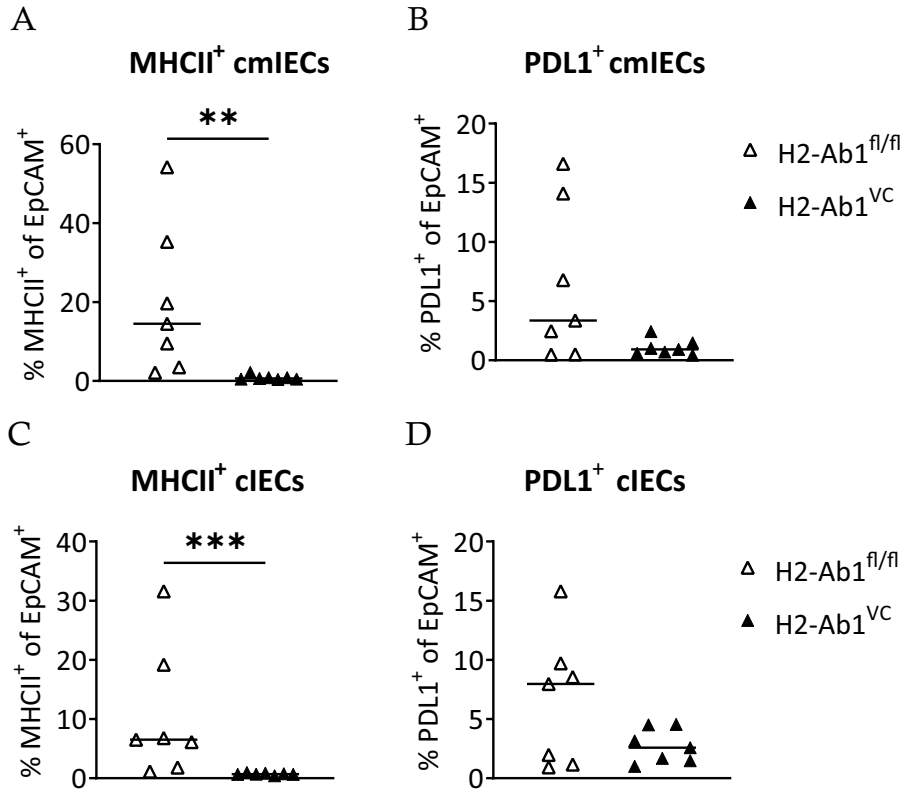


Figure 6.6: *H. hepaticus* colonisation induces MHC class II and PD-L1 expression by IECs in the caecum and colon of H2-Ab1$^{fl/fl}$ mice. 20000 FACS sorted naïve HH7-2tgIL10GFP CD4 T cells were adoptively transferred into *H. hepaticus* colonised H2-Ab1$^{fl/fl}$ and H2-Ab1^{VC} littermates. Mice were sacrificed 17 d after colonisation and MHC class II expression by IECs assessed by flow cytometry. Symbols denote MHC class II expression by caecal (A) and colonic (C) IECs as well as PD-L1 expression by caecal (B) and colonic (D) IECs. Horizontal bars indicate group medians. Statistical significance between the groups was determined by the Mann-Whitney test. P-value summary: **$p<0.01$. Data from one experiment with total mouse numbers per group as follows; n=7 H2-Ab1^{VC} and n=7 H2-Ab1$^{f/fl}$ littermates. Mice were housed in the new SPF-B animal facility.

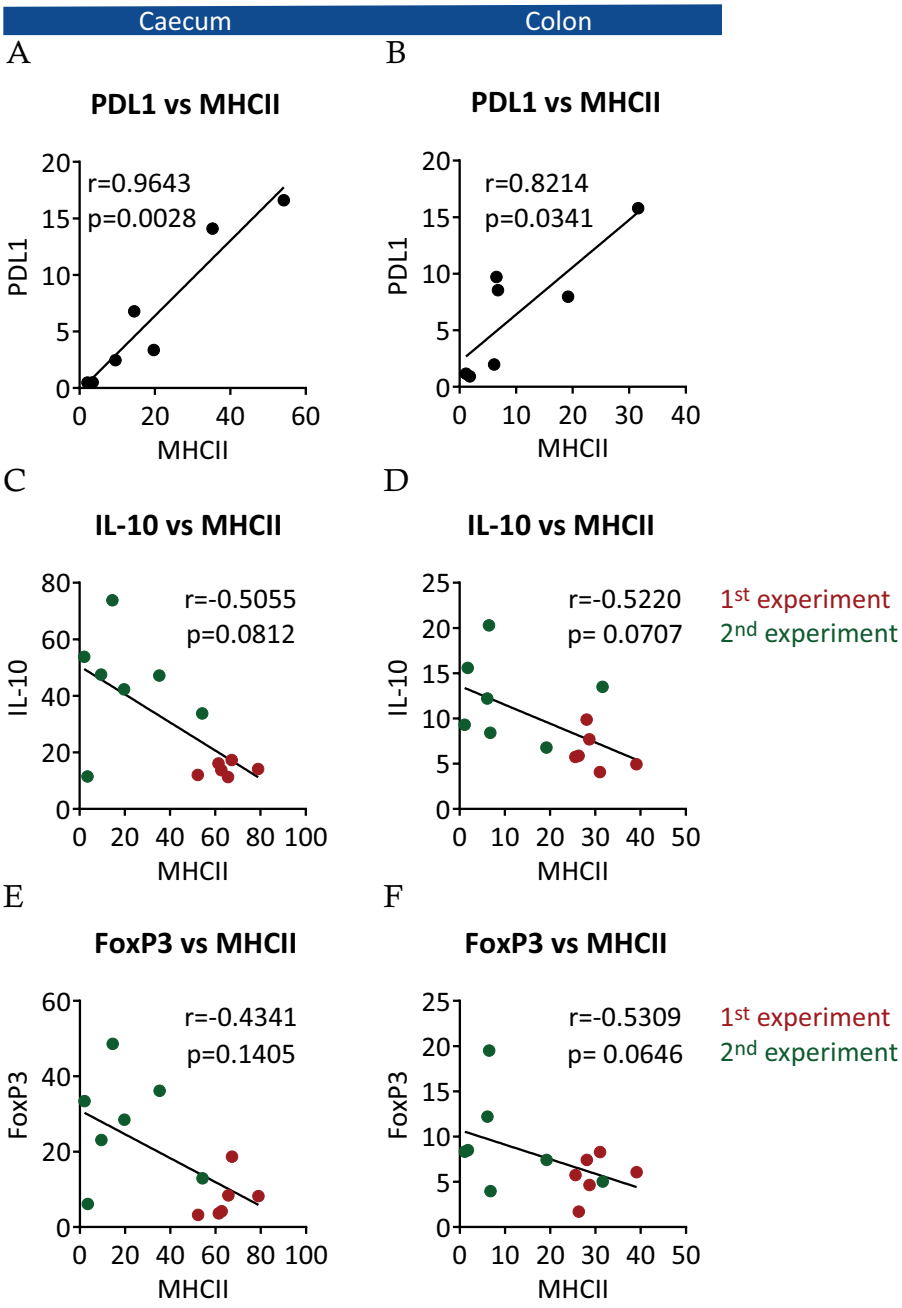


Figure 6.7: MHC class II and PD-L1 expression by caecal and colonic IECs show very strong positive correlation. FACS sorted naïve HH7-2tgIL10GFP CD4 T cells were adoptively transferred into *H. hepaticus* colonised H2-Ab1$^{fl/fl}$ and H2-Ab1^{VC} littermates. Mice were sacrificed 17 d after colonisation and MHC class II and PD-L1 expression by IECs assessed by flow cytometry. Spearman's correlation analysis was performed on MHC class II and PD-L1 expression by IECs. Symbols denote paired data of MHC class II and PD-L1 in caecal (A) and colonic (B) IECs of the second adoptive transfer experiment, showing low IEC MHC class II expression. Spearman's correlation analysis was performed on IL-10 expression by HH7-2tgIL10GFP CD4 T cells and MHC class II expression by caecal (C) and colonic (D) IECs of both adoptive transfer experiments.

Figure 6.7 (continuation): 2000 FACS sorted naïve HH7-2tgIL10GFP T cells were adoptively transferred in the first and 20000 in the second adoptive transfer experiment. Spearman's correlation analysis between FoxP3 expression by HH7-2tg CD4 T cells and MHC class II expression by caecal (E) and colonic (F) IECs of both experiments. Lines denotes simple linear regression. Correlation was determined by two-tailed nonparametric Spearman's correlation. P-values and Spearman's correlation coefficients (r) are depicted in each of the graphs. P-value summary: *$p<0.05$ (A and B) Data from one experiment with n=7 H2-Ab1$^{f/fl}$ mice. (C-F) Data from two independent experiments with n=6 H2-Ab1$^{fl/fl}$ for the first (high MHCII) and n=7 H2-Ab1$^{fl/fl}$ for the second experiment (low MHCII). Mice were housed in the new SPF-B animal facility.

6.2.2 HH7-2tg CD4 T cells are activated and their effector functions modulated by colonic organoid MHC class II expression

The varying degrees of MHC class II expression by IECs between different *in vivo* experiments made it challenging to investigate whether IECs can function as non-professional antigen presenting cells but allowed us to develop hypotheses about the potential role of IEC MHC class II expression. We hypothesised that upon intestinal inflammation caecal and colonic IECs upregulate MHC class II and PD-L1 expression. We further hypothesised, that the interaction of CD4 T cells with their cognate antigen presented on MHC class II molecules expressed by IECs results in the upregulation of the activation maker PD-1, which in turn can interact with PD-L1 expressed by IECs. The activation of the PD-1-PD-L1 pathway then leads to the inhibition of CD4 T cell effector functions. To model $CD4^+$ T cell interactions with IEC, we used a reductionist approach and developed a 3D intestinal organoid co-culture system (see Methods section 2.10.3). Using colonic organoids allowed us to consistently upregulate MHC class II expression by IFNγ stimulation. In addition, the co-culture only consists of colonic organoids and CD4 T cells, which allowed us to investigate changes in CD4 T cell phenotypes exclusively in response to IECs. As we had previously used *H. hepaticus* specific CD4 T cells in our *in vivo* mouse models, we continued to investigate whether MHC class II expression by colonic organoids modulates HH7-2tg CD4 T cell phenotype and function.

CD4 T cell priming occurs in secondary lymphoid tissues and after activation, CD4 T cells migrate into the intestinal tissue where they encounter further antigen presenting cell populations. The vast majority of CD4 T cells located in the intestinal tissue is therefore antigen experienced, with very few of them being naïve. We FACS sorted naïve HH7-2tg CD4 T cells and pre-activated them by stimulation with anti-CD3/anti-CD28 for three days, followed by two days of rest prior to co-culture with H2-$Ab1^{fl/fl}$ IEC organoids. To test the role of MHC class II expression by cIECs in modulating CD4 T cell responses, we pre-treated cIEC organoids with

IFNγ to upregulate MHC class II expression and subsequently pulsed them with the *H. hepaticus* MHC II peptide epitope HH_1713. We used both H2-Ab1^{VC} organoids and αMHCII treatment as negative controls. The experimental co-culture setup is depicted in Figure 6.8 A and the experimental conditions are described in Figure 6.8 B.

First, we wanted to determine whether antigen presentation via MHC class II molecules expressed by cIECs can activate CD4 T cells in an antigen specific manner. FACS sorted naïve HH7-2tg CD4 T cells were pre-activated for 3 d, rested for 2 d, and the effector HH7-2tg CD4 T cells subsequently co-cultured for 3 d with H2-Ab1$^{fl/fl}$ and H2-Ab1^{VC} colonic organoids. We observed the co-culture over the incubation period and brightfield images for the HH7-2tg CD4 T cell co-culture with H2-Ab1$^{fl/fl}$ organoids can be seen in Figure 6.9. Organoids continued to grow during the co-culture period, indicating that the co-culture setup supports organoid growth and survival. In addition, we observed organoid differentiation, which becomes apparent in thicker walled organoids shedding dead cells into their lumen. Some organoids also died throughout the period, which is visible by burst organoid fragments. Overall, the majority of organoids were viable throughout the co-culture with HH7-2tg CD4 T cells (Figure 6.9).

After three days of co-culture, cells were analysed by flow cytometry. First, we detected between around 10 % and 30 % HH7-2tg CD4 T cells among the cells harvested from the co-cultures (Figure 6.10 A and Figure 6.11 A). We found the viability of HH7-2tg CD4 T cells after 3 d of co-culture was between 60 % to 80 % (Figure 6.10 B and Figure 6.11 A). We then wanted to understand whether antigen presentation by cIECs leads to the activation of HH7-2tg CD4 T cells and used upregulated expression of PD-1 and CD44 as a proxy for TCR-mediated activation. When co-cultured with IFNγ-treated H2-Ab1$^{fl/fl}$ organoids in the presence of cognate peptide, we observed that 10-15 % of HH7-2tg CD4 T cells significantly upregulated PD-1 and CD44^{hi} expression (Figure 6.10 C and D, Figure 6.11 B and C). We did

not observe PD-1 or CD44^{hi} upregulation when antigen recognition was either not possible (H2-Ab1^{VC} organoids) or blocked (αMHCII treatment) (Figure 6.10 C and D, Figure 6.11 B and C). These results demonstrate, that HH7-2tg CD4 T cells survived the three day co-culture period and that they upregulate PD-1 and CD44 expression upon antigen specific activation by cIECs expressing MHC class II. This highlights that cIECs can function as non-professional antigen presenting cells *in vitro*.

Next, we assessed whether co-cultured HH7-2tg CD4 T cells phentopically resembled effector or central memory T cells, as defined by CD44 and CD62L expression. We detected a significant increase in the proportion of effector memory T cells (CD44^{Hi}CD62L^{-}) and a corresponding decrease in central memory T cells (CD44^{Hi}CD62L^{+}) only when HH7-2tg CD4 T cells were co-cultured with IFNγ-treated H2-Ab1$^{fl/fl}$ organoids in the presence of cognate peptide (Figure 6.12 A and B).

Next, we wanted to investigate whether antigen specific activation of HH7-2tg CD4 T cells by cIECs modulated their effector phenotype. When HH7-2tg CD4 T cells were co-cultured with IFNγ-treated H2-Ab1$^{fl/fl}$ organoids in the presence of cognate peptide there was almost no effect on the proportion of classical Treg cells (Foxp3^{+}RoRγt^{-}) (Figure 6.13 A and Figure 6.14 A). However, under these conditions we detected the presence of about 10 % RoRγt^{+} cells (Figure 6.13 B and Figure 6.14 B) and around 20 % Tbet^{+} cells (Figure 6.13 C and Figure 6.14 C). These RoRγt^{+} and Tbet^{+} populations were not observed when cognate peptide presentation was ablated by using H2-Ab1^{VC} organoids or αMHCII treatment (Figure 6.13 and Figure 6.14). Overall, these data suggest that antigen specific activation of HH7-2tg CD4 T cells by cIECs modulates their phenotype towards the Th1 and Th17 lineages, but does not enhance expression of the Treg transcription factor FoxP3.

H. hepaticus colonisation drives peripheral differentiation of Treg cells, expressing both the transcription factors FoxP3 and RoRγt, as well as Th1 and Th17 cells, expressing T-bet and RoRγt respectively [318]. We therefore assessed whether antigen specific activation mediated by cIECs supports peripherally induced RoRγt$^+$ Treg cells. We found that although co-culture of HH7-2tg CD4 T cells with IFNγ-treated H2-Ab1$^{fl/fl}$ cIECs in the presence of cognate peptide did not alter FoxP3$^+$ RoRγt$^-$ frequencies (Figure 6.15 A), it did support the emergence of a small population (3 %) of FoxP3$^+$ RoRγt$^+$ T cells (Figure 6.15 B). In addition, we detected a similarly sized population of FoxP3$^-$ RoRγt$^+$ T cell in the same co-cultures (Figure 6.15 C). Further analysis of HH7-2tg CD4 T cells co-cultured with IFNγ-treated H2-Ab1$^{fl/fl}$ cIECs in the presence of cognate peptide revealed a more sizable population (15 %) of Tbet$^+$ RoRγt$^-$ T cells (Figure 6.15 D) and a small proportion (4 %) of Tbet$^+$ RoRγt$^+$ T cells (Figure 6.15 E). Finally, around 2 % of HH7-2tg CD4 T cells in these co-cultures were Tbet$^-$ RoRγt$^+$ T cells (Figure 6.15 F). Altogether, these results suggest antigen specific activation of HH7-2tg CD4 T cells by cIECs modulates transcription factor expression in a way that supports the emergence and/or survival of RoRγt and/or T-bet expressing cells.

We further analysed how antigen presentation by cIECs modulates HH7-2tg CD4 T cell functions by assessing expression of canonical effector cytokines. Upon co-culture of HH7-2tg CD4 T cells with IFNγ-treated H2-Ab1$^{fl/fl}$ cIECs in the presence of cognate peptide, we detected small, but significantly increased, populations of IL-17A$^+$ (Figure 6.16 A and Figure 6.17 A), IFNγ^+ (Figure 6.16 B and Figure 6.17 B) and TNFα^+ HH7-2tg CD4 T cells (Figure 6.16 C and 6.17 C). Overall, these results indicate that antigen presentation by cIECs modulates HH7-2tg CD4 T cell functions by supporting pro-inflammatory cytokine expression of IL-17A, IFNγ and TNFα.

We also determined IFNγ concentrations in the co-culture supernatants of a separate experiment. IFNγ was detected in all co-culture conditions, suggesting

that HH7-2tg CD4 T cells produced IFNγ after their pre-activation (Figure 6.18). However, consistent with our flow cytometry results (see Figure 6.17 B), elevated IFNγ concentrations were detected when HH7-2tg CD4 T cells were co-cultured with IFNγ-treated H2-Ab1$^{fl/fl}$ cIECs in the presence of cognate peptide (Figure 6.18). It is noticable however, that we also detected increased IFNγ concentrations when HH7-2tg CD4 T cells were co-cultured with H2-Ab1^{VC} cIECs in the presence of cognate peptide (Figure 6.18), suggesting that there was insufficient Cre mediated deletion of MHC class II in some cIECs (see section 3.2.5). MHC class II blockade ablated the increase in IFNγ secretion by HH7-2tg CD4 T cells when co-cultured with both H2-Ab1$^{fl/fl}$ and H2-Ab1^{VC} organoids (Figure 6.18). Unexpectedly, we detected comparable increases in IFNγ secretion when only the HH_1713 peptide was added to HH7-2tg CD4 T cells co-cultured with cIECs that had not been treated with IFN-γ (Figure 6.18). This suggesting that the baseline IFNγ expression by the pre-activated HH7-2tg CD4 T cells may have been sufficient to upregulate MHC class II expression by cIECs organoids, resulting in increased IFNγ secretion (Figure 6.18). Taken together, these results highlight that HH7-2tg CD4 T cells produce IFNγ after pre-activation, but they increase IFNγ secretion upon co-culture with cIECs in the presence of cognate peptide.

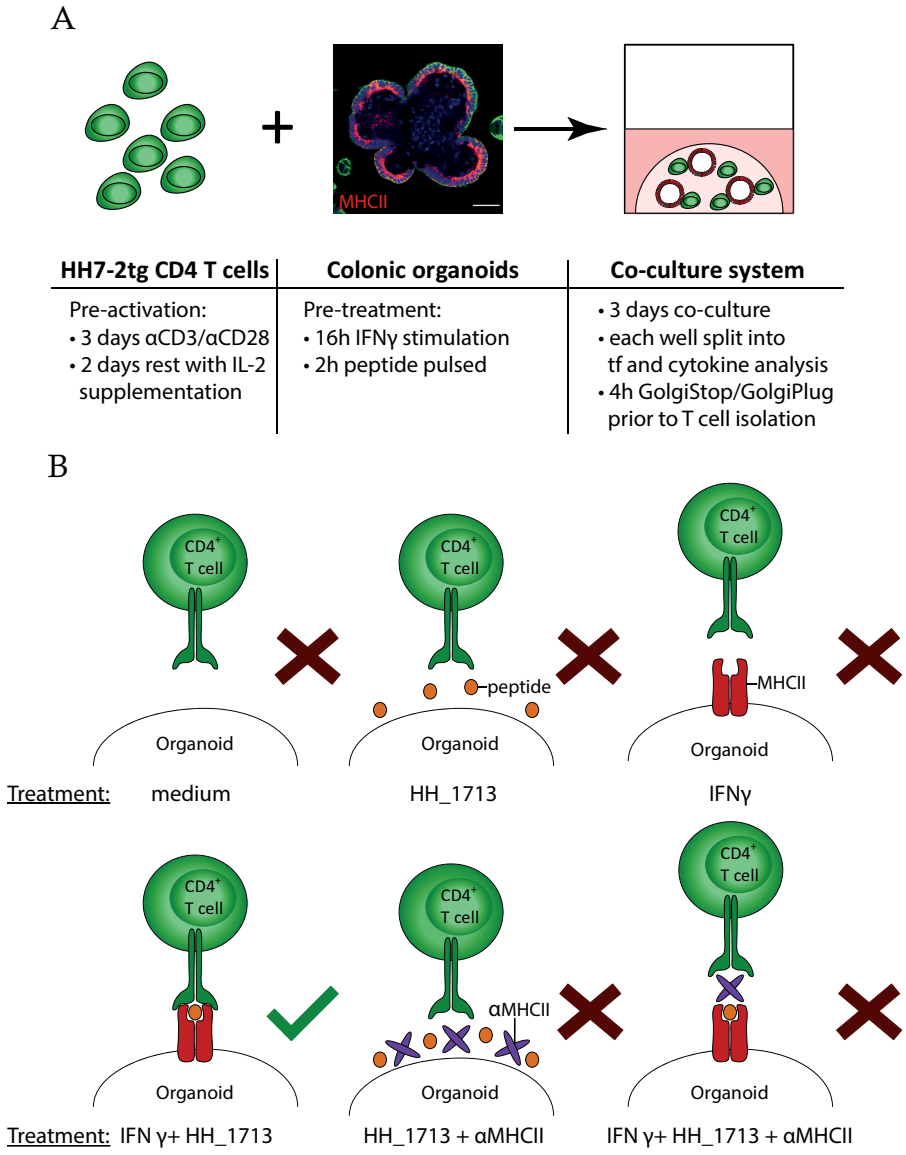


Figure 6.8: Experimental setup of colonic organoid and CD4 T cell co-culture and culture conditions. (A) Experimental setup of colonic organoid and CD4 T cell co-culture. FACS sorted naïve HH7-2tg CD4 T cells were pre-activated for 3d, rested for 2d, prior to their three day co-culture with IFNγ pre-treated and HH_1713 peptide-pulsed colonic organoids. (B) Schematic of co-culture conditions and details on whether they lead to CD4 T cell activation. Cross: no CD4 T cell activation; check: CD4 T cell activation.

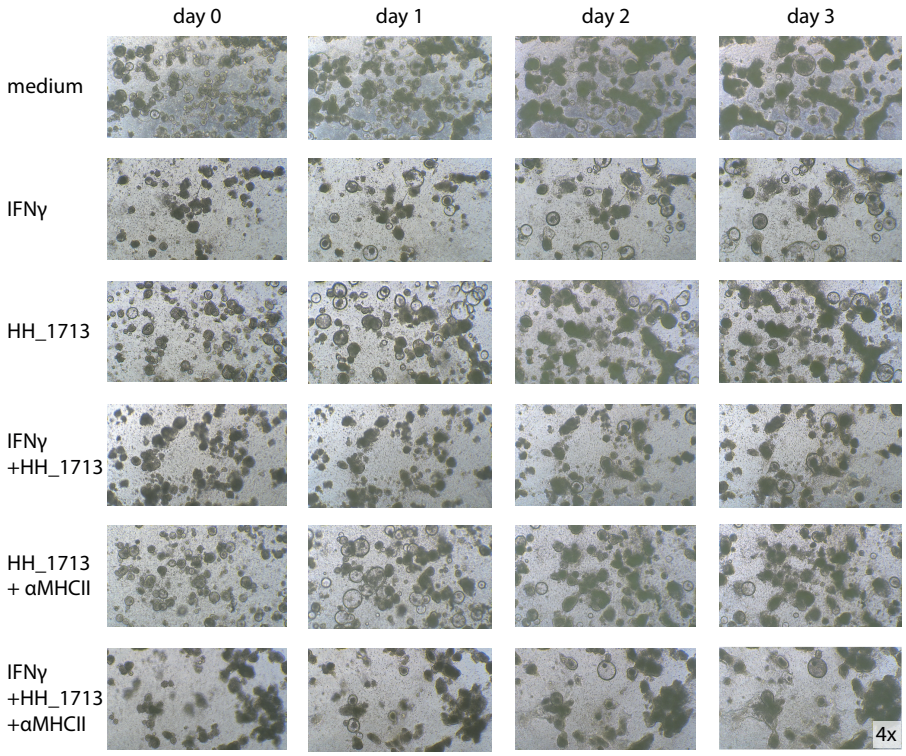


Figure 6.9: Three day co-culture of HH7-2tg CD4 T cells with colonic H2-Ab1$^{fl/fl}$ organoids. Pre-activated HH7-2tg CD4 T cells were co-cultured with H2-Ab1$^{fl/fl}$ for three days. Brightfield microscopy images were acquired each day of the co-culture of roughly the same location of the HH7-2tg CD4 T cell and H2-Ab1$^{fl/fl}$ co-culture under 4 X magnification.

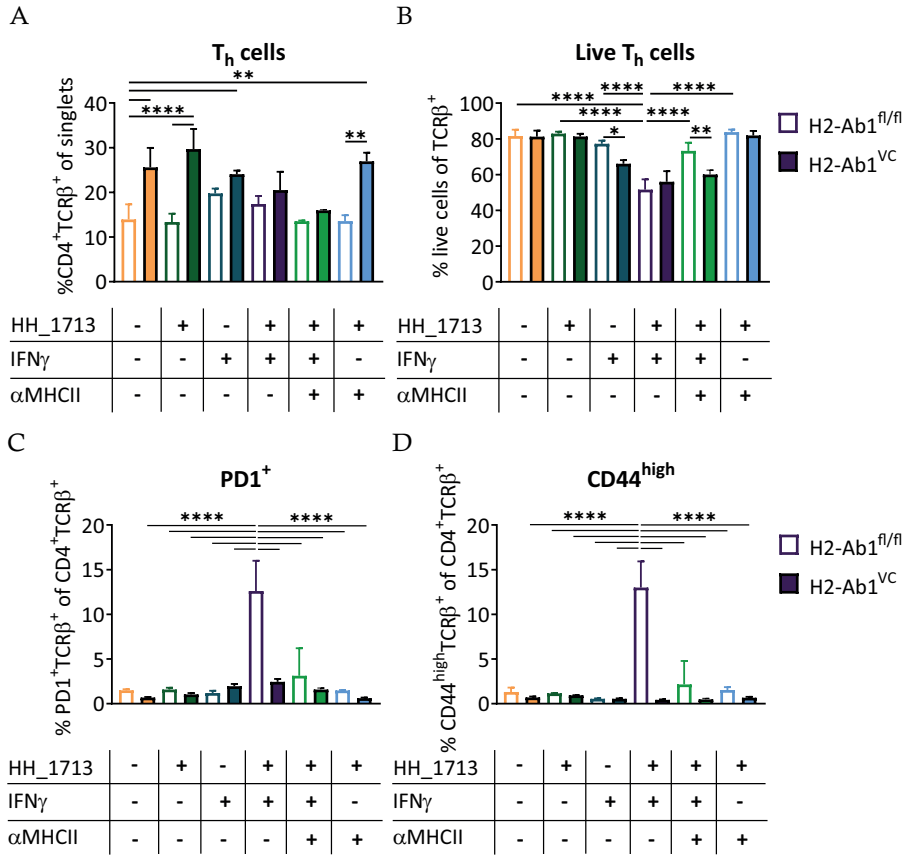


Figure 6.10: Upregulation of PD-1 and CD44 expression by HH7-2tg CD4 T cells upon antigen specific activation by cIECs. 100000 pre-activated HH7-2tg CD4 T cells were co-cultured with H2-Ab1$^{fl/fl}$ and H2-Ab1^{VC} organoids for three days. Then, HH7-2tg CD4 T cells were isolated and analysed by flow cytometry. Frequencies of live cells (A) and CD4$^+$ T cells (B). Frequencies of PD-1$^+$ (C) and CD44^{high} (D) HH7-2tg CD4 T cells. Bars represent mean (± SD). Statistical significance between the groups was determined by repeated measure mixed-effects analysis with Tukey's multiple comparisons test, with a single pooled variance. P-value summary: *p<0.05; **p<0.01; ****p<0.0001. Representative data from one of two independent experiments, with three technical replicates for each co-culture condition, except for the HH_1713 + αMHCII condition, which consists of two technical replicates.

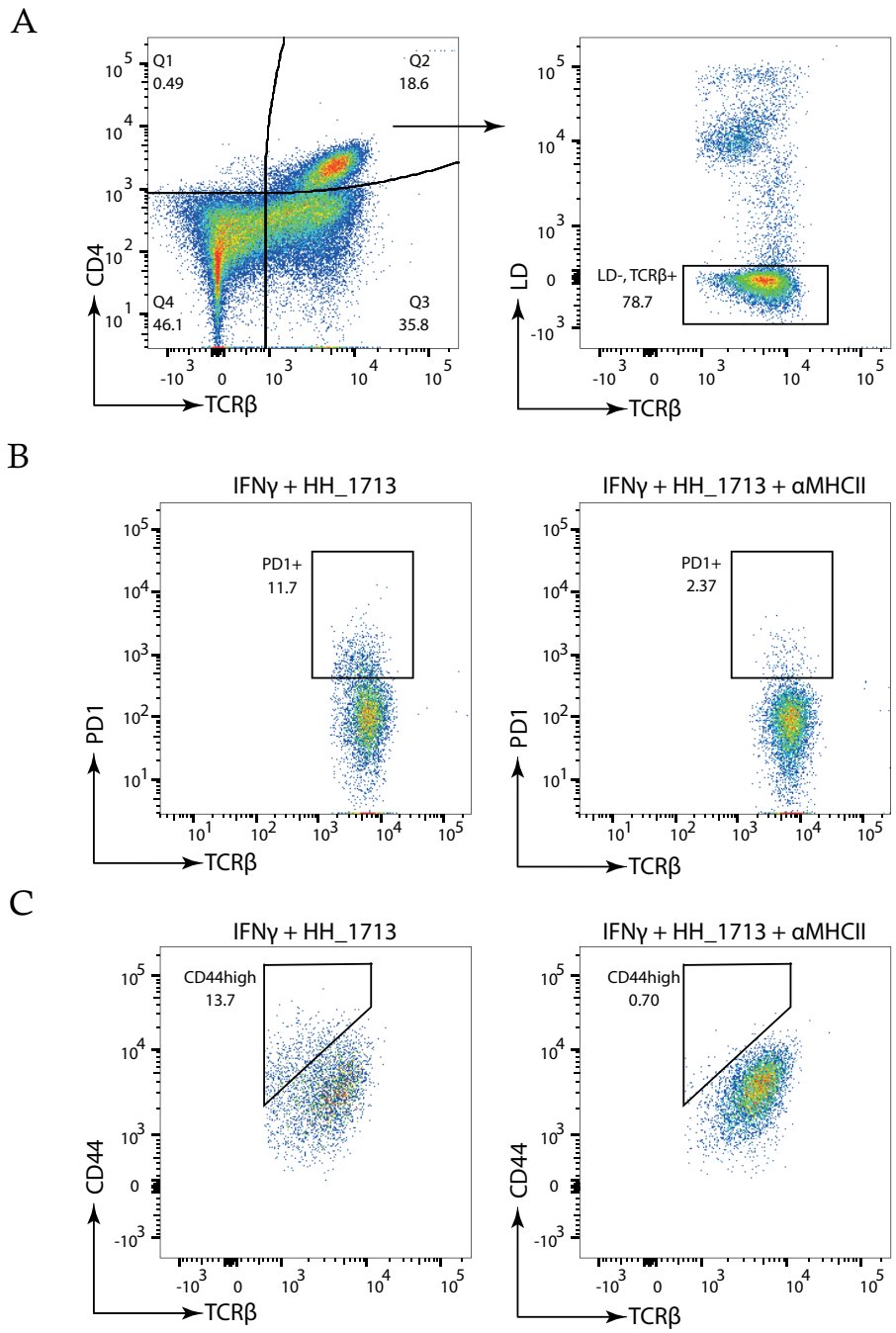


Figure 6.11: Flow cytometric analysis of PD-1 and CD44 expression by HH7-2tg CD4 T cells upon antigen specific activation by cIECs. 100000 pre-activated HH7-2tg CD4 T cells were co-cultured with H2-Ab1$^{fl/fl}$ and H2-Ab1^{VC} organoids for three days. (A) HH7-2tg CD4 T cells were isolated and analysed by flow cytometry. Representative FACS plots of PD-1^{+} (B) and CD44^{high} of CD44^{+} (C) HH7-2tg CD4 T cell frequencies, when co-cultured with colonic H2-Ab1$^{fl/fl}$ organoids pre-treated with IFNγ, to upregulated MHC class II expression, and peptide pulsed with HH_1713 on the left and additional αMHCII treatment on the right.

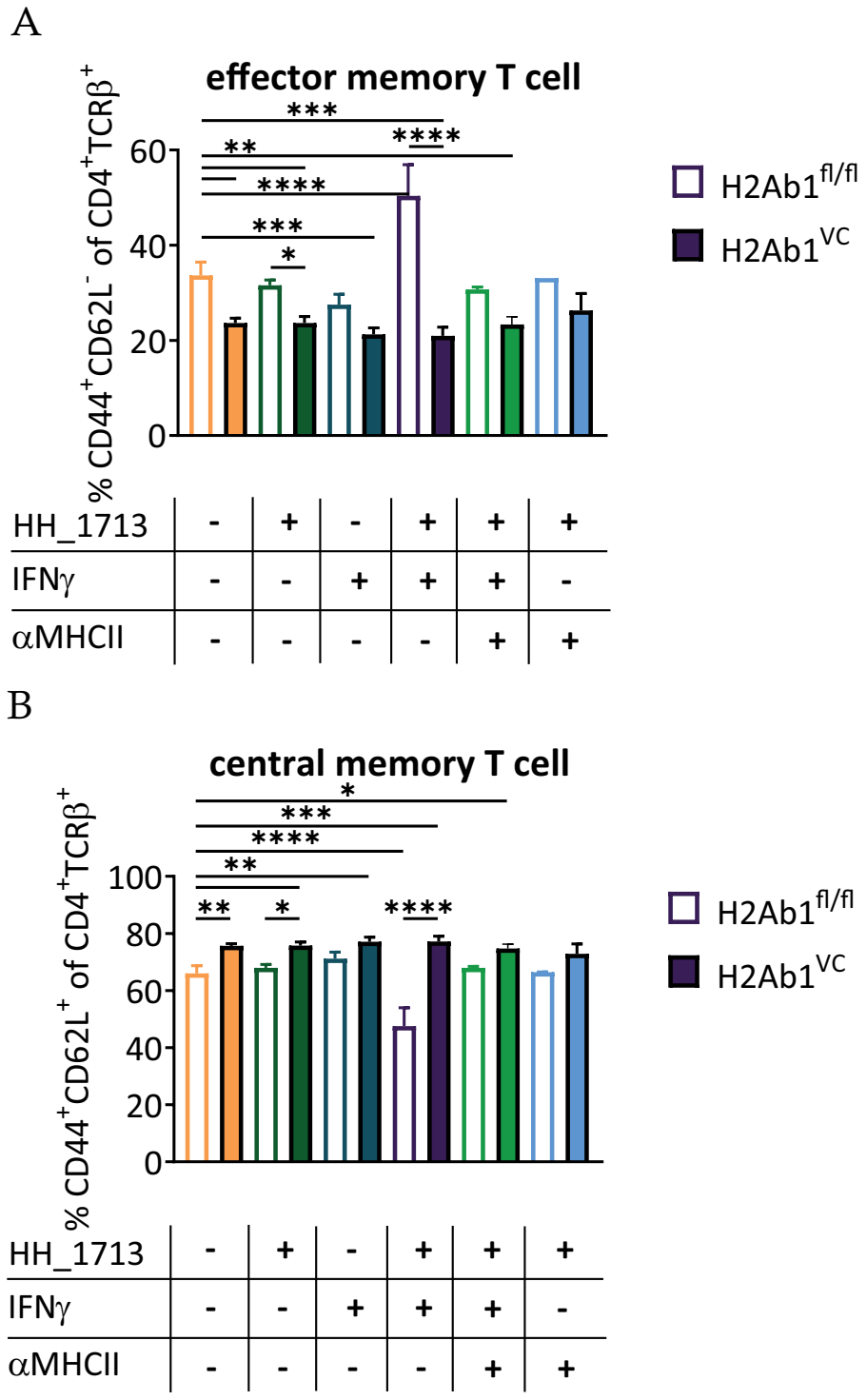


Figure 6.12: Co-culture supports central memory T cell differentiation. 100000 pre-activated HH7-2tg CD4 T cells were co-cultured with H2-Ab1$^{fl/fl}$ and H2-Ab1^{VC} organoids for three days. HH7-2tg CD4 T cells were isolated and analysed by flow cytometry. Frequencies of effector memory (A) and central memory (B) T cells. Bars represent mean (± SD). Statistical significance between the groups was determined by repeated measure mixed-effects analysis with Tukey's multiple comparisons test, with a single pooled variance. P-value summary: ***p<0.0001. Representative data from one of two independent experiments, with three technical replicates for each co-culture condition, except for the HH_1713 + αMHCII condition, which consists of two technical replicates.

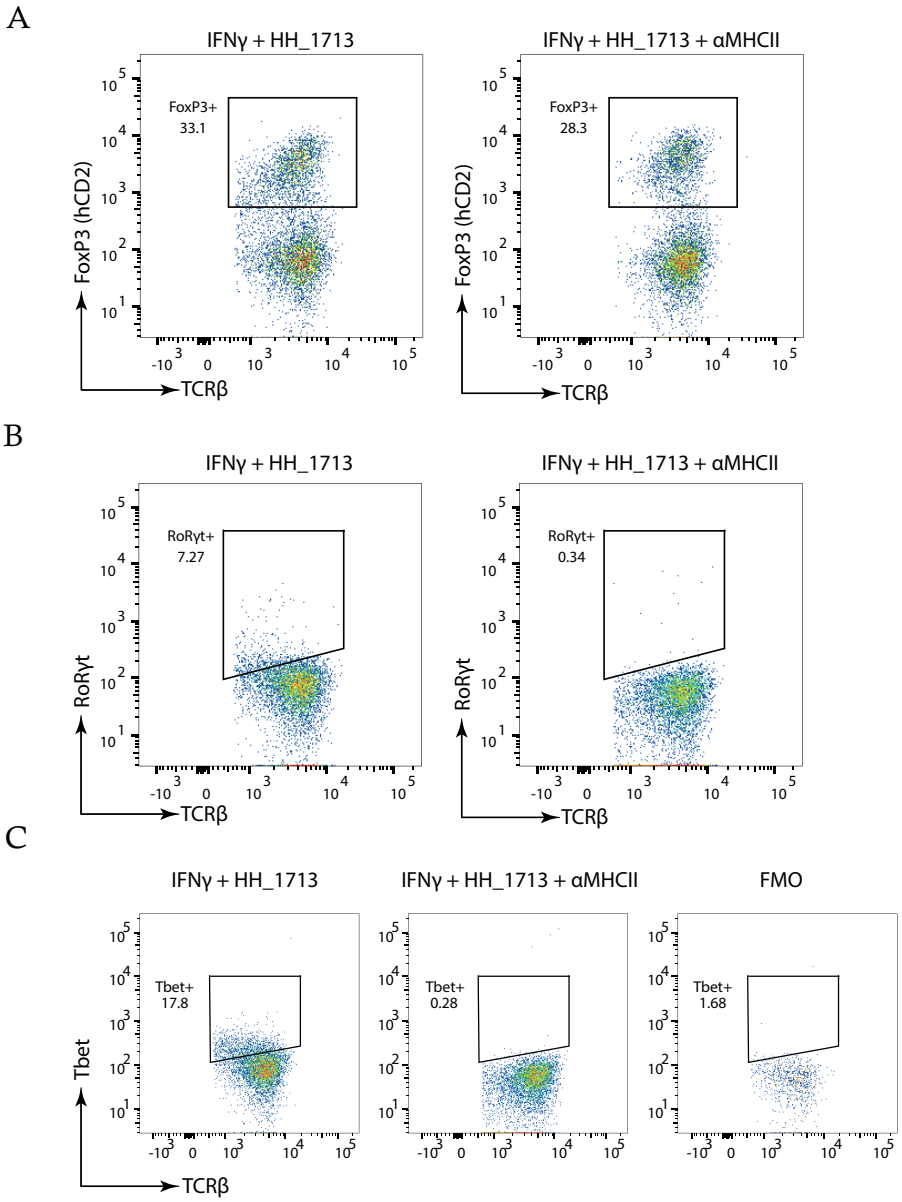


Figure 6.13: Upregulation of RoRγt and T-bet but not FoxP3 expression by HH7-2tg CD4 T cells upon antigen specific activation. 100000 pre-activated HH7-2tg CD4 T cells were co-cultured with H2-Ab1$^{fl/fl}$ and H2-Ab1^{VC} organoids for three days. HH7-2tg CD4 T cells were isolated and analysed by flow cytometry. Representative FACS plots of FoxP3^{+} (A), RoRγt^{+} (B) and Tbet^{+} (C) HH7-2tg CD4 T cell frequencies. HH7-2tg CD4 T cells were co-cultured with colonic H2-Ab1$^{fl/fl}$ organoids pre-treated with IFNγ to upregulated MHC class II expression and peptide pulsed with HH_1713 on the left and experienced additional αMHCII treatment on the right. FMO was obtained from HH7-2tg CD4 T cells co-cultured with IFNγ treated and HH_1713 peptide pulsed colonic H2-Ab1$^{fl/fl}$ organoids.

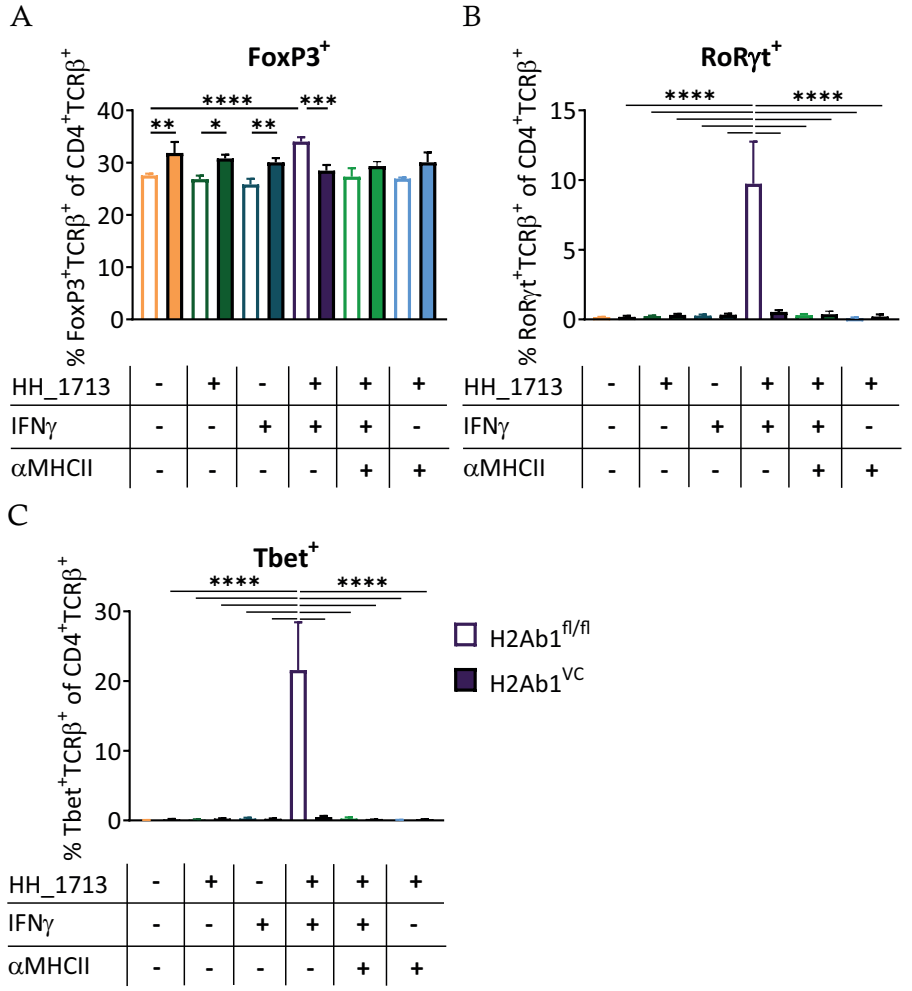


Figure 6.14: Upregulation of RoRγt and T-bet but not FoxP3 expression by HH7-2tg CD4 T cells upon antigen specific activation. 100000 pre-activated HH7-2tg CD4 T cells were co-cultured with H2-Ab1$^{fl/fl}$ and H2-Ab1^{VC} organoids for three days. HH7-2tg CD4 T cells were isolated and analysed by flow cytometry. Frequencies of FoxP3$^+$ (A), RoRγt$^+$ (B) and Tbet$^+$ (C) HH7-2tg CD4 T cells. Bars represent mean ($\pm$ SD). Statistical significance between the groups was determined by repeated measure mixed-effects analysis with Tukey's multiple comparisons test, with a single pooled variance. P-value summary: *p<0.05; **p<0.01; ***p<0.001; ****p<0.0001. Representative data from one of two independent experiments, with three technical replicates for each co-culture condition, except for the HH_1713 + αMHCII condition, which consists of two technical replicates.

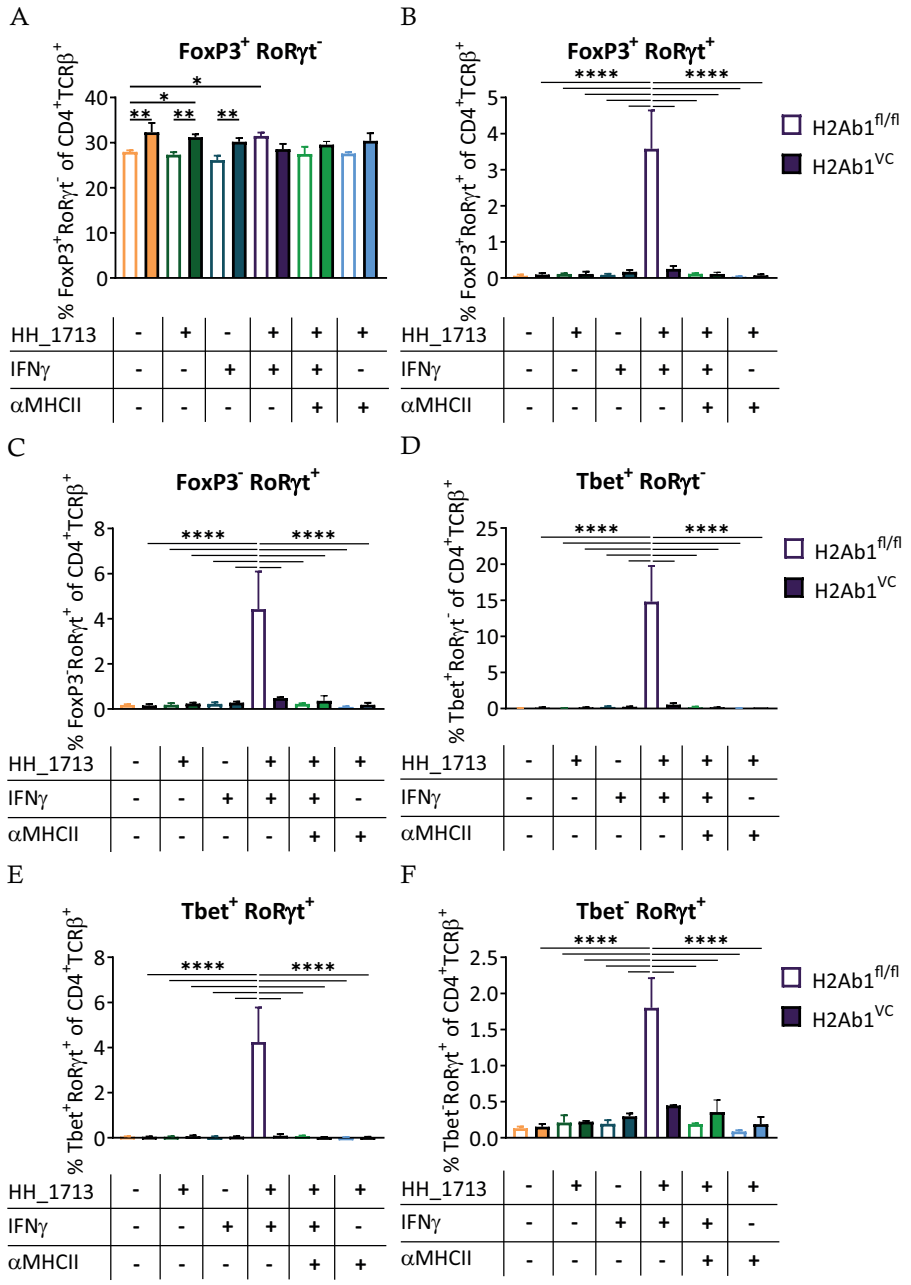


Figure 6.15: Antigen specific activation of HH7-2tg CD4 T cells by MHC class II expressing cIECs supports RoRγt and T-bet expression. 100000 pre-activated HH7-2tg CD4 T cells were co-cultured with H2-Ab1$^{fl/fl}$ and H2-Ab1^{VC} organoids for three days. HH7-2tg CD4 T cells were isolated and analysed by flow cytometry. Frequencies of FoxP3^{+} RoRγt^{-} (A), FoxP3^{+} RoRγt^{+} (B) and FoxP3^{-} RoRγt^{+} (C), Tbet^{+} RoRγt^{-} (D), Tbet^{+} RoRγt^{+} (E) and Tbet^{-} RoRγt^{+} (F) HH7-2tg CD4 T cells. Bars represent mean (± SD). Statistical significance between the groups was determined by repeated measure mixed-effects analysis with Tukey's multiple comparisons test, with a single pooled variance. P-value summary: *p<0.05; **p<0.01; ****p<0.0001. Representative data from one of two independent experiments, with three technical replicates for each co-culture condition, except for the HH_1713 + αMHCII condition, which consists of two technical replicates.

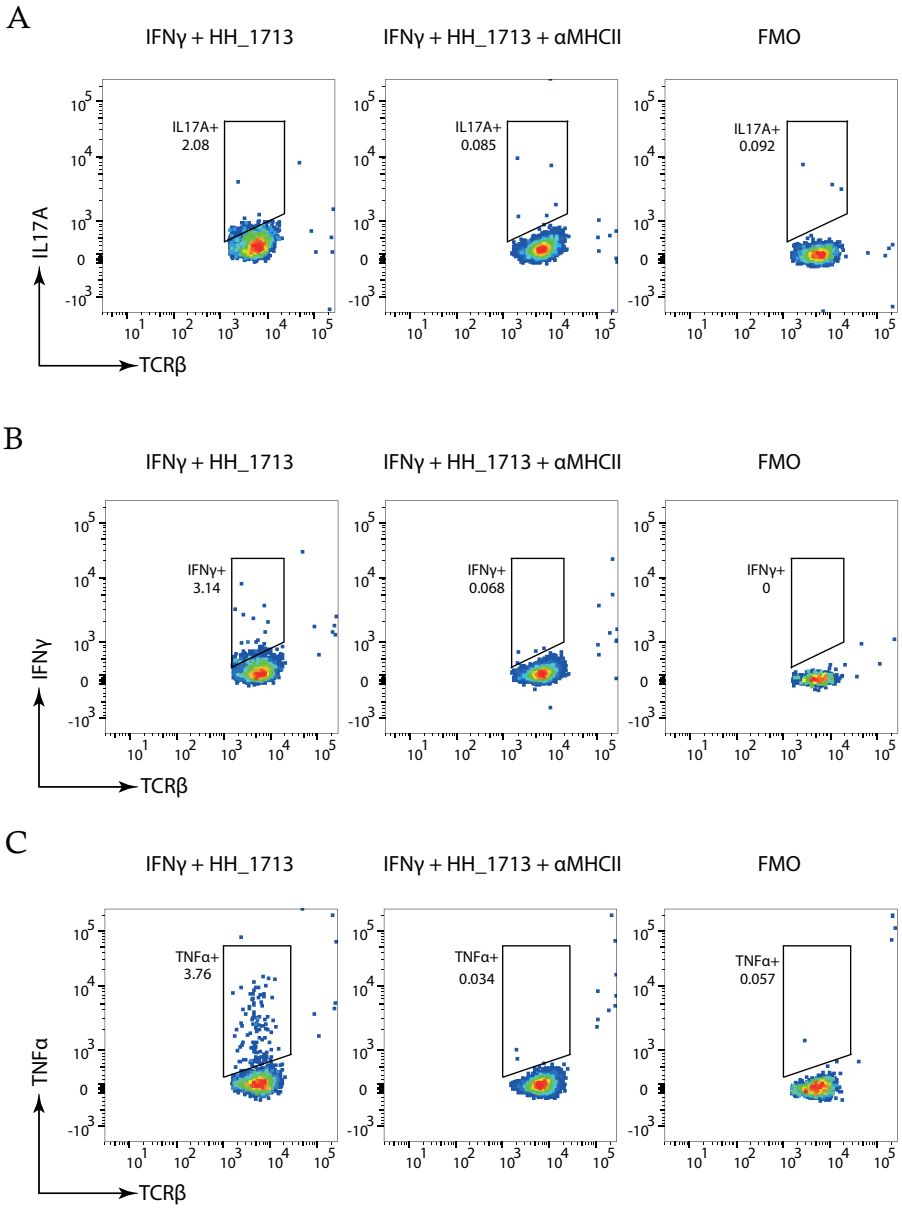


Figure 6.16: Upregulation of IFNγ, IL-17A and TNFα cytokine production upon antigen specific activation of HH7-2tg CD4 T cells. 100000 p-re-activated HH7-2tg CD4 T cells were co-cultured with H2-Ab1$^{fl/fl}$ and H2-Ab1^{VC} organoids for three days. Prior to cell isolation, the co-culture was treated with GolgiPlug and GolgiStop for 4 h and HH7-2tg CD4 T cells isolated and analysed by flow cytometry. Representative FACS plots of IL-17A$^+$ (A), IFNγ^+ (B) and TNFα^+ (C) HH7-2tg CD4 T cell frequencies. HH7-2tg CD4 T cells were co-cultured with colonic H2-Ab1$^{fl/fl}$ organoids pre-treated with IFNγ to upregulated MHC class II expression and peptide pulsed with HH_1713 on the left and experienced additional αMHCII treatment in the middle graphs. FMOs on the right were obtained from HH7-2tg CD4 T cells co-cultured with IFNγ treated and HH_1713 peptide pulsed colonic H2-Ab1$^{fl/fl}$ organoids.

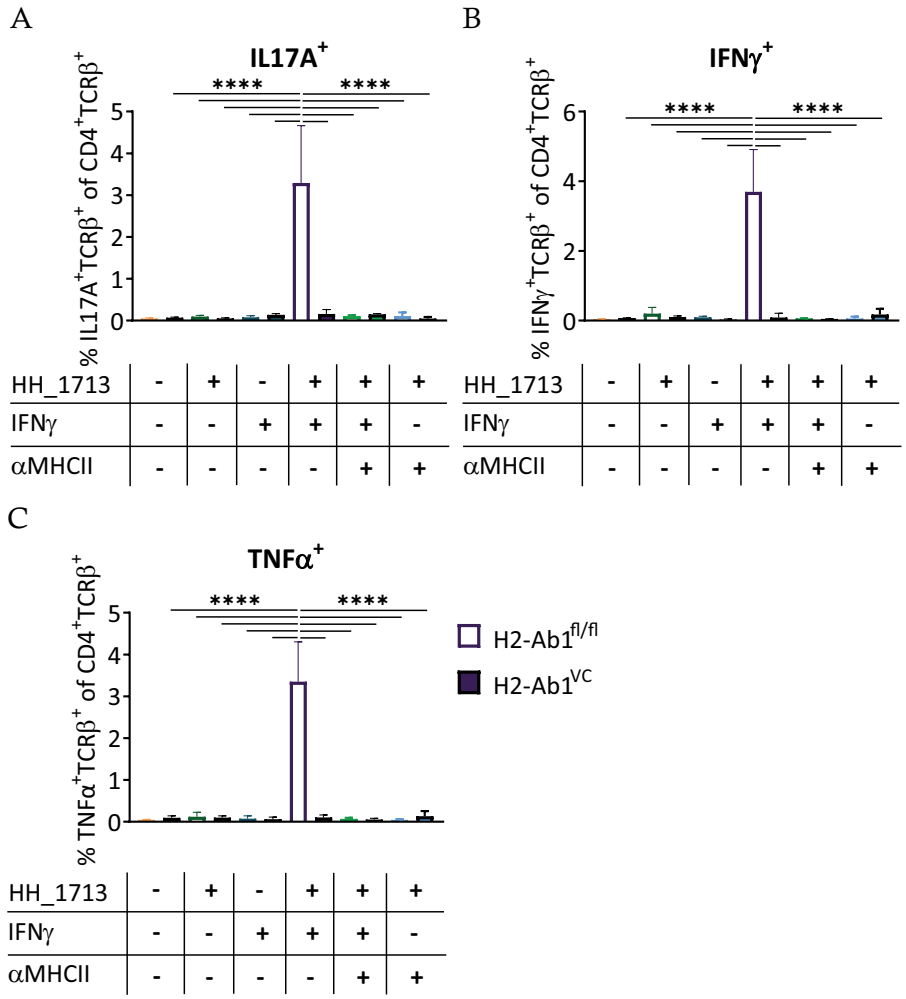


Figure 6.17: Upregulation of IFNγ, IL-17A and TNFα cytokine production upon antigen specific activation of HH7-2tg CD4 T cells. 100000 pre-activated HH7-2tg CD4 T cells were co-cultured with H2-Ab1$^{fl/fl}$ and H2-Ab1^{VC} organoids for three days. HH7-2tg CD4 T cells were isolated and analysed by flow cytometry. Frequencies of IL-17A$^+$ (A), IFNγ^+ (B) and TNFα^+ (C) HH7-2tg CD4 T cells. Bars represent mean ($\pm$ SD). Statistical significance between the groups was determined by repeated measure mixed-effects analysis with Tukey's multiple comparisons test, with a single pooled variance. P-value summary: ***p<0.0001. Representative data from two independent experiments, with three technical replicates for each co-culture condition, except for the HH_1713 + αMHCII condition, which consists of two technical replicates.

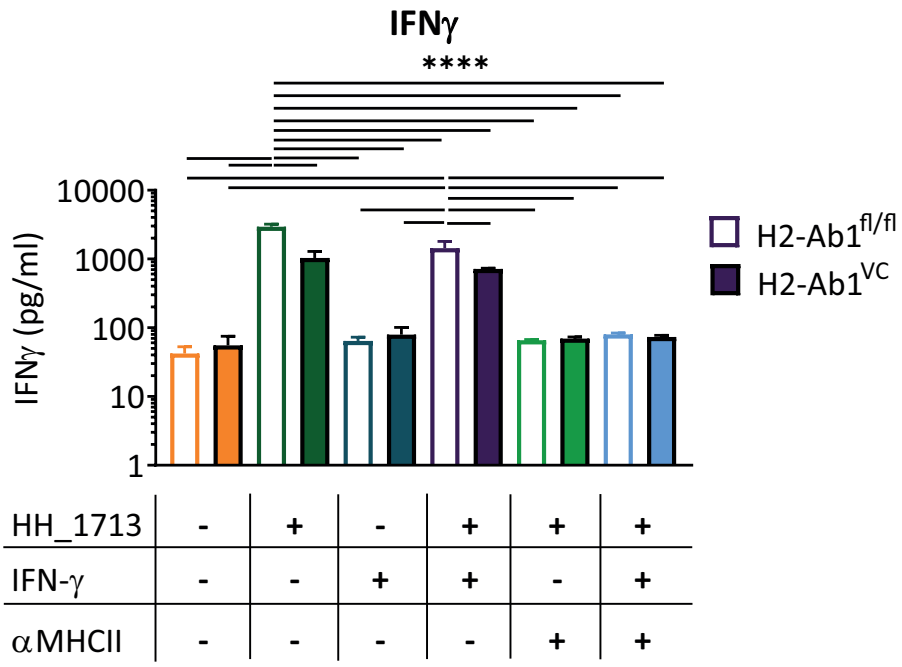


Figure 6.18: Antigen specific stimulation of HH7-2tg CD4 T cells leads to IFNγ release. 100000 pre-activated HH7-2tg CD4 T cells were co-cultured with H2-Ab1$^{fl/fl}$ and H2-Ab1^{VC} organoids for three days. Co-culture supernatant was collected and IFNγ secretion measured by ELISA. Bars represent mean ($\pm$ SD). Statistical significance between the groups was determined by repeated measure mixed-effects analysis with Tukey's multiple comparisons test, with a single pooled variance. P-value summary: ****p<0.0001. Data from one experiment, with four technical replicates for each co-culture condition, except for both the IFNγ + HH_1713 + αMHCII and the HH_1713 + αMHCII condition, which consist of two technical replicates.

6.3 Discussion

In chapter 3, we determined that IECs have important features to function as non-conventional APCs, and existing literature suggests that antigen presentation by IECs shapes CD4 T cell phenotypes and function. The colonisation of wild-type mice with *H. hepaticus* induces regulatory CD4 T cell responses, however it is currently not clear whether IEC MHC class II expression might modulate these adaptive immune responses in the mucosa. We hypothesised that antigen presentation by large intestinal IECs plays an important role in the modulation of CD4 T cell phenotype and function in response to *H. hepaticus*, thereby supporting the maintenance of intestinal homeostasis. We studied this by investigating the modulation of *H. hepaticus*-specific HH7-2tgIL10GFP CD4 T cells within the colonic and caecal mucosa. In addition, we established an *in vitro* co-culture system of HH7-2tg CD4 T cell and colonic organoids, to detect differences in HH7-2tg CD4 T cell phenotype and function exclusively in response to IEC-T cell interactions.

We show that lack of MHC class II expression by caecal IECs induces increased FoxP3 as well as IL-10 expression by HH7-2tgIL10GFP CD4 T cells in the caecal LP. This phenotype appears to be dependent on the proportion of MHC class II expressing cmIECs in the intestinal epithelium, as an experimental repeat, characterised by lower cmIEC MHC class II expression, did not find an increase in FoxP3 expression and IL-10 production by HH7-2tgIL10GFP CD4 T cells.

HH7-2tg CD4 T cells were shown to adopt their phenotype to the tissue micro-environment of *H. hepaticus* colonised mice. They differentiate into Tfh cells in lymphoid tissues and into Treg cells in the intestinal lamina propria, despite recognising the same antigen at either tissue site [318]. This highlights the importance of extrinsic signals shaping *H. hepaticus*-specific T cell differentiation and responses. Here we show, that *H. hepaticus* colonisation induces the expression of MHC class II by large intestinal IECs, though to a varying extent between experimental repeats. This finding is supported by studies performed in HFD treated

mice, which showed that *Helicobacter* species induced MHC class II expression by siIECs [377]. The different levels of MHC class II expression by cmIECs might reflect different colonisation levels of *H. hepaticus* between the experimental repeats. In addition, variations in pro-inflammatory cytokines levels in the intestinal mucosa, potentially driven by additional environmental factors, could have caused these differences of IEC MHC class II expression. Further studies could assess *H. hepaticus* colonisation levels both in caecal contents and caecal tissue to determine whether colonisation levels correlate with cmIEC MHC class II expression. In addition, the assessment of tissue cytokine levels at the different tissue sites across the experiments could provide a more detailed characterisation of the tissue micro-environment influencing epithelial antigen presentation. We further observed an increased differentiation into FoxP3$^+$ HH7-2tgIL10GFP CD4 T cells and an increased IL-10 production by HH7-2tgIL10GFP CD4 T cells in MHC class II deficient mice compared to littermate controls expressing high proportions of MHC class II. These results were unexpected, as we hypothesised that epithelial antigen presentation is supporting peripherally-induced Treg cell differentiation. Therefore, we anticipated higher FoxP3$^+$ HH7-2tgIL10GFP proportions in H2-Ab1$^{\mathrm{fl/fl}}$ mice compared to H2-Ab1$^{\mathrm{VC}}$ littermate controls, though the opposite was detected. Interestingly, this phenotype was lost, when fewer cmIECs expressed MHC class II. Suggesting, that the tissue micro-environment might play an important role in shaping IEC antigen presentation and thereby adaptive immune responses.

It has been reported that murine siIECs express PD-L1 under steady state conditions [378] and low PD-L1 protein expression was detected in IBD patient cIECs, but not in healthy individuals [169]. These findings suggest that large intestinal IEC PD-L1 protein expression is upregulated by inflammatory conditions, similar to IEC MHC class II expression. In our study we detected a trend towards increased PD-L1 expression in MHC class II sufficient mice compared to MHC class II deficient littermate controls in our second adoptive transfer experiment. Unfortunately, we did not acquire the PD-L1 expression by large intestinal IECs in our first adoptive

transfer experiment, showing higher IEC MHC class II expression, so we can not be certain whether heightened frequencies of MHCII$^+$ IECs are accompanied by heightened PD-L1$^+$ IECs and whether lack of MHC class II expression by IECs influences IEC PD-L1 expression. Interestingly, we detected a positive correlation between IEC MHC class II expression and PD-L1 expression. This raised the question whether MHC class II and PD-L1 expression might be driven by the same stimuli. A previous study showed that PD-L1 expression by siIECs depends on IFNγ signalling [378]. They reported a concentration-dependent increase in PD-L1 expression in small intestinal organoids following IFNγ treatment, and IFNγR-/- mice as well as mice treated with IFNγ-neutralising antibodies showed reduced siIEC PD-L1 expression [378]. These findings highlight that IFNγ signalling induced PD-L1 expression by siIECs and we confirmed IFNγ to be a potent inducer of IEC MHC class II expression in our study. Of note, lack of siIEC PD-L1 did not affect siIEC MHC class II expression levels and vice versa [378]. As our study assessed PD-L1$^+$ IEC frequencies, future studies could investigate whether IEC PD-L1 protein expression levels differ between H2-Ab1^{VC} and littermate controls. Furthermore, it would be of interest whether an IEC MHC class II-PD-L1 double-knock-out mouse, lacking both antigen presentation and PD-L1 co-inhibitory signalling capacity of IECs, would show changes in CD4 T cell differentiation and function in the mucosa.

Our study further suggests that an increase in MHC class II expression by caecal and colonic IECs negatively influences IL-10 production and FoxP3 expression, although these findings need to be further validated. One could speculate, that during low intestinal inflammation epithelial MHC class II expression is low and that the tissue micro-environment supports Treg cell differentiation and function, reflected in the higher IL-10 production and FoxP3 expression in the second adoptive transfer experiment. During increased intestinal inflammation, higher levels of IFNγ induce increased MHC class II, and potentially PD-L1, expression by large intestinal IECs, which allows the CD4 T cells to interact with their cognate antigen presented by the epithelium. This interaction supports the modulation of effector CD4 T cell

phenotypes and functions, the modulation potentially being dependent on both peptide:MHC class II complex recognition and PD-L1-PD-1 engagement. This interaction could retain CD4 T cells at the epithelial barrier, to locally secrete their effector cytokines and support the epithelium in its barrier functions before their functions are being constrained by the PD-1-PD-L1 interaction. This could establish a local niche for antigen-experienced CD4 T cells at the barrier site. To investigate, whether CD4 T cells accumulate at the intestinal epithelium during intestinal inflammation, future studies could perform immuno-fluorescent imaging of HH7-2tgIL10GFP CD4 T cells in intestinal swiss rolls and perform distance analysis between HH7-2tgIL10GFP CD4 T cells and MHCII^{+} IECs. However, these studies would not be able to provide information about recent TCR engagement with epithelial peptide:MHC class II complexes. Two-photon *in vivo* live cell imaging of adoptively transferred HH7-2tgDsRed CD4 T cells into H2-Ab1$^{fl/fl}$ and H2-Ab1^{VC} recipients at the intestinal barrier could provide information about the duration of the interaction between HH7-2tgDsRed CD4 T cells and IECs [407]. TCR engagement results in reduced motility of T cells [408, 409], so spacial-temporal analysis could provide further insights into the CD4 T cells-IEC interaction dynamics, as HH7-2tgDsRed CD4 T cells halt to actively engage with their cognate antigen presented by IECs.

As a large proportion of HH7-2tgIL10GFP CD4 T cells did not express FoxP3 or IL-10 in our experiments, it would be of interest to assess which additional phenotypes and functions they possess in future analysis. To this end, HH7-2tg CD4 T cells could be isolated from the different intestinal tissue sites of *H. hepaticus* colonised H2-Ab1$^{fl/fl}$ and H2-Ab1^{VC} mice, FACS sorted and subjected to targeted RTqPCR or RNAseq analysis. This would allow us to assess whether epithelial antigen presentation rather modulates *H. hepaticus*-specific CD4 T effector cells than Treg cells. To further strengthen our hypothesis that different levels of IEC MHC class II expressions result in varied microbe-specific CD4 T cells phenotype and function, it would be ideal to develop an *in vivo* system, which allows a reproducible

induction of epithelial MHC class II expression. Our data often shows a large spread of MHCII$^+$ IEC frequencies (see Figure 6.6) within the H2-Ab1$^{fl/fl}$ mouse group, which might result in different functional outcomes of CD4 T cells. The administration of a low dose of the pro-inflammatory and MHC class II inducing IFNγ prior to *H. hepaticus* colonisation, might decrease variability of MHC class II expression by IECs.

In order to understand whether *H. hepaticus*-specific CD4 T cell responses are modulated by epithelial antigen presentation, we further established a co-culture system of pre-activated HH7-2tg CD4 T cells and colonic organoids. Here we report, that HH7-2tg CD4 T cells were viable after three days of co-culture. We detected upregulated PD-1 and CD44 expression by HH7-2tg CD4 T cells that were able to interact with their cognate antigen, which we used as a surrogate for TCR-mediated activation. Upon antigen recognition, HH7-2tg CD4 T cells increased their RoRγt and T-bet expression levels. Interestingly, FoxP3 expression was not affected by epithelial antigen presentation but we detected the induction of FoxP3$^+$ RoRγt$^+$ HH7-2tg CD4 T cells. In addition to these phenotypic changes, we report the induction of TNFα, IFNγ and IL-17A cytokine expression upon antigen specific activation of HH7-2tg CD4 T cells. When assessing IFNγ concentrations in the co-culture supernatant of another co-culture experiment, we detected increased IFNγ release by HH7-2tg CD4 T cells activated by their cognate antigen. These findings show that cIECs can function as non-conventional APCs in an *in vitro* setting and that epithelial antigen presentation modulates HH7-2tg CD4 T cell phenotypes and functions towards the Th1 and Th17 lineage but does not enhance the expression of FoxP3. A schematic overview of the CD4 T cell IEC interaction mechanism is shown in Figure 6.19. In our *in vivo* study we detected increased FoxP3 expression by HH7-2tg CD4 T cells in the absence of epithelial MHC class II, which might suggest that also in the *in vivo* setting epithelial antigen presentation supports the modulation of Teff functions during inflammatory conditions.

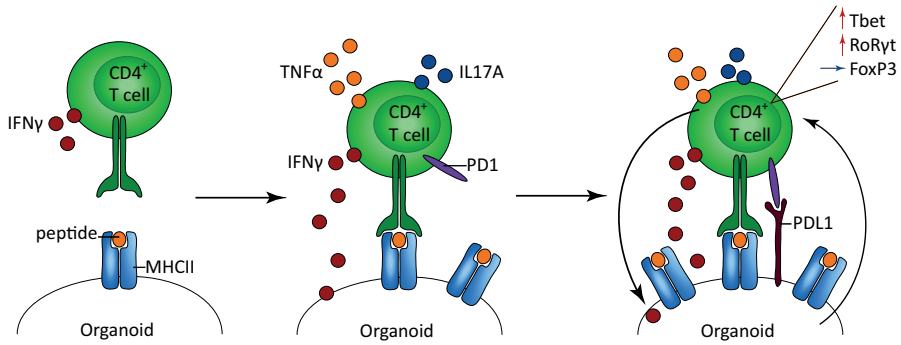


Figure 6.19: Schematic overview of antigen-specific interaction of HH7-2tg CD4 T cell with colonic organoids. Pre-activated $CD4^+$ T cells produce IFNγ and interact with their cognate antigen presented on MHC class II molecules by IECs. Upon TCR mediated activation, $CD4^+$ T cells express PD-1, increase their IFNγ production and produce TNF-α and IL-17A. In addition, they upregulate the expression of the TF T-bet and RoRγt, whereas FoxP3 remains unchanged.

In our study we used PD-1 and CD44 expression as a proxy for TCR-mediated activation [410, 411] and observed upregulation of both markers upon antigen specific activation of HH7-2tg CD4 T cells. Future studies could use calcium sensing dyes or HH7-2tgNur77GFP mice to assess TCR-specific activation. The expression of Nur77 is rapidly upregulated upon TCR signalling and Nur77GFP reporter mice therefore allows the investigation of antigen specific T cell activation [412]. *In vitro* studies performed in the Powrie lab (unpublished data by Dr. Yisu Gu) show that the Nur77GFP signal returns to its baseline expression at around 72 h following TCR stimulation. Therefore, all HH7-2tgNur77GFP CD4 T cells not receiving TCR signalling will be Nur77GFP low/negative, while HH7-2tgNur77GFP CD4 T cells engaging with peptide:MHC class II complexes presented by cIECs will be Nur77GFP high/positive after the co-culture with colonic organoids. The two day resting phase after pre-activation of HH7-2tgNur77GFP CD4 T cells as well as the three day co-culture period should allow the return of the Nur77GFP signal to baseline in the non-activation condition. These studies would provide further confirmation of TCR engagement by HH7-2tg CD4 T cells with antigen presenting IECs.

PD-1 engagement was described to deliver inhibitory signals to restrain TCR signalling and T cell activation [413–415]. However, a recent study showed that PD-1 interacts with the TIM-3 ligand Galectin-9 to attenuate Galectin-9/TIM-3-induced apoptosis of exhausted PD-1$^+$ TIM-3$^+$ T cells, thereby contributing to their persistence [416]. PD-1 surface protein expression can be detected within 24 h of TCR signalling, with maximal levels observed after 48 h of stimulation [417]. We detected between 10-15 % of HH7-2tg CD4 T cell expressing PD-1. As we co-culture HH7-2tg CD4 T cells for three days with colonic organoids, it could be possible that we are not detecting recently activated CD4 T cells but rather CD4 T cells activated at the very start of the co-culture and thereby missing HH7-2tg CD4 T cells which are in the process of upregulating PD-1 expression. The lower proportions of PD-1 expressing HH7-2tg CD4 T cells might additionally reflect the fact, that HH7-2tg CD4 T cells have to migrate through the co-culture matrigel to find their cognate antigen presented by cIECs. Preliminary experiments confirmed the migration of HH7-2tg CD4 T cells through the matrigel for the first 4 h of the co-culture by live cell imaging (data not shown), but this data needs to be further validated and the duration of imaging extended.

We detected the modulation of HH7-2tg CD4 T cells into the Th1 and Th17 lineage rather than the Treg lineage. In order to clarify whether antigen presentation by cIECs specifically modulates Teff rather than Treg cells, future studies could pre-differentiate naïve HH7-2tg CD4 T cells into different effector and regulatory T cell subsets [418] and subsequently co-culture them with antigen presenting colonic organoids. As Treg cells were described to express high levels of PD-1, it would be interesting to assess whether their PD-1 expression is modulated by epithelial antigen presentation. In addition, further co-stimulatory and co-inhibitory interactions could be assessed, such as ICOS-ICOS-L or CD40-CD40-L. The secretion of effector cytokines by activated HH7-2tg CD4 T cells might influence the expression of these co-stimulatory and co-inhibitory molecules. Studies have shown that TNFα, IL-17A and IFNγ induce the expression of PD-L1, CD40 or intercellular adhesion molecule

(ICAM) 1 in IECs [167, 419, 420]. Activated HH7-2tg CD4 T cells, expressing lymphocyte function-associated antigen-1 (LFA-1), could bind to ICAM-1, thereby facilitating prolonged adhesion to the epithelium [421]. In addition, the secretion of effector cytokines could feed back into the epithelium. Studies have described that the secretion of IL-10 by Treg cells maintains the small intestinal ISC niche, while Th effector cytokines, including IFNγ and IL-17A, promote small intestinal ISC differentiation [134]. The local secretion of CD4 T cell effector cytokines could therefore support the epithelial turn-over and shedding of infected IECs to re-establish the intestinal barrier during inflammatory conditions. It would be interesting to investigate, whether the composition of cIECs differ in H2-Ab1$^{fl/fl}$ and H2-Ab1^{VC} mice during intestinal inflammation and future studies could perform single cell RNAseq analysis to determine which cIEC subset expresses MHC class II and whether the lack of MHC class II expression changes the composition of the intestinal epithelium and leads to the loss and/or expansion of a certain IEC subset.

It was further described that activated human CD4 T cells have the ability to express MHC class II themselves (reviewed in [422]). The interaction with antigen presenting human CD4 T cells is thought to maintain T cell homeostasis by providing inhibitory signals to the interacting CD4 T cell [422]. However, murine CD4 T cells are not described to express MHC class II themselves [422]. To exclude the possibility of antigen presentation by activated HH7-2tg CD4 T cells, we determined MHC class II expression of HH7-2tg CD4 T cells in one of our co-culture experiments and could not detect MHC class II expression (data not shown). However these findings were preliminary and have to be further validated. But if the upregulation of PD-1 and CD44 expression would have been mediated by antigen presenting activated HH7-2tg CD4 T cells, we should have detected increased PD-1 and CD44 expression also in the co-culture of HH7-2tg CD4 T cells with H2-Ab1^{VC} organoids, which was not the case (see Figure 6.10).

Of note, we detected increased secretion of IFNγ into the co-culture supernatants when HH7-2tg CD4 T cells were co-cultured both with antigen presenting and peptide-pulsed colonic organoids. As we detected IFNγ secretion also in the untreated condition, we concluded that the pre-activation of HH7-2tg CD4 T cells with anti-CD3/anti-CD28 induces low levels of IFNγ production. The secreted IFNγ by HH7-2tg CD4 T cells appeared to be sufficient to induce MHC class II expression by colonic organoids, the MHC class II molecules were loaded with HH_1713 peptide and subsequently induced antigen specific activation and IFNγ secretion by HH7-2tg CD4 T cells. These findings highlight that the production of IFNγ by HH7-2tg CD4 T cells alone induced MHC class II expression by cIECs. HH7-2tg CD4 T cells thereby mediated their own antigen specific activation. However, we also detected increased secretion of IFNγ by HH7-2tg C4 T cells co-cultured with MHC class II deficient colonic organoids, which could be caused by insufficient Villin-Cre mediated deletion of MHC class II expression in cIECs (see section 3.2.5) and/or by very small numbers of bona fide APCs carried over during the sorting of the naïve HH7-2tg CD4 T cells. However, this seems very unlikely as HH7-2tg CD4 T cells were FACS sorted and cultured in T cell growing conditions for five days prior to their addition to the co-culture. In subsequent experiments we did not detect PD-1 upregulation by HH7-2tg CD4 T cells co-cultured with H2-Ab1^{VC} colonic organoids, which excludes the possibility of bona fide APCs inducing antigen specific activation of HH7-2tg CD4 T cells in these experiments. These results also suggest that cytokine release by HH7-2tg CD4 T cells may be a more sensitive readout of antigen specific activation and follow-up studies of the co-culture supernatants are warranted.

Depending on the tissue-microenvironment HH7-2tg CD4 T cells are able to differentiate into Tfh, Treg or Th17 cells. Our results show, that during increased inflammatory conditions, lack of MHC class II expression by cIECs induces increased expression of FoxP3 and IL-10 by HH7-2tg CD4 T cells. Colonic IEC MHC class II and PD-L1 expression were correlated, which might suggest that antigen presenting cIECs can provide co-inhibitory signals. We detected the induction

of PD-1 expression by HH7-2tg CD4 T cells upon antigen specific activation by colonic organoids *in vitro*. This activation was accompanied by the induction of IFNγ, IL-17A and TNFα expression and by the modulation of the HH7-2tg CD4 T cells into the Th1 and Th17 lineage. We therefore were able to show that cIECs can function as non-conventional APCs in an *in vitro* setting and that they modulate Teff phenotypes and functions.

7
General discussion

The intestinal epithelium consists of a single layer of IECs and physically separates the microbiota present in the gut lumen from the mucosal immune system of the host. Being exposed to vast amounts of microbial and dietary antigens, the epithelium has the challenging task to allow the continuous absorption of nutrients and water, while distinguishing potential pathogenic antigens from commensal antigens to maintain intestinal homeostasis. Far from being merely a physical barrier, the intestinal epithelium actively participates in the sensing of its environment and the initiation of immune cell effector responses.

In order to recognise MAMPs and DAMPs, IECs are equipped with a variety of different PRRs and TLR signalling was shown to maintain barrier function [104, 105]. In addition to initiating innate immune pathways, IECs have been described to express MHC class II [127–130], the critical molecule of APCs to activate adaptive immune cells in an antigen-specific manner. Multiple studies showed that siIECs constitutively express MHC class II [128, 130–134], while cIECs do not express MHC class II at steady state [340]. Inflammatory conditions upregulate MHC class II expression by IECs at both tissue sites and MHCII$^+$ IECs have been detected in immune-mediated disorders, such as IBD or GvHD [137, 138]. CD4 T cells reside within both the intestinal epithelium and the lamina propria and IECs have

been proposed to modulate antigen-specific CD4 T cell responses via MHC class II expression. However, it is currently not clear whether epithelial antigen presentation enhances Treg or Teff cell activity.

A critical feature of professional APCs is their ability to take up and process antigen, which will then be presented on MHC class II molecules to CD4 T cells. TCR engagement with the peptide:MHC class II complex presented by APCs will provide the first activating signal to CD4 T cells. Professional APCs further provide co-stimulatory or co-inhibitory signals, as well as cytokines, to CD4 T cells to either promote or inhibit their activation, differentiation and function. However, the intestinal mucosa mainly harbours activated CD4 T cells, which are less dependent on co-stimulatory signal for their re-activation. Therefore, IECs may not need to express co-stimulatory and/or co-inhibitory molecules in order to activate CD4 T cells via MHC class II and whether they do express co-stimulatory and co-inhibitory molecules is a matter of ongoing debate.

We identified that cIECs upregulate MHC class II expression in response to IFNγ signalling and that they are able to take up and process protein, thereby possessing important prerequisites to function as non-conventional APCs. In addition, we detected low expression of the co-inhibitory molecule PD-L1 by large intestinal IECs in *H. hepaticus* colonised mice, suggesting that IECs may be able to provide co-inhibitory signals to CD4 T cells. We further used different mouse models of colonic inflammation to investigate the role of cIEC antigen presentation in intestinal inflammation. We detected neither an aggravating nor ameliorating effect on disease severity during both acute and chronic intestinal inflammation. However, cIEC MHC class II expression might be important during the resolution of chronic inflammation.

As siIECs constitutively express MHC class II, we further wanted to understand whether antigen presentation by siIECs plays an important role in the maintenance of intestinal tolerance. The small intestinal epithelium hosts a variety of different

IEL subsets, which form an additional line of defence against invading pathogens and support barrier integrity. We detected the near loss of CD8$\alpha\alpha^+$ CD4$^+$ IELs in the ileal epithelial layer of MHC class II deficient mice, which was accompanied by an increase in conventional CD4 IELs, expressing increased proportions of RoRγt or FoxP3. However, the functional consequences of the loss of these CD8$\alpha\alpha^+$ CD4$^+$ IELs remain to be determined.

Additionally, multiple studies have reported that antigen presentation by IECs induces regulatory CD4 T cell responses [390, 391, 423, 424]. We therefore investigated the role of cIEC MHC class II expression in modulating Treg cell responses to maintain intestinal homeostasis. The *H. hepaticus* infection model of wild-type mice allows the investigation of Treg cell responses suppressing inflammatory immune responses towards *H. hepaticus* to maintain intestinal homeostasis during steady state [425]. We used the recently developed *H. hepaticus* TCR tg mouse model [318] to investigate the role of large intestinal IEC antigen presentation in modulating *H. hepaticus*-specific CD4 T cell responses. We did not block regulatory circuits in these experiments to be able to assess *H. hepaticus*-specific Treg cell responses. Using this model, we showed the induction of FoxP3 expression and IL-10 production by *H. hepaticus*-specific CD4 T cells in mice lacking cmIEC MHC class II expression compared to littermate controls during intestinal inflammation. In an experimental repeat with lower cmIEC MHC class II expression we did not detect these changes in FoxP3 expression or IL-10 production. So there appears to be an inverse relationship between IEC MHC class II expression and IL-10 and FoxP3 expression by *H. hepaticus*-specific CD4 T cells. Furthermore, we showed that large intestinal MHC class II expression correlates with PD-L1 expression. Our data highlights the importance of the tissue microenvironment, and most likely the tissue level of IFNγ, in supporting the expression of IEC MHC class II and thereby influencing the local niche of microbe-specific CD4 T cells and their effector functions.

To be able to control and manipulate the micro-environment of CD4 T cells interacting with MHCII$^+$ IECs we developed an *in vitro* co-culture system of colonic organoids and *H. hepaticus*-specific CD4 T cells. This allowed us to gain further insights into the modulation of CD4 T cell phenotype and function by cIEC MHC class II expression. Antigen specific activation of *H. hepaticus*-specific CD4 T cells resulted in the upregulation of PD-1 and facilitated the modulation of CD4 T cells into the Th1 and Th17 lineage, while FoxP3 expression was unchanged. In addition, it induced the production of the effector cytokines IFNγ, IL-17A and TNFα by *H. hepaticus*-specific CD4 T cells. These data show that IECs can function as non-conventional APC in an *in vitro* setting and that epithelial antigen presentation modulates microbe-specific CD4 Teff cell phenotypes and functions.

Future studies could investigate how the cross-talk of CD4 T cells with antigen presenting IECs re-establishes and maintains intestinal homeostasis in the large intestine. Single-cell RNA sequencing analysis of the large intestine could provide further insights into changes of ISC differentiation in response to different CD4 T cell effector cytokines, potentially validating data obtained from the small intestine where IL-10 supported the ISC niche, while IFNγ or IL-17A supported ISC differentiation [318]. In addition, this could provide information about which large intestinal IEC subset is expressing MHC class II and whether loss of epithelial antigen presentation leads to the loss and/or expansion of a distinct IEC subset. It could further provide information about changes in the transcriptomic profile of CD4 T cells caused by the absence of IEC MHC class II expression and whether their TCR specificity is shaped by epithelial antigen presentation. This data would allow future studies to tailor their inflammatory conditions in a way that best supports the functional analysis of epithelial antigen presentation in maintaining intestinal homeostasis.

IEC MHC class II "inducing" and "suppressing" bacteria have been described [377] and MHC class II "inducing" bacteria, such as Proteobacteria, have been associated with a dysregulated microbiome in IBD patients [426]. In addition, HFD has been

associated with a reduction in siIEC MHC class II expression [372, 377], which was accompanied by the loss of IL-10 production of $CD4^+$ IELs [372]. In our study, we detected MHC class II expression by large intestinal IECs in *H. hepaticus* colonised mice. These results suggest, that the microbiota influences epithelial antigen presentation either through direct interactions or indirectly through nutritional supply or by activating other immune cells in the mucosa. Future studies could investigate the underlying mechanisms of microbial and food antigens in inducing epithelial MHC class II expression and how these processes influence disease severity.

In addition, antigen recognition by CD4 T cells is a critical mechanism of the adaptive immune system to initiate anti-tumour immunity [427]. Many tumours have been described to actively down-regulate antigen presentation pathways to evade the recognition by the adaptive immune response and this has been associated with poor prognosis [428, 429]. Future studies could investigate the role of epithelial antigen presentation in the initiation of intestinal tumourigenesis. Indeed, previous studies detected more intestinal tumours in mice lacking the tumour suppressor gene *Apc* and MHC class II expression in $Lgr5^+$ ISC than in MHC class II expressing littermate controls [377]. These data suggest that epithelial antigen presentation might be important in controlling anti-tumour responses, as loss of epithelial MHC class II expression appears to promote tumour initiation in a genetically susceptible setting. How microbial and/or dietary composition mediate the expression of MHC class II expression by IECs and thereby influence tumour initiation needs to be further investigated. It is possible that CD4 Teff responses are involved and that epithelial antigen presentation plays a supporting function in mediating their effector functions.

References

[1] Cornelia Heuberger, Johanna Pott, and Kevin Joseph Maloy. "Why do intestinal epithelial cells express MHC class II?" In: *Immunology* 162.4 (Apr. 2021), pp. 357–367.

[2] Rao JN, Wang JY., and San Rafael. "Intestinal Architecture and Development". In: *Regulation of Gastrointestinal Mucosal Growth.* (2010), pp. 1–5.

[3] Allan M. Mowat and William W. Agace. "Regional specialization within the intestinal immune system". In: *Nature Reviews Immunology* 14.10 (Oct. 2014), pp. 667–685.

[4] Ruth E. Ley, Daniel A. Peterson, and Jeffrey I. Gordon. "Ecological and evolutionary forces shaping microbial diversity in the human intestine". In: *Cell* 124.4 (Feb. 2006), pp. 837–848.

[5] Steven R. Gill et al. "Metagenomic analysis of the human distal gut microbiome". In: *Science* 312.5778 (June 2006), pp. 1355–1359.

[6] June L. Round and Sarkis K. Mazmanian. "The gut microbiota shapes intestinal immune responses during health and disease". In: *Nature Reviews Immunology* 9.5 (May 2009), pp. 313–323.

[7] Yasmine Belkaid and Timothy W. Hand. "Role of the microbiota in immunity and inflammation". In: *Cell* 157.1 (Mar. 2014), pp. 121–141.

[8] Roberta Caruso, Bernard C. Lo, and Gabriel Núñez. "Host–microbiota interactions in inflammatory bowel disease". In: *Nature Reviews Immunology* 20.7 (July 2020), pp. 411–426.

[9] Alina Janney, Fiona Powrie, and Elizabeth H. Mann. "Host–microbiota maladaptation in colorectal cancer". In: *Nature* 585.7826 (Sept. 2020), pp. 509–517.

[10] Peter J. Turnbaugh et al. "An obesity-associated gut microbiome with increased capacity for energy harvest". In: *Nature* 444.7122 (Dec. 2006), pp. 1027–1031.

[11] Arthur Kaser, Sebastian Zeissig, and Richard S. Blumberg. "Inflammatory bowel disease". In: *Annual Review of Immunology* 28 (Apr. 2010), pp. 573–621.

[12] Clara Abraham and Judy H Cho. "Mechanisms of Disease: Inflammatory Bowel Diseases". In: *New England Journal of Medicine* 361.21 (2009), pp. 2066–78.

[13] Barbara A. Hendrickson, Ranjana Gokhale, and Judy H. Cho. "Clinical aspects and pathophysiology of inflammatory bowel disease". In: *Clinical Microbiology Reviews* 15.1 (2002), pp. 79–94.

[14] Dominic King et al. "Changing patterns in the epidemiology and outcomes of inflammatory bowel disease in the United Kingdom: 2000-2018". In: *Alimentary Pharmacology and Therapeutics* 51.10 (May 2020), pp. 922–934.

[15] Heitor S.P. De Souza and Claudio Fiocchi. “Immunopathogenesis of IBD: Current state of the art”. In: *Nature Reviews Gastroenterology and Hepatology* 13.1 (Jan. 2016), pp. 13–27.

[16] T R Mosmann et al. “Two types of murine helper T cell clone. I. Definition according to profiles of lymphokine activities and secreted proteins.” In: *Journal of immunology (Baltimore, Md. : 1950)* 136.7 (1986), pp. 2348–57.

[17] Paola Parronchi et al. “Type 1 T-helper cell predominance and lnterleukin-12 expression in the gut of patients with Crohn’s disease”. In: *American Journal of Pathology* 150.3 (1997), pp. 823–832.

[18] I J Fuss et al. “Disparate CD4+ lamina propria (LP) lymphokine secretion profiles in inflammatory bowel disease. Crohn’s disease LP cells manifest increased secretion of IFN-gamma, whereas ulcerative colitis LP cells manifest increased secretion of IL-5.” In: *Journal of immunology (Baltimore, Md. : 1950)* 157.3 (1996), pp. 1261–70.

[19] Frank Heller et al. “Interleukin-13 Is the Key Effector Th2 Cytokine in Ulcerative Colitis That Affects Epithelial Tight Junctions, Apoptosis, and Cell Restitution”. In: *Gastroenterology* 129.2 (Aug. 2005), pp. 550–564.

[20] Shigeo Inoue et al. “Characterization of cytokine expression in the rectal mucosa of ulcerative colitis: Correlation with disease activity”. In: *American Journal of Gastroenterology* 94.9 (Sept. 1999), pp. 2441–2446.

[21] S. Fujino et al. “Increased expression of interleukin 17 in inflammatory bowel disease”. In: *Gut* 52.1 (Jan. 2003), pp. 65–70.

[22] Ole Haagen Nielsen et al. “Upregulation of interleukin-12 and -17 in active inflammatory bowel disease”. In: *Scandinavian Journal of Gastroenterology* 38.2 (Feb. 2003), pp. 180–185.

[23] Akira Andoh et al. “Interleukin-22, a member of the IL-10 subfamily, induces inflammatory responses in colonic subepithelial myofibroblasts”. In: *Gastroenterology* 129.3 (2005), pp. 969–984.

[24] T. Kobayashi et al. “IL23 differentially regulates the Th1/Th17 balance in ulcerative colitis and Crohn’s disease”. In: *Gut* 57.12 (Dec. 2008), pp. 1682–1689.

[25] Marika C. Kullberg et al. “IL-23 plays a key role in Helicobacter hepaticus-induced T cell-dependent colitis”. In: *Journal of Experimental Medicine* 203.11 (Oct. 2006), pp. 2485–2494.

[26] Sophie Hue et al. “Interleukin-23 drives innate and T cell-mediated intestinal inflammation”. In: *Journal of Experimental Medicine* 203.11 (Oct. 2006), pp. 2473–2483.

[27] Charles O. Elson et al. “Monoclonal Anti-Interleukin 23 Reverses Active Colitis in a T Cell-Mediated Model in Mice”. In: *Gastroenterology* 132.7 (June 2007), pp. 2359–2370.

[28] Philip J. Morrissey et al. “CD4+ T cells that express high levels of CD45RB induce wasting disease when transferred into congenic severe combined immunodeficient mice. disease development is prevented by cotransfer of purified CD4+ T Cells”. In: *Journal of Experimental Medicine* 178.1 (July 1993), pp. 237–244.

[29] Fiona Powrie et al. “Phenotypically distinct subsets of cd4+t cells induce or protect from chronic intestinal inflammation in c. B-17 scid mice”. In: *International Immunology* 5.11 (Nov. 1993), pp. 1461–1471.

[30] Fiona Powrie et al. “Regulatory Interactions between CD45RBhigh and CD45RBlow CD4 + T Cells are important for the balance between protective and pathogenic cell-mediated immunity”. In: *Journal of Experimental Medicine* 179.2 (Feb. 1994), pp. 589–600.

[31] Christian Mottet, Holm H. Uhlig, and Fiona Powrie. “Cutting Edge: Cure of Colitis by CD4 + CD25 + Regulatory T Cells”. In: *The Journal of Immunology* 170.8 (Apr. 2003), pp. 3939–3943.

[32] Alexander Swidsinski et al. “Spatial organization and composition of the mucosal flora in patients with inflammatory bowel disease”. In: *Journal of Clinical Microbiology* 43.7 (July 2005), pp. 3380–3389.

[33] Daniel N. Frank et al. “Molecular-phylogenetic characterization of microbial community imbalances in human inflammatory bowel diseases”. In: *Proceedings of the National Academy of Sciences of the United States of America* 104.34 (Aug. 2007), pp. 13780–13785.

[34] Uri Gophna et al. “Differences between tissue-associated intestinal microfloras of patients with Crohn’s disease and ulcerative colitis”. In: *Journal of Clinical Microbiology* 44.11 (Nov. 2006), pp. 4136–4141.

[35] Warren Strober, Ivan J. Fuss, and Richard S. Blumberg. “The immunology of mucosal models of inflammation”. In: *Annual Review of Immunology* 20 (2002), pp. 495–549.

[36] Wendy S. Garrett et al. “Enterobacteriaceae Act in concert with the gut microbiota to induce spontaneous and maternally transmitted colitis”. In: *Cell Host and Microbe* 8.3 (Sept. 2010), pp. 292–300.

[37] Aurélie Couturier-Maillard et al. “NOD2-mediated dysbiosis predisposes mice to transmissible colitis and colorectal cancer”. In: *Journal of Clinical Investigation* 123.2 (Feb. 2013), pp. 700–711.

[38] Monika Schaubeck et al. “Dysbiotic gut microbiota causes transmissible Crohn’s disease-like ileitis independent of failure in antimicrobial defence”. In: *Gut* 65.2 (Feb. 2016), pp. 225–237.

[39] R. K. Russell and J. Satsangi. “IBD: A family affair”. In: *Best Practice and Research: Clinical Gastroenterology* 18.3 (June 2004), pp. 525–539.

[40] Bernard Khor, Agnès Gardet, and Ramnik J. Xavier. “Genetics and pathogenesis of inflammatory bowel disease”. In: *Nature* 474.7351 (June 2011), pp. 307–317.

[41] Daniel B. Graham and Ramnik J. Xavier. “Pathway paradigms revealed from the genetics of inflammatory bowel disease”. In: *Nature* 578.7796 (Feb. 2020), pp. 527–539.

[42] Richard H. Duerr et al. “A genome-wide association study identifies IL23R as an inflammatory bowel disease gene”. In: *Science* 314.5804 (Dec. 2006), pp. 1461–1463.

[43] Erik-Oliver Glocker et al. “Inflammatory Bowel Disease and Mutations Affecting the Interleukin-10 Receptor”. In: *New England Journal of Medicine* 361.21 (Nov. 2009), pp. 2033–2045.

[44] Brian G. Feagan et al. “A Comparison of Methotrexate with Placebo for the Maintenance of Remission in Crohn’s Disease”. In: *New England Journal of Medicine* 342.22 (June 2000), pp. 1627–1632.

[45] Daniel Rachmilewitz et al. “Infliximab, Azathioprine, or Combination Therapy for Crohn’s Disease”. In: *New England Journal of Medicine* 362.15 (Apr. 2013), pp. 1383–1395.

[46] Stephen B. Hanauer et al. “Maintenance infliximab for Crohn’s disease: The ACCENT I randomised trial”. In: *Lancet* 359.9317 (May 2002), pp. 1541–1549.

[47] D. B. Schauer and S. Falkow. “Attaching and effacing locus of a Citrobacter freundii biotype that causes transmissible murine colonic hyperplasia”. In: *Infection and Immunity* 61.6 (1993), pp. 2486–2492.

[48] Siouxsie Wiles et al. “Organ specificity, colonization and clearance dynamics in vivo following oral challenges with the murine pathogen Citrobacter rodentium”. In: *Cellular Microbiology* 6.10 (Oct. 2004), pp. 963–972.

[49] Rosanna Mundy et al. “Citrobacter rodentium of mice and man”. In: *Cellular Microbiology* 7.12 (Dec. 2005), pp. 1697–1706.

[50] Caroline Mullineaux-Sanders et al. “Citrobacter rodentium–host–microbiota interactions: immunity, bioenergetics and metabolism”. In: *Nature Reviews Microbiology* 17.11 (Nov. 2019), pp. 701–715.

[51] James W. Collins et al. “Citrobacter rodentium: Infection, inflammation and the microbiota”. In: *Nature Reviews Microbiology* 12.9 (Aug. 2014), pp. 612–623.

[52] Wanyin Deng et al. “Dissecting virulence: Systematic and functional analyses of a pathogenicity island”. In: *Proceedings of the National Academy of Sciences of the United States of America* 101.10 (Mar. 2004), pp. 3597–3602.

[53] Valerie F. Crepin et al. “Citrobacter rodentium mouse model of bacterial infection”. In: *Nature Protocols* 11.10 (Oct. 2016), pp. 1851–1876.

[54] Lisa M. Higgins et al. “Citrobacter rodentium infection in mice elicits a mucosal Th1 cytokine response and lesions similar to those in murine inflammatory bowel disease”. In: *Infection and Immunity* 67.6 (1999), pp. 3031–3039.

[55] S W Barthold et al. “Transmissible Murine Colonic Hyperplasia”. In: *Veterinary Pathology* 15.2 (1978), pp. 223–236.

[56] S. A. Luperchio et al. “Citrobacter rodentium, the causative agent of transmissible murine colonic hyperplasia, exhibits clonality: Synonymy of C. rodentium and mouse-pathogenic Escherichia coli”. In: *Journal of Clinical Microbiology* 38.12 (2000), pp. 4343–4350.

[57] Bruce A. Vallance et al. “Mice lacking T and B lymphocytes develop transient colitis and crypt hyperplasia yet suffer impaired bacterial clearance during Citrobacter rodentium infection”. In: *Infection and Immunity* 70.4 (2002), pp. 2070–2081.

[58] Cameron P. Simmons et al. “Central role for B lymphocytes and CD4+ T cells in immunity to infection by the attaching and effacing pathogen Citrobacter rodentium”. In: *Infection and Immunity* 71.9 (Sept. 2003), pp. 5077–5086.

[59] Christian Maaser et al. “Clearance of Citrobacter rodentium requires B cells but not secretory immunoglobulin A (IgA) or IgM antibodies”. In: *Infection and Immunity* 72.6 (June 2004), pp. 3315–3324.

[60] Sarah L. Lebeis et al. “TLR Signaling Mediated by MyD88 Is Required for a Protective Innate Immune Response by Neutrophils to Citrobacter rodentium”. In: *The Journal of Immunology* 179.1 (July 2007), pp. 566–577.

[61] Paul R. Mangan et al. “Transforming growth factor-β induces development of the T H17 lineage”. In: *Nature* 441.7090 (May 2006), pp. 231–234.

[62] Yan Zheng et al. “Interleukin-22 mediates early host defense against attaching and effacing bacterial pathogens”. In: *Nature Medicine* 14.3 (Mar. 2008), pp. 282–289.

[63] Claudia Lupp et al. “Host-Mediated Inflammation Disrupts the Intestinal Microbiota and Promotes the Overgrowth of Enterobacteriaceae”. In: *Cell Host and Microbe* 2.3 (Sept. 2007), p. 204.

[64] Christian Hoffmann et al. “Community-wide response of the gut microbiota to enteropathogenic Citrobacter rodentium infection revealed by deep sequencing”. In: *Infection and Immunity* 77.10 (Oct. 2009), pp. 4668–4678.

[65] Ivaylo I. Ivanov et al. “Induction of Intestinal Th17 Cells by Segmented Filamentous Bacteria”. In: *Cell* 139.3 (Oct. 2009), pp. 485–498.

[66] J. G. Fox et al. “Helicobacter hepaticus sp. nov., a microaerophilic bacterium isolated from livers and intestinal mucosal scrapings from mice”. In: *Journal of Clinical Microbiology* 32.5 (1994), pp. 1238–1245.

[67] Jerrold M. Ward et al. “Chronic active hepatitis and associated liver tumors in mice caused by a presistent bacterial infection with a novel Helicobacter Species”. In: *Journal of the National Cancer Institute* 86.16 (Aug. 1994), pp. 1222–1227.

[68] Jerrold M. Ward et al. “Inflammatory Large Bowel Disease in Immunodeficient Mice Naturally Infected with Helicobacter hepaticus”. In: *Laboratory Animal Science* 46.1 (Feb. 1996), pp. 15–20.

[69] Charmaine J Foltz et al. “Spontaneous inflammatory bowel disease in multiple mutant mouse lines: Association with colonization by Helicobacter hepaticus”. In: *Helicobacter* 3.2 (1998), pp. 69–78.

[70] Marika C. Kullberg et al. “Helicobacter hepaticus triggers colitis in specific-pathogen-free interleukin-10 (IL-10)-deficient mice through an IL-12-and gamma interferon- dependent mechanism”. In: *Infection and Immunity* 66.11 (1998), pp. 5157–5166.

[71] Andrew Burich et al. “Helicobacter-induced inflammatory bowel disease in IL-10- and T cell-deficient mice”. In: *American Journal of Physiology - Gastrointestinal and Liver Physiology* 281.3 44-3 (Sept. 2001), G764–G778.

[72] M. C. Kullberg et al. “Helicobacter hepaticus-induced colitis in interleukin-10-deficient mice: Cytokine requirements for the induction and maintenance of intestinal inflammation”. In: *Infection and Immunity* 69.7 (2001), pp. 4232–4241.

[73] David Yen et al. “IL-23 is essential for T cell-mediated colitis and promotes inflammation via IL-17 and IL-6”. In: *Journal of Clinical Investigation* 116.5 (May 2006), pp. 1310–1316.

[74] I. C. Arnold et al. “CD11c+ monocyte/macrophages promote chronic Helicobacter hepaticus-induced intestinal inflammation through the production of IL-23”. In: *Mucosal Immunology* 9.2 (Mar. 2016), pp. 352–363.

[75] Claire L. Langrish et al. “IL-12 and IL-23: Master regulators of innate and adaptive immunity”. In: *Immunological Reviews* 202.1 (Dec. 2004), pp. 96–105.

[76] Marika C. Kullberg et al. “Bacteria-triggered CD4+ T regulatory cells suppress Helicobacter hepaticus-induced colitis”. In: *Journal of Experimental Medicine* 196.4 (Aug. 2002), pp. 505–515.

[77] Hamed Laroui et al. “Dextran sodium sulfate (DSS) induces colitis in mice by forming nano-lipocomplexes with medium-chain-length fatty acids in the colon”. In: *PLoS ONE* 7.3 (Mar. 2012). Ed. by Jan-Hendrik Niess, e32084.

[78] Isao Okayasu et al. “A novel method in the induction of reliable experimental acute and chronic ulcerative colitis in mice”. In: *Gastroenterology* 98.3 (1990), pp. 694–702.

[79] Stefan Wirtz et al. “Chemically induced mouse models of intestinal inflammation”. In: *Nature Protocols* 2.3 (Mar. 2007), pp. 541–546.

[80] Martina Perše and Anton Cerar. “Dextran sodium sulphate colitis mouse model: Traps and tricks”. In: *Journal of Biomedicine and Biotechnology* 2012 (2012).

[81] Levinus A. Dieleman et al. “Dextran sulfate sodium-induced colitis occurs in severe combined immunodeficient mice”. In: *Gastroenterology* 107.6 (Dec. 1994), pp. 1643–1652.

[82] Christian F. Krieglstein et al. “Collagen-binding integrin $\alpha 1\beta 1$ regulates intestinal inflammation in experimental colitis”. In: *Journal of Clinical Investigation* 110.12 (Dec. 2002), pp. 1773–1782.

[83] L. A. Dieleman et al. “Chronic experimental colitis induced by dextran sulphate sodium (DSS) is characterized by Th1 and Th2 cytokines”. In: *Clinical and Experimental Immunology* 114.3 (Dec. 1998), pp. 385–391.

[84] Nabeetha A. Nagalingam, John Y. Kao, and Vincent B. Young. “Microbial ecology of the murine gut associated with the development of dextran sodium sulfate-induced colitis”. In: *Inflammatory Bowel Diseases* 17.4 (Apr. 2011), pp. 917–926.

[85] Håkansson et al. “Immunological alteration and changes of gut microbiota after dextran sulfate sodium (DSS) administration in mice”. In: *Clinical and Experimental Medicine* 15.1 (Feb. 2015), pp. 107–120.

[86] J. N. Lieberkühn. “De Fabrica et Actione villorum intestinorum tenuium Hominis”. In: *Journal of Physiology and Biochemistry* 64.4 (2008), pp. 393–414.

[87] Adam L. Haber et al. “A single-cell survey of the small intestinal epithelium”. In: *Nature* 551.7680 (Nov. 2017), pp. 333–339.

[88] Yalong Wang et al. “Single-cell transcriptome analysis reveals differential nutrient absorption functions in human intestine”. In: *Journal of Experimental Medicine* 217.2 (Feb. 2020).

[89] Michael H. Ross and Wojciech. Pawlina. *Histology : a text and atlas : with correlated cell and molecular biology*. Wolters Kluwer/Lippincott Williams & Wilkins Health, 2011, p. 974.

[90] N. A. Mabbott et al. "Microfold (M) cells: Important immunosurveillance posts in the intestinal epithelium". In: *Mucosal Immunology* 6.4 (July 2013), pp. 666–677.

[91] Harvey Miller et al. "Intestinal M cells: The fallible sentinels?" In: *World Journal of Gastroenterology* 13.10 (Mar. 2007), pp. 1477–1486.

[92] Toshiro Sato et al. "Paneth cells constitute the niche for Lgr5 stem cells in intestinal crypts". In: *Nature* 469.7330 (Jan. 2011), pp. 415–418.

[93] M. Neutra and C. P. Leblond. "Synthesis of the carbohydrate of mucus in the golgi complex as shown by electron microscope radioautography of goblet cells from rats injected with glucose-H3." In: *The Journal of cell biology* 30.1 (July 1966), pp. 119–136.

[94] Malin E.V. Johansson and Gunnar C. Hansson. "Immunological aspects of intestinal mucus and mucins". In: *Nature Reviews Immunology* 16.10 (Oct. 2016), pp. 639–649.

[95] Jens Madsen et al. "Tissue localization of human trefoil factors 1, 2, and 3". In: *Journal of Histochemistry and Cytochemistry* 55.5 (May 2007), pp. 505–513.

[96] J. J. Worthington, F. Reimann, and F. M. Gribble. "Enteroendocrine cells-sensory sentinels of the intestinal environment and orchestrators of mucosal immunity". In: *Mucosal Immunology* 11.1 (Jan. 2018), pp. 3–20.

[97] François Gerbe et al. "Intestinal epithelial tuft cells initiate type 2 mucosal immunity to helminth parasites". In: *Nature* 529.7585 (Jan. 2016), pp. 226–230.

[98] Jakob Von Moltke et al. "Tuft-cell-derived IL-25 regulates an intestinal ILC2-epithelial response circuit". In: *Nature* 529.7585 (Jan. 2016), pp. 221–225.

[99] Alex Gregorieff et al. "Expression Pattern of Wnt Signaling Components in the Adult Intestine". In: *Gastroenterology* 129.2 (Aug. 2005), pp. 626–638.

[100] Henner F. Farin, Johan H. Van Es, and Hans Clevers. "Redundant sources of Wnt regulate intestinal stem cells and promote formation of paneth cells". In: *Gastroenterology* 143.6 (Dec. 2012), 1518–1529.e7.

[101] Michael E. Rothenberg et al. "Identification of a cKit+ colonic crypt base secretory cell that supports Lgr5+ stem cells in mice". In: *Gastroenterology* 142.5 (May 2012), 1195–1205.e6.

[102] Nobuo Sasaki et al. "Reg4+ deep crypt secretory cells function as epithelial niche for Lgr5+ stem cells in colon". In: *Proceedings of the National Academy of Sciences of the United States of America* 113.37 (Sept. 2016), E5399–E5407.

[103] Charles A. Herring et al. "Unsupervised Trajectory Analysis of Single-Cell RNA-Seq and Imaging Data Reveals Alternative Tuft Cell Origins in the Gut". In: *Cell Systems* 6.1 (Jan. 2018), 37–51.e9.

[104] Juan F. Burgueño and Maria T. Abreu. "Epithelial Toll-like receptors and their role in gut homeostasis and disease". In: *Nature Reviews Gastroenterology and Hepatology* 17.5 (May 2020), pp. 263–278.

[105] Johanna Pott and Mathias Hornef. “Innate immune signalling at the intestinal epithelium in homeostasis and disease”. In: *EMBO reports* 13.8 (Aug. 2012), pp. 684–698.

[106] Sophie Chabot et al. “TLRs Regulate the Gatekeeping Functions of the Intestinal Follicle-Associated Epithelium”. In: *The Journal of Immunology* 176.7 (Apr. 2006), pp. 4275–4283.

[107] April E. Price et al. “A Map of Toll-like Receptor Expression in the Intestinal Epithelium Reveals Distinct Spatial, Cell Type-Specific, and Temporal Patterns”. In: *Immunity* 49.3 (Sept. 2018), 560–575.e6.

[108] Megan L. Stanifer et al. “Asymmetric distribution of TLR3 leads to a polarized immune response in human intestinal epithelial cells”. In: *Nature Microbiology* 5.1 (Jan. 2020), pp. 181–191.

[109] Michael R. Howitt et al. “Tuft cells, taste-chemosensory cells, orchestrate parasite type 2 immunity in the gut”. In: *Science* 351.6279 (Mar. 2016), pp. 1329–1333.

[110] Nick Barker. “Adult intestinal stem cells: Critical drivers of epithelial homeostasis and regeneration”. In: *Nature Reviews Molecular Cell Biology* 15.1 (Jan. 2014), pp. 19–33.

[111] Toshiro Sato et al. “Single Lgr5 stem cells build crypt-villus structures in vitro without a mesenchymal niche”. In: *Nature* 459.7244 (May 2009), pp. 262–265.

[112] Neil McCarthy, Judith Kraiczy, and Ramesh A. Shivdasani. “Cellular and molecular architecture of the intestinal stem cell niche”. In: *Nature Cell Biology* 22.9 (Sept. 2020), pp. 1033–1041.

[113] Shiro Yui et al. “Functional engraftment of colon epithelium expanded in vitro from a single adult Lgr5 + stem cell”. In: *Nature Medicine* 18.4 (Apr. 2012), pp. 618–623.

[114] Aneta Rogoz et al. “A 3-D enteroid-based model to study T-cell and epithelial cell interaction”. In: *Journal of Immunological Methods* 421 (June 2015), pp. 89–95.

[115] Kengo Nozaki et al. “Co-culture with intestinal epithelial organoids allows efficient expansion and motility analysis of intraepithelial lymphocytes”. In: *Journal of Gastroenterology* 51.3 (2016), pp. 206–213.

[116] Agnieszka Pastuła et al. “Three-Dimensional Gastrointestinal Organoid Culture in Combination with Nerves or Fibroblasts: A Method to Characterize the Gastrointestinal Stem Cell Niche”. In: *Stem Cells International* 2016 (2016).

[117] Devanjali Dutta, Inha Heo, and Hans Clevers. “Disease Modeling in Stem Cell-Derived 3D Organoid Systems”. In: *Trends in Molecular Medicine* 23.5 (May 2017), pp. 393–410.

[118] Peter Jung et al. “Isolation and in vitro expansion of human colonic stem cells”. In: *Nature Medicine* 17.10 (Oct. 2011), pp. 1225–1227.

[119] Nick Barker et al. “Lgr5+ve Stem Cells Drive Self-Renewal in the Stomach and Build Long-Lived Gastric Units In Vitro”. In: *Cell Stem Cell* 6.1 (Jan. 2010), pp. 25–36.

[120] Sylvia F. Boj et al. “Organoid models of human and mouse ductal pancreatic cancer”. In: *Cell* 160.1-2 (Jan. 2015), pp. 324–338.

[121] Meritxell Huch et al. “In vitro expansion of single Lgr5 + liver stem cells induced by Wnt-driven regeneration”. In: *Nature* 494.7436 (Feb. 2013), pp. 247–250.

[122] Meritxell Huch et al. “Long-term culture of genome-stable bipotent stem cells from adult human liver”. In: *Cell* 160.1-2 (Jan. 2015), pp. 299–312.

[123] Marc Van De Wetering et al. “Prospective derivation of a living organoid biobank of colorectal cancer patients”. In: *Cell* 161.4 (May 2015), pp. 933–945.

[124] Georgios Vlachogiannis et al. “Patient-derived organoids model treatment response of metastatic gastrointestinal cancers”. In: *Science* 359.6378 (Feb. 2018), pp. 920–926.

[125] Johanna F. Dekkers et al. “Characterizing responses to CFTR-modulating drugs using rectal organoids derived from subjects with cystic fibrosis”. In: *Science Translational Medicine* 8.344 (June 2016).

[126] Masayuki Fujii, Hans Clevers, and Toshiro Sato. “Modeling Human Digestive Diseases With CRISPR-Cas9–Modified Organoids”. In: *Gastroenterology* 156.3 (Feb. 2019), pp. 562–576.

[127] Klas Wiman et al. “Occurrence of Ia antigens on tissues of non-lymphoid origin”. In: *Nature* 276.5689 (1978), pp. 711–713.

[128] H. Scott et al. “HLA-DR-like Antigens in the Epithelium of the Human Small Intestine”. In: *Scandinavian Journal of Immunology* 12.1 (July 1980), pp. 77–82.

[129] Earl L. Parr and Ian F.C. McKenzie. “Demonstration of Ia antigens on mouse intestinal epithelial cells by immunoferritin labeling”. In: *Immunogenetics* 8.1 (Dec. 1979), pp. 499–508.

[130] L. Madrigal et al. “Flow cytometric analysis of surface major histocompatibility complex class II expression on human epithelial cells prepared from small intestinal biopsies”. In: *Journal of Immunological Methods* 158.2 (Feb. 1993), pp. 207–214.

[131] J. Kelly, D. G. Weir, and C. Feighery. “Differential expression of HLA-D gene products in the normal and coeliac small bowel”. In: *Tissue Antigens* 31.3 (Mar. 1988), pp. 151–160.

[132] Brendan Byrne et al. “Human duodenal epithelial cells constitutively express molecular components of antigen presentation but not costimulatory molecules”. In: *Human Immunology* 63.11 (Nov. 2002), pp. 977–986.

[133] Gheorghe Hundorfean et al. “Luminal antigens access late endosomes of intestinal epithelial cells enriched in MHC I and MHC II molecules: in vivo study in Crohn’s ileitis”. In: *American Journal of Physiology-Gastrointestinal and Liver Physiology* 293.4 (Oct. 2007), G798–G808.

[134] Moshe Biton et al. “T Helper Cell Cytokines Modulate Intestinal Stem Cell Renewal and Differentiation”. In: *Cell* 175.5 (Nov. 2018), 1307–1320.e22.

[135] Ichiro Hirata et al. “Immunoelectron microscopic localization of HLA-DR antigen in control small intestine and colon and in inflammatory bowel disease”. In: *Digestive Diseases and Sciences* 31.12 (Dec. 1986), pp. 1317–1330.

[136] Iris Dotan et al. “Intestinal epithelial cells from inflammatory bowel disease patients preferentially stimulate CD4+ T cells to proliferate and secrete interferon-γ”. In: *American Journal of Physiology - Gastrointestinal and Liver Physiology* 292.6 (June 2007), G1630–G1640.

[137] Motoko Koyama et al. “MHC Class II Antigen Presentation by the Intestinal Epithelium Initiates Graft-versus-Host Disease and Is Influenced by the Microbiota”. In: *Immunity* 51.5 (Nov. 2019), 885–898.e7.

[138] Christopher S. Smillie et al. “Intra- and Inter-cellular Rewiring of the Human Colon during Ulcerative Colitis”. In: *Cell* 178.3 (July 2019), 714–730.e22.

[139] Robert M. Hershberg et al. “Intestinal epithelial cells use two distinct pathways for HLA class II antigen processing”. In: *Journal of Clinical Investigation* 100.1 (July 1997), pp. 204–215.

[140] Robert M. Hershberg et al. “Highly polarized HLA class II antigen processing and presentation by human intestinal epithelial cells”. In: *Journal of Clinical Investigation* 102.4 (Aug. 1998), pp. 792–803.

[141] Satoshi Matsumoto, Hiromi Setoyama, and Yoshimori Umesaki. “Differential induction of major histocompatibility complex molecules on mouse intestine by bacterial colonization”. In: *Gastroenterology* 103.6 (Dec. 1992), pp. 1777–1782.

[142] S. Fais et al. “Gliadin induced changes in the expression of MHC-class II antigens by human small intestinal epithelium. Organ culture studies with coeliac disease mucosa”. In: *Gut* 33.4 (Apr. 1992), pp. 472–475.

[143] K. P. Zimmer et al. “Translocation of gliadin into HLA-DR antigen containing lysosomes in coeliac disease enterocytes”. In: *Gut* 36.5 (May 1995), pp. 703–709.

[144] F. Arnaud-Battandier et al. “Increased HLA-DR Expression by Enterocytes in Children With Celiac Disease”. In: *Gastroenterology* 91.5 (Nov. 1986), pp. 1206–1212.

[145] G Mayrhofer and L D Spargo. “Distribution of class II major histocompatibility antigens in enterocytes of the rat jejunum and their association with organelles of the endocytic pathway.” In: *Immunology* 70.1 (May 1990), pp. 11–9.

[146] Robert C. Piper and David J. Katzmann. “Biogenesis and function of multivesicular bodies”. In: *Annual Review of Cell and Developmental Biology* 23.1 (Nov. 2007), pp. 519–547.

[147] F. Bär et al. “Inflammatory bowel diseases influence major histocompatibility complex class I (MHC I) and II compartments in intestinal epithelial cells”. In: *Clinical & Experimental Immunology* 172.2 (May 2013), pp. 280–289.

[148] Jonathan E. Wosen et al. “Human intestinal enteroids model MHC-II in the gut epithelium”. In: *Frontiers in Immunology* 10.AUG (Aug. 2019), p. 1970.

[149] P. A. Roche and P. Cresswell. “Proteolysis of the class II-associated invariant chain generates a peptide binding site in intracellular HLA-DR molecules”. In: *Proceedings of the National Academy of Sciences of the United States of America* 88.8 (Apr. 1991), pp. 3150–3154.

[150] C A Lamb and P Cresswell. “Assembly and transport properties of invariant chain trimers and HLA-DR- invariant chain complexes”. In: *Journal of Immunology* 148.11 (June 1992), pp. 3478–3482.

[151] J. S. Blum and P. Cresswell. "Role for intracellular proteases in the processing and transport of class II HLA antigens". In: *Proceedings of the National Academy of Sciences of the United States of America* 85.11 (June 1988), pp. 3975–3979.

[152] Melanie A. Sherman, Dominique A. Weber, and Peter E. Jensen. "DM enhances peptide binding to class II MHC by release of invariant chain-derived peptide". In: *Immunity* 3.2 (Aug. 1995), pp. 197–205.

[153] Lisa K. Denzin and Peter Cresswell. "HLA-DM induces clip dissociation from MHC class II $\alpha\beta$ dimers and facilitates peptide loading". In: *Cell* 82.1 (July 1995), pp. 155–165.

[154] Victor S. Sloan et al. "Mediation by HLA-DM of dissociation of peptides from HLA-DR". In: *Nature* 375.6534 (1995), pp. 802–806.

[155] Jörn Dengjel et al. "Autophagy promotes MHC class II presentation of peptides from intracellular source proteins". In: *Proceedings of the National Academy of Sciences of the United States of America* 102.22 (May 2005), pp. 7922–7927.

[156] Delu Zhou et al. "Lamp-2a facilitates MHC class II presentation of cytoplasmic antigens". In: *Immunity* 22.5 (May 2005), pp. 571–581.

[157] Casper Paludan et al. "Endogenous MHC class II processing of a viral nuclear antigen after autophagy". In: *Science* 307.5709 (Jan. 2005), pp. 593–596.

[158] Leonia Bozzacco et al. "Mass spectrometry analysis and quantitation of peptides presented on the MHC II molecules of mouse spleen dendritic cells". In: *Journal of Proteome Research* 10.11 (Nov. 2011), pp. 5016–5030.

[159] Roman M. Chicz et al. "Specificity and promiscuity among naturally processed peptides bound to HLA-DR alleles". In: *Journal of Experimental Medicine* 178.1 (July 1993), pp. 27–47.

[160] Paul A. Roche and Kazuyuki Furuta. "The ins and outs of MHC class II-mediated antigen processing and presentation". In: *Nature Reviews Immunology* 15.4 (Mar. 2015), pp. 203–216.

[161] Domenico Tortorella et al. "Viral subversion of the immune system". In: *Annual Review of Immunology* 18 (Nov. 2000), pp. 861–926.

[162] Kenneth P. Murphy. *Janeway's Immunobiology*. 8th editio. Garland Science, 2012.

[163] Walter Reith and Bernard Mach. "The bare lymphocyte syndrome and the regulation of MHC expression". In: *Annual Review of Immunology* 19.1 (Apr. 2001), pp. 331–373.

[164] Lieping Chen and Dallas B. Flies. "Molecular mechanisms of T cell co-stimulation and co-inhibition". In: *Nature Reviews Immunology* 13.4 (Apr. 2013), pp. 227–242.

[165] A. Nakazawa et al. "Functional expression of costimulatory molecule CD86 on epithelial cells in the inflamed colonic mucosa". In: *Gastroenterology* 117.3 (Sept. 1999), pp. 536–545.

[166] I R Sanderson et al. "Differential regulation of B7 mRNA in enterocytes and lymphoid cells." In: *Immunology* 79.3 (July 1993), pp. 434–8.

[167] Frauke Borcherding et al. "The CD40-CD40L Pathway contributes to the proinflammatory function of intestinal epithelial cells in inflammatory bowel disease". In: *American Journal of Pathology* 176.4 (Apr. 2010), pp. 1816–1827.

[168] S. Bloom, D. Simmons, and D. P. Jewell. "Adhesion molecules intercellular adhesion molecule-1 (ICAM-1), ICAM-3 and B7 are not expressed by epithelium in normal or inflamed colon". In: *Clinical and Experimental Immunology* 101.1 (June 1995), pp. 157–163.

[169] Atsushi Nakazawa et al. "The Expression and Function of Costimulatory Molecules B7h and B7-H1 on Colonic Epithelial Cells". In: *Gastroenterology* 126.5 (May 2004), pp. 1347–1357.

[170] M Croft, L M Bradley, and S L Swain. "Naive versus memory CD4 T cell response to antigen. Memory cells are less dependent on accessory cell costimulation and can respond to many antigen-presenting cell types including resting B cells." In: *Journal of immunology (Baltimore, Md. : 1950)* 152.6 (Mar. 1994), pp. 2675–85.

[171] Phillip D. Smith, Richard S. Blumberg, and Thomas T. MacDonald. *Principles of Mucosal Immunology*. Garland Science, Apr. 2020.

[172] K W Beagley et al. "Differences in intraepithelial lymphocyte T cell subsets isolated from murine small versus large intestine." In: *Journal of immunology (Baltimore, Md. : 1950)* 154.11 (1995), pp. 5611–9.

[173] Craig L. Maynard and Casey T. Weaver. "Intestinal Effector T Cells in Health and Disease". In: *Immunity* 31.3 (Sept. 2009), pp. 389–400.

[174] Gerard E. Kaiko et al. "Immunological decision-making: How does the immune system decide to mount a helper T-cell response?" In: *Immunology* 123.3 (Mar. 2008), pp. 326–338.

[175] A. C. Mullen et al. "Role of T-bet in commitment of TH1 cells before IL-12-dependent selection". In: *Science* 292.5523 (June 2001), pp. 1907–1910.

[176] Maryam Afkarian et al. "T-bet is a STATI-induced regulator for IL-12R expression in naïve CD4+ T cells". In: *Nature Immunology* 3.6 (May 2002), pp. 549–557.

[177] Atsunobu Takeda et al. "Cutting Edge: Role of IL-27/WSX-1 Signaling for Induction of T-Bet Through Activation of STAT1 During Initial Th1 Commitment". In: *The Journal of Immunology* 170.10 (May 2003), pp. 4886–4890.

[178] Sadahiro Kamiya et al. "An Indispensable Role for STAT1 in IL-27-Induced T-bet Expression but Not Proliferation of Naive CD4 + T Cells". In: *The Journal of Immunology* 173.6 (Sept. 2004), pp. 3871–3877.

[179] Fiona Powrie et al. "Inhibition of Thl responses prevents inflammatory bowel disease in scid mice reconstituted with CD45RBhi CD4+ T cells". In: *Immunity* 1.7 (Oct. 1994), pp. 553–562.

[180] M. F. Neurath et al. "The transcription factor T-bet regulates mucosal T cell activation in experimental colitis and Crohn's disease". In: *Journal of Experimental Medicine* 195.9 (May 2002), pp. 1129–1143.

[181] Thomas Krausgruber et al. "T-bet is a key modulator of IL-23-driven pathogenic CD4 + T cell responses in the intestine". In: *Nature Communications* 7.1 (May 2016), pp. 1–12.

[182] Booki Min et al. "Basophils produce IL-4 and accumulate in tissues after infection with a Th2-inducing parasite". In: *Journal of Experimental Medicine* 200.4 (Aug. 2004), pp. 507–517.

[183] André Gessner, Katja Mohrs, and Markus Mohrs. "Mast Cells, Basophils, and Eosinophils Acquire Constitutive IL-4 and IL-13 Transcripts during Lineage Differentiation That Are Sufficient for Rapid Cytokine Production". In: *The Journal of Immunology* 174.2 (Jan. 2005), pp. 1063–1072.

[184] Jinzhao Hou et al. "An interleukin-4-induced transcription factor: IL-4 Stat". In: *Science* 265.5179 (1994), pp. 1701–1706.

[185] H. Takeda et al. "Essential role of Stat6 in IL-4 signalling". In: *Nature* 380.6575 (1996), pp. 627–630.

[186] H. Shimoda et al. "Lack of IL-4-induced Th2 response and IgE class switching in mice with disrupted Stat6 gene". In: *Nature* 380.6575 (1996), pp. 630–633.

[187] Mark H. Kaplan et al. "Stat6 is required for mediating responses to IL-4 and for the development of Th2 cells". In: *Immunity* 4.3 (Mar. 1996), pp. 313–319.

[188] Wei Ping Zheng and Richard A. Flavell. "The transcription factor GATA-3 is necessary and sufficient for Th2 cytokine gene expression in CD4 T cells". In: *Cell* 89.4 (May 1997), pp. 587–596.

[189] Dong Hong Zhang et al. "Transcription factor GATA-3 is differentially expressed in murine Th1 and Th2 cells and controls Th2-specific expression of the interleukin-5 gene". In: *Journal of Biological Chemistry* 272.34 (Aug. 1997), pp. 21597–21603.

[190] William C. Gause and David Artis. *The th2 type immune response in health and disease: From host defense and allergy to metabolic homeostasis and beyond*. 2015, pp. 1–172.

[191] Jinfang Zhu et al. "Conditional deletion of Gata3 shows its essential function in TH1-TH2 responses". In: *Nature Immunology* 5.11 (Nov. 2004), pp. 1157–1165.

[192] Takashi Usui et al. "GATA-3 suppresses Th1 development by downregulation of Stat4 and not through effects on IL-12Rβ2 chain or T-bet". In: *Immunity* 18.3 (Mar. 2003), pp. 415–428.

[193] Madeline M. Fort et al. "IL-25 Induces IL-4, IL-5, and IL-13 and Th2-associated pathologies in vivo". In: *Immunity* 15.6 (Dec. 2001), pp. 985–995.

[194] Tiffany A. Reese et al. "Chitin induces accumulation in tissue of innate immune cells associated with allergy". In: *Nature* 447.7140 (May 2007), pp. 92–96.

[195] Fred D. Finkelman et al. "Interleukin-4- and interleukin-13-mediated host protection against intestinal nematode parasites". In: *Immunological Reviews* 201.1 (Oct. 2004), pp. 139–155.

[196] Bali Pulendran and David Artis. "New paradigms in type 2 immunity". In: *Science* 337.6093 (July 2012), pp. 431–435.

[197] Kenneth M. Murphy and Steven L. Reiner. "The lineage decisions of helper T cells". In: *Nature Reviews Immunology* 2.12 (Dec. 2002), pp. 933–944.

[198] Catherine M. Evans and Richard G. Jenner. "Transcription factor interplay in t helper cell differentiation". In: *Briefings in Functional Genomics* 12.6 (Nov. 2013), pp. 499–511.

[199] Wenjun Ouyang et al. “Inhibition of Th1 development mediated by GATA-3 through an IL-4- independent mechanism”. In: *Immunity* 9.5 (Nov. 1998), pp. 745–755.

[200] Ryoji Yagi et al. “The Transcription Factor GATA3 Actively Represses RUNX3 Protein-Regulated Production of Interferon-γ”. In: *Immunity* 32.4 (Apr. 2010), pp. 507–517.

[201] Susetta Finotto et al. “Development of spontaneous airway changes consistent with human asthma in mice lacking T-bet”. In: *Science* 295.5553 (Jan. 2002), pp. 336–338.

[202] Luisa Camoglio et al. “Altered expression of interferon-γ and interleukin-4 in inflammatory bowel disease”. In: *Inflammatory Bowel Diseases* 4.4 (1998), pp. 285–290.

[203] Tomomasa Kakazu and Junichi Hara. “Type 1 T-helper cell predominance in granulomas of Crohn’s disease”. In: *American Journal of Gastroenterology* 94.8 (Aug. 1999), pp. 2149–2155.

[204] Kiyotaka Ohtani et al. “Increased mucosal expression of GATA-3 and STAT-4 in pediatric ulcerative colitis”. In: *Pediatrics International* 52.4 (Aug. 2010), pp. 584–589.

[205] Ji Li et al. “Profiles of Lamina Propria T Helper Cell Subsets Discriminate between Ulcerative Colitis and Crohn’s Disease”. In: *Inflammatory Bowel Diseases* 22.8 (May 2016), pp. 1779–1792.

[206] Anne Brüstle et al. “The development of inflammatory TH-17 cells requires interferon-regulatory factor 4”. In: *Nature Immunology* 8.9 (Sept. 2007), pp. 958–966.

[207] Francisco J. Quintana et al. “Control of Treg and TH17 cell differentiation by the aryl hydrocarbon receptor”. In: *Nature* 453.7191 (May 2008), pp. 65–71.

[208] Barbara U. Schraml et al. “The AP-1 transcription factor Batf controls T H 17 differentiation”. In: *Nature* 460.7253 (July 2009), pp. 405–409.

[209] Marc Veldhoen et al. “The aryl hydrocarbon receptor links TH17-cell-mediated autoimmunity to environmental toxins”. In: *Nature* 453.7191 (May 2008), pp. 106–109.

[210] Xuexian O. Yang et al. “T Helper 17 Lineage Differentiation Is Programmed by Orphan Nuclear Receptors RORα and RORγ”. In: *Immunity* 28.1 (Jan. 2008), pp. 29–39.

[211] Heon Park et al. “A distinct lineage of CD4 T cells regulates tissue inflammation by producing interleukin 17”. In: *Nature Immunology* 6.11 (Nov. 2005), pp. 1133–1141.

[212] Laurie E. Harrington et al. “Interleukin 17-producing CD4+ effector T cells develop via a lineage distinct from the T helper type 1 and 2 lineages”. In: *Nature Immunology* 6.11 (Nov. 2005), pp. 1123–1132.

[213] Marc Veldhoen et al. “TGFβ in the context of an inflammatory cytokine milieu supports de novo differentiation of IL-17-producing T cells”. In: *Immunity* 24.2 (Feb. 2006), pp. 179–189.

[214] Yan Zheng et al. “Interleukin-22, a TH17 cytokine, mediates IL-23-induced dermal inflammation and acanthosis”. In: *Nature* 445.7128 (Feb. 2007), pp. 648–651.

[215] Liang Zhou et al. “IL-6 programs TH-17 cell differentiation by promoting sequential engagement of the IL-21 and IL-23 pathways”. In: *Nature Immunology* 8.9 (Sept. 2007), pp. 967–974.

[216] Roza Nurieva et al. “Essential autocrine regulation by IL-21 in the generation of inflammatory T cells”. In: *Nature* 448.7152 (July 2007), pp. 480–483.

[217] Thomas Korn et al. “IL-21 initiates an alternative pathway to induce proinflammatory T H17 cells”. In: *Nature* 448.7152 (July 2007), pp. 484–487.

[218] Claire L. Langrish et al. “IL-23 drives a pathogenic T cell population that induces autoimmune inflammation”. In: *Journal of Experimental Medicine* 201.2 (Jan. 2005), pp. 233–240.

[219] Mandy J. McGeachy et al. “The interleukin 23 receptor is essential for the terminal differentiation of interleukin 17-producing effector T helper cells in vivo”. In: *Nature Immunology* 10.3 (2009), pp. 314–324.

[220] Kamran Ghoreschi et al. “Generation of pathogenic TH 17 cells in the absence of TGF-β 2 signalling”. In: *Nature* 467.7318 (Oct. 2010), pp. 967–971.

[221] Christina E. Zielinski et al. “Pathogen-induced human T H17 cells produce IFN-γ or IL-10 and are regulated by IL-1β”. In: *Nature* 484.7395 (Apr. 2012), pp. 514–518.

[222] Song Zhang. “The role of transforming growth factor β in T helper 17 differentiation”. In: *Immunology* 155.1 (Sept. 2018), pp. 24–35.

[223] Estelle Bettelli et al. “Reciprocal developmental pathways for the generation of pathogenic effector TH17 and regulatory T cells”. In: *Nature* 441.7090 (May 2006), pp. 235–238.

[224] Veera Hölttä et al. “IL-23/IL-17 immunity as a hallmark of Crohn’s disease”. In: *Inflammatory Bowel Diseases* 14.9 (Sept. 2008), pp. 1175–1184.

[225] Luke Jostins et al. “Host-microbe interactions have shaped the genetic architecture of inflammatory bowel disease”. In: *Nature* 491.7422 (Nov. 2012), pp. 119–124.

[226] Hailiang Huang et al. “Fine-mapping inflammatory bowel disease loci to single-variant resolution”. In: *Nature* 547.7662 (July 2017), pp. 173–178.

[227] Holm H. Uhlig et al. “Differential Activity of IL-12 and IL-23 in Mucosal and Systemic Innate Immune Pathology”. In: *Immunity* 25.2 (Aug. 2006), pp. 309–318.

[228] Philip P. Ahern et al. “Interleukin-23 Drives Intestinal Inflammation through Direct Activity on T Cells”. In: *Immunity* 33.2 (Aug. 2010), pp. 279–288.

[229] Moritz Leppkes et al. “RORγ-Expressing Th17 Cells Induce Murine Chronic Intestinal Inflammation via Redundant Effects of IL-17A and IL-17F”. In: *Gastroenterology* 136.1 (2009), pp. 257–267.

[230] Yasuaki Nishizuka and Teruyo Sakakura. “Thymus and reproduction: Sex-linked dysgenesia of the gonad after neonatal thymectomy in mice”. In: *Science* 166.3906 (Nov. 1969), pp. 753–755.

[231] R K Gershon and K Kondo. “Cell interactions in the induction of tolerance: the role of thymic lymphocytes.” In: *Immunology* 18.5 (May 1970), pp. 723–37.

[232] Shimon Sakaguchi, Toshitada Takahashi, and Yasuaki Nishizuka. “Study on cellular events in postthymectomy autoimmune oophoritis in mice: I. Requirement of lyt-1 effector cells for oocytes damage after adoptive transfer”. In: *Journal of Experimental Medicine* 156.6 (Dec. 1982), pp. 1565–1576.

[233] Fiona Powrie and Don Mason. “OX-22high CD4+ T cells induce wasting disease with multiple organ pathology: Prevention by the ox-22low subset”. In: *Journal of Experimental Medicine* 172.6 (Dec. 1990), pp. 1701–1708.

[234] S Sakaguchi et al. “Immunologic self-tolerance maintained by activated T cells expressing IL-2 receptor alpha-chains (CD25). Breakdown of a single mechanism of self-tolerance causes various autoimmune diseases.” In: *Journal of immunology (Baltimore, Md. : 1950)* 155.3 (1995), pp. 1151–64.

[235] Jason D. Fontenot, Marc A. Gavin, and Alexander Y. Rudensky. “Foxp3 programs the development and function of CD4+CD25+ regulatory T cells”. In: *Nature Immunology* 4 (Feb. 2003), pp. 330–336.

[236] Shimon Sakaguchi et al. “Regulatory T Cells and Immune Tolerance”. In: *Cell* 133.5 (May 2008), pp. 775–787.

[237] Mary E. Brunkow et al. “Disruption of a new forkhead/winged-helix protein, scurfin, results in the fatal lymphoproliferative disorder of the scurfy mouse”. In: *Nature Genetics* 27.1 (2001), pp. 68–73.

[238] Craig L. Bennett et al. “The immune dysregulation, polyendocrinopathy, enteropathy, X-linked syndrome (IPEX) is caused by mutations of FOXP3”. In: *Nature Genetics* 27.1 (2001), pp. 20–21.

[239] Robert S. Wildin et al. “X-linked neonatal diabetes mellitus, enteropathy and endocrinopathy syndrome is the human equivalent of mouse scurfy”. In: *Nature Genetics* 27.1 (2001), pp. 18–20.

[240] Thomas R. Malek and Allison L. Bayer. “Tolerance, not immunity, crucially depends on IL-2”. In: *Nature Reviews Immunology* 4.9 (Sept. 2004), pp. 665–674.

[241] Amy A. Caudy et al. “CD25 deficiency causes an immune dysregulation, polyendocrinopathy, enteropathy, X-linked-like syndrome, and defective IL-10 expression from CD4 lymphocytes”. In: *Journal of Allergy and Clinical Immunology* 119.2 (Feb. 2007), pp. 482–487.

[242] Simon Read, Vivianne Malmström, and Fiona Powrie. “Cytotoxic T lymphocyte-associated antigen 4 plays an essential role in the function of CD25+CD4+ regulatory cells that control intestinal inflammation”. In: *Journal of Experimental Medicine* 192.2 (July 2000), pp. 295–302.

[243] Holm H. Uhlig et al. “ Characterization of Foxp3 + CD4 + CD25 + and IL-10-Secreting CD4 + CD25 + T Cells during Cure of Colitis ”. In: *The Journal of Immunology* 177.9 (Nov. 2006), pp. 5852–5860.

[244] Craig L. Maynard et al. “Regulatory T cells expressing interleukin 10 develop from Foxp3+ and Foxp3- precursor cells in the absence of interleukin 10”. In: *Nature Immunology* 8.9 (Sept. 2007), pp. 931–941.

[245] Harald Von Boehmer. "Mechanisms of suppression by suppressor T cells". In: *Nature Immunology* 6.4 (Mar. 2005), pp. 338–344.

[246] Navid Sobhani et al. "CTLA-4 in regulatory T cells for cancer immunotherapy". In: *Cancers* 13.6 (Mar. 2021), pp. 1–18.

[247] Vassiliki A. Boussiotis. "Molecular and Biochemical Aspects of the PD-1 Checkpoint Pathway". In: *New England Journal of Medicine* 375.18 (Nov. 2016). Ed. by Dan L. Longo, pp. 1767–1778.

[248] Liliana E. Lucca and Margarita Dominguez-Villar. "Modulation of regulatory T cell function and stability by co-inhibitory receptors". In: *Nature Reviews Immunology* 20.11 (Nov. 2020), pp. 680–693.

[249] Takeshi Tanoue, Koji Atarashi, and Kenya Honda. "Development and maintenance of intestinal regulatory T cells". In: *Nature Reviews Immunology* 16.5 (Apr. 2016), pp. 295–309.

[250] Ana Izcue, Janine L. Coombes, and Fiona Powrie. "Regulatory lymphocytes and intestinal inflammation". In: *Annual Review of Immunology* 27 (Mar. 2009), pp. 313–338.

[251] Koji Atarashi et al. "Induction of colonic regulatory T cells by indigenous Clostridium species". In: *Science* 331.6015 (Jan. 2011), pp. 337–341.

[252] Markus B. Geuking et al. "Intestinal Bacterial Colonization Induces Mutualistic Regulatory T Cell Responses". In: *Immunity* 34.5 (May 2011), pp. 794–806.

[253] Jonathan M. Weiss et al. "Neuropilin 1 is expressed on thymus-derived natural regulatory T cells, but not mucosagenerated induced Foxp3+ T reg cells". In: *Journal of Experimental Medicine* 209.10 (Sept. 2012), pp. 1723–1742.

[254] Andrew T. Stefka et al. "Commensal bacteria protect against food allergen sensitization". In: *Proceedings of the National Academy of Sciences of the United States of America* 111.36 (Sept. 2014), pp. 13145–13150.

[255] Kwang Soon Kim et al. "Dietary antigens limit mucosal immunity by inducing regulatory T cells in the small intestine". In: *Science* 351.6275 (Feb. 2016), pp. 858–863.

[256] Michael J. Barnes and Fiona Powrie. "Regulatory T Cells Reinforce Intestinal Homeostasis". In: *Immunity* 31.3 (Sept. 2009), pp. 401–411.

[257] Wan Jun Chen et al. "Conversion of Peripheral CD4+CD25- Naive T Cells to CD4+CD25+ Regulatory T Cells by TGF-β Induction of Transcription Factor Foxp3". In: *Journal of Experimental Medicine* 198.12 (Dec. 2003), pp. 1875–1886.

[258] Ming O. Li, Shomyseh Sanjabi, and Richard A A. Flavell. "Transforming Growth Factor-β Controls Development, Homeostasis, and Tolerance of T Cells by Regulatory T Cell-Dependent and -Independent Mechanisms". In: *Immunity* 25.3 (Sept. 2006), pp. 455–471.

[259] Koji Atarashi et al. "Treg induction by a rationally selected mixture of Clostridia strains from the human microbiota". In: *Nature* 500.7461 (July 2013), pp. 232–236.

[260] Micah J. Benson et al. "All-trans retinoic acid mediates enhanced T reg cell growth, differentiation, and gut homing in the face of high levels of co-stimulation". In: *Journal of Experimental Medicine* 204.8 (Aug. 2007), pp. 1765–1774.

[261] Janine L. Coombes et al. "A functionally specialized population of mucosal CD103+ DCs induces Foxp3+ regulatory T cells via a TGF-β -and retinoic acid-dependent mechanism". In: *Journal of Experimental Medicine* 204.8 (Aug. 2007), pp. 1757–1764.

[262] Angela M. Thornton et al. "Expression of Helios, an Ikaros Transcription Factor Family Member, Differentiates Thymic-Derived from Peripherally Induced Foxp3 + T Regulatory Cells". In: *The Journal of Immunology* 184.7 (Apr. 2010), pp. 3433–3441.

[263] Mahesh Yadav et al. "Neuropilin-1 distinguishes natural and inducible regulatory T cells among regulatory T cell subsets in vivo". In: *Journal of Experimental Medicine* 209.10 (Sept. 2012), pp. 1713–1722.

[264] Edyta Szurek et al. "Differences in expression level of Helios and neuropilin-1 do not distinguish thymus-derived from extrathymically-induced CD4+Foxp3+ regulatory T cells". In: *PLoS ONE* 10.10 (Oct. 2015). Ed. by Antonio A Freitas, e0141161.

[265] Ye Zheng et al. "Role of conserved non-coding DNA elements in the Foxp3 gene in regulatory T-cell fate". In: *Nature* 463.7282 (Feb. 2010), pp. 808–812.

[266] Clarissa Campbell et al. "Extrathymically Generated Regulatory T Cells Establish a Niche for Intestinal Border-Dwelling Bacteria and Affect Physiologic Metabolite Balance". In: *Immunity* 48.6 (June 2018), 1245–1257.e9.

[267] Steven Z. Josefowicz et al. "Extrathymically generated regulatory T cells control mucosal T H 2 inflammation". In: *Nature* 482.7385 (Feb. 2012), pp. 395–399.

[268] Liang Zhou et al. "TGF-B-induced Foxp3 inhibits TH17 cell differentiation by antagonizing RORγt function". In: *Nature* 453.7192 (May 2008), pp. 236–240.

[269] Makoto Miyara et al. "Functional Delineation and Differentiation Dynamics of Human CD4+ T Cells Expressing the FoxP3 Transcription Factor". In: *Immunity* 30.6 (June 2009), pp. 899–911.

[270] Esen Sefik et al. "Individual intestinal symbionts induce a distinct population of RORγ+ regulatory T cells". In: *Science* 349.6251 (Aug. 2015), pp. 993–997.

[271] Caspar Ohnmacht et al. "The microbiota regulates type 2 immunity through RORγt+ T cells". In: *Science* 349.6251 (Aug. 2015), pp. 989–993.

[272] Yunqi Wang, Maureen A. Su, and Yisong Y. Wan. "An Essential Role of the Transcription Factor GATA-3 for the Function of Regulatory T Cells". In: *Immunity* 35.3 (Sept. 2011), pp. 337–348.

[273] Gang Wei et al. "Global Mapping of H3K4me3 and H3K27me3 Reveals Specificity and Plasticity in Lineage Fate Determination of Differentiating CD4+ T Cells". In: *Immunity* 30.1 (Jan. 2009), pp. 155–167.

[274] Marc Bonneville et al. "Intestinal intraepithelial lymphocytes are a distinct set of $\gamma\delta$ T cells". In: *Nature* 336.6198 (1988), pp. 479–481.

[275] Thomas Goodman and Leo Lefrançois. "Expression of the γ-δ T-cell receptor on intestinal CD8+ intraepithelial lymphocytes". In: *Nature* 333.6176 (1988), pp. 855–858.

[276] Hilde Cheroutre, Florence Lambolez, and Daniel Mucida. "The light and dark sides of intestinal intraepithelial lymphocytes". In: *Nature Reviews Immunology* 11.7 (July 2011), pp. 445–456.

[277] Makoto Iwata et al. "Retinoic acid imprints gut-homing specificity on T cells". In: *Immunity* 21.4 (Oct. 2004), pp. 527–538.

[278] Loui T. Madakamutil et al. "CD8$\alpha\alpha$-Mediated Survival and Differentiation of CD8 Memory T Cell Precursors". In: *Science* 304.5670 (Apr. 2004), pp. 590–593.

[279] Timothy L. Denning et al. "Mouse TCR$\alpha\beta$ + CD8$\alpha\alpha$ Intraepithelial Lymphocytes Express Genes That Down-Regulate Their Antigen Reactivity and Suppress Immune Responses". In: *The Journal of Immunology* 178.7 (Apr. 2007), pp. 4230–4239.

[280] Robert Hershberg et al. "Expression of the thymus leukemia antigen in mouse intestinal epithelium". In: *Proceedings of the National Academy of Sciences of the United States of America* 87.24 (Dec. 1990), pp. 9727–9731.

[281] A. J. Leishman et al. "T cell responses modulated through interaction between CD8$\alpha\alpha$ and the nonclassical MHC class I molecule, TL". In: *Science* 294.5548 (Nov. 2001), pp. 1936–1939.

[282] Yiwei Liu et al. "The crystal structure of a TL/CD8$\alpha\alpha$ complex at 2.1 Å resolution: Implications for modulation of T cell activation and memory". In: *Immunity* 18.2 (Feb. 2003), pp. 205–215.

[283] Christiaan N. Levelt et al. "High- and low-affinity single-peptide/MHC ligands have distinct effects on the development of mucosal CD8$\alpha\alpha$ and CD8$\alpha\beta$ T lymphocytes". In: *Proceedings of the National Academy of Sciences of the United States of America* 96.10 (May 1999), pp. 5628–5633.

[284] R. Lee Mosley, Daniel Styre, and John R. Klein. "CD4+ CD8+ murine intestinal intraepithelial lymphocytes". In: *International Immunology* 2.4 (Apr. 1990), pp. 361–365.

[285] L. Helgeland et al. "Sequential development of intraepithelial $\gamma\delta$ and $\alpha\beta$ T lymphocytes expressing CD8$\alpha\beta$ in neonatal rat intestine: Requirement for the thymus". In: *Immunology* 92.4 (Dec. 1997), pp. 447–456.

[286] Jessica C.A. Ter Steege, Wim A. Buurman, and Pierre Philippe Forget. "The neonatal development of intraepithelial and lamina propria lymphocytes in the murine small intestine". In: *Developmental Immunology* 5.2 (1997), pp. 121–128.

[287] Y Umesaki et al. "Expansion of alpha beta T-cell receptor-bearing intestinal intraepithelial lymphocytes after microbial colonization in germ-free mice and its independence from thymus." In: *Immunology* 79.1 (May 1993), pp. 32–7.

[288] Manish Latthe, Linda Terry, and Thomas T. Macdonald. "High frequency of CD8$\alpha\alpha$ homodimer-bearing T cells in human fetal intestine". In: *European Journal of Immunology* 24.7 (July 1994), pp. 1703–1705.

[289] Hajime Komano et al. “Homeostatic regulation of intestinal epithelia by intraepithelial $\gamma\delta$ T cells”. In: *Proceedings of the National Academy of Sciences of the United States of America* 92.13 (June 1995), pp. 6147–6151.

[290] Delphine Guy-Grand et al. “Small bowel enteropathy: Role of intraepithelial lymphocytes and of cytokines (IL-12, IFN-γ, TNF) in the induction of epithelial cell death and renewal”. In: *European Journal of Immunology* 28.2 (Feb. 1998), pp. 730–744.

[291] Scott J. Roberts et al. “T-cell $\alpha\beta$+ and $\gamma\delta$+ deficient mice display abnormal but distinct phenotypes toward a natural, widespread infection of the intestinal epithelium”. In: *Proceedings of the National Academy of Sciences of the United States of America* 93.21 (Oct. 1996), pp. 11774–11779.

[292] Stefan Müller, Myriam Bühler-Jungo, and Christoph Mueller. “Intestinal Intraepithelial Lymphocytes Exert Potent Protective Cytotoxic Activity During an Acute Virus Infection”. In: *The Journal of Immunology* 164.4 (Feb. 2000), pp. 1986–1994.

[293] T Dharakul et al. “Immunization with baculovirus-expressed recombinant rotavirus proteins VP1, VP4, VP6, and VP7 induces CD8+ T lymphocytes that mediate clearance of chronic rotavirus infection in SCID mice”. In: *Journal of Virology* 65.11 (Nov. 1991), pp. 5928–5932.

[294] A C Lepage et al. “Gut-derived intraepithelial lymphocytes induce long term immunity against Toxoplasma gondii.” In: *Journal of immunology (Baltimore, Md. : 1950)* 161.9 (1998), pp. 4902–8.

[295] Gobardhan Das et al. “An important regulatory role for CD4+CD8$\alpha\alpha$ T cells in the intestinal epithelial layer in the prevention of inflammatory bowel disease”. In: *Proceedings of the National Academy of Sciences of the United States of America* 100.9 (2003), pp. 5324–5329.

[296] P A Offit and K I Dudzik. “Rotavirus-specific cytotoxic T lymphocytes appear at the intestinal mucosal surface after rotavirus infection”. In: *Journal of Virology* 63.8 (Aug. 1989), pp. 3507–3512.

[297] John Shires, Efstathios Theodoridis, and Adrian C. Hayday. “Biological insights into TCR$\gamma\delta$+ and TCR$\alpha\beta$+ intraepithelial lymphocytes provided by serial analysis of gene expression (SAGE)”. In: *Immunity* 15.3 (Sept. 2001), pp. 419–434.

[298] M. M.W. Yeung et al. “Characterisation of mucosal lymphoid aggregates in ulcerative colitis: Immune cell phenotype and TcR-$\gamma\delta$ expression”. In: *Gut* 47.2 (Aug. 2000), pp. 215–227.

[299] H. Kanazawa et al. “Multiple accumulation of Vδ2+ $\gamma\delta$ T-cell clonotypes in intestinal mucosa from patients with Crohn’s disease”. In: *Digestive Diseases and Sciences* 46.2 (2001), pp. 410–416.

[300] R. Giacomelli et al. “Increase of circulating γ/δ T lymphocytes in the peripheral blood of patients affected by active inflammatory bowel disease”. In: *Clinical and Experimental Immunology* 98.1 (June 1994), pp. 83–88.

[301] Stephen J. Simpson et al. “Expression of pro-inflammatory cytokines by TCR$\alpha\beta$+ and TCR$\gamma\delta$+ T cells in an experimental model of colitis”. In: *European Journal of Immunology* 27.1 (Jan. 1997), pp. 17–25.

[302] Mariko Kawaguchi-Miyashita et al. “An accessory role of TCR$\gamma\delta$+ cells in the exacerbation of inflammatory bowel disease in TCRα mutant mice”. In: *European Journal of Immunology* 31.4 (Apr. 2001), pp. 980–988.

[303] Atsushi Mizoguchi et al. “Role of the CD5 molecule on TCR $\gamma\delta$ T cell-mediated immune functions: Development of germinal centers and chronic intestinal inflammation”. In: *International Immunology* 15.1 (Jan. 2003), pp. 97–108.

[304] Bertrand Meresse et al. “Coordinated induction by IL15 of a TCR-independent NKG2D signaling pathway converts CTL into lymphokine-activated killer cells in celiac disease”. In: *Immunity* 21.3 (Sept. 2004), pp. 357–366.

[305] Sophie Hüe et al. “A direct role for NKG2D/MICA interaction in villous atrophy during celiac disease”. In: *Immunity* 21.3 (Sept. 2004), pp. 367–377.

[306] Karen Smith, Kathy D. McCoy, and Andrew J. Macpherson. “Use of axenic animals in studying the adaptation of mammals to their commensal intestinal microbiota”. In: *Seminars in Immunology* 19.2 (Apr. 2007), pp. 59–69.

[307] Seth Rakoff-Nahoum et al. “Recognition of commensal microflora by toll-like receptors is required for intestinal homeostasis”. In: *Cell* 118.2 (July 2004), pp. 229–241.

[308] Inna Sekirov et al. “Antibiotic-induced perturbations of the intestinal microbiota alter host susceptibility to enteric infection”. In: *Infection and Immunity* 76.10 (Oct. 2008), pp. 4726–4736.

[309] D. A. Hill et al. “Metagenomic analyses reveal antibiotic-induced temporal and spatial changes in intestinal microbiota with associated alterations in immune cell homeostasis”. In: *Mucosal Immunology* 3.2 (Mar. 2010), pp. 148–158.

[310] Ivaylo I. Ivanov et al. “Specific Microbiota Direct the Differentiation of IL-17-Producing T-Helper Cells in the Mucosa of the Small Intestine”. In: *Cell Host and Microbe* 4.4 (Oct. 2008), pp. 337–349.

[311] Koji Atarashi et al. “Th17 Cell Induction by Adhesion of Microbes to Intestinal Epithelial Cells”. In: *Cell* 163.2 (Oct. 2015), pp. 367–380.

[312] Tze Guan Tan et al. “Identifying species of symbiont bacteria from the human gut that, alone, can induce intestinal Th17 cells in mice”. In: *Proceedings of the National Academy of Sciences of the United States of America* 113.50 (Dec. 2016), E8141–E8150.

[313] Bertrand Routy et al. “Gut microbiome influences efficacy of PD-1-based immunotherapy against epithelial tumors”. In: *Science* 359.6371 (Jan. 2018), pp. 91–97.

[314] Eduard Ansaldo et al. “Akkermansia muciniphila induces intestinal adaptive immune responses during homeostasis”. In: *Science* 364.6446 (June 2019), pp. 1179–1184.

[315] Stephanie K. Lathrop et al. “Peripheral education of the immune system by colonic commensal microbiota”. In: *Nature* 478.7368 (Oct. 2011), pp. 250–254.

[316] Katherine Nutsch et al. “Rapid and Efficient Generation of Regulatory T Cells to Commensal Antigens in the Periphery”. In: *Cell Reports* 17.1 (Sept. 2016), pp. 206–220.

[317] Jiani N. Chai et al. “Helicobacter species are potent drivers of colonic T cell responses in homeostasis and inflammation”. In: *Science Immunology* 2.13 (July 2017), p. 5068.

[318] Mo Xu et al. “C-MAF-dependent regulatory T cells mediate immunological tolerance to a gut pathobiont”. In: *Nature* 554.7692 (Feb. 2018), pp. 373–377.

[319] Kahoko Hashimoto, Sunil K. Joshi, and Pandelakis A. Koni. “A conditional null allele of the major histocompatibility IA-beta chain gene”. In: *Genesis* 32.2 (Feb. 2002), pp. 152–153.

[320] Blair B. Madison et al. “cis elements of the villin gene control expression in restricted domains of the vertical (crypt) and horizontal (duodenum, cecum) axes of the intestine”. In: *Journal of Biological Chemistry* 277.36 (Sept. 2002), pp. 33275–33283.

[321] Masahito Kamanaka et al. “Expression of Interleukin-10 in Intestinal Lymphocytes Detected by an Interleukin-10 Reporter Knockin tiger Mouse”. In: *Immunity* 25.6 (Dec. 2006), pp. 941–952.

[322] Noriko Komatsu et al. “Heterogeneity of natural Foxp3+ T cells: A committed regulatory T-cell lineage and an uncommitted minor population retaining plasticity”. In: *Proceedings of the National Academy of Sciences of the United States of America* 106.6 (Feb. 2009), pp. 1903–1908.

[323] Takako Sasaki et al. “Expression and distribution of laminin α1 and α2 chains in embryonic and adult mouse tissues: An immunochemical approach”. In: *Experimental Cell Research* 275.2 (May 2002), pp. 185–199.

[324] Axel U. Dignass and Andreas Sturm. “Peptide growth factors in the intestine”. In: *European Journal of Gastroenterology and Hepatology* 13.7 (2001), pp. 763–770.

[325] James C.H. Hardwick et al. “Bone Morphogenetic Protein 2 Is Expressed by, and Acts Upon, Mature Epithelial Cells in the Colon”. In: *Gastroenterology* 126.1 SUPPL. 1 (2004), pp. 111–121.

[326] Anna Pavlina G. Haramis et al. “De Novo Crypt Formation and Juvenile Polyposis on BMP Inhibition in Mouse Intestine”. In: *Science* 303.5664 (Mar. 2004), pp. 1684–1686.

[327] Daniel Pinto et al. “Canonical Wnt signals are essential for homeostasis of the intestinal epithelium”. In: *Genes and Development* 17.14 (July 2003), pp. 1709–1713.

[328] Frank Kuhnert et al. “Essential requirement for Wnt signaling in proliferation of adult small intestine and colon revealed by adenoviral expression of Dickkopf-1”. In: *Proceedings of the National Academy of Sciences of the United States of America* 101.1 (Jan. 2004), pp. 266–271.

[329] Kyung Ah Kim et al. “Mitogenic influence of human R-spondin1 on the intestinal epithelium”. In: *Science* 309.5738 (Aug. 2005), pp. 1256–1259.

[330] Kiichi Watanabe et al. “A ROCK inhibitor permits survival of dissociated human embryonic stem cells”. In: *Nature Biotechnology* 25.6 (June 2007), pp. 681–686.

[331] Toshiro Sato et al. “Long-term expansion of epithelial organoids from human colon, adenoma, adenocarcinoma, and Barrett’s epithelium”. In: *Gastroenterology* 141.5 (2011), pp. 1762–1772.

[332] Taku Kambayashi and Terri M. Laufer. "Atypical MHC class II-expressing antigen-presenting cells: Can anything replace a dendritic cell?" In: *Nature Reviews Immunology* 14.11 (Jan. 2014), pp. 719–730.

[333] Jennifer E. Smith-Garvin, Gary A. Koretzky, and Martha S. Jordan. "T cell activation". In: *Annual Review of Immunology* 27 (Mar. 2009), pp. 591–619.

[334] Julie M. Curtsinger and Matthew F. Mescher. "Inflammatory cytokines as a third signal for T cell activation". In: *Current Opinion in Immunology* 22.3 (June 2010), pp. 333–340.

[335] Lieping Chen and Dallas B. Flies. "Molecular mechanisms of T cell co-stimulation and co-inhibition". In: *Nature Reviews Immunology* 13.4 (Apr. 2013), pp. 227–242.

[336] S. Danese, M. Sans, and C. Fiocchi. "The CD40/CD40L costimulatory pathway in inflammatory bowel disease". In: *Gut* 53.7 (July 2004), pp. 1035–1043.

[337] David G. Saliba et al. "Composition and structure of synaptic ectosomes exporting antigen receptor linked to functional CD40 ligand from helper T cells". In: *eLife* 8 (Aug. 2019).

[338] John Attanasio and E. John Wherry. "Costimulatory and Coinhibitory Receptor Pathways in Infectious Disease". In: *Immunity* 44.5 (May 2016), pp. 1052–1068.

[339] Leonard J. Appleman and Vassiliki A. Boussiotis. "T cell anergy and costimulation". In: *Immunological Reviews* 192.1 (Apr. 2003), pp. 161–180.

[340] G. B. McDonald and D. P. Jewell. "Class II antigen (HLA-DR) expression by intestinal epithelial cells in inflammatory diseases of colon". In: *Journal of Clinical Pathology* 40.3 (Mar. 1987), pp. 312–317.

[341] Claudio Franceschi et al. "Inflamm-aging. An evolutionary perspective on immunosenescence". In: *Annals of the New York Academy of Sciences*. Vol. 908. New York Academy of Sciences, 2000, pp. 244–254.

[342] Netusha Thevaranjan et al. "Age-Associated Microbial Dysbiosis Promotes Intestinal Permeability, Systemic Inflammation, and Macrophage Dysfunction". In: *Cell Host and Microbe* 21.4 (Apr. 2017), 455–466.e4.

[343] Mark T. Whary et al. "Chapter 3 - Biology and Diseases of Mice". In: *Laboratory Animal Medicine: Third Edition*. Elsevier Inc., Jan. 2015, pp. 43–149.

[344] D. J. Mathis et al. "Several mechanisms can account for defective E alpha gene expression in different mouse haplotypes." In: *Proceedings of the National Academy of Sciences of the United States of America* 80.1 (Jan. 1983), pp. 273–277.

[345] Dominic Cosgrove et al. "Mice lacking MHC class II molecules". In: *Cell* 66.5 (Sept. 1991), pp. 1051–1066.

[346] J. M. Waldburger et al. "Selective abrogation of major histocompatibility complex class II expression on extrahematopoietic cells in mice lacking promoter IV of the class II transactivator gene". In: *Journal of Experimental Medicine* 194.4 (Aug. 2001), pp. 393–406.

[347] Laura Santambrogio et al. "Extracellular antigen processing and presentation by immature dendritic cells". In: *Proceedings of the National Academy of Sciences of the United States of America* 96.26 (Dec. 1999), pp. 15056–15061.

[348] Elizabeth Daro et al. "Polyethylene Glycol-Modified GM-CSF Expands CD11b high CD11c high But Not CD11b low CD11c high Murine Dendritic Cells In Vivo: A Comparative Analysis with Flt3 Ligand". In: *The Journal of Immunology* 165.1 (July 2000), pp. 49–58.

[349] J. M. Waldburger et al. "Lessons from the bare lymphocyte syndrome: Molecular mechanisms regulating MHC class II expression". In: *Immunological Reviews* 178 (2000), pp. 148–165.

[350] Yuanshu Dong et al. "The Smad3 Protein Is Involved in TGF-β Inhibition of Class II Transactivator and Class II MHC Expression". In: *The Journal of Immunology* 167.1 (July 2001), pp. 311–319.

[351] W Rohn et al. "IL-1 beta inhibits IFN-gamma-induced class II MHC expression by suppressing transcription of the class II transactivator gene." In: *Journal of immunology (Baltimore, Md. : 1950)* 162.2 (Jan. 1999), pp. 886–96.

[352] Guangming Zhong, Tao Fan, and Li Liu. "Chlamydia inhibits interferon γ-inducible major histocompatibility complex class II expression by degradation of upstream stimulatory factor 1". In: *Journal of Experimental Medicine* 189.12 (June 1999), pp. 1931–1937.

[353] Daniel M. Miller et al. "Human cytomegalovirus inhibits major histocompatibility complex class II expression by disruption of the Jak/Stat pathway". In: *Journal of Experimental Medicine* 187.5 (Mar. 1998), pp. 675–683.

[354] Emmanuelle Le Roy et al. "Escape of Human Cytomegalovirus from HLA-DR-Restricted CD4+ T-Cell Response Is Mediated by Repression of Gamma Interferon-Induced Class II Transactivator Expression". In: *Journal of Virology* 73.8 (Aug. 1999), pp. 6582–6589.

[355] George M. O'Keefe, Vince T. Nguyen, and Etty N. Benveniste. "Class II transactivator and class II MHC gene expression in microglia: Modulation by the cytokines TGF-β, IL-4, IL-13 and IL-10". In: *European Journal of Immunology* 29.4 (Apr. 1999), pp. 1275–1285.

[356] Marie Pierik et al. "Toll-like receptor-1, -2, and -6 polymorphisms influence disease extension in inflammatory bowel diseases". In: *Inflammatory Bowel Diseases* 12.1 (Jan. 2006), pp. 1–8.

[357] Andrew T. Gewirtz et al. "Dominant-negative TLR5 polymorphism reduces adaptive immune response to flagellin and negatively associates with Crohn's disease". In: *American Journal of Physiology - Gastrointestinal and Liver Physiology* 290.6 (June 2006), pp. 1157–1163.

[358] D. Franchimont et al. "Deficient host-bacteria interactions in inflammatory bowel disease? the toll-like receptor (TLR)-4 Asp299gly polymorphism is associated with Crohn's disease and ulcerative colitis". In: *Gut* 53.7 (July 2004), pp. 987–992.

[359] Mark J. Asquith et al. "Pathogenic and protective roles of MyD88 in leukocytes and epithelial cells in mouse models of inflammatory bowel disease". In: *Gastroenterology* 139.2 (Aug. 2010), 519–529.e2.

[360] Masayuki Fukata et al. "Constitutive activation of epithelial TLR4 augments inflammatory responses to mucosal injury and drives colitis-associated tumorigenesis". In: *Inflammatory Bowel Diseases* 17.7 (July 2011), pp. 1464–1473.

[361] Rishu Dheer et al. “Intestinal epithelial Toll-like receptor 4 signaling affects epithelial function and colonic microbiota and promotes a risk for transmissible colitis”. In: *Infection and Immunity* 84.3 (Mar. 2016), pp. 798–810.

[362] Ian R. Sanderson et al. “Age and diet act through distinct isoforms of the class II transactivator gene in mouse intestinal epithelium”. In: *Gastroenterology* 127.1 (July 2004), pp. 203–212.

[363] Valli De Re, Raffaella Magris, and Renato Cannizzaro. “New insights into the pathogenesis of celiac disease”. In: *Frontiers in Medicine* 4.AUG (Aug. 2017), p. 1.

[364] Anja Fuchs et al. “Intraepithelial type 1 innate lymphoid cells are a unique subset of il-12- and il-15-responsive ifn-γ-producing cells”. In: *Immunity* 38.4 (Apr. 2013), pp. 769–781.

[365] M J Skeen and H K Ziegler. “Activation of gamma delta T cells for production of IFN-gamma is mediated by bacteria via macrophage-derived cytokines IL-1 and IL-12.” In: *Journal of immunology (Baltimore, Md. : 1950)* 154.11 (June 1995), pp. 5832–41.

[366] Jet Phey Lim and Paul A Gleeson. “Macropinocytosis: An endocytic pathway for internalising large gulps”. In: *Immunology and Cell Biology* 89.8 (Nov. 2011), pp. 836–843.

[367] Linda Chia Hui Yu et al. “Enteric dysbiosis promotes antibiotic-resistant bacterial infection: Systemic dissemination of resistant and commensal bacteria through epithelial transcytosis”. In: *American Journal of Physiology - Gastrointestinal and Liver Physiology* 307.8 (Oct. 2014), G824–G835.

[368] Mark S. Ladinsky et al. “Endocytosis of commensal antigens by intestinal epithelial cells regulates mucosal T cell homeostasis”. In: *Science* 363.6431 (Mar. 2019), eaat4042.

[369] Claudio Franceschi et al. “Inflammaging: a new immune–metabolic viewpoint for age-related diseases”. In: *Nature Reviews Endocrinology* 14.10 (Oct. 2018), pp. 576–590.

[370] Elena Biagi et al. “Through ageing, and beyond: Gut microbiota and inflammatory status in seniors and centenarians”. In: *PLoS ONE* 5.5 (May 2010). Ed. by Niyaz Ahmed, e10667.

[371] Simone Rampelli et al. “Functional metagenomic profiling of intestinal microbiome in extreme ageing”. In: *Aging* 5.12 (Dec. 2013), pp. 902–912.

[372] Timur Tuganbaev et al. “Diet Diurnally Regulates Small Intestinal Microbiome-Epithelial-Immune Homeostasis and Enteritis”. In: *Cell* 182.6 (Sept. 2020), 1441–1459.e21.

[373] Tushar Singh and Anne B. Newman. “Inflammatory markers in population studies of aging”. In: *Ageing Research Reviews* 10.3 (July 2011), pp. 319–329.

[374] W. Zac Stephens et al. “Epithelial-myeloid exchange of MHC class II constrains immunity and microbiota composition”. In: *Cell Reports* 37.5 (Nov. 2021), p. 109916.

[375] Ryan J. Cummings et al. “Different tissue phagocytes sample apoptotic cells to direct distinct homeostasis programs”. In: *Nature* 539.7630 (Nov. 2016), pp. 565–569.

[376] Bruce R. Blazar, William J. Murphy, and Mehrdad Abedi. "Advances in graft-versus-host disease biology and therapy". In: *Nature Reviews Immunology* 12.6 (June 2012), pp. 443–458.

[377] Semir Beyaz et al. "Dietary suppression of MHC class II expression in intestinal epithelial cells enhances intestinal tumorigenesis". In: *Cell Stem Cell* 28.11 (2021), 1922–1935.e5.

[378] Sookjin Moon et al. "Niche-specific MHC II and PD-L1 regulate CD4+CD8$\alpha\alpha$+ intraepithelial lymphocyte differentiation". In: *Journal of Experimental Medicine* 218.4 (Apr. 2021).

[379] Angelina M. Bilate et al. "T Cell Receptor Is Required for Differentiation, but Not Maintenance, of Intestinal CD4+ Intraepithelial Lymphocytes". In: *Immunity* 53.5 (Nov. 2020), 1001–1014.e20.

[380] Bernardo Sgarbi Reis et al. "Mutual expression of the transcription factors Runx3 and ThPOK regulates intestinal CD4 + T cell immunity". In: *Nature Immunology* 14.3 (Jan. 2013), pp. 271–280.

[381] Daniel Mucida et al. "Transcriptional reprogramming of mature CD4 + helper T cells generates distinct MHC class II-restricted cytotoxic T lymphocytes". In: *Nature Immunology* 14.3 (Jan. 2013), pp. 281–289.

[382] Tomohisa Sujino et al. "Tissue adaptation of regulatory and intraepithelial CD4+ T cells controls gut inflammation". In: *Science* 352.6293 (June 2016), pp. 1581–1586.

[383] Luisa Cervantes-Barragan et al. "Lactobacillus reuteri induces gut intraepithelial CD4+CD8$\alpha\alpha$+ T cells". In: *Science* 357.6353 (Aug. 2017), pp. 806–810.

[384] Bernardo S. Reis et al. "Transcription factor T-bet regulates intraepithelial lymphocyte functional maturation". In: *Immunity* 41.2 (Aug. 2014), pp. 244–256.

[385] Hilde Cheroutre and Florence Lambolez. "Doubting the TCR Coreceptor Function of CD8$\alpha\alpha$". In: *Immunity* 28.2 (Feb. 2008), pp. 149–159.

[386] Joshua Oluoch Amimo et al. "Rotavirus Interactions With Host Intestinal Epithelial Cells". In: *Frontiers in Immunology* 12 (Dec. 2021), p. 5544.

[387] Mayumi K. Holly and Jason G. Smith. "Adenovirus Infection of Human Enteroids Reveals Interferon Sensitivity and Preferential Infection of Goblet Cells". In: *Journal of Virology* 92.9 (May 2018).

[388] Iliyan D. Iliev and Ken Cadwell. "Effects of Intestinal Fungi and Viruses on Immune Responses and Inflammatory Bowel Diseases". In: *Gastroenterology* 160.4 (Mar. 2021), pp. 1050–1066.

[389] Adam Sateriale et al. "A Genetically Tractable, Natural Mouse Model of Cryptosporidiosis Offers Insights into Host Protective Immunity". In: *Cell Host and Microbe* 26.1 (July 2019), 135–146.e5.

[390] A. M Westendorf et al. "Intestinal Epithelial Antigen Induces CD4+ T Cells with Regulatory Phenotype in a Transgenic Autoimmune Mouse Model". In: *Annals of the New York Academy of Sciences* 1072.1 (Aug. 2006), pp. 401–406.

[391] Christoph Thelemann et al. "Interferon-γ induces expression of MHC class II on intestinal epithelial cells and protects mice from colitis". In: *PLoS ONE* 9.1 (Jan. 2014). Ed. by Muriel Moser, e86844.

[392] Deepa R. Jamwal et al. “Intestinal Epithelial Expression of MHCII Determines Severity of Chemical, T Cell-Induced, and Infectious Colitis in Mice”. In: *Gastroenterology* (June 2020).

[393] Ryo Hatano et al. “Antigen presentation by small intestinal epithelial cells uniquely enhances IFN-γ secretion from CD4+ intestinal intraepithelial lymphocytes”. In: *Biochemical and Biophysical Research Communications* 435.4 (June 2013), pp. 592–596.

[394] Lillian Maggio-Price et al. “Lineage targeted MHC-II transgenic mice demonstrate the role of dendritic cells in bacterial-driven colitis”. In: *Inflammatory Bowel Diseases* 19.1 (Jan. 2013), pp. 174–184.

[395] Ralf Kühn et al. “Interleukin-10-deficient mice develop chronic enterocolitis”. In: *Cell* 75.2 (Oct. 1993), pp. 263–274.

[396] Daniel J. Berg et al. “Enterocolitis and colon cancer in interleukin-10-deficient mice are associated with aberrant cytokine production and CD4+ Th1-like responses”. In: *Journal of Clinical Investigation* 98.4 (Aug. 1996), pp. 1010–1020.

[397] Chrystelle Asseman et al. “An essential role for interleukin 10 in the function of regulatory T cells that inhibit intestinal inflammation”. In: *Journal of Experimental Medicine* 190.7 (Oct. 1999), pp. 995–1003.

[398] David Ruano-Gallego et al. “Type III secretion system effectors form robust and flexible intracellular virulence networks”. In: *Science* 371.6534 (Mar. 2021).

[399] Nobuhiko Kamada et al. “Humoral immunity in the gut selectively targets phenotypically virulent attaching-and-effacing bacteria for intraluminal elimination”. In: *Cell Host and Microbe* 17.5 (May 2015), pp. 617–627.

[400] S. W. Barthold, G. W. Osbaldiston, and A. M. Jonas. “Dietary, bacterial, and host genetic interactions in the pathogenesis of transmissible murine colonic hyperplasia”. In: *Laboratory Animal Science* 27.6 (Dec. 1977), pp. 938–945.

[401] Rosanna Mundy et al. “Citrobacter rodentium of mice and man”. In: *Cellular Microbiology* 7.12 (Dec. 2005), pp. 1697–1706.

[402] Nobuhiko Kamada et al. “Role of the gut microbiota in immunity and inflammatory disease”. In: *Nature Reviews Immunology* 13.5 (May 2013), pp. 321–335.

[403] Benjamin L. Duell et al. “Recent insights into microbial triggers of interleukin-10 production in the host and the impact on infectious disease pathogenesis”. In: *FEMS Immunology and Medical Microbiology* 64.3 (Apr. 2012), pp. 295–313.

[404] Graham J. Britton et al. “Microbiotas from Humans with Inflammatory Bowel Disease Alter the Balance of Gut Th17 and RORγt+ Regulatory T Cells and Exacerbate Colitis in Mice”. In: *Immunity* 50.1 (Jan. 2019), 212–224.e4.

[405] Loise M. Francisco et al. “PD-L1 regulates the development, maintenance, and function of induced regulatory T cells”. In: *Journal of Experimental Medicine* 206.13 (Dec. 2009), pp. 3015–3029.

[406] Candelaria Ponce de León et al. “Dysregulation of the PD-1/PD-L1 pathway contributes to the pathogenesis of celiac disease”. In: *Cellular and Molecular Immunology* 16.9 (2019), pp. 777–779.

[407] Claire Pearson et al. “ILC3 GM-CSF production and mobilisation orchestrate acute intestinal inflammation”. In: *eLife* 5.JANUARY2016 (Jan. 2016).

[408] Thorsten R. Mempel, Sarah E. Henrickson, and Ulrich H. Von Andrian. “T-cell priming by dendritic cells in lymph nodes occurs in three distinct phases”. In: *Nature* 427.6970 (Jan. 2004), pp. 154–159.

[409] Bernd H. Zinselmeyer et al. “In situ characterization of CD4+ T cell behavior in mucosal and systemic lymphoid tissues during the induction of oral priming and tolerance”. In: *Journal of Experimental Medicine* 201.11 (June 2005), pp. 1815–1823.

[410] Yasutoshi Agata et al. “Expression of the PD-1 antigen on the surface of stimulated mouse T and B lymphocytes”. In: *International Immunology* 8.5 (May 1996), pp. 765–772.

[411] H C DeGrendele et al. “CD44 activation and associated primary adhesion is inducible via T cell receptor stimulation.” In: *Journal of immunology (Baltimore, Md. : 1950)* 159.6 (1997), pp. 2549–53.

[412] Judith F. Ashouri and Arthur Weiss. “Endogenous Nur77 Is a Specific Indicator of Antigen Receptor Signaling in Human T and B Cells”. In: *The Journal of Immunology* 198.2 (Jan. 2017), pp. 657–668.

[413] Gordon J. Freeman et al. “Engagement of the PD-1 immunoinhibitory receptor by a novel B7 family member leads to negative regulation of lymphocyte activation”. In: *Journal of Experimental Medicine* 192.7 (Oct. 2000), pp. 1027–1034.

[414] Mary E Keir et al. “PD-1 and its ligands in tolerance and immunity”. In: *Annual Review of Immunology* 26 (2008), pp. 677–704.

[415] Tadashi Yokosuka et al. “Programmed cell death 1 forms negative costimulatory microclusters that directly inhibit T cell receptor signaling by recruiting phosphatase SHP2”. In: *Journal of Experimental Medicine* 209.6 (June 2012), pp. 1201–1217.

[416] Riyao Yang et al. “Galectin-9 interacts with PD-1 and TIM-3 to regulate T cell death and is a target for cancer immunotherapy”. In: *Nature Communications* 12.1 (Dec. 2021), pp. 1–17.

[417] Jens M. Chemnitz et al. “SHP-1 and SHP-2 Associate with Immunoreceptor Tyrosine-Based Switch Motif of Programmed Death 1 upon Primary Human T Cell Stimulation, but Only Receptor Ligation Prevents T Cell Activation”. In: *The Journal of Immunology* 173.2 (July 2004), pp. 945–954.

[418] Daniel J. Puleston et al. “Polyamine metabolism is a central determinant of helper T cell lineage fidelity”. In: *Cell* 184.16 (Aug. 2021), 4186–4202.e20.

[419] Youping Wu et al. “A novel role for programmed cell death receptor ligand-1 in sepsis-induced intestinal dysfunction”. In: *Molecular Medicine* 22 (2016), pp. 830–840.

[420] Xun Wang et al. “Inflammatory cytokines IL-17 and TNF-α up-regulate PD-L1 expression in human prostate and colon cancer cells”. In: *Immunology Letters* 184 (Apr. 2017), pp. 7–14.

[421] Brandon L. Walling and Minsoo Kim. “LFA-1 in T cell migration and differentiation”. In: *Frontiers in Immunology* 9.MAY (May 2018), p. 952.

[422] Tjadine M. Holling, Erik Schooten, and Peter J. Van Den Elsen. "Function and regulation of MHC class II molecules in T-lymphocytes: Of mice and men". In: *Human Immunology* 65.4 (Apr. 2004), pp. 282–290.

[423] S M Cruickshank et al. "Colonic epithelial cell mediated suppression of CD4 T cell activation". In: *Gut* 53.5 (May 2004), pp. 678–684.

[424] A M Westendorf et al. "CD4+Foxp3+ regulatory T cell expansion induced by antigen-driven interaction with intestinal epithelial cells independent of local dendritic cells". In: *Gut* 58.2 (Feb. 2009), pp. 211–219.

[425] J. G. Fox et al. "Helicobacter hepaticus infection in mice: Models for understanding lower bowel inflammation and cancer". In: *Mucosal Immunology* 4.1 (Jan. 2011), pp. 22–30.

[426] Dirk Gevers et al. "The treatment-naive microbiome in new-onset Crohn's disease". In: *Cell Host and Microbe* 15.3 (Mar. 2014), pp. 382–392.

[427] Matthew Vanneman and Glenn Dranoff. "Combining immunotherapy and targeted therapies in cancer treatment". In: *Nature Reviews Cancer* 12.4 (Apr. 2012), pp. 237–251.

[428] Anuradha Tarafdar et al. "CML cells actively evade host immune surveillance through cytokine-mediated downregulation of MHC-II expression". In: *Blood* 129.2 (2017), pp. 199–208.

[429] Tone Løvig et al. "Strong HLA-DR expression in microsatellite stable carcinomas of the large bowel is associated with good prognosis". In: *British Journal of Cancer* 87.7 (Sept. 2002), pp. 756–762.